Bulletin
of
The Geological Society of America

VOLUME 63 April 1952 NUMBER 4

CONTENTS

Pages

Mechanism of limestone replacement at low temperatures and pressures. By R. M. Garrels and R. M. Dreyer 325–380

Structure and petrology of the Sunapee quadrangle, New Hampshire. By Carleton A. Chapman 381–426

Short Notes

Use of equal-area or other projections in the statistical treatment of joints. By John Rodgers 427–430

Some methods for operating on orientation data. By Howard J. Pincus 431–434

Subscription $15.00 per year.

Publication Office: Mt. Royal & Guilford Aves., Baltimore 2, Md.

Communications for publication should be addressed to The Geological Society of America, Dr. H. R. Aldrich, Secretary, 419 West 112th Street, New York, N. Y.

NOTICE—Four weeks notice of change of address is necessary. In accordance with the rules established by the Council, claims for for non-receipt of the preceding number of the Bulletin must be sent the Secretary of the Society within three months of the date of the receipt of this number in order to be filled gratis.

Entered as second-class matter at the Post-Office at Baltimore, Md., under the Act of Congress of July 16, 1894.

Accepted for mailing at special rate of postage provided for in Section 1103 Act of October 3, 1917, authorized on July 8, 1918.

PAPERS IN PRESS FOR FORTHCOMING ISSUES

BIOGEOCHEMICAL INVESTIGATIONS IN THE PACIFIC NORTHWEST. By Harry V. Warren, Robert E. Delavault, and Ruth I. Irish

QUATERNARY VOLCANISM ON SUMATRA. By J. Westerveld

MAGMATIC DIFFERENTIATION IN TERTIARY AND QUATERNARY VOLCANIC ROCKS FROM ADAK AND KANAGA ISLANDS, ALEUTIAN ISLANDS, ALASKA. By Robert R. Coats

GEOLOGY OF AGUA FRIA QUADRANGLE, BREWSTER COUNTY, TEXAS. By C. Gardley Moon

STATISTICAL METHODS APPLIED TO TRENTONIAN STRATIGRAPHY IN NEW YORK. By Philip A. Chenoweth

ANNOTATED AND ILLUSTRATED BIBLIOGRAPHIC MATERIAL ON THE MORPHOLOGY OF RIVERS. By P. F Neményi

BULLETIN OF THE GEOLOGICAL SOCIETY OF AMERICA
VOL. 63, PP. 325-380, 36 FIGS., 3 PLS. APRIL 1952

MECHANISM OF LIMESTONE REPLACEMENT AT LOW TEMPERATURES AND PRESSURES

By R. M. Garrels and R. M. Dreyer

Abstract

The replacement of limestone by supergene copper minerals provides a key to some of the mechanisms of metasomatism at low temperatures and pressures. The replacements studied were of the type in which the host and guest have no ions in common. Although numerous physical and chemical variables were studied, pH is noted to be the major control of metasomatism. The reaction of hydrolyzed, slightly acid solutions provided replacement always essentially volume-for-volume and with duplication of textures. The replacement of limestone by sulfides probably is analogous. Access of mineralizing solutions again is shown to be a function of secondary permeability. Movement outward from secondary openings is indicated to be mainly by diffusion rather than by forced flow. Under special conditions an impenetrable replacement layer, resembling crustification, may form as a result of diffusional replacement. The replacement layer formed where forced flow is a major factor commonly is more irregular than layers formed by diffusion alone. Natural replacement textures resemble the synthetic. The composition of natural replacement products is more complex than those formed synthetically as a result of oscillation in ionic content of the natural solutions.

CONTENTS

TEXT

	Page
Introduction	326
Acknowledgment	327
Previous work	328
Solubility of calcium carbonate	329
Calculation of equilibrium constants at various temperatures	329
Effect of pressure on carbonate equilibria	331
Relation of equilibrium constants and observed solubility	332
Introduction	332
Determination of activity coefficients	334
Calculation of the dissociation constant of $CaCO_3$ soluble	335
Correspondence of calculated and observed K′ values	335
Temperature coefficient of activity coefficients	336
Calculation of calcium carbonate solubility at 0°C.: a check with previous determinations	336
Discussion and summary	338
Solubility and rate of solution of calcite	341
General statement	341
Experimental procedure	341
Experimental results	342
Discussion	342
Relative rates of solution of calcite and other carbonates	344
Precipitation curves and Ksp values for atacamite and brochantite	344
Application of precipitation curves for atacamite and brochantite to the malachite problem	346
Petrography of synthetic replacements	347
Replacement under pressure	350
Natural copper mineral replacements	353
Replacement of calcite by iron oxide	355
Discussion	355
Oxidation-reduction relations	357
Replacement of limestone by mixed iron and copper solutions	358
Transportation of iron and copper from oxidizing chalcopyrite	360
Relation of grain size to rate of crystallization and to the effects of aging	361
Statement	361
Discussion	362
Effect of aging on grain size	362
Discussion	362
Replacement of calcite by sulfides	363
General	363
The silver bisulfide complex	364
Possibility of bisulfide complexes of other heavy metals	365
Differential effect of complexes on metal solubility	366
Replacement of sulfides by other sulfides	368
Statement	368
Discussion of results	368
Some mechanisms of precipitation, exclusive of reaction with solids	370
Introduction	370
Precipitation by dilution	370
Precipitation by gas loss	371
Relative roles of porosity and permeability in control of mineral deposition	372
Time necessary for replacement by diffusion	373
Time necessary for replacement by forced flow	375
Discussion	375
Summary	376
References cited	378

ILLUSTRATIONS

Figure — Page

1. Effect of pressure on equilibrium constant of $CaCO_3$, H_2CO_3 and HCO_3 at 25°C..... 331
2. Effect of pressure on the ionization constant of water..... 331
3. Effect of added salt on change of equilibrium constant with pressure at 25°C..... 331
4. Equilibrium constants of carbonate equilibria as a function of temperature, pressure, and added salts..... 332
5. K′ as a function of pH..... 332
6. Ionic strength versus chlorinity for sea water..... 334
7. Activity coefficients of the important components necessary for the calculation of calcium carbonate solubility..... 334
8. Comparison of calculated and empirical values for K′ as a function of pH..... 336
9. The effect of temperature on the activity coefficient of bicarbonate and carbonate ions..... 337
10. The effect of temperature, pressure, pH and salinity on the solubility of calcium carbonate..... 339
11. Solubility of calcium carbonate as a function of total CO_2 in solution at constant pH..... 340
12. Rate of solution of calcite in HCl solution buffered with sodium acetate..... 341
13. Rate of solution of calcite in HCl solution buffered with sodium acetate..... 341
14. Rate of solution of calcite in HCl solution buffered with sodium acetate..... 342
15. Rate of solution of calcite as a function of pH and temperature in HCl solutions buffered with sodium acetate..... 342
16. Rate of solution of calcite as a function of solubility and temperature in HCl solutions buffered with sodium acetate..... 342
17. Rate of solution of halite in NaCl solutions..... 343
18. Precipitation—pH curve for atacamite..... 345
19. Precipitation—pH curve for brochantite..... 346
20. Forced flow of water and 0.5M $CuCl_2$ solution through limestone at 5 lbs./sq. in..... 350
21. Forced flow of 0.5M $CuCl_2$ solution through limestone at 15 lbs./sq. in..... 351
22. Forced flow of 0.5M $CuCl_2$ solution through limestone with increasing pressure..... 351
23. Forced flow of 0.05M $CuCl_2$ solution through limestone at 10 lbs./sq. in..... 351
24. Forced flow of $FeCl_2$ solution through limestone at 10 lbs./sq. in. and various concentrations..... 351
25. Sections of a core replaced by atacamite..... 352
26. Changes in pH and in activity of ferrous and ferric ions..... 357
27. Maximum activity of ferrous ion as a function of Eh and pH..... 358
28. Adaptation of Figure 27 showing the Eh-pH stability field boundary separating solutions which can carry appreciable amounts of ferrous ion from those that cannot..... 358
29. Relation of grain size of precipitates to degree of supersaturation of solution in which they form..... 361
30. Distribution of major ionic species resulting from the ionization of H_2CO_3 and H_2S as a function of pH..... 363
31. Solubility of silver as a function of pH..... 365
32. Graph showing effects of various types of complexes on sulfide solubility..... 367
33. Solubility of CO_2 in water as a function of hydrostatic pressure and temperature..... 371
34. Solubility of H_2S in water as a function of hydrostatic pressure and temperature..... 371
35. Solubility of CO_2 as a function of depth..... 372
36. pH and CO_2 solubility as a function of depth..... 372

Plate — Facing page

1. Photomicrographs..... 348
2. Photomicrographs..... 354
3. Photomicrographs..... 356

TABLES

Page

1. Calculated values of the constants at different temperatures..... 330
2. Chlorinity..... 337
3. Equilibrium constants for carbonate equilibria as a function of temperature, pressure and ionic strength..... 340
4. Relative rates of solution of various carbonates..... 344
5. Typical results of calcite replacement in copper chloride solution..... 348
6. Analyses of chrysocolla..... 354
7. Changes in Eh and pH during reaction of ferrous chloride solution with sodium chloride solution containing solid calcium carbonate..... 355
8. Relation of grain diameter to degree of supersaturation..... 361
9. Solubility of silver in H_2S bearing solutions..... 365
10. Reaction of solutions with sulfides..... 368
11. Permeability of major ore beds in the Tri-State lead-zinc district..... 373
12. Time for formation of a replacement deposit of galena 32 centimeters thick at the wall of a planar vein..... 374
13. Replacement of rock..... 375

Introduction

The geological literature is replete with descriptions of mineral replacements. Many studies have been made of natural replacements to determine the process by which they have formed. A surprisingly small amount of study, however, has been devoted to laboratory experimentation on the factors that expedite or impede the replacement process. Our work was activated by a hope that a systematic laboratory study of the replacement process would augment the field studies and clarify some aspects of the replacement process. In particular, we have long felt the need of quantitative, experimentally ascertained data in

developing theories relative to the manner of mineral replacement. A project was submitted to the Geological Society of America and a substantial grant from the Penrose fund was awarded us in 1946.

Most natural solutions and the natural containers in which they circulate are complex chemical bodies. Since, in most cases, it is not possible to make quantitative determinations of the factors effecting mineral replacement where many chemical components and several physical phases are involved, it became apparent, early in this study, that it would be advisable to select a condition both chemically simple and geologically possible.

One of the simplest conditions, geologically speaking, obtains where supergene copper sulfate solutions replace calcite or limestone. The temperature and pressure are essentially atmospheric. The copper solutions resulting from oxidation of a simple copper sulfide ore body can be assumed, with reasonable accuracy in many cases, to consist predominantly of copper, iron, and sulfate ions. Limestone provides calcium and carbonate ions to the circulating solutions. In view of the relative simplicity of the natural system, it was decided first to investigate the reaction of copper salts with limestone and then to study the added effect of iron ions in the solutions. We hoped not only to determine the chemical reactions involved, but also to interpret textural relationships. With this in mind, laboratory studies were compared with natural copper replacements in limestone from selected areas.

The problem of the mechanism of limestone replacement revolves around two basic problems. How do the replacing solutions move into the limestone? How is the limestone simultaneously dissolved and carried away to provide a locus of replacement? It has long been known —and is again confirmed by this study—that mineral replacements are not molecular but, rather, volume for volume. The replacement mechanism must be of such a nature that a continuous supply of replacing ions can move to the replacement interface at the same time and in the same volume as the dissolved calcium carbonate moves away. In the case of copper solutions moving into limestone, the solubility and rate of solution of calcium carbonate are obviously the key to the replacement process. We therefore attempt to evaluate limestone solubility as affected by temperature, pressure, pH, total CO_2 content, and salinity. If the factors controlling the solution of calcium carbonate are known, we can then proceed with the problem of the introduction of the guest mineral. Does introduction occur by mass movement of the copper solutions into the limestone or by diffusion of ions through fluids contained in the host limestone? The two process are vastly different. Current literature does not yet provide an answer to the problem. We have therefore initiated experiments on mass movement of solutions into chalk and limestone under pressure and we have studied ionic diffusion into the same rocks. The two processes have been studied both chemically and petrographically. The resulting replacements are compared petrographically with natural replacements, both as to form and composition of the replacement developed. We also consider the effect of iron ions in the penetrating solutions as well as the factors which would control replacement by sulfides. Classic studies already have been made of the effect of porosity and permeability on replacement and such studies are somewhat augmented by data here presented.

We are fully aware of the difficulties of simulating natural conditions in the laboratory. To the extent that laboratory studies can reconstruct natural conditions, these studies should supplement our present knowledge of the mechanism of limestone replacement.

Acknowledgment

We wish gratefully to acknowledge the encouragement of the Geological Society of America in advancing very substantial financial assistance toward the pursuit of this study.

The work on replacement of limestones under pressure was done by Professor A. L. Howland, Northwestern University, and we have consulted with him frequently during the course of the rest of this work. We also appreciate the advice of Drs. C. A. Anderson, C. H. Behre, Jr., S. C. Creasey, J. W. Gruner, T. S. Lovering, Charles Milton, H. T. Morris, Harrison Schmitt, and G. M. Schwartz.

Dr. H. R. Aldrich, in his capacity as Secretary of the Geological Society, has done everything within his power to expedite this study.

The following persons have assisted the authors in various phases of the work: Miss Rose Marie Annos, Miss Anne Marie Anrod, Miss Betty Brestel, Mr. Neil Crow, Miss Dorothy Dietrich, Mrs. Barbara Dunlap, Mr. Robert O. Fay, Miss Dorothy Martin, Miss Marjorie Mooberry, Mr. R. T. Runnels, and Mr. Lawrence Stine.

Previous Work

The numerous mineral replacement zones in carbonate rocks indicate the importance of ready solubility in localizing replacement. There is, however, much discussion as to the manner in which solutions gain access to such carbonate rocks—whether by mass movement of solution or ionic diffusion. Although there is general agreement that both mass movement and ionic diffusion occur, there is much difference of opinion as to the relative importance of each process. The literature on the subject of replacement is great. A few selected quotations may illustrate the major concepts regarding the mode of occurrence of this process.

Lindgren (1933, p. 91) has defined replacement as:

"The process of practically simultaneous capillary solution and deposition by which a new mineral of partly or wholly differing chemical composition may grow in the body of an old mineral or mineral aggregate . . . . It is necessary to distinguish between metasomatic changes proceeding in free crystals or grains or in loose or plastic aggregates under light load where the force can easily overcome the restraining pressure; and (2) metasomatic changes proceeding in rigid rocks where the new mineral is forced to make room for itself by the solution of the host mineral. In the first case, the volume changes proceed according to the chemical formula. In the second case, the replacing mineral occupies exactly the space formerly filled by the primary mineral . . . .The most fundamental changes in rocks take place with practical constancy of volume." He states further (p. 173): "Many deposits have been formed by solutions containing various salts and gases and capable of attacking certain kinds of rocks. Guided by fissures or other open ducts, the solutions deposit part of their load in the open super-capillary spaces whenever supersaturation takes place; thus is produced the filling of fissures. As almost all rocks are porous and as the solutions frequently are under heavy pressure, they will be forced into the rocks and will produce chemical and mineralogical changes in them. At the same time, the porous rock acts, undoubtedly, as a semi-permeable membrane through which various substances will diffuse at differing rates—electrolytes and gases most easily, colloids and difficultly ionized compounds very slowly."

Lindgren notes further (pp. 176–177):

"By diffusion is meant the movement of the molecules in a solution from a place of higher concentration to a place of lower concentration. This process is most important for the phenomena of replacement and ore deposition in general. . . . But the process . . . is exceedingly slow, does not act over large distances and ceases after a certain time. Diffusion is incompetent to originate mineral deposits; it must be supplemented by the movement of solution on fractures or other open spaces."

Lindgren thus, without presenting laboratory evidence, postulated a replacement process essentially by mass movement of solution along open spaces with diffusion accorded a minor role.

G. F. Becker (1897) first calculated the rate of diffusion under geological conditions.

Whitman (1928) studied quantitatively the rate of diffusion of potassium iodide in marble. He states (pp. 483–484):

"The spheroid of dilution of a substance passing into solution in the depths of the earth must expand with exceeding slowness after reaching a certain radius. Becker showed that sodium chloride diffusion through massive water in the course of 100,000 years would have progressed only 731 feet. But 100,000 years is only 1 per cent of the time that may be reasonably allowed for the period of accumulation of some mineral deposits according to the quoted ideas of the magnitude of geologic time; and, for arguments sake, we may say that 2,000 feet shall be the maximum radius allowed for mineral migration through the pore spaces of rock in a spherical field of diffusion. Then, in the formation of ore deposits more than that distance from the supposed source of mineral, water circulation through unsealed passages may be invoked where diffusion is equal in all directions; but that leaves a large proportion of significant metasomatic deposits within this assumed radius and requires no passage of water through cemented fractures; it also permits the formation of mineral deposits nearly a half a mile from any significant water course in a homogeneous medium. However, the radius of diffusion, or the influence of precipitation, is not necessarily the theoretical radius of diffusion, but a greatly modified form of it. The field of diffusion is rarely spherical but enormously distorted by lines of relatively easy diffusion; in consequence the diffusing substance will move chiefly along some relatively open channel for the major part of its migration, the practical field of diffusion thus being, simply or complexly, essentially tabular. This would greatly alter the radius of diffusion because the volume or space to be occupied by the diffusing substance would thus be more or less elongated,

and commonly would more than double the radius of diffusion."

Whitman then concludes (p. 482) that:

"Diffusion is a large factor if not the major factor in the formation of metasomatic metalliferous deposits."

Duffell (1937) also experimented on the diffusion of solutions through rocks. He notes the inadequacy of the process in the replacement of both dry and water saturated rocks.

Bateman (1950, p. 139) states:

"It has been repeatedly demonstrated ... that replacement is definitely a volume for volume interchange. Consequently, ordinary balanced chemical equations do not express what actually happens in volume for volume replacement, and the oft-quoted equations must be considered only as indicating the trend and end products of the exchange. The process is not yet fully understood." And further (p. 140): "Replacement involves the necessity of continuing supplies of new material and the removal of the dissolved material. How does the new material arrive at the point of deposition? ... Diffusion is probably the answer. This is the movement of molecules or ions in a solution from a point of supply to a point of deposition or from a place of higher to one of lower concentration. Particles of ionic or molecular size can move through a layer where a bodily flow of solution could not. But diffusion is known to be exceedingly slow and to act only over short distances. Therefore, it cannot be a means of transporting large quantities of replacing substances over long distances; it is incompetent by itself to build up large mineral deposits. However, it is an effective process for supplying and removing the products and by-products of replacement over the short distances at the actual front of replacement where voluminous moving solutions could not gain entry."

Bateman thus follows Lindgren in assigning to diffusion only a minor role in the replacement process.

Holser (1947, p. 389) notes that:

"A number of the authors cited have pointed out the fact that diffusion through a fluid phase is a particularly convenient mechanism of transport in replacement, because it easily allows the movement of matter to the replacing front and away from it, within the same volume of fluid, each ion moving down its own concentration gradient. Furthermore, the precipitation of an ion at the replacement front automatically provides the impetus for further supply because removal decreases the concentration of that ion. Another convenient property of diffusion is the decrease of diffusion rate with increasing (ionic) radius, which might separate complex solutions ... to give the zoning observed in many replacement deposits."

The reader is referred to Holser's paper for a detailed review of the literature on metasomatism.

From the wide range of opinion expressed concerning the relative importance of mass movement of solution down a pressure gradient (permeability), versus movement of ions down a concentration gradient (diffusion), it is clear that an understanding of the replacement processes cannot evolve until the relative importance of these two mechanisms of material transport can be assessed.

Solubility of Calcium Carbonate

Calculation of Equilibrium Constants at Various Temperatures

The fundamental equilibrium constants used in the calculation of the solubility of calcium carbonate at 25°C. are well known, but it is necessary to resort to a method similar to that used for the calculation of the solubility of sulfides by Verhoogen (1938) to determine the necessary values at higher temperatures.

To calculate the solubility of calcium carbonate at a given pH at an elevated temperature, the activity product of the carbonate and the two dissociation constants of carbonic acid must be known at that temperature:

$$\frac{(a_{H^+})(a_{CO_3^{''}})}{(a_{HCO_3^-})} = K_{e_{HCO_3^-}} \qquad (1)$$

$$\frac{(a_{H^+})(a_{HCO_3^-})}{(a_{H_2CO_3})} = K_{e_{H_2CO_3}} \qquad (2)$$

$$(a_{Ca^{++}})(a_{CO_3^{''}}) = K_{e_{CaCO_3}} \qquad (3)$$

These can be computed from the free energy relations. For equation #1:

$$H^+ + CO_3^{''} = HCO_3^- \; ; \quad \Delta F^0_{(T)} = \Delta F^0 + AT$$

(Kelley and Anderson, 1935, p. 7)

$$\Delta F^0_{(T)} = -5370 - 29.64T \qquad (4)$$

$\Delta F^0_{(T)}$ is related to $K_{e_{HCO_3^-}}$ by the following equation:

$$\Delta F^0_{(T)} = -RT \ln \frac{(a_{HCO_3^-})}{(a_{H^+})(a_{CO_3^{''}})} = -RT \ln \frac{1}{K_{e_{HCO_3^-}}} \qquad (5)$$

Substituting from equation 4:

$$\Delta F^0_{(T)} = \Delta F^0 + AT = -5370 - 29.64T = -RT \ln \frac{1}{K_{e_{HCO_3^-}}}$$

The parallel equation for $Ke_{H_2CO_3}$ is (Kelley, 1935, p. 7):

$$\Delta F^0_{(T)} = \Delta F^0 + BT = -2890 - 19.84T = -RT \ln \frac{1}{Ke_{H_2CO_3}}$$

Unfortunately, a similar equation for the dissociation of calcium carbonate is not available, but the free energy change for the equation can be written:

$$Ca^{++} + CO_3'' = CaCO_3 \quad (7)$$

$$\Delta F^0_{(T)} = \Delta F^0_{(T)CaCO_3} - [\Delta F^0_{(T)Ca^{++}} + \Delta F^0_{(T)CO_3''}]$$

and it is possible to determine the temperature coefficients of the individual components.

For $\Delta F^0_{(T)CaCO_3}$ at a given temperature, Kelley (p. 16) gives:

$$\Delta F^0_{(T)} = -283{,}800 - 1.64T \log T + 2.78 \times 10^{-3}T^2 + 0.454 \times 10^5 T^{-1} + 66.32T \quad (8)$$

Similar equations are not available for $\Delta F^0_{(T)Ca^{++}}$ and $\Delta F^0_{(T)CO_3''}$ but it is possible to calculate them for a limited temperature range by taking advantage of the relations (Lewis and Randall, 1923, p. 168–173):

$$-\Delta F_i^0 = nE_i^0F \quad (9)$$

and:

$$E_i^0 + \frac{\Delta H_i}{nF} = T\frac{dE_i^0}{dT} \quad (10)$$

where ΔF_i^0 is the free energy of formation of the ion; where E_i^0 is the standard electrode potential for the formation of the calcium or carbonate ion; ΔH_i^0 is the heat of formation of the ion; n is the number of electrons lost in the ionization; F is the Faraday, expressed in calories per mol; and T the absolute temperature.

The free energy of ionization of Ca^{++} ion is $-127{,}340$ calories at 25°C. (Kelley and Anderson, 1935, p. 15). Substituting this value in equation 9, along with 2 for n, and 23,060 for F, gives a value for $E^0_{Ca^{++}}$ of 2.76 volts. The heat of ionization (ΔH^{0*}) at 18°C. is $-128{,}500$ calories (International Critical Tables, 1929, vol. 5, p. 196). Ignoring the 7° difference for the moment, and substituting the value of $E^0_{Ca^{++}}$ at 25°C. in equation #10

TABLE 1.—CALCULATED VALUES OF THE CONSTANTS

	Temperature			
	0°C.	25°C.	45°C.	65°C.
Ke_{CaCO_3}	$10^{-7.97}$	$10^{-8.29}$	$10^{-8.40}$	$10^{-8.75}$
Ke_{HCO_3}	$10^{-10.75}$	$10^{-10.33}$	$10^{-10.20}$	$10^{-9.91}$
$Ke_{H_2CO_3}$	$10^{-6.61}$	$10^{-6.45}$	$10^{-6.34}$	$10^{-6.21}$

gives:

$$2.76 + \frac{-128{,}500}{2 \times 23060} = 291\frac{dE^0_{Ca^{++}}}{dT}$$

$$\frac{dE^0_{Ca^{++}}}{dT} = -0.000086 \text{ volts/degree}$$

Then, using this value for $\frac{dE^0_{Ca^{++}}}{dT}$, $E^0_{Ca^{++}}$ at 18°C. remains within the limit of error at 2.76 volts. Substituting the same value in equation #10, a value of $\frac{dE^0_{Ca^{++}}}{dT}$ of -0.000086 volts/degree is obtained. Assuming that the value of $\frac{dE^0_{Ca^{++}}}{dT}$ is constant from 25°C. to 65°C., an equation for the change of $\Delta F^0_{Ca^{++}}$ can be obtained from equation #9:

$$-\Delta F^0_{Ca^{++}} = nF[2.76 - (0.000086[T - 298])] \quad (11)$$

A similar expression can be derived for $\Delta F^0_{CO_3''}$:

$$-\Delta F^0_{CO_3''} = nF[2.74 - (0.00260[T - 298])] \quad (12)$$

In obtaining this relation, the value for $\Delta F^0_{CO_3''}$ (298°) = $-126{,}390$ was taken from Kelley (p. 15); that used for $\Delta H^0_{CO_3''}$ (291°) = $-161{,}000$ is taken from the International Critical Tables (1929, p. 181).

A combination of equations #8, #11, and #12 gives the desired expression for the free energy of ionization of calcium carbonate as a function of temperature.

$$\Delta F^0_{(T)CaCO_3} = [-283{,}800 - 1.64T \log T + 2.78 \times 10^{-3}T^2 + 0.454\ 10^5T^{-1} + 66.32T] - [(-nF(2.76 - (0.000086[T - 298])] - [-nF(2.74 - (0.00260[T - 298])] \quad (13)$$

It must be remembered that the equation is derived on the assumption of the constancy of the value $\frac{dE^0}{dT}$, but the error introduced probably is not large for a range of 40° or 50°C.

$\Delta F^0_{(T)}$ is related to Ke_{CaCO_3} by the equation:

$$\Delta F^0_{(T)} = -RT \ln \frac{1}{Ke_{CaCO_3}} \qquad (14)$$

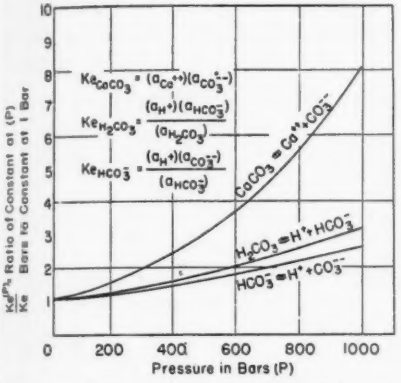
$Ke_{CaCO_3} = (a_{Ca^{++}})(a_{CO_3^{--}})$
$Ke_{H_2CO_3} = \frac{(a_{H^+})(a_{HCO_3^-})}{(a_{H_2CO_3})}$
$Ke_{HCO_3^-} = \frac{(a_{H^+})(a_{CO_3^{--}})}{(a_{HCO_3^-})}$
$CaCO_3 = Ca^{++} + CO_3^{--}$
$H_2CO_3 = H^+ + HCO_3^-$
$HCO_3^- = H^+ + CO_3^{--}$
$K_e^{(P)}/K_e$ Ratio of Constant at (P) Bars to Constant at 1 Bar
Pressure in Bars (P)

FIGURE 1.—EFFECT OF PRESSURE ON EQUILIBRIUM CONSTANT OF $CaCO_3$, H_2CO_3 AND HCO_3^- AT 25°C. (Owen and Brinkley, 1941, p. 468).

Effect of Pressure on Carbonate Equilibria

The effect of hydrostatic pressure on the activity product of calcium carbonate and on other ionic equilibria of interest in the problem of calcium carbonate solubility has been investigated by Owen and Brinkley (1941, p. 461–474). They have determined the ratio of equilibrium constants at higher pressures to those at one bar of pressure for solutions with pure water as the solvent, and also with artificial sea water as the dissolving medium (Figs. 1–3).

In summary, the effect of hydrostatic pressure of as much as 1000 bars (approximately 1000 atmospheres) is to increase the equilibrium constants by a maximum factor of 8 in the case of $CaCO_3$, by much less for the other equilibria. In general the pressure effect is less at higher temperatures and also is lessened by the presence of added salts.

This investigation is arbitrarily limited to low temperatures and low pressures, duplicating conditions likely to be encountered in the upper few hundreds of feet of the crust. In Figure 4, the activity product of calcium carbonate and the equilibrium constants for the first and second ionizations of carbonic acid are plotted as functions of temperature, pressure, and added salts. The same percentage decreases in pressure effect with increased temperature and

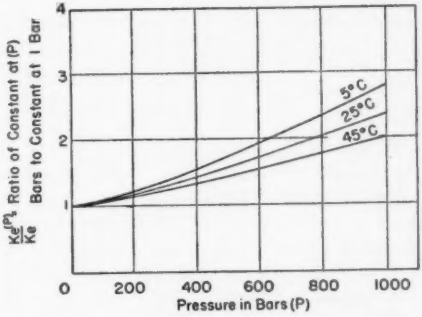

FIGURE 2.—EFFECT OF PRESSURE ON THE IONIZATION CONSTANT OF WATER

Showing typical decrease of pressure effect with higher temperatures (Owen and Brinkley, 1941, p. 467).

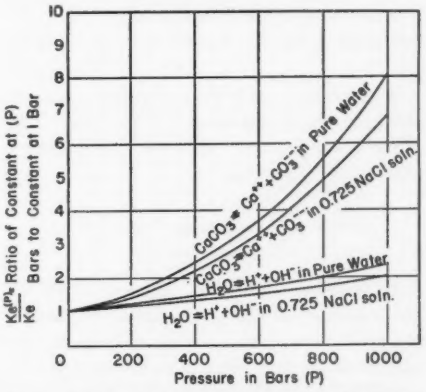
$CaCO_3 = Ca^{++} + CO_3^{--}$ in Pure Water
$CaCO_3 = Ca^{++} + CO_3^{--}$ in 0.725 NaCl soln.
$H_2O = H^+ + OH^-$ in Pure Water
$H_2O = H^+ + OH^-$ in 0.725 NaCl soln.
$K_e^{(P)}/K_e$ Ratio of Constant at (P) Bars to Constant at 1 Bar
Pressure in Bars (P)

FIGURE 3.—EFFECT OF ADDED SALT (0.725) mNaCl) ON CHANGE OF EQUILIBRIUM CONSTANT WITH PRESSURE AT 25°C.

(Owen and Brinkley, 1941, p. 472).

with added salt calculated by Owen and Brinkley for water are applied to the carbonate equilibria. This has justification in the comparable percentage change of the pressure effect with added salt on the ionization of water and on that of calcium carbonate (Fig. 3), and in the conclusion by Owen and Brinkley that the general effect of increase of temperature is to decrease the effect of pressure on the equilibrium

constant of the weak electrolytes. At any rate, it is certain that the adjustment is in the right direction. Even if the temperature effect and the salt effect were ignored completely, the total resulting error in the equilibrium constant probably would not exceed 30 per cent; with adjustment, the error probably is not greater than 10 or 15 per cent.

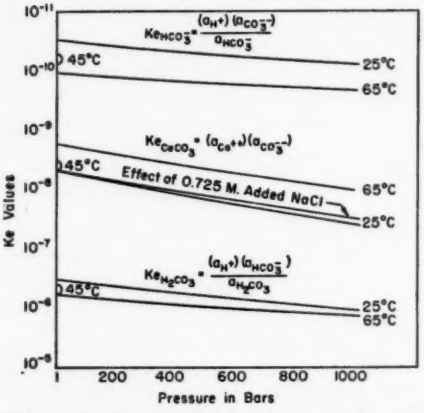

FIGURE 4.—EQUILIBRIUM CONSTANTS OF CARBONATE EQUILIBRIA AS A FUNCTION OF TEMPERATURE, PRESSURE, AND ADDED SALTS

Salt effect is shown only for Ke_{CaCO_3} at 25°C.

Relation of Equilibrium Constants and Observed Solubility

Introduction.—Of the exhaustive studies made of the solubility of calcium carbonate, the most relevant to the study of limestone replacement are those cited in Sverdrup, Johnson, and Fleming (1942, p. 205–208). The problem of solubility in sea water is analogous to the solubility in solutions migrating through rocks; the effect of a variety of dissolved substances must be considered. The treatment in Sverdrup *et al.* is essentially empirical—a number of equations and graphs are developed relating solubility to pH and chlorinity. It is necessary, in order to estimate calcium carbonate solubility in any stipulated environment, to develop general theoretical equations relating observed solubility to pH, concentration of other components in the solution, pressure, and temperature.

It has already been shown that the equilibrium constants of $CaCO_3$, H_2CO_3, and HCO_3^- are known as functions of temperature and pressure over the range of 25°–65°C. and 1 to 1000 bars. The problem can be completed if a relation can be found between the observed solubility and the equilibrium constants.

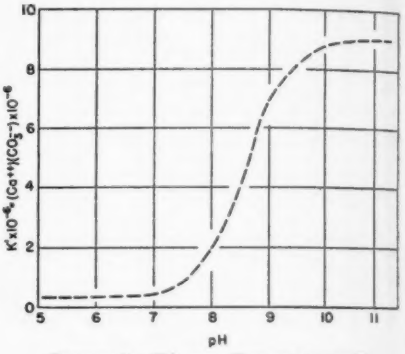

FIGURE 5.—K′ AS A FUNCTION OF pH (Sverdrup *et al.*, 1942, p. 206)

In the excellent summary of observed solubility relations in Sverdrup *et al.*, the product $[Ca^{++}]\,[CO_3'']$, which they call K', is shown as a function of pH and chlorinity (Fig. 5). If their curves can be duplicated entirely from theoretical considerations, the way is pointed to a very broad extension of the conditions under which calcium carbonate solubility can be predicted.

The product $[Ca^{++}]\,[CO_3'']$ warrants analysis, for the relation required is a method of calculating this product from the known values of the activity product:

$$(a_{Ca^{++}})(a_{CO_3''}) = K_{\text{activity}\,CaCO_3}.$$

$[Ca^{++}]$ seems to be the concentration of *soluble calcium* in the solution, whereas $[CO_3'']$ is the stoichiometric concentration of carbonate ions $-m_{CO_3''}$. $[Ca^{++}]$ is generally determined by direct analysis; whereas $[CO_3'']$ is a partially calculated value based upon a combination of analysis and theory. Consequently, it is possible to rewrite the product:

$$(\text{Total soluble calcium})(m_{CO_3''}) = K' \qquad (1)$$

This change is necessary, because it is conceivable that the total soluble calcium in solu-

tion may comprise not only the concentration of calcium ions ($m_{Ca^{++}}$), but may also represent a contribution from other soluble ionic or molecular species containing calcium.

A partial bridge between K' and $K_{activity}$ may be made from the relation between the activity product and the classical solubility product constant K_{sp}:

$$(a_{Ca^{++}})(a_{CO_3''}) = K_{activity\ CaCO_3} \quad (2)$$

$$(m_{Ca^{++}})(m_{CO_3''}) = K_{sp} \quad (3)$$

but:

$$(a_{Ca^{++}}) = m_{Ca^{++}}\gamma_{Ca^{++}} \quad (4)$$

$$(a_{CO_3''}) = m_{CO_3''}\gamma_{CO_3''} \quad (5)$$

where the coefficient γ is the *activity coefficient*. Combining the equations:

$$(m_{Ca^{++}})(m_{CO_3''}) = \frac{K_{activity\ CaCO_3}}{\gamma_{Ca^{++}}\gamma_{CO_3''}} \quad (6)$$

Once the relation is established, it becomes certain that the K' listed by Sverdrup *et al.* is not the same as K_{sp}. In other words, $[Ca^{++}]$ must represent a contribution from ionic or molecular species other than simple calcium ion. If all the calcium in solution were present in this simple form, K' would not change with pH in sea water of constant chlorinity. γ values are affected by changes in concentration in a solution, but the effect of the small change represented by a difference of a few pH units in the middle of the pH range is negligible. Consequently, from equation # 6, since $K_{activity}$ is a true constant, and since neither $\gamma_{Ca^{++}}$ nor $\gamma_{CO_3''}$ should change solely with change in pH, the product of $(m_{Ca^{++}})$ and $(m_{CO_3''})$ must remain constant. But K' does not remain constant; it changes from 0.62×10^{-6} at a pH of 7.4 to 8.8×10^{-6} at a pH of 10. Therefore, calcium must be present not only as simple ions, but in important quantities in some combined soluble form.

The equation for K′ can then be written:

$$(m_{Ca^{++}} + m_{soluble\ calcium\ complex})(m_{CO_3''}) = K' \quad (7)$$

The nature of the soluble calcium complex is indicated by the correlation of the increase of K' with increasing pH to that of CO_3'' ion. CO_3'' ion increases with increasing pH in much the same way that K' changes (Sverdrup *et al.*, p. 201). Therefore, the term $(m_{Ca^{++}} + m_{soluble\ calcium\ complex})$ presumably remains nearly constant. Such behavior might be expected if the soluble calcium is present largely as molecular calcium carbonate. In this case, solid calcium carbonate would dissolve to give soluble molecular calcium carbonate, which in turn would ionize to Ca^{++} and CO_3'' ions:

$$CaCO_{3\,solid} = CaCO_{3\,soluble} = Ca^{++} + CO_3'' \quad (8)$$

As CO_3'' ion concentration increases with increasing pH, Ca^{++} ion concentration would correspondingly decrease, as indicated by equation # 6, the total mass action effect would be to keep $(CaCO_{3\,soluble})$ constant. On the basis of this assumption, the following equilibria are of importance in sea water in equilibrium with calcium carbonate:

$$CaCO_{3\,solid} = CaCO_{3\,soluble} = Ca^{++} + CO_3''$$

$$\frac{(a_{Ca^{++}})(a_{CO_3''})}{(a_{CaCO_3\,soluble})} = Ke_{CaCO_3\,soluble} = \frac{(\gamma_{Ca^{++}} m_{Ca^{++}})(\gamma_{CO_3''} m_{CO_3''})}{(\gamma_{CaCO_3\,soluble}\, m_{CaCO_3\,soluble})} \quad (9)$$

$$H_2CO_3 = H^+ + HCO_3^-$$

$$\frac{(a_{H^+})(a_{HCO_3^-})}{(a_{H_2CO_3})} = Ke_{H_2CO_3} = \frac{(a_{H^+})(\gamma_{HCO_3^-} m_{HCO_3^-})}{(\gamma_{H_2CO_3}\, m_{H_2CO_3})} \quad (10)$$

$$HCO_3^- = H^+ + CO_3''$$

$$\frac{(a_{H^+})(a_{CO_3''})}{(a_{HCO_3^-})} = Ke_{HCO_3^-} = \frac{(a_{H^+})(\gamma_{CO_3''} m_{CO_3''})}{(\gamma_{HCO_3^-} m_{HCO_3^-})} \quad (11)$$

$$H_2CO_3 = H_2O + CO_2$$

$$\frac{(a_{CO_2})(a_{H_2O})}{(a_{H_2CO_3})} = Ke_{CO_2} = \frac{(\gamma_{CO_2} m_{CO_2})(\gamma_{H_2O} m_{H_2O})}{(\gamma_{H_2CO_3}\, m_{H_2CO_3})} \quad (12)$$

Since it is generally considered that the activity of water in such solutions is nearly constant, and that all the CO_2 in solution is present in combined form, Ke_{CO_2} is not necessary. Instead, we can write (Sverdrup *et al.*, p. 197):

$$(m_{CO_2}) = \text{solubility } CO_2 = m_{H_2CO_3} + m_{HCO_3^-} + m_{CO_3''} \quad (13)$$

Thus, if γ_i values are known, there are five equations with six unknowns, if all the Ke's

are known. All are available except $Ke_{CaCO_3\ soluble}$.

Determination of activity coefficients.—From the preceding equations, it is noted that values

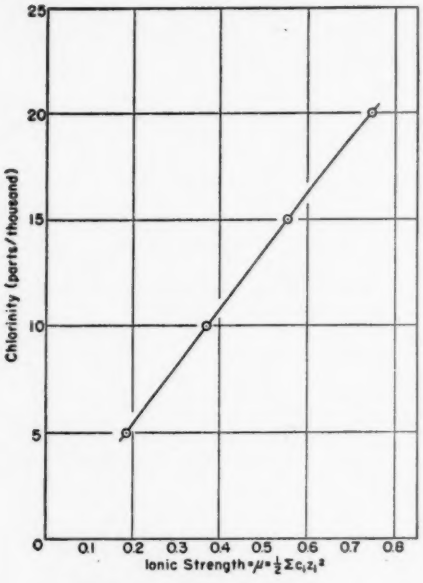

FIGURE 6.—IONIC STRENGTH VERSUS CHLORINITY FOR SEA WATER

of $\gamma_{Ca^{++}}$, $\gamma_{CO_3^{--}}$, $\gamma_{H_2CO_3}$, $\gamma_{HCO_3^-}$, and $\gamma_{CaCO_3\ soluble}$ are needed. In Sverdrup *et al.* (p. 205), values of $\gamma_{CO_3^{--}}$, $\gamma_{HCO_3^-}$, and $\gamma_{H_2CO_3}$ are given for sea water of 19 parts per thousand chlorinity as 0.019, 0.36, and 1.13 respectively. These values are satisfactory for this single value of chlorinity, but for general utility it is necessary to know them over a wide range of concentration of added salts. According to a first approximation of the DeBye-Hückel theory, the activity coefficient in solutions of low ionic strength can be calculated from the formula:

$$-\log \gamma_i = Az_i^2\sqrt{\mu} \qquad (14)$$

where γ_i is the activity coefficient of the ion in question, A is a constant at a given temperature (0.5 at 18°C.), z_i is the valence of the ion, and μ the ionic strength. The ionic strength is defined as:

$$\mu = \tfrac{1}{2}\Sigma c_i z_i^2 \qquad (15)$$

where c_i is the concentration of each ion in solution, and z_i its valence. Although this first approximation is usually valid only to values of μ of a few hundredths, and the ionic strength of sea water of 19 parts per thousand chlorinity

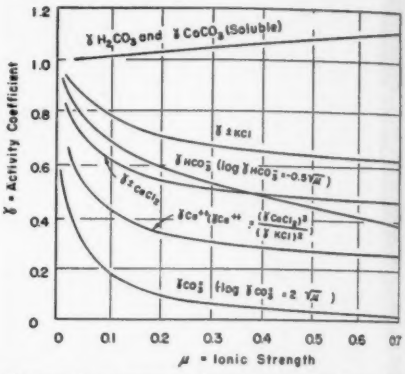
γ = Activity Coefficient
γ H2CO3 and γ CoCO3 (Soluble)
γ ±KCl
γ HCO3 (log γ HCO3 = -0.5√μ)
γ ±CaCl2
γ Ca++ γ ±KCl2 = (γ CaCl2)3 / (γ KCl)2
γ CO3 (log γ CO3 = -2 √μ)
μ = Ionic Strength

FIGURE 7.—ACTIVITY COEFFICIENTS OF THE IMPORTANT COMPONENTS NECESSARY FOR THE CALCULATION OF CALCIUM CARBONATE SOLUBILITY

The basis for calculation is indicated on the graph.

is about 0.7 (Fig. 6), a calculation using the first approximation (equation #14) yields 0.021 as $\gamma_{CO_3^{--}}$, and 0.38 as $\gamma_{HCO_3^-}$, a truly remarkable check. On the basis of this correspondence of theory and observation, additional values were calculated for other ionic strengths. The plot is shown in (Fig. 7).

No values are available for $\gamma_{Ca^{++}}$, but they can be obtained indirectly. So-called mean values ($\gamma_\pm$) are known for KCl and for $CaCl_2$ (Robinson and Stokes, 1949, p. 593–604); these mean values are related to those of the individual ions by the equation:

$$\gamma_\pm = (\gamma_+^{\nu_+}\gamma_-^{\nu_-})^{1/\nu_+ + \nu_-} \qquad (16)$$

where γ_+ is the activity coefficient of the positive ion; γ_- that of the negative ion, ν_+ the number of positive ions produced by ionization of one molecule of the salt, and ν_- the number of negative ions. For example, for KCl:

$$\gamma_{\pm KCl} = (\gamma'_{K^+}\gamma'_{Cl^-})^{1/1+1} \qquad (17)$$

Since γ_{K^+} and γ_{Cl^-} are nearly equal, $\gamma_\pm$ can be used for γ_{Cl^-}. For $CaCl_2$:

$$\gamma_{\pm CaCl_2} = (\gamma_{Ca^{++}}\gamma^2_{Cl^-})^{1/1+2} \qquad (18)$$

By substituting values of γ_{Cl^-} ($\gamma_{\pm KCl}$) and the measured values of $\gamma_{\pm CaCl_2}$, $\gamma_{Ca^{++}}$ is obtained (Fig. 7).

Activity coefficients of unionized molecules are close to unity and have similar values at comparable ionic strengths; thus the values graphed for $\gamma_{CaCO_3\ soluble}$ and $\gamma_{H_2CO_3}$ (Fig. 7) are calculated from the Sverdrup equation for $\gamma_{H_2CO_3}$ (p. 204).

By such devious methods the necessary γ_i values are obtained, and five of the unknowns are removed.

Calculation of the dissociation constant of $CaCO_3$ soluble.—The next step is to calculate a value for $Ke_{CaCO_3\ soluble}$. Until this value is known, there are still five equations and seven unknowns. Also, the existence of such a constant still is unproved. To obtain it, the values of K' as a function of pH can be used (Fig. 5).

According to the interpretation developed in the preceding pages:

$$(m_{Ca^{++}} + m_{CaCO_3\ soluble})(m_{CO_3''}) = K' \qquad (7)$$

The validity of this interpretation can be checked by obtaining a value of $Ke_{CaCO_3\ soluble}$ for a given value of K', and then determining if other values of K', calculated using $Ke_{CaCO_3\ soluble}$, fit the empirical values of K' at the various pH values.

Assume for convenience that the sea water is saturated with CO_2 at 1 atmosphere pressure. Under this condition, 0.03 mols are in solution (Sverdrup *et al.*, p. 202), and:

$$m_{HCO_3^-} + m_{H_2CO_3} + m_{CO_3''} = 0.03 \qquad (13)$$

At 20°C. (Sverdrup *et al.*, p. 204):

$$\frac{(a_{H^+})(\gamma_{CO_3^-}\ m_{CO_3^-})}{(\gamma_{HCO_3^-}\ m_{HCO_3^-})} = 10^{-10.288} \qquad (11)$$

Substituting γ_i values from Figure 7, for a chlorinity of 19‰, and 10^{-10} (pH = 10) for a_{H^+}

$$\frac{(m_{CO_3''})}{(m_{HCO_3^-})} = \frac{10^{-10.288} \times 0.28}{0.021 \times 10^{-10}} = 9.3 \qquad (19)$$

Also:

$$\frac{(a_{H^+})(\gamma_{HCO_3^-}\ m_{HCO_3^-})}{(\gamma_{H_2CO_3}\ m_{H_2CO_3})} = 10^{-6.47} \qquad (10)$$

$$\frac{(m_{HCO_3^-})}{(m_{H_2CO_3})} = \frac{10^{-6.47} \times 1.13}{0.38 \times 10^{-10}} = 10^4; \qquad (20)$$

$$\frac{(m_{H_2CO_3})}{(m_{HCO_3^-})} = 10^{-4}$$

Returning to equation #13, and using these ratios:

$$m_{HCO_3^-} + 10^{-4} m_{HCO_3^-} + 9.3\ m_{HCO_3^-} = 0.030$$

$$(m_{HCO_3^-}) = 0.0029 \qquad (13)$$

$$(m_{H_2CO_3}) = 0.00000029$$

$$(m_{CO_3''}) = 0.027$$

Since (equation #6):

$$(\gamma_{Ca^{++}} m_{Ca^{++}})(\gamma_{CO_3''}\ m_{CO_3''}) = 5 \times 10^{-9}\ (20°C.) \qquad (6)$$

Substituting γ values from Figure 7 and the value of $m_{CO_3''}$ from equation #13:

$$(0.26\ m_{Ca^{++}})(0.021 \times 0.027) = 5 \times 10^{-9}$$

$$m_{Ca^{++}} = \frac{5 \times 10^{-9}}{0.26 \times 0.021 \times 0.027}$$

$$= 3.4 \times 10^{-5} \qquad (21)$$

But:

$$(m_{Ca^{++}} + m_{CaCO_3\ soluble})(m_{CO_3''}) = 8.8 \times 10^{-6}$$

(equation #7 and Fig. 5)

$$(3.4 \times 10^{-5} + m_{CaCO_3\ soluble})(2.7 \times 10^{-3}) = 8.8 \times 10^{-6}$$

$$m_{CaCO_3\ soluble} = 3 \times 10^{-4} \qquad (22)$$

and:

$$\frac{(\gamma_{Ca^{++}}\ m_{Ca^{++}})(\gamma_{CO_3''}\ m_{CO_3''})}{(\gamma_{CaCO_3\ soluble}\ m_{CaCO_3\ soluble})} = Ke_{CaCO_3\ soluble}$$

Substituting values from the preceding equations:

$$\frac{(0.26 \times 3.4 \times 10^{-5})(0.021 \times 0.027)}{1.13 \times 3 \times 10^{-4}} \qquad (23)$$

$$= 1.48 \times 10^{-5}$$

which is the desired constant.

Correspondence of calculated and observed K' values.—Now the five equations with six unknowns are available, and K' values can be determined at any arbitrary pH. A sample calculation should suffice to show the method.

One of the empirical points on the Sverdrup graph (Fig. 5) is at a pH of 7.4. Using this value:

$$\frac{(a_{H^+})(\gamma_{CO_3^{''}}\ m_{CO_3^{''}})}{(\gamma_{HCO_3^-}\ m_{HCO_3^-})} = 10^{-10.288} \qquad (11)$$

$$\frac{(m_{CO_3^{''}})}{(m_{HCO_3^-})} = \frac{0.38 \times 10^{-10.288}}{0.021 \times 10^{-7.4}} = 2.32 \times 10^{-3}$$

Similarly:

$$\frac{(m_{HCO_3^-})}{(m_{H_2CO_3})} = \frac{1.13 \times 10^{-6.47}}{0.38 \times 10^{-7.4}} = 25.4;$$

$$\frac{(m_{H_2CO_3})}{(m_{HCO_3^-})} = 0.0394$$

Then since:

$$m_{HCO_3^-} + m_{H_2CO_3}\ m_{CO_3^{''}} = 0.03 \qquad (13)$$

$$m_{HCO_3^-} + 0.0394\ m_{HCO_3^-} + 0.0232\ m_{HCO_3^-} = 0.03$$

$$m_{HCO_3^-} = 0.0282$$

$$m_{CO_3^{''}} = 6.55 \times 10^{-4}$$

Further:

$$(\gamma_{Ca^{++}} m_{Ca^{++}})(\gamma_{CO_3^{''}}\ m_{CO_3^{''}}) = Ke_{CaCO_3} = 5.0 \times 10^{-9}$$

$$(m_{Ca^{++}}) = \frac{5 \times 10^{-9}}{0.26 \times 0.021 \times 6.55 \times 10^{-4}} = 1.41 \times 10^{-3}$$

From equation #23:

$$\frac{(\gamma_{Ca^{++}} m_{Ca^{++}})(\gamma_{CO_3^{''}} m_{CO_3^{''}})}{(\gamma_{CaCO_3\ soluble} m_{CaCO_3\ soluble})} = 1.48 \times 10^{-6}$$

$$\frac{(0.26 \times 1.41 \times 10^{-3})(0.021 \times 6.55 \times 10^{-4})}{(1.13 \times m_{CaCO_3\ soluble})} = 1.48 \times 10^{-6}$$

$$m_{CaCO_3\ soluble} = 2.98 \times 10^{-4}$$

Since:

$$(m_{Ca^{++}} + m_{CaCO_3\ soluble})(m_{CO_3^{''}}) = K' \qquad (7)$$

Substituting:

$$(1.41 \times 10^{-3} + 2.98 \times 10^{-4})(6.55 \times 10^{-4}) = 1.12 \times 10^{-6}$$

The listed value is 0.62×10^{-6}.

Figure 8 shows the good correspondence of the observed and calculated K' values, indicating that in spite of all the approximations necessary, the method is a valid one. Also, it is possible to calculate the change in K' at constant pH but with changing chlorinity, using

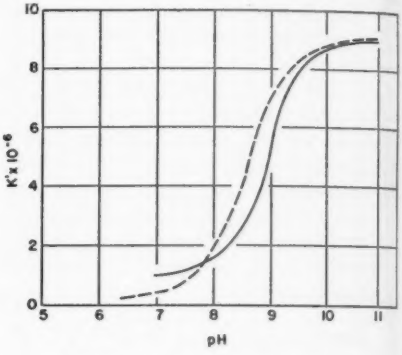

FIGURE 8.—COMPARISON OF CALCULATED AND EMPIRICAL VALUES FOR K' AS A FUNCTION OF pH

(---------- empirical values, Sverdrup; ——— calculated values, this paper).

similar methods, but using values of γ_i at the appropriate chlorinity. The empirical values given in Sverdrup *et al.* (p. 207) compare well with the calculated ones.

Temperature coefficient of activity coefficients.—The temperature coefficient of the activity coefficients must be known if calculations of solubility are to be made above or below 25°C. The temperature coefficients are quite small; γ_i changes a maximum of approximately 10 per cent at an ionic strength of 0.7 in the range 25–65°C. Figure 9 shows the change of $\gamma_{HCO_3^-}$ and $\gamma_{CO_3^{''}}$ with temperature and ionic strength. The values are calculated from the equation:

$$-\log \gamma_i = Az_i^2\sqrt{\mu}$$

Values of A for the various temperatures are from Manov *et al.*, 1943.

Calculation of calcium carbonate solubility at 0°C.: a check with previous determinations.—Now the temperature coefficients of all the important variables except $Ke_{CaCO_3\ soluble}$ are known, and it is possible, if it is assumed that $Ke_{CaCO_3\ soluble}$ has a small temperature coefficient, to calculate calcium carbonate solu-

bility at various temperatures, pressures, and ionic strengths. A partial justification of this assumption can be made by calculating K' at 0°C., and comparing it with the empirical value listed by Sverdrup *et al.* (p. 206). According to Sverdrup, K' at 25°C. in sea water of pH 7.4 is 5.5 × 10^{-7}, at 0° is 8.1 × 10^{-7}; the ratio is 1.47. The calculated value at 25°C. (this paper) is 11.2 × 10^{-7}. Accordingly, the next step is to calculate K' at 0°C. and to see how it compares with the empirical Sverdrup value.

TABLE 2.—CHLORINITY
(parts per thousand)

	5	10	15	20
Empirical K′ (Sverdrup)	1.8 × 10^{-7}	4 × 10^{-7}	5 × 10^{-7}	6.2 × 10^{-7}
Calculated K′ (This paper)	1.74 × 10^{-7}	3.5 × 10^{-7}	8.6 × 10^{-7}	11.2 × 10^{-7}

At 0°C.,

$$Ke_{CaCO_3} = 10^{-7.95}; \quad Ke_{HCO_3^-} = 10^{-10.75};$$

$$Ke_{H_2CO_3} = 10^{-6.61} \text{ (Table 1)}$$

Following the procedure outlined before:

$$\frac{(a_{H^+})(\gamma_{CO_3''} m_{CO_3''})}{(\gamma_{HCO_3^-} m_{HCO_3^-})} = 10^{-10.75}$$

Taking into consideration the small increase in γ_i values caused by this decrease in temperature (Fig. 9):

$$\frac{(a_{H^+})(0.022 \times m_{CO_3^-})}{(0.41 \times m_{HCO_3^-})} = 10^{-10.75}$$

$$\frac{m_{CO_3''}}{m_{HCO_3^-}} = \frac{0.41 \times 10^{-10.75}}{0.022 \times 10^{-7.40}} = 0.0083$$

Similarly:

$$\frac{(a_{H^+})(\gamma_{HCO_3^-} \times m_{HCO_3^-})}{(\gamma_{H_2CO_3} m_{H_2CO_3})} = 10^{-6.61}$$

$$\frac{(a_{H^+})(0.41 \times m_{HCO_3^-})}{(1.14 \times m_{H_2CO_3})} = 10^{-6.61}$$

$$\frac{m_{HCO_3^-}}{m_{H_2CO_3}} = \frac{1.14 \times 10^{-6.61}}{0.41 \times 10^{-7.4}}; \qquad \frac{m_{H_2CO_3}}{m_{HCO_3^-}} = 0.0583$$

Assuming, as before (equation #13), that the total carbon dioxide components in solution are 0.03 molal:

$$m_{HCO_3^-} + 0.0583 m_{HCO_3^-} + 0.0083 m_{HCO_3^-} = 0.030$$

$$m_{HCO_3^-} = 0.0282$$

$$m_{CO_3''} = 0.000234$$

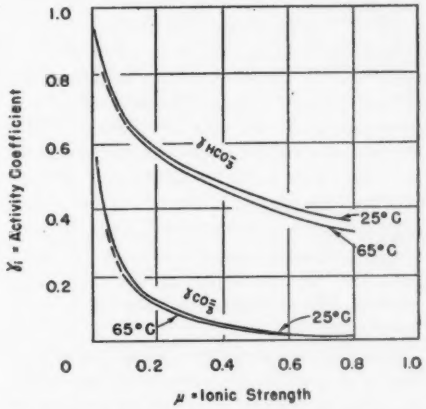

FIGURE 9.—EFFECT OF TEMPERATURE ON THE ACTIVITY COEFFICIENT OF BICARBONATE AND CARBONATE IONS

Then:

$$(\gamma_{Ca^{++}} m_{Ca^{++}})(\gamma_{CO_3''} m_{CO_3''}) = 10^{-7.95}$$

$$m_{Ca^{++}} = \frac{10^{-7.95}}{0.27 \times 0.022 \times 2.34 \times 10^{-4}}$$

$$= 7.2 \times 10^{-3}$$

Using the assumption that $Ke_{CaCO_3 \text{ soluble}}$ is unchanged:

$$\frac{(\gamma_{Ca^{++}} m_{Ca^{++}})(\gamma_{CO_3''} m_{CO_3''})}{(\gamma_{CaCO_3 \text{ soluble}} m_{CaCO_3 \text{ soluble}})} = 1.48 \times 10^{-8}$$

$$\frac{(0.27 \times 7.2 \times 10^{-3})(0.022 \times 2.34 \times 10^{-4})}{(1.14 \times m_{CaCO_3 \text{ soluble}})}$$

$$= 1.48 \times 10^{-8}$$

$$m_{CaCO_3 \text{ soluble}} = 5.9 \times 10^{-4}$$

Then, from equation #7:

$$(m_{Ca^{++}} + m_{CaCO_3\ soluble})(m_{CO_3''}) = K'$$

$$(7.2 \times 10^{-3} + 5.9 \times 10^{-4})(2.34 \times 10^{-4}) = 18 \times 10^{-7}$$

Consequently, the ratio of the calculated K' at 0°C. and that at 25°C. is:

$$\frac{18 \times 10^{-7}}{11.2 \times 10^{-7}} = 1.61$$

as compared with a ratio of the observed values of 1.47.

Although this is a fair check on the change in solubility with temperature, the check is at a pH where the major contribution to total calcium is from free calcium ion, and not from undissociated calcium carbonate. Consequently, although the amount of undissociated calcium carbonate could not have increased markedly without affecting this check calculation, it could have decreased to any smaller value without affecting the check. If the Sverdrup values were measured at a higher pH, then the contribution of undissociated $CaCO_3$ would have accounted for essentially all the calcium in solution, and a check calculation would have been unequivocal.

Discussion and summary.—It has been shown that it is possible to calculate values of the solubility of calcium carbonate that duplicate empirical results within relatively narrow limits. Changes in solubility with pH, added salts, and temperature have been investigated, and in each instance the calculated values change with these variables in the same manner as the empirical ones. The maximum difference between the calculated and the observed values comes at relatively low pH and at high salinity (Fig. 8, Table 2); here the calculated value of K' is approximately twice the observed value.

It is now possible to calculate solubilities at any temperature from 0° to 65°C., at any pressure up to 1000 bars, at concentration of added salts up to an ionic strength of 0.7, and over the entire pH range, at a given total CO_2 content of the system. Because of the many variables, there is no simple graphic method of representing the solubilities; a sample calculation must suffice to show the method of obtaining values.

Suppose that water in a formation has the following characteristics: pH, 7; Total Salt (μ), 0.6; Temperature, 45°C.; Pressure (Hydrostatic), 500 bars; Total CO_2, 0.001 molal. What is the solubility of $CaCO_3$?

The first step is to obtain values of the activity constants under these conditions. Table 1 lists values at 45°C. and at 1 bar pressure for an ionic strength of zero. The effect of a pressure of 500 bars in pure water at 25° is shown in Figure 1; Ke_{CaCO_3} is increased by a factor of 3; $Ke_{HCO_3^-}$ by a factor of 1.7; $Ke_{H_2CO_3}$ by a factor of 1.8. However, this solution contains salts sufficient to give an ionic strength of 0.6; the effect of these salts is to reduce the pressure effect (Fig. 3). Also, the pressure effect is less in a solution at 45° than in one at 25° (Fig. 2). The ratio of the pressure effect in a solution of ionic strength of 0.6 at 500 bars to that in pure water is *0.93*; the ratio of the pressure effect at 45° and 500 bars to that at 25° is *0.92*; both these effects decrease the pressure effect. Consequently, the equilibrium constants are decreased by these ratios; Ke_{CaCO_3} becomes:

$$0.93 \times 0.92 \times 3 \times 10^{-8.40} = 10.6 \times 10^{-9}$$

That for $Ke_{H_2CO_3}$ becomes:

$$0.93 \times 0.92 \times 1.8 \times 10^{-6.34} = 7 \times 10^{-7}$$

That for $Ke_{HCO_3^-}$ becomes:

$$0.93 \times 0.92 \times 1.7 \times 10^{-10.3} = 9.1 \times 10^{-11}$$

Decrease of the pressure effect with increased temperature and the presence of added salts is a minor effect; no serious error would result by ignoring them.

With known values of Ke, it is possible to calculate the molality of the various ions if the activity coefficients are known. The effect of ionic strength on γ_i values is shown in Figure 7; the effect of temperature on these values in Figure 9. The effect of a change from 25° to 45° can be ignored. Using values for an ionic strength of 0.6 from Figure 7 gives $\gamma_{Ca^{++}} = 0.26$; $\gamma_{CO_3''} = 0.028$; $\gamma_{H_2CO_3} = 1.10$; $\gamma_{HCO_3^-} = 0.41$; and $\gamma_{CaCO_3\ soluble} = 1.10$.

Then, using equation #9:

$$\frac{(a_{H^+})(\gamma_{CO_3''}\, m_{CO_3''})}{(\gamma_{HCO_3^-}\, m_{HCO_3^-})} = 9.1 \times 10^{-11}$$

Substituting:

$$\frac{m_{CO_3''}}{m_{HCO_3^-}} = \frac{9.1 \times 10^{-11} \times 0.41}{10^{-7} \times 0.028} = 0.0133$$

Similarly:

$$\frac{(a_{H^+})(\gamma_{HCO_3^-}\, m_{HCO_3^-})}{(\gamma_{H_2CO_3}\, m_{HCO_3^-})} = 7 \times 10^{-7}$$

Substituting:

$$\frac{m_{HCO_3^-}}{m_{H_2CO_3}} = \frac{7 \times 10^{-7} \times 1.10}{10^{-7} \times 0.41} = 18.8;$$

$$\frac{m_{H_2CO_3}}{m_{HCO_3^-}} = 0.053$$

Since total $CO_2 = 0.001$, then:

$$m_{HCO_3^-} + m_{CO_3''} + m_{H_2CO_3} = 0.001$$

Substituting:

$$m_{HCO_3^-} + 0.0133 m_{HCO_3^-} + 0.053 m_{HCO_3^-} = 0.001$$

$$m_{HCO_3^-} = 0.000943$$

$$m_{CO_3''} = 0.000943 \times 0.0133 = 12.5 \times 10^{-6}$$

Then $m_{Ca^{++}}$ can be obtained from equation #6:

$$(\gamma_{Ca^{++}} m_{Ca^{++}})(\gamma_{CO_3''} m_{CO_3''}) = Ke_{CaCO_3} = 10.6 \times 10^{-9}$$

Substituting:

$$m_{Ca^{++}} = \frac{10.6 \times 10^{-9}}{0.26 \times 0.028 \times 12.5 \times 10^{-6}} = 1.16 \times 10^{-1}$$

The amount of calcium tied up in the calcium carbonate complex can now be obtained from the equation #23:

$$\frac{(\gamma_{Ca^{++}}\, m_{Ca^{++}})(\gamma_{CO_3''}\, m_{CO_3''})}{(\gamma_{CaCO_3\ soluble}\, m_{CaCO_3\ soluble})} = Ke_{CaCO_3\ soluble}$$

We are not sure of the change of $Ke_{CaCO_3\text{-}soluble}$ with temperature and pressure, but if its behavior is at all comparable with the other constants investigated, it is unlikely that it is changed more than tenfold. Its value at 25° and 1 bar pressure is 1.48×10^{-5} (Equation #23). Using this value tentatively:

$$\frac{10.6 \times 10^{-9}}{1.10 \times m_{CaCO_3\ soluble}} = 1.48 \times 10^{-5}$$

$$m_{CaCO_3\ soluble} = 6.5 \times 10^{-4}$$

and the contribution from the complex is negligible, even for a large range in $Ke_{CaCO_3\text{-}soluble}$. Therefore, the solubility of calcium carbonate is almost entirely from free calcium ion, and is 1.16×10^{-1} mols per liter. It is

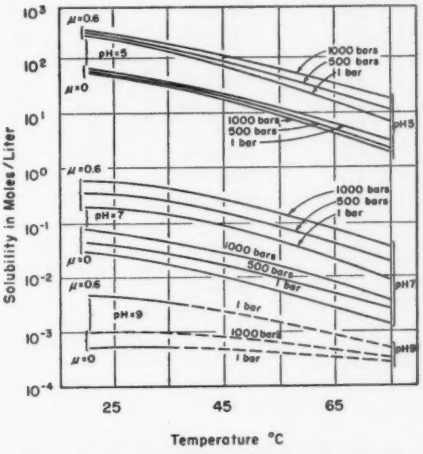

FIGURE 10.—EFFECT OF TEMPERATURE, PRESSURE, pH, AND SALINITY (μ) ON THE SOLUBILITY OF CALCIUM CARBONATE

The curves are calculated for a total CO_2 content of 0.001 mols per liter. The uncertainty indicated by the dashed lines at pH = 9 results from lack of knowledge of change of Ke_{CaCO_3} soluble with temperature and pressure.

difficult to assess the total magnitude of the errors involved, but at most, the solubility should not be greater than 1.5×10^{-1}, nor less than approximately 0.90×10^{-1} mols per liter.

Using this method, a graph has been made to show the change of calcium carbonate solubility with the major variables (Fig. 10). Since there are five such variables, it has been necessary to show their effects over a limited range. The equilibrium constants necessary for the calculation of the points on the graph are given in Table 3. The effect of change of CO_2 content, other factors remaining constant, is shown in Figure 11.

The overall relations can be summarized as follows:

1. Calcium carbonate solubility in natural solutions changes with five important variables: temperature, pressure, added salts, pH, and amount of total CO_2 in the solution.

TABLE 3.—EQUILIBRIUM CONSTANTS FOR CARBONATE EQUILIBRIA AS A FUNCTION OF TEMPERATURE, PRESSURE, AND IONIC STRENGTH

Temp. °C.	Pressure (bars)	Ionic Strength	$K_{e_{CaCO_3}}$	$K_{e_{HCO_3^-}}$	$K_{e_{H_2CO_3}}$
25°	1 bar	0	5.1×10^{-9}	3.2×10^{-11}	3.5×10^{-7}
25°	500 bars	0	1.5×10^{-8}	5.4×10^{-11}	6.2×10^{-7}
25°	1000 bars	0	4.1×10^{-8}	8.3×10^{-11}	1.1×10^{-6}
25°	1 bar	0.6	5.1×10^{-9}	3.2×10^{-11}	3.5×10^{-7}
25°	500 bars	0.6	1.4×10^{-8}	5.0×10^{-11}	5.8×10^{-7}
25°	1000 bars	0.6	3.4×10^{-8}	6.9×10^{-11}	9.2×10^{-7}
45°	1 bar	0	4.0×10^{-9}	6.3×10^{-11}	4.55×10^{-7}
45°	500 bars	0	1.1×10^{-8}	9.8×10^{-11}	7.5×10^{-7}
45°	1000 bars	0	2.8×10^{-8}	1.4×10^{-10}	1.2×10^{-6}
45°	1 bar	0.6	4.0×10^{-9}	6.3×10^{-11}	4.55×10^{-7}
45°	500 bars	0.6	1.02×10^{-8}	9.1×10^{-11}	7.0×10^{-7}
45°	1000 bars	0.6	2.4×10^{-8}	1.2×10^{-10}	1.1×10^{-6}
65°	1 bar	0	1.8×10^{-9}	1.1×10^{-10}	6.2×10^{-7}
65°	500 bars	0	4.6×10^{-9}	1.5×10^{-10}	9.3×10^{-7}
65°	1000 bars	0	1.0×10^{-8}	2.0×10^{-10}	1.4×10^{-6}
65°	1 bar	0.6	1.8×10^{-9}	1.1×10^{-10}	6.2×10^{-7}
65°	500 bars	0.6	3.8×10^{-9}	1.3×10^{-10}	7.8×10^{-7}
65°	1000 bars	0.6	8.7×10^{-9}	1.7×10^{-10}	1.2×10^{-6}

2. The effect of the variables is to a considerable extent independent; for example, the effect of 0.7 molal added salts changes the effect of 1000 bars pressure by about 20 per cent.

3. Solubility decreases with increase of temperature; with other factors constant, the effect of a change from 25° to 65° causes approximately a tenfold decrease in solubility. The general independence of the variables is shown by the fact that a similar change in temperature at a pressure of 1000 bars causes a change of almost exactly the same magnitude.

4. Solubility increases with increase in pressure; a hydrostatic pressure of 1000 bars causes approximately a threefold increase in solubility. Again this effect is almost the same at 25° as at 65°C.

5. Solubility increases with decreasing pH, and the effect is very marked. In acid solutions, the solubility increases 100-fold for each decrease of 1 pH unit; at pH values higher than seven, this effect diminishes, and a low (approximately 10^{-4} mols/liter) and nearly constant solubility is reached at pH of approximately 10. This "relict" solubility is apparently caused by the presence of undissociated $CaCO_3$.

6. Solubility increases with addition of salts to the solution. The effect of an ionic strength of 0.6 (such as a 0.6 m_{NaCl} solution) is to increase solubility by a factor of about six over that in pure water. Again this effect is nearly independent of other variables, although influenced somewhat by pH.

7. Solubility is strongly dependent upon the amount of dissolved CO_2, and is inversely proportional to it for small amounts of CO_2 under

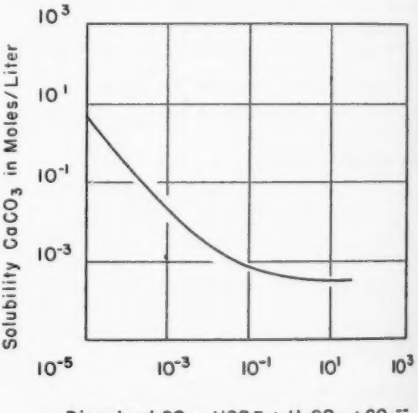

FIGURE 11.—SOLUBILITY OF CALCIUM CARBONATE AS A FUNCTION OF TOTAL CO_2 IN SOLUTION AT CONSTANT pH
The calculation has been made at a pH of 7 and a temperature of 25°C.

constant conditions. At a given pH, adding CO_2 increases the carbonate ion and decreases the amount of *free* calcium ion present. If pressure is sufficient, the amount of free calcium finally becomes so small that the solubility reaches a limiting value controlled by the amount of undissociated $CaCO_3$ present. The amount of undissociated $CaCO_3$ is independent of total CO_2. This general statement may seem contrary to the experimental fact that $CaCO_3$ solubility increases with increased CO_2 pressure; the apparent anomaly is explained if it is remembered that experimentally addition of CO_2 results in a decrease of pH, which is more effective in increasing solubility than the addition of more total carbon dioxide components. Nevertheless, at constant pH, increase of CO_2 will decrease solubility.

Solubility and Rate of Solution of Calcite

General Statement

The solubility of calcite is a measure of the amount that can be carried at equilibrium in a given environment; it is important now to know the rate at which this equilibrium is attained. To this end, a series of experiments was devised to measure the rate of solution over a wide range of solubilities, with pH and temperature as the controls.

Experimental Procedure

Cleavage rhombs of optical calcite were suspended in a slowly moving solution at constant temperature and pH. Solutions were made up with hydrochloric acid buffered with sodium acetate; pH was measured before and after each determination with a regularly calibrated Beckman type G pH meter. The calcite rhombs were weighed and the total area exposed to the solution determined before and after each run; from these measurements, the weight loss per square centimeter was calculated. The rate of flow of the solution past the rhombs was the same in each experiment; approximately 1 centimeter per second. The rhombs used were large enough to give accurate determinations of weight loss per unit area within a reasonable time without significant change in surface area, but still so small relative to the bulk of the solution that no measurable changes in solution characteristics resulted from the dissolving of the calcite. pH values, for example, were identical within the accuracy of the instrument before and after each run. Consequently, each run is a determination at constant solubility.

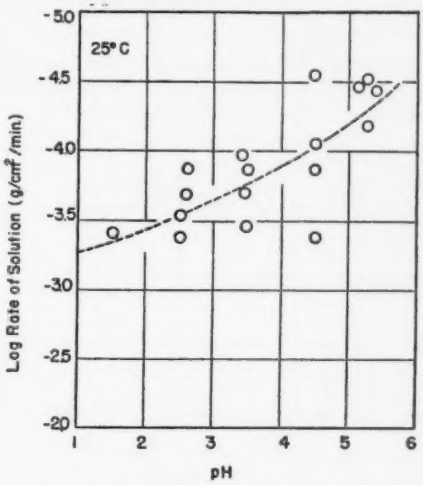

Figure 12.—Rate of Solution of Calcite in HCl Solution Buffered with Sodium Acetate
Rate of flow of solution equals 1 cm. per second. Open circles represent original data.

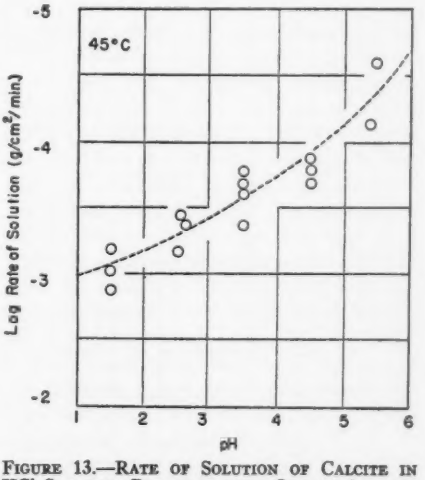

Figure 13.—Rate of Solution of Calcite in HCl Solution Buffered with Sodium Acetate
Rate of flow of solution equals 1 cm. per second. Open circles represent original data.

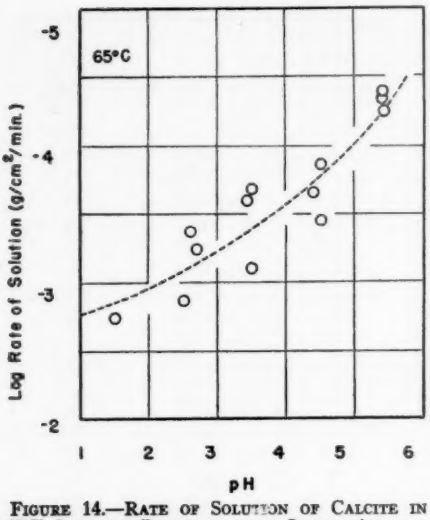

FIGURE 14.—RATE OF SOLUTION OF CALCITE IN HCl SOLUTION BUFFERED WITH SODIUM ACETATE
Rate of flow of solution equals 1 cm. per second. Open circles represent original data.

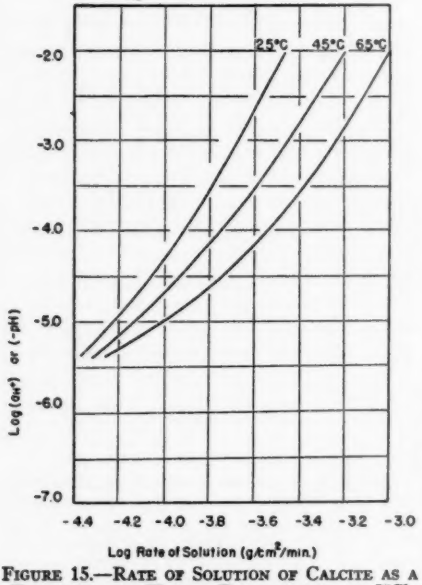

FIGURE 15.—RATE OF SOLUTION OF CALCITE AS A FUNCTION OF pH AND TEMPERATURE IN HCl SOLUTIONS BUFFERED WITH SODIUM ACETATE

Experimental Results

The results of the runs at 25°, 45°, and 65°C. are shown in Figures 12, 13, and 14. The wide scatter of the points can be attributed to erratic carbon dioxide bubble formation on the rhombs. The data are summarized in Figures 15 and 16. The solubilities plotted as

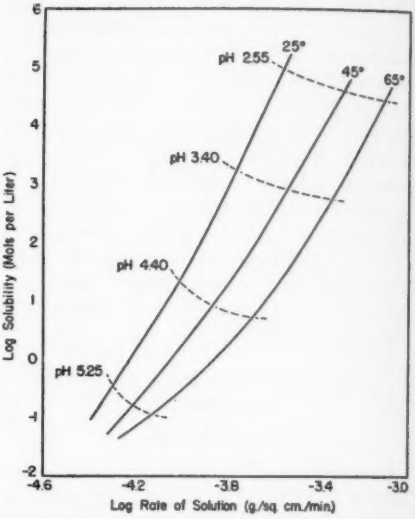

FIGURE 16.—RATE OF SOLUTION OF CALCITE AS A FUNCTION OF SOLUBILITY AND TEMPERATURE IN HCl SOLUTIONS BUFFERED WITH SODIUM ACETATE

ordinate in Figure 16 are calculated without taking into consideration the effect of the ionic strength of the acetate used as a buffer. The effect would be constant and small relative to the range of solubility involved. Corrected solubility values would be somewhat higher.

Discussion

The rate of solution of a substance is correlated roughly with its solubility; very broadly the greater the solubility, the higher the rate of solution. However, there are many and very striking exceptions to this rule. The data for calcite show that it behaves fairly consistently; the rate of solution increases with increasing solubility, although by a very small ratio compared to the increase in solubility. Also rate of solution shows an increase with increasing temperature at constant solubility, although the increase in rate is considerably less than the general rule that reaction rates double for each 10°C. rise in temperature.

These rates of solution are rates into a

medium containing essentially no calcium ion, and, furthermore, the characteristics of the solution did not change during the process. In nature such conditions might occur, as in the case where a stream flows across a patch of limestone, but only where the rate of renewal and removal of the reacting solution is very large compared to the changes occurring while it is in contact with the reacting surfaces. In most cases, as where a solution moves slowly through a limestone, the limestone is dissolving into a constantly changing medium. The rate of solution usually decreases because: (1) The ability of the solvent to hold calcium carbonate in solution is decreased as the dissolved calcium increases; and (2) pH of the solution increases as reaction continues.

These are separate effects. The first effect is exemplified by the dissolving of a nonreactive substance, such as common salt, in water. The rate of solution continually decreases as the medium becomes saturated. This effect is well demonstrated by Figure 17. Rate of solution is plotted against the term $\frac{So - S}{So}$, which is a measure of the departure of the solution from saturation. So is the solubility of salt in pure water, and S is its solubility in the partially saturated solution. Therefore, $So - S$ is a measure of the amount of salt that still can be dissolved, and $\frac{So - S}{So}$ is a convenient ratio showing a range from one in pure water to zero in a saturated solution. The rate of solution increases linearly with departure of the solution from saturation in a stirred solution, as exemplified by curves A and B, but the rate increases at an increasing rate without stirring (curve C).

This difference in behavior can be explained (Taylor, 1925, p. 942–947) on the assumption that rate of solution is controlled by rate of diffusion of ions or molecules of the solid into the solution. When a fragment of solid is placed in pure water, for example, it begins to dissolve, and a concentrated solution, saturated at the interface, forms at the solid surface. Further solution must take place by diffusion through this layer.

When the solution is stirred (in this case by spinning a cleavage fragment of halite), the solid is separated from the bulk of the solution by a very thin layer of fluid saturated at the surface of the crystal and grading regularly in concentration outward to the bulk of the solution. Reasonably constant conditions result,

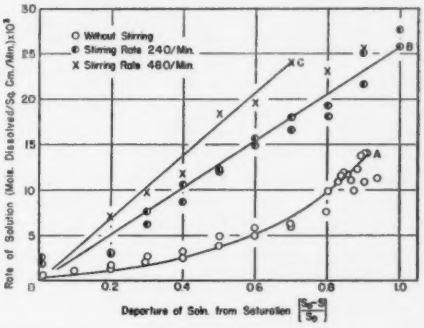

FIGURE 17.—RATE OF SOLUTION OF HALITE IN NaCl SOLUTIONS

with diffusion taking place through this fluid layer into the bulk of the solution.

An increase in stirring rate presumably thins this film of gradational composition, providing a steeper concentration gradient and consequent more rapid rate of solution. According to Taylor (p. 945), the rate of solution should increase with the 3/2 power of the stirring rate; this prediction is checked very closely by the experiments on halite (curves A and B).

The data shown by curve C were obtained by suspending a halite cube motionless in a beaker of solution. The halite began to dissolve, the solution at the solid-liquid interface became denser than the remainder of the solvent, and slid downward to start a convectional system. Under these conditions, the rate is controlled not only by the concentration gradient from crystal to solution, but by the speed of circulation set up by convection.

In nearly pure water, the density convection reaches its greatest speed, and the concentration difference between the saturated solution at the solid surface and the bulk of the solution is at a maximum. As a result of these two effects, both of which tend to increase the rate of solution as the solvent approaches pure water, the rate does not increase linearly, but at an increasing rate.

Consequently, the rates of solution of calcite

shown in Figure 16 or 17 represent a special case—the maximum rate of solution likely to be encountered in nature for the particular pH values or solubilities listed. They are the rates into flowing solutions of constant composition. When calcite dissolves in a stagnant solution, as one confined in rock pores, the rate progressively slows for two reasons. In the beginning, the concentration gradient, from the infinitely thin layer of saturated solution immediately at the crystal surface to the surrounding solution, is relatively great. As time goes on, a zone of high calcium concentration develops as the ions diffuse outward, and the gradient is reduced. Also, with the reaction between the solution and the calcite, the pH of the solution is increased, and the ability of the solution to hold calcite in solution is decreased. The rate of solution is decreased (1) as calcium goes into the solvent, and (2) as the solvent's ability to hold calcium is decreased by reaction.

The original rate is controlled chiefly by the pH, but the total amount of calcite that will dissolve in infinite time is, to a considerable extent, a function of the source of the hydrogen ions that react with the calcite. For example, a solution of pH 4 made up by adding hydrochloric acid to distilled water has almost no capacity for dissolving calcite; all the acid is ionized, and the 10^{-4} mols per liter of hydrogen ion soon react to equilibrium. If, on the other hand, the pH of 4 is the result of hydrolysis of a salt, such as copper or iron chloride, hydrogen ion used up by reaction is renewed as hydrolysis continues. In such cases, as will be seen later, the hydrolyzing salt usually is removed by precipitation, but the solution will continue to dissolve calcite until essentially all the salt is precipitated. Therefore, the ability of solutions to dissolve calcite depends to a considerable extent upon their action as buffers. Each solution can be considered to have a *potential* and a *capacity* for dissolving calcite. The *potential* is measured by the pH, and the *capacity* by total amount of hydrogen ion available for reaction. An unbuffered solution of low pH will react rapidly with calcite, but will dissolve very little; a heavily buffered solution of higher pH will react originally more slowly, will move toward equilibrium more slowly, dissolving much larger quantities of calcite.

Relative Rates of Solution of Calcite and Other Carbonates

A comprehensive study of the relative rates of solution of various carbonates has been made by Ferrari and Sessi (1937). The determinations were made at constant solubility in 8 per cent hydrochloric acid at 25°C. Some of their results are given in Table 4.

TABLE 4.—RELATIVE RATES OF SOLUTION OF VARIOUS CARBONATES

Carbonate	Relative Velocity of Solution
$CaCO_3$	100,000
$ZnCO_3$	6,500
$MnCO_3$	850
$(Mg, Fe)CaCO_3$	650
$FeCO_3$	570
$MgCO_3$	9

Ferrari and Sessi also have studied rate of solution of calcium carbonate as a function of temperature in the range 0°–40°C. They found that rate increases by a factor of approximately 1.8 for each 10°C. Their results for other carbonates were comparable. This checks fairly well with the results obtained in this study for calcium carbonate, in which the rate of solution was increased by a factor of about 1.5 for each 10° increase in temperature. The temperature coefficient of the rate of solution presumably is less than the coefficient for rates of reaction because of the role of diffusion processes in controlling rate of solution. It can be seen from our data (Fig. 15), that the temperature coefficient of rate of solution is somewhat dependent upon the pH, and decreases with increase in pH. Consequently, it seems that, if our experiments had been carried out in solutions as concentrated as those of Ferrari and Sessi, the temperature coefficient would have been approximately the same. The necessity for distinction between solubility and the rate of solution is emphasized by the data; whereas solubility decreases with increase in temperature, rate of solution increases (Fig. 16).

PRECIPITATION CURVES AND K_{sp} VALUES FOR ATACAMITE AND BROCHANTITE

Earlier work (Garrels and Stine, 1946) showed that the green products forming at

a calcite surface when copper sulfate or chloride solutions reacted with calcite were basic sulfates or chlorides, rather than the basic carbonates found in nature. It was hoped that a study of the stability of the basic copper chloride and sulfate would give a clue to the reasons for the absence of malachite, the expected product. Malachite is the common product under natural conditions, but many experiments over a considerable range of copper concentration failed to produce it by reaction at a calcite surface.

Accordingly, solutions of copper chloride and copper sulfate were made up over a wide range of concentration, and concentrated sodium hydroxide solution was added to each until a precipitate formed. The pH was measured at the time of precipitation and after a 24-hour interval, to assure that equilibrium was established (Figs. 18, 19).

From these curves it is possible to check the formula of the supposed product; to prove that the salts are true basic salts, in the sense that the hydroxyl has a place in the lattice comparable to that of the other ions; and to obtain a value for the solubility product constant K_{sp}.

For example, it was assumed that the green precipitate formed by addition of NaOH to copper chloride solution was atacamite, which has a formula listed as $Cu_4(OH)_6Cl_2$. If so, then the equation for its ionization is:

$$Cu_4(OH)_6Cl_2 = 4Cu^{++} + 6OH^- + 2Cl^- \quad (1)$$

and its classical solubility product constant:

$$(m_{Cu++})^4(m_{OH-})^6(m_{Cl-})^2 = K_{sp} \quad (2)$$

But because the original solution was made up solely of copper chloride:

$$CuCl_2 = Cu^{++} + 2Cl^- \quad (3)$$

Thus:

$$2m_{Cu++} = m_{Cl-} \quad (4)$$

Substituting in equation #2:

$$(m_{Cu++})^4(m_{OH-})^6(2m_{Cu++})^2 = K_{sp}$$

$$4(m_{Cu++})^6(m_{OH-})^6 = K_{sp}$$

Taking the logarithms:

$$\log 4 + 6 \log (m_{Cu++}) + 6 \log (m_{OH-}) = \log K_{sp}$$

$$\log (m_{Cu++}) = \frac{\log K_{sp}}{6} - \frac{\log 4}{6} - \log (m_{OH-})$$

Since, according to equation #3, $m_{Cu++} = m_{CuCl_2}$ or:

$$\log (m_{CuCl_2}) = \frac{\log K_{sp}}{6} - \frac{\log 4}{6} - \log (m_{OH^-}) \quad (5)$$

Therefore, a plot of *log* m_{CuCl_2} against *log* m_{OH-} should give a straight line with a 1:1

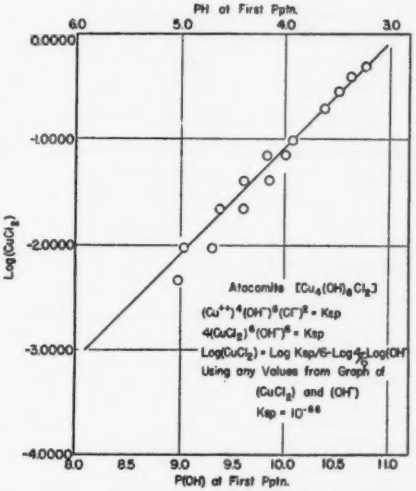

FIGURE 18.—PRECIPITATION—pH CURVE FOR ATACAMITE

slope. This prediction, based on the assumption that the precipitate is atacamite, checks with the observed relations of Figure 18.

Also, calculation of K_{sp} depends only on a knowledge of the concentration of copper chloride and the pH of precipitation, so it is readily calculated from the graph.

The argument for the composition and K_{sp} for brochantite is parallel to that for atacamite, and the essentials of the calculation are shown in Figure 19. Although the K_{sp} values are very small, they do not necessarily mean a small solubility of atacamite or brochantite, for K_{sp} has as one of its factors (m_{OH-}) to the sixth power, and m_{OH-} is very small in acid solutions.

Knowledge of the K_{sp} values makes it possible to calculate conditions under which the basic copper salts will precipitate, and also to calculate the completeness of precipitation.

For example, at a pH of 8, $(m_{OH^-})^6 = (10^{-6})^6 = 10^{-36}$, and since.

$$(m_{Cu^{++}})^4(m_{OH^-})^6(m_{Cl^-})^2 = 10^{-66}$$

$$(m_{Cu^{++}})^4(m_{Cl^-})^2 = \frac{10^{-66}}{10^{-36}} = 10^{-30}$$

So the product of $(m_{Cu^{++}})^4$ and $(m_{Cl^-})^2$ cannot be greater than 10^{-30}. Even if the original

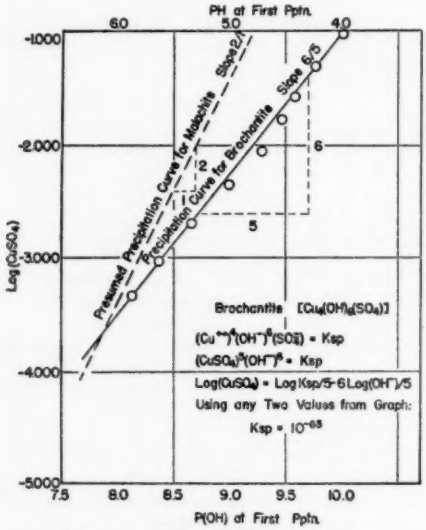

FIGURE 19.—PRECIPITATION—pH CURVE FOR BROCHANTITE

m_{Cl^-} is as small as 10^{-5}, $m_{Cu^{++}}$ cannot be greater than about 10^{-5} and precipitation of copper is essentially complete.

Precipitations of atacamite and brochantite were carried out at 35° and 45°C., but the curves are not shown, for they are essentially identical to those at 25°C., showing that the temperature coefficient of the K_{sp} values is negligible.

APPLICATION OF PRECIPITATION CURVES FOR ATACAMITE AND BROCHANTITE TO THE MALACHITE PROBLEM

If the concentration—pH curves for the precipitation of atacamite and brochantite are known, it is possible to give a reasonable explanation of the formation of these two salts, in preference to malachite, when copper solutions react at a calcite surface. A copper sulfate solution is acid because of hydrolysis:

$$\begin{array}{ccccc} CuSO_4 & \rightleftharpoons & Cu^{++} & + & SO_4'' \\ & & + & & + \\ 2H_2O & \rightleftharpoons & 2OH^- & & 2H^+ \\ & & \downarrow\uparrow & & \downarrow\uparrow \\ & & Cu(OH)_2 & & H_2SO_4 \end{array}$$

When a piece of calcite is placed in solution, it begins to dissolve, and the excess hydrogen ions of the solution react with the carbonate ions from the calcite. Undoubtedly an equilibrium is reached among carbonate ions, bicarbonate ions, and carbonic acid. The reaction thus reduces the hydrogen ion concentration at the solid surface; there, in addition to others, are hydrogen ions, hydroxyl ions, carbonate ions, copper ions, and sulfate ions. The experimental results indicate that the K_{sp} value of brochantite is exceeded, whereas that of malachite is not. Thus the result at the calcite surface is similar to the effect of adding sodium hydroxide to the copper sulfate solution; an insoluble copper hydroxy-sulfate is formed.

Apparently, in these experiments, the concentration of carbonate ion is not sufficient to force the formation of the copper hydroxy-carbonate in preference to the basic sulfate. This conclusion was corroborated by saturating copper sulfate solutions with CO_2, and then adding sodium hydroxide; as before the basic sulfate precipitated.

Under what conditions, then, does malachite form? It was suspected that, in very dilute copper sulfate solutions, the sulfate ion concentration might be so small that there would be a chance for formation of the basic carbonate. This is corroborated by an analysis of the slope expected of a malachite precipitation curve. The formula for malachite is $Cu_2(CO_3)(OH)_2$; its K_{sp} should be:

$$(m_{Cu^{++}})^2(m_{CO_3''})(m_{OH^-})^2 = K_{sp}$$

The slope of the precipitation curve can be predicted if a relation can be found between $m_{CO_3''}$ and m_{OH^-}.

In these solutions, carbon dioxide is released by reaction of the solution with the calcite, so the solution is saturated with CO_2:

$$m_{H_2CO_3} + m_{CO_3''} + m_{HCO_3^-} = 0.03$$

If we solve for $m_{CO_3''}$ at various pH values, as has been done, the relation is obtained for pH values of 3, 4, and 5, where essentially all the CO_2 is in the form of H_2CO_3:

$$m_{CO_3''} \alpha \frac{1}{(m_{H+})^2}$$

or, since the activity product of water must be satisfied:

$$m_{CO_3''} \alpha (m_{OH-})^2$$

or:

$$m_{CO_3''} = k(m_{OH-})^2$$

Substituting in equation #2:

$$(m_{Cu++})^2 (m_{OH-})^2 k(m_{OH-})^2 = K_{sp}$$

$$(m_{Cu++})^2 (m_{OH-})^4 = \frac{K_{sp}}{k} = k'$$

Taking logs of both sides:

$$2 \log m_{Cu++} + 4 \log m_{OH-} = \log k'$$

$$\log m_{Cu++} = \frac{\log k'}{2} - 2 \log m_{OH-}$$

Thus, a plot of log m_{Cu++} against log m_{OH-} should give a straight line with a slope of 2. Such a precipitation curve would tend to intersect the brochantite curve at low concentrations of the copper salt, as indicated by the hypothetical curve in Figure 19. This development subtantiates the suspicion that malachite might form in solutions of low copper content—comparable to those found in nature.

Attempts were made to form malachite from solutions of copper sulfate of $10^{-3.5}$ molal and less, but, at such low concentration, the rate of reaction with the calcite was so low, and the amount of precipitate so small, that it was very difficult to make a positive identification of the precipitate. Several particles of precipitate, formed at a calcite surface from a solution of $10^{-3.7}$ molal copper sulfate were observed under the microscope to effervesce strongly when treated with hydrochloric acid, and presumably were malachite. This evidence is the basis for the position chosen for the intersection of the brochantite—malachite curves in Figure 19.

Consequently, low concentrations of copper sulfate might favor the primary formation of malachite. Brochantite should form in solutions saturated with CO_2 at concentrations of about 10^{-3} molal copper sulfate or more. With solutions undersaturated with CO_2, brochantite might form at concentrations lower than 10^{-3} molal.

It seems quite possible, however, that primary brochantite may be altered to malachite by reaction with carbonate waters deficient in copper. It is significant, nevertheless, that such brochantite relics are not commonly found. Of the many malachite samples dissolved in acid, none gave test for sulfate ion. In summary, the evidence indicates that most supergene solutions derived from the weathering of primary copper sulfides contain less than 0.001 mols of copper ion per liter.

Petrography of Synthetic Replacements

The laboratory synthesis of replacement cannot provide more than a first approximation to the natural process. Laboratory replacements are made within inert containers by allowing one or, at most, a very few ions to react with one wall rock at constant temperatures and pressures. A natural solution not only reacts with its natural container, but also varies in composition, temperature, and pressure as it moves through a changing physical and chemical environment. It was decided to attempt to simulate what seemed to be the simplest type of natural replacement. The replacement of limestone by supergene type copper solutions provided the opportunity to study the effect of one common metallic ion on a common and essentially monominerallic rock at known low temperatures and pressures.

As the simplest approach to the problem of supergene copper replacement of limestone, a study was made of replacement resulting from reaction of dilute solutions of copper salts with calcite rhombs at low temperatures and atmospheric pressures.

In an earlier paper (Garrels, Dreyer, and Howland, 1949), we investigated the diffusion of ions through rocks. The major conclusions are summarized here. (1) The rate of diffusion of a given concentration front on nonreacting ions is independent of the porosity and permeability of the rock. The amount of diffusion is a linear function of the effective porosity so that there is a relatively small range in the

amount which will diffuse through the most and least porous rocks as opposed to the vastly greater range in the amount transferred by mass movement of solution. (2) The rate of diffusion increases with temperature. (3) Over a sufficient, but geologically reasonable, period of time, ions can diffuse great distances through rocks. (4) Large quantities of a material can diffuse through rocks only under conditions approximating steady-state diffusion. Steady-state diffusion can be expected during replacement.

The calcite rhombs were suspended from the "c" axis in various dilute copper solutions at known low temperatures and at atmospheric pressures. Each rhomb to be studied petrographically was suspended in copper-bearing solutions ranging from $0.1M$–$0.65M$, and at a temperature of 55°C. for an hour. Further details of this experiment are provided in an earlier paper (Garrels and Stine, 1947). As a result of reaction between the calcite and copper chloride solution, a green replacement layer formed on the rhombohedral surfaces. Although the replacement product expected was malachite, all of the replacement layers were formed by the basic copper chloride, atacamite ($Cu_4OH_6Cl_2$). Electron photomicrographs (Garrels and Stine, 1947, p. 24–25) indicate that the atacamite is very fine-grained—individual crystals reaching only a few microns in diameter. Data presented later indicate that prolonged aging at room temperature does not materially increase the crystal size. The reason for the formation of atacamite (or, in the case of sulfate solutions, of brochantite) is considered in a preceding section.

Table 5 gives data for the replacement of calcite rhombs by atacamite. Were the replacement process a molecular interchange, the

TABLE 5.—TYPICAL RESULTS OF CALCITE REPLACEMENT IN COPPER CHLORIDE SOLUTION

Sample Number	97	99	102	103	105	107
Concentration (Mols/liter)	0.15	0.35	0.45	0.1	0.25	0.65
Time (Hours)	1	1	1	1	1	1
Temperature (°C.)	55°	55°	55°	55°	55°	55°
Original Weight Calcite Rhomb (mg.)	48.8	44.6	56.7	61.6	54.4	60.6
Surface Calcite (in Sq. Cm.)	.44	.413	.483	.511	.472	.505
Weight after Run (mg.)	48.9	45.1	57.2	61.7	55.0	61.3
Weight after Solution Atacamite in NH_4OH (mg.)	47.7	43.7	55.5	60.9	53.1	58.0
Dissolved Calcite (Relative Mols)	1.1	0.9	1.2	0.7	1.3	2.6
Added Atacamite (Relative Mols)	1.2	1.4	1.7	0.8	1.9	3.3
Ratio Added: Dissolved	1.09	1.55	1.42	1.14	1.46	1.27

PLATE 1.—PHOTOMICROGRAPHS

FIGURE 1. ATACAMITE REPLACEMENT LAYER ON CALCITE RHOMB
Note sharpness and thinness of layer. × 50.

FIGURE 2. ATACAMITE PENETRATING ALONG CALCITE CLEAVAGE PLANES (× 50)

FIGURE 3. ENLARGEMENT OF FIGURE 21 SHOWING ATACAMITE REPLACING OUTWARD FROM CLEAVAGE PLANES (× 200)

FIGURE 4. ATACAMITE REPLACEMENT LAYER ON PERMEABLE CHALK
Note thinness of layer formed after maximum replacement and sharpness of contact as well as thinning over crystalline microfossils. × 50.

FIGURE 5. ATACAMITE REPLACEMENT LAYER ON CHALK
Note thinning of layer over crystalline areas. × 50.

FIGURE 6. ATACAMITE REPLACEMENT LAYER ON CHALK SHOWING CLEAN BREAK FROM UNREPLACED ROCK (× 50)

FIGURE 7. ATACAMITE REPLACEMENT LAYERS CORRODING CORNER OF CHALK CUBE. (× 50)

FIGURE 1

FIGURE 2

FIGURE 3

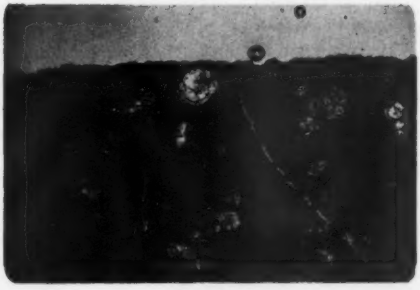

FIGURE 4

FIGURE 5

FIGURE 6

FIGURE 7

PHOTOMICROGRAPHS

ratio of the weight of atacamite added to the weight of calcite dissolved should be approximately 4.3:1. If the replacement is volume-for-volume, the ratio of weight of atacamite added to weight of calcite dissolved should be 1.39:1. Table 5 indicates that the ratio varies from 1.09 to 1.55 with an average of 1.32—showing that the replacement is very nearly volume-for-volume. The ratio of atacamite formed to calcite dissolved is probably slightly greater than 1.39:1 for all the replacements, because a small amount of colloidal sloughing was noted in many of the experiments.

Although the atacamite layer was known to form by replacement, the atacamite-calcite contact was very sharp (Pl. 1, fig. 1). If the process of formation of the atacamite layer had not been known, it would have been assumed that the atacamite was a crustification rather than a replacement. Moreover, the replacement layer, like a crustification, breaks cleanly from the unreplaced calcite. The corroded rhombohedral corners furnish the best evidence of replacement.

After the atacamite replacement layer reached an average thickness of 0.05 mm (0.006–0.1 mm), there was no further replacement of the calcite regardless of the concentration of the solution or of the period of time during which the calcite was left in the copper solution. Only at places where the solutions moved inward along cleavage planes (Pl. 1, figs. 2, 3) was there any penetration beyond this thin surficial barrier layer.

It was thought possible that the formation of thin replacement rims on calcite rhombs might be a function of the lack of porosity of the atacamite layer formed on crystalline calcite. Similar experiments were, therefore, performed on 1 cm. cubes of porous and permeable limestones and chalk. The initial tests were run at atmospheric pressure. Temperature ranged from 35° to 75°C.; concentration of copper chloride from 0.001*M* to 0.5*M*; and time of exposure of cubes to copper solutions from 1 to 40 hours. The reactions were tested on both dry and water-saturated cubes. The resulting replacements on the dry and water-saturated cubes were identical and were essentially volume-for-volume. Here again, after the atacamite replacement layer reached an average thickness of 0.08 mm. (0.008–0.2 mm) there was no further replacement by the copper-bearing solutions—even when the very porous and permeable chalk was placed in solutions for long periods of time. Thus, even though a rock was very porous, the replacement deposit acted as a sealing agent to prevent more than a thin surficial replacement.

Within the narrow limits given above, the thickness of the surficial replacement layer and the sharpness of the contact are a function of porosity. Thus, in the chalk, there are a number of micro-fossils composed of crystalline calcite. Where these fossils formed a portion of the surface of the chalk cube, the atacamite layer was much thinner and the contact much sharper than over the adjacent chalk (Pl. 1, figs. 4, 5). The contact between carbonate and atacamite on chalk is slightly less sharp than that on limestone although, even with chalk, the contact looks more like crustification than replacement and the atacamite breaks cleanly from the chalk and limestone (Pl. 1, fig. 6). The transition between pure atacamite and unreplaced carbonate is only 0.002–0.004 mm. wide. Here again, the corrosion of corners (Pl. 1, fig. 7) is better evidence of replacement than the sharpness of the contact.

In all these experiments, copper solutions were reacted with calcite in such a way that the pH of the system was changed very little as a result of the reaction. In a sense, the system can be said to have been flooded with solution. The amount of atacamite (or brochantite) deposited was slightly in excess of the volume of calcium carbonate dissolved. The solutions were acid as a result of the hydrolysis of the copper salts; they were neutralized at the calcium carbonate surfaces, with attendant precipitation of the basic copper salts. As each cubic micron of calcite dissolved, an equal or slightly larger volume of basic salt precipitated, thereby duplicating the texture of the material being replaced. It is evident that reaction cannot be expected to continue if calcite is the host. Although the original film of copper compound may have a very slight porosity, the interstices become plugged by further precipitation. When the host is chalk or limestone, the process continues a little longer, for the copper compound can fill not only the space made available by solution of calcium carbonate, but the original pore spaces as well.

This particular type of replacement, therefore, can be called "replacement in which guest is in excess of host." The result is a thin sharply bounded replacing layer.

A test was made of the accuracy of this conclusion by powdering calcite and allowing a very dilute solution of copper sulfate to diffuse into it. It was predicted that, in this case where the porosity was very high, the excess in volume of the copper salt formed over the calcium carbonate dissolved would not be sufficient to replace the calcite, and fill the interstices as well. The prediction was justified. Over a 3-week period, it was found that replacement of the calcite took place to a depth of slightly more than a centimeter. The same result can be achieved by adding excess free acid to a more concentrated copper chloride or copper sulfate solution. With very large concentrations of free acid, the excess of solution over precipitation is so great that a cavernous texture with irregular crusts of basic copper salt results. With intermediate amounts, the precipitation is continuous and yields good textural duplication. Every gradation can be observed between almost instantaneous clogging, when the volume of host precipitated markedly exceeds the original volume of host plus pore space, to the development of cavernous crustified masses, when conditions are arranged so that the rate of solution of the host is far in excess of the rate of precipitation of the guest.

In an earlier paper (Garrels, Dreyer, Howland, 1949), we demonstrated the ability of ions to diffuse long distances through rocks. An elaboration of these data is presented subsequently as related to the roles of porosity and permeability in mineral deposition. Rove (1947) and Brown (1947) stress the importance of secondary openings as affording primary avenues of access for the mass movement of mineralizing solutions. It is further evident that wall rock replacement outward from secondary openings can be effected only by (1) mass movement of solution at elevated pressure or (2) ionic diffusion.

Replacement under Pressure

Data recorded in the preceding section show the type of replacement resulting from ionic diffusion at atmospheric pressure. This section will discuss the efficacy of mass movement of solution under forced flow as an agency of replacement.

Cores of limestones, 1 cm in diameter and 1 cm long, with different permeabilities, were mounted in plastic tubes. Replacing solutions were forced through the rock by nitrogen under pressures up to 15 pounds/sq. in. Cores were tested for rate of transmitted flow of liquid first with water and then with copper chloride solutions. In limestones of low permeability, the flow of both water and copper chloride solution was so slight that irregularities of flow resulting from leakage at the tube-rock contact made the interpretation of results impossible. A limestone of high permeability (approximately 14 millidarcies) was therefore chosen for systematic treatment. In Figure 20, cumulative flow is plotted against time for both water and a 0.5*M* solution of copper chloride under a differential pressure of 5 lbs/sq. in. The flow of the copper chloride falls off steadily. The rate at zero time is shown by the dashed line. Here again, as in the case of replacement effected by ionic diffusion at atmospheric pressure, the precipitation of replacing mineral from solution gradually decreases the volume of flow and hence the further replacement. The results for a similar solution under a differential pressure of 15 lbs/sq. in. are shown in Figure 21. The flow, and hence the replacement process, continues at a measurable rate for a longer

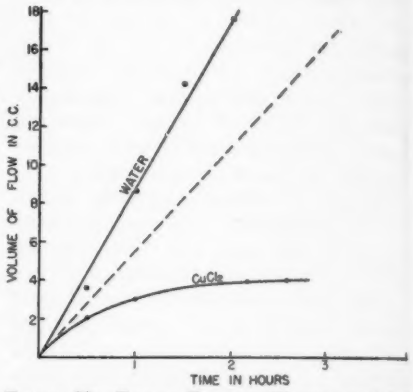

Figure 20.—Forced Flow of Water and 0.5M $CuCl_2$ Solution Through Limestone at 5 lbs./sq. inch

period of time. When pressures were increased from 2 to 10 pounds and 10 to 15 pounds on the same run (Fig. 22), volume of flow increased with each increase in pressure.

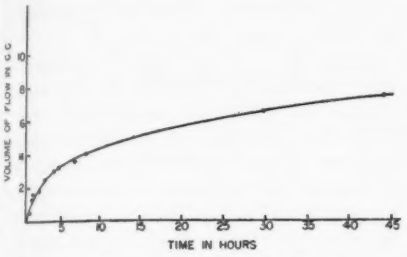

FIGURE 21.—FORCED FLOW OF 0.5M $CuCl_2$ SOLUTION THROUGH LIMESTONE AT 15 LBS./SQ. INCH

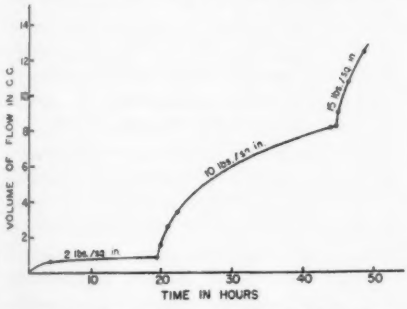

FIGURE 22.—FORCED FLOW OF 0.5M $CuCl_2$ SOLUTION THROUGH LIMESTONE WITH INCREASING PRESSURE

With a more dilute solution (Fig. 23), flow decreased much more slowly owing to less rapid sealing of open spaces by the precipitating copper salt.

The solution that emerged from the cores was entirely spent; it always had a pH of approximately 7.5. At this pH, the copper content is reduced almost to zero, and the solution has no capacity for dissolving more calcite. It follows that the amount of basic copper salt deposited in the limestone can be calculated from the amount of solution transmitted, and is directly proportional to the amount of solution for any given original concentration of solution. The same general relation holds for amount of calcite dissolved.

The total amount of copper salt precipitated is approximately a linear function of the pressure applied (Fig. 22). More accurately, it is a function of the pressure gradient. Although the pressures used were not high, compared with those expected in nature, the pressure

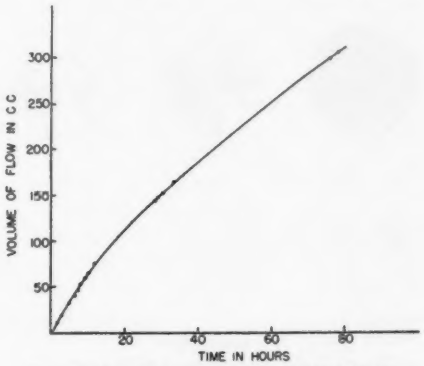

FIGURE 23.—FORCED FLOW OF 0.05M $CuCl_2$ SOLUTION THROUGH LIMESTONE AT 10 LBS./SQ. INCH

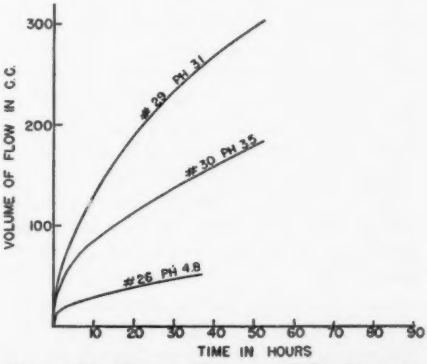

FIGURE 24.—FORCED FLOW OF $FeCl_2$ SOLUTION THROUGH LIMESTONE AT 10 LBS./SQ. INCH AND VARIOUS CONCENTRATIONS

gradient was extreme. A gradient of 15 pounds per square inch per centimeter (core length) is probably almost unknown in nature, for it would correspond to a pressure of 1000 atmospheres in one fissure, as opposed to a pressure of one atmosphere in another parallel fissure 35 feet away.

In the diffusion experiments, reaction stopped after the formation of a thin nonporous layer. In these forced flow experiments, the effect of pressure was apparently sufficient to break

through the layer mechanically and to push precipitated material along those avenues of easier solution flow, resulting in further reaction along such channels and the formation of a very irregular replacement front controlled by high permeability channels. The mechanism of reaction apparently is the same; the hydrolyzed acid copper solution is neutralized at calcium carbonate surfaces, and an amount of basic copper salt precipitated slightly in excess of the calcium carbonate dissolved, resulting in eventual clogging and removal of all porosity.

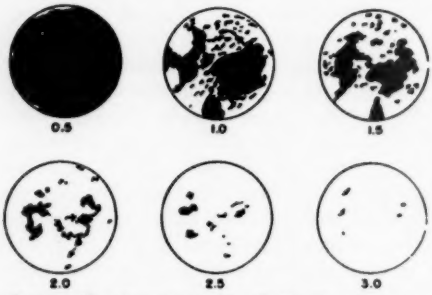

FIGURE 25.—SECTIONS OF A CORE REPLACED BY ATACAMITE (DARK)

Formed from 0.5M copper chloride solution acting on limestone at pressure of 10 lbs./sq. inch for 78 hours. Sections taken at 0.5 mm. intervals.

Experiments with ferrous chloride show an extremely important relation: the ratio of guest precipitated to host dissolved does not necessarily remain constant during the neutralization process. Figure 24 shows the results of a series of runs using different concentrations of ferrous chloride, and hence solutions of different original reaction rate with calcite. The highly acid solution replaced much more limestone before clogging than did the weaker one. Not only was more iron precipitated from each cubic centimeter of solution, but many more cubic centimeters passed through before clogging ensued. These experiments emphasize that replacement will eventually stop if the ratio volume of guest precipitated/volume of host dissolved is greater than unity, and the amount of replacement depends only on the ratio, and not at all upon the actual concentrations or rates of reaction. In the neutralization of the concentrated iron solutions, it must be assumed that the ratio above is nearly unity; in the less concentrated solutions, the ratio is markedly larger. Such a relation is to be expected; there is no *a priori* reason to assume that the pH of a hydrolyzed salt solution should change in such a way with concentration as to yield an exactly linear relation with its ability to dissolve calcium carbonate.

In the case of copper salts, the amount of basic copper salt precipitated from dilute solutions before replacement ceases shows a rough equivalence with that from more concentrated solutions; this must be ascribed to coincidence. In nature, various types of behavior may be expected: from solutions that precipitate an excess of guest over host dissolved in the pH range from three to four and a deficiency in the range from six to seven to those of exactly contrary behavior.

A greater volume of solution penetrates a limestone under forced flow than with simple diffusion before mineral precipitation seals the rock against further penetration. It therefore follows, as a corollary, that there must be a greater amount of replacement and hence a greater penetration of the replacing mineral. There is no sharply bounded dense barrier replacement layer formed under forced flow as is the case during diffusion at atmospheric pressures. Under pressures up to 15 pounds, the form of the replacing layer is rather irregular with a relatively wide transition zone between completely replaced and unreplaced limestone. Figure 25 shows sections of a core replaced by atacamite formed from 0.5 *M*. copper chloride solution acting on limestone at pressures of 10 lbs./sq. in. for 78 hours. The core was sectioned at 0.5 mm intervals and shows a rather irregular penetration averaging 3 mm. Under 15 pounds pressure, a replacement layer 5 mm. thick was formed in 48 hours. It is also noticeable that, under pressure, the coarse and finely crystalline portions of the limestone are replaced with equal ease, although in both cases significant replacement occurs only after available open spaces have been filled by the precipitating mineral.

The efficiency of mass movement of solution in replacement increases with applied pressure although, if guest exceeds host, there must be a continual decrease in the flow of solution after a finite replacement.

Natural Copper Mineral Replacements

As a type example of replacement at atmospheric temperatures and pressures by relatively simple solutions in a mono-minerallic rock, natural examples of supergene copper mineralization in limestone were studied. During the course of the collecting, it became apparent that in some cases it would be desirable not to limit the collection to limestone replacements. Collections were made from several areas including Jerome, Tintic, Bisbee, Morenci, and several small mines around Tucson.

One of the best examples of replacement under surficial conditions is furnished by an occurrence of oxidized copper minerals in Recent canyon gravels directly downstream from the main ore body at Jerome, Arizona. These gravels form the bed of a small canyon and consist of large, angular, poorly sorted pebbles and cobbles of limestone, dolomite, and volcanics. The introduced copper minerals were formed, presumably, from sulphate solutions moving down the stream bed from the main sulphide ore body, although no copper chloride or sulphate minerals are present. The introduced copper minerals consist of malachite and chrysocolla with minor amounts of azurite. It was not until the open spaces (pores and fractures) had been filled that any significant replacement occurred. The first replacement started in the carbonate cement and then moved outward into carbonate pebbles (Pl. 2, figs. 1–4). The replacement layer on many carbonate pebbles is chrysocolla, not malachite. The anion of the replaced rock is thus not always instrumental in determining the anion of the replacing supergene mineral. The replacement of carbonate rocks by chrysocolla was found to occur in many areas (Pl. 2, figs. 5, 6). The formation of a chrysocolla replacement layer several millimeters thick in the absence of forced flow indicates solution of calcite in excess of chrysocolla precipitated.

Any minute opening will provide a channel from which replacement can be initiated. Figure 7 of Plate 2 (from the Desert Tungsten Mine, Tintic, Utah) shows malachite replacement penetrating outward from rhombohedral calcite cleavage planes. The intricacy of a typical micro-vein system is illustrated by Figure 8 of Plate 2, showing chalcedonic veinlets from the Desrte Tungsten Mine. Not only are the micro-vein systems intricate, but, in the case of oxidized copper minerals, the resulting vein fillings are complex. Figure 1 of Plate 3 shows a micro-vein system from the Mineral Hill area, Pima county, Arizona. The veins and bordering replacement zones consist of an intimate intergrowth of malachite and chrysocolla. This intimate intergrowth of chrysocolla and malachite is a common feature of supergene copper mineralization. Figure 2 of Plate 3 shows two generations of malachite with a central core of chrysocolla in a specimen from the Daylight Mine, Helvetia District, Pima County, Arizona. This intergrowth must reflect a delicate balance between carbonate and silicate anions in the copper-bearing solutions and, very likely, a pH control.

It has been noted that no basic copper sulphate or chloride minerals were found in the Jerome gravels although, when the solutions left the ore body, they must certainly have been in the form of copper sulphate. The absence of sulphates and chlorides is also characteristic of most of the other supergene copper replacement zones in limestones. This absence of copper sulphate is especially surprising since, when solutions of concentration greater than $10^{-3.5}$ M were reacted with limestones in the laboratory, the basic sulphate—not the carbonate—replaced the limestone. The presence of malachite as a common replacement product in limestones indicates that the supergene mineralizing solutions probably were very dilute in composition.

The optical properties and chemical composition of chrysocolla vary widely. The mineral commonly occurs in bands showing varying intensity of blue-green coloration. The bands commonly are intimately associated with chalcedony (Pl. 3, figs. 3, 4, 5). In thin section, the color ranges from black through blue-green to a typical chalcedony with only a slight greenish tinge. The birefringence increases with increasing color.

Table 6 gives analyses of ten typical chrysocollas. The break in the table separates green chrysocolla above from black chrysocolla (below). (Incidentally, it is our impression that much black chrysocolla has, in the field, been incorrectly called tenorite.) It is apparent that

the black color is caused by manganese oxide. However, none of the chrysocolla analyzed has the same composition and none has the percentages of copper oxide, silica, and water required by the commonly assigned composition—$CuSiO_3 \cdot 2H_2O$ (CuO 45.2%, SiO_2 34.3%, H_2O 20.5%). An X-Ray examination by Charles Milton and Joseph Axelrod gave indefinite results (personal communication). The chrysocolla occurs in some places in gradational bands (Pl. 3, fig. 6) in which the color grades from blue-green to nearly colorless and in which the optical properties grade from those of chrysocolla to those of chalcedony. This gradation from chrysocolla toward chalcedony would suggest that chrysocolla, rather than being a distinct mineral, might be a solution of copper salt trapped during deposition in a silica gel. There is, however, a major impediment to this interpretation: in all of the chrysocolla tested, there is no anion other than silicate. It is possible, however, that chrysocolla, as commonly found, may be a solution of copper silicate in silica.

TABLE 6.—ANALYSES OF CHRYSOCOLLA*

Sample	SiO_2	Al_2O_3	Fe_2O_3	R_2O_3	MnO	CuO	CaO	MgO	H_2O	Total
201	45.76	N.D.	N.D.	N.D.	N.D.	45.81	N.D.	N.D.	7.32	98.9
Mor-1	45.49	—	—	1.65	N.D.	42.36	N.D.	N.D.	7.74	97.25
Mor-3	53.03	N.D.	N.D.	N.D.	N.D.	34.02	N.D.	N.D.	10.46	97.5
Mor-13	52.61	N.D.	N.D.	N.D.	N.D.	35.91	N.D.	N.D.	9.38	97.4
Mor-24	48.82	N.D.	N.D.	N.D.	N.D.	38.92	N.D.	N.D.	9.56	97.3
Jer-10B	42.39	—	—	3.88	1.24	34.26	0.87	0.31	12.90	95.85
1001-G	42.45	7.83	0.28	—	0.79	33.07	N.D.	N.D.	12.90	97.3
1001-B	35.42	11.61	3.18	—	6.40	26.64	1.49	0.41	13.05	98.2
Mor-31	44.79	—	—	9.50	12.41	18.63	1.58	1.37	9.88	98.16
Tu-2A	46.54	N.D.	N.D.	N.D.	13.26	29.84	N.D.	N.D.	10.00	99.6

R. T. Runnels, analyst, State Geological Survey of Kansas.

* Top 7 samples are green chrysocolla; bottom 3 samples are black.

The noted variation in the composition of chrysocolla is in agreement with published data (Foote and Bradley, 1913) showing the wide range in composition of chrysocolla. Foote

PLATE 2.—PHOTOMICROGRAPHS

FIGURE 1. MALACHITE AND CHRYSOCOLLA REPLACING CEMENT AND LIMESTONE PEBBLES IN GRAVEL BELOW ORE BODY
Jerome, Arizona. × 0.6.

FIGURE 2. MALACHITE FILLING FRACTURES AND REPLACING CARBONATE CEMENT IN STREAM GRAVEL
Pebbles are volcanics. Transmitted and oblique illumination. × 10.

FIGURE 3. CHRYSOCOLLA REPLACING CEMENT AROUND VOLCANIC PEBBLES
Jerome, Arizona. Oblique illum. × 10.

FIGURE 4. MALACHITE REPLACEMENT OF CARBONATE PEBBLES IN GRAVEL
Jerome, Arizona. × 0.7.

FIGURE 5. THICK CHRYSOCOLLA REPLACEMENT LAYER ON DOLOMITE PEBBLE
Jerome, Arizona. × 1.1.

FIGURE 6. DETAIL OF CHRYSOCOLLA REPLACEMENT LAYER ON DOLOMITE PEBBLE
Oblique illum. × 10.

FIGURE 7. MALACHITE ENTERING CALCITE ALONG CLEAVAGE PLANES AS IN ARTIFICIAL REPLACEMENT
Desert Tungsten Mine, Tintic, Utah, × Nicols. × 40.

FIGURE 8. CHALCEDONY VEINS IN INTRICATE MICRO-VEIN SYSTEM
Desert Tungsten Mine, Tintic, Utah. × Nicols, × 10.

FIGURE 1

FIGURE 2

FIGURE 3

FIGURE 4

FIGURE 5

FIGURE 6

FIGURE 7

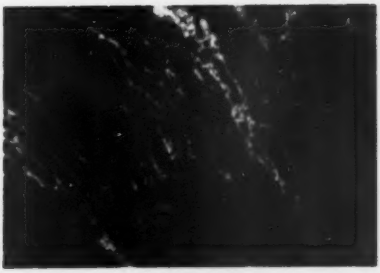

FIGURE 8

PHOTOMICROGRAPHS

and Bradley also believed that chrysocolla, rather than being a distinct mineral species, is an amorphous silica gel with varying amounts of copper salts in solution.

When precipitation of copper salts is induced in artificial copper solutions, crystallization proceeds as fine needles growing outward from nuclei. In many localities, natural wall rock replacement by malachite also was observed to develop by the coalescence of needles growing out into the country rock from such nuclei as shown in two photomicrographs of Bisbee ores (Pl. 3, figs. 7, 8). Such spherules also may form as surface crustifications. Subsequent layering over the spherules then will produce a botryoidal surface. Incidentally, several such botryoidal masses show alternate or interfingering bands of malachite and chrysocolla illustrating again the apparently delicate balance between silicate and carbonate depcsition from supergene copper solutions.

The malachite crystals shown in Figures 7 and 8 of Plate 3 are much larger than any crystals formed as limestone replacements in the laboratory. Dr. J. W. Gruner supplied us with calcite rhombs which had been immersed in 0.1 M copper sulphate for 20 years. These rhombs showed only a thin, sharp, surficial barrier replacement layer comparable to those we were able to form in a few hours. The additional aging did not thicken the replacement layer. Moreover, just as in the case of the replacement layer formed on calcite from copper solutions in a few hours, the brochantite precipitate, aged at room temperature for 20 years, was too fine-grained to permit detection of individual crystals even under the highest petrographic magnification. The coarse size of the natural malachite crystals, plus the fact that malachite rather than brochantite commonly forms as a limestone replacement from sulphate solutions, attests that these supergene replacements must form from extremely dilute solutions over a long period of time.

Replacement of Calcite by Iron Oxide

Discussion

After the work with copper salts, an obvious extension into replacement of calcite by iron compounds was begun. Solutions of iron salts hydrolyze to form acid solutions. The experiments with atacamite and brochantite indicated that reaction of iron solutions with calcite might well form an insoluble hydroxide or hydroxy-salt at the calcite surface, with attendant solution of the calcite.

Table 7.—Changes in Eh and pH During Reaction of Ferrous Chloride Solution With Sodium Chloride Solution Containing Solid Calcium Carbonate

Elapsed time (hours and minutes)	Eh, Volts	pH	Temp. °C.
Original $FeCl_2$ solution (0.01 M)	0.546	3.5	25
0:25	0.251	6.4	24
1:35	0.421	7.08	24
3:00	0.521	7.65	24
8:20	0.546	7.6	25
12:03	0.566	7.8	24.5
25:12	0.564	7.85	24

Preliminary experiments showed that both ferric and ferrous salts react with calcite to form ferric oxide. The reaction of ferric salts was a direct analogue of the cupric salt reactions, but the production of a ferric compound from the ferrous salt pointed up the necessity of investigating the role of oxidation-reduction reactions in replacement.

When the ferric chloride solution reacts with solid calcium carbonate, the ferric ion is precipitated at the solid-solution interface as ferric oxide. Apparently the hydroxide is formed momentarily, but almost immediately breaks down to the oxide (Weiser, 1939, p. 125):

$$2Fe^{+++} + 6OH^- = 2Fe(OH)_3 = Fe_2O_3 + 3H_2O$$

No study of the degree of hydration of the oxide was made, although the work of Kulp and Trites (1951) indicates that it probably was hematite.

When ferrous chloride solution reacts with calcite, the end product is the same:

$$2Fe^{++} = 2Fe^{+++} + 2e$$

$$2Fe^{+++} + 6OH^- = 2Fe(OH)_3 = 2Fe_2O_3 + 3H_2O$$

In a paper on the origin of the Clinton type iron ores, Castano and Garrels (1950) investigated the reactions that occur when ferrous

chloride solution is added to a sodium chloride solution in equilibrium with solid calcium carbonate. The results provide a useful quantitative example of one aspect of the reactions of iron-bearing solutions with limestone.

They made a study of the oxidation-reduction potential (Eh) and pH changes during attainment of equilibrium after mixing a 0.01 M $FeCl_2$ solution with a 0.6 M sodium chloride solution containing solid calcium carbonate grains of sand size (Table 7). Some of the more important variables are graphed in Figure 26.

This work shows that ferrous chloride solutions react with solid calcium carbonate in essentially the same way as copper-bearing solutions. The solution contains both ferrous and ferric ions and, although the ratio of ferrous to ferric is relatively high, there still is sufficient ferric ion present to react with the hydroxyl ion at the calcium carbonate surface, causing the formation of ferric oxide. As ferric oxide is formed, more of the ferrous ion is converted to ferric to maintain the original ferrous-ferric ratio, and this process continues until essentially all the iron in solution has been precipitated as the ferric oxide (or, of course, until all the calcium carbonate present is used up). In addition, the table illustrates that ferric oxide precipitation "keeps up" with the neutralization of the solution and that iron is removed at the rate expected from the progressive change in pH. If this were no so, the calculated value for the activity product of ferric hydroxide would not remain constant. The pH curve in Figure 26 has the shape expected from the reaction of almost any hydrolyzed heavy metal salt with calcium carbonate, and essentially the same equilibrium pH is attained as in the copper experiments.

The precipitate of iron oxide formed at the calcium carbonate surface is even finer-grained than the atacamite film developed by reaction of copper chloride solutions with calcite. Electron photomicrographs show that the individual "grains" are quite uniform, nearly spherical, and have a diameter of approximately 0.1 microns.

A number of experiments were performed using calcium carbonate "reaction tubes". A 10 mm. glass tube 15 cm. long was filled with powdered calcite (less than 200 mesh) and ferrous chloride solution was allowed to drip through the column from a reservoir. Precipitation apparently was nearly instantaneous, and the upper part of the calcite eventually became heavily stained with iron oxide for a distance of several centimeters from the top of the tube. The solution emerging from the lower end of the reaction tube had a pH of 7.8, and was free from dissolved iron. Reference to Figure 26 shows that the total concentra-

---

PLATE 3.—PHOTOMICROGRAPHS

FIGURE 1. MICRO-VEIN SYSTEM WITH REPLACEMENT BORDERS

Veins consist of an intricate, and here indistinguishable, intergrowth of malachite and chrysocolla. Mineral Hill area, Pima County, Arizona. × 10.

FIGURE 2. VEIN SYSTEM CONTAINING TWO GENERATIONS OF MALACHITE AND AN INTERNAL FILLING OF CHRYSOCOLLA

Daylight Mine Helvetia district, Pima County, Arizona. Oblique illum. × 10.

FIGURE 3. BANDED CHRYSOCOLLA

Miami, Arizona. × 0.7.

FIGURE 4. DETAIL OF GRADATIONAL BANDS IN FIGURE 21. × 2

FIGURE 5. BANDED CHRYSOCOLLA VEINS WITH A CORE OF CHALCEDONY

Desert Tungsten Mine, Tintic, Utah. Oblique and transmitted light, × Nicols. × 10.

FIGURE 6. BASAL LAYER OF MALACHITE INTERFINGERED WITH BLACK CHRYSOCOLLA ABOVE WHICH IS A BOTRYOIDAL SURFACE SHOWING CHRYSOCOLLA GRADING INTO CHALCEDONY

Jerome, Arizona. × 10.

FIGURE 7. TYPICAL MALACHITE SPHERULES IN LIMESTONE GROWING OUTWARD FROM CALCITE CRYSTAL BOUNDARIES

Bisbee, Arizona. Transmitted and oblique illum. × 10.

FIGURE 8. MALACHITE NEEDLES GROWING OUTWARD FROM NUCLEUS IN LIMESTONE

Bisbee, Arizona. Transmitted and oblique illum. × 45.

FIGURE 1

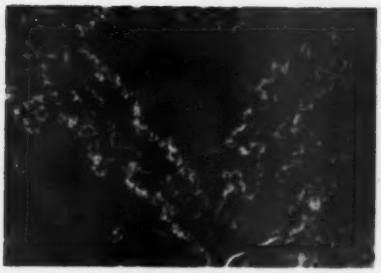

FIGURE 2

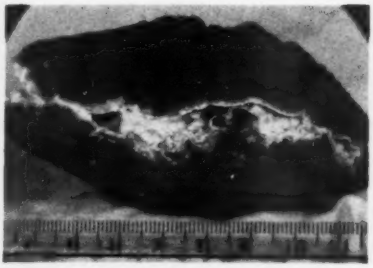

FIGURE 3

FIGURE 4

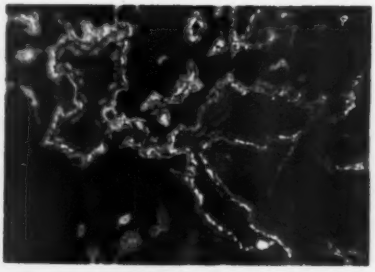

FIGURE 5

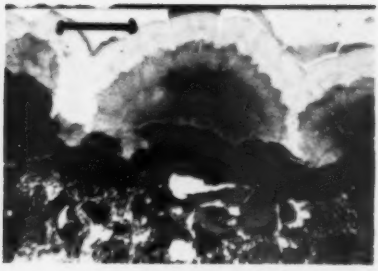

FIGURE 6

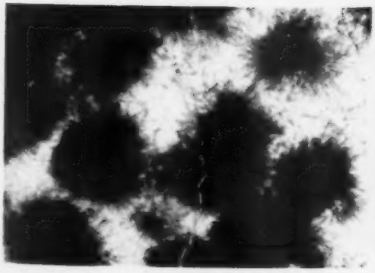

FIGURE 7

FIGURE 8

PHOTOMICROGRAPHS

9
7
5
3
0

tion of iron ($\Sigma Fe^{++} + Fe^{+++}$) should have been of the order of magnitude of 10^{-14} mols per liter. Some of the iron moved through the tube in a colloidal state. After heating to coagulate the colloid, a small amount of iron oxide could be collected by filtering.

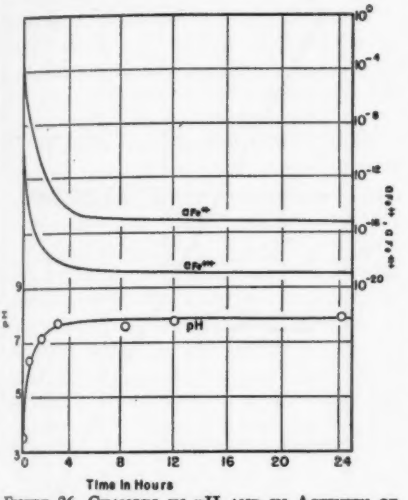

FIGURE 26. CHANGES IN pH AND IN ACTIVITY OF FERROUS AND FERRIC IONS

Resulting from the reaction of a 0.01 molar ferrous chloride solution with a 0.6 molar sodium chloride solution containing calcium carbonate grains of sand size. The pH curve is typical of the reaction to completion of a hydrolyzed metal salt solution with solid calcium carbonate.

In summary, the reaction of ferrous and ferric solutions with calcite is analogous to the reaction of solutions of copper salts. The hydrolyzed acid solution is neutralized by reaction with the calcite, and the iron essentially completely precipitated. During the period of attainment of equilibrium, calcite is dissolved, and replacement results at the grain surface from these simultaneous processes. The major difference between the reactions of iron and copper solutions with calcite (without forced flow) is in the attainment of equilibrium with iron salts as opposed to the incompleteness of reaction when copper solutions are the reactants. The explanation seems to lie in the difference in crystallization characteristics between iron oxide and the basic copper compounds, and also in the difference in their ability to adhere to the surface of the calcite. The iron oxide films are gelatinous rather than crystalline, and continuously slough away from the calcite surface, re-exposing it to attack.

Oxidation-Reduction Relations

Perhaps one of the most important lessons to be learned from the reaction of ferrous chloride solutions with calcite is the danger of assuming the state of oxidation of the components of a solution from the materials that precipitate from it. In the experiments with ferrous chloride solutions, the ferrous-ferric ratio was never less than 1000 to 1 (Fig. 26), yet the iron was entirely precipitated as ferric oxide. In cases where there are two oxidation states of a metal ion, there are two major controls of the compound that will precipitate—the solubility of the least soluble compound that can be formed by each of the oxidation states, and the relative abundance of the two states in the solution. If ferrous hydroxide were as slightly soluble as ferric hydroxide, it would have been the predominant solid phase formed.

These experiments raise again the question of the oxidation state of natural solutions. Even though the precipitates from such solutions commonly are *sulfides* as opposed to *sulfates*, and even though there is a tendency for the metals in veins to precipitate in their lower oxidation states, it still is conceivable that the ratio of sulfate ions to sulfide ions in the solutions is relatively great, and that at least part of the obviously rather high solubility of sulfides in vein solutions comes from a "repression" of sulfide ion into sulfate.

The experiments on replacement of calcite by ferric oxide were carried out in well-aerated solutions and represent conditions under which the ratio of ferrous to ferric ions is at a minimum. With decreasing oxygen saturation, the ratio would increase, and the likelihood of precipitating ferrous compounds would increase. Figure 27 shows the effect of a change of oxidation potential on the amount of ferrous ion that can be carried in any solution in equilibrium with solid ferric oxide (Cooper, 1937, p. 305). With decreasing Eh, the ratio of ferrous to ferric ion in solution becomes so large that there are not enough ferric ions to cause precipitation even of the extremely insoluble ferric oxide.

In primary mineral deposits formed below the water table, hematite is a minor mineral except in those deposits presumed to have been formed at high temperatures and pressures. Iron minerals almost always contain ferrous ion. Among the most common are pyrite and siderite. If we restrict our attention to deposits generally classified as epithermal, the effect of temperatures and pressure on the various chemical equilibria may not be so great as to make a discussion based on relationships at 25° C. and 1 atmosphere pressure completely inapplicable. Figure 28 is adapted from Figure 27, and shows the Eh and pH values at which 10^{-6} mols per liter of ferrous ion can exist in equilibrium with solid ferric oxide. The graph shows the limiting values of Eh and pH at which appreciable quantities of ferrous ion can exist. Any solution with Eh and pH characteristics that lies to the right of the curve cannot carry more than 10^{-6} mols per liter of ferrous ion. This concentration was chosen as a limiting amount on the assumption that smaller concentrations could not possibly be effective in causing some of the tremendous pyrite and

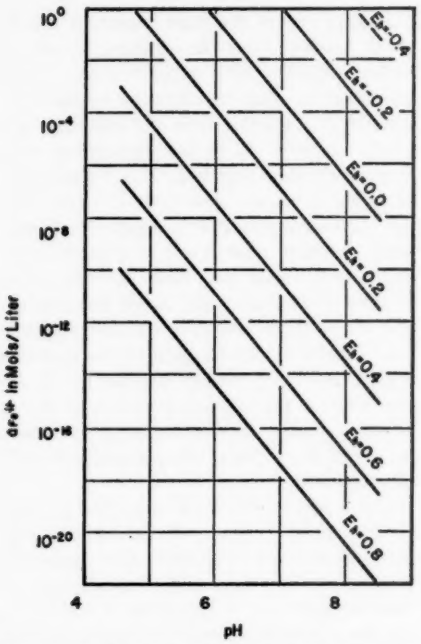

FIGURE 27.—MAXIMUM ACTIVITY OF FERROUS ION AS A FUNCTION OF Eh AND pH

At any greater values of ferrous ion activity, ferric hydroxide will precipitate.

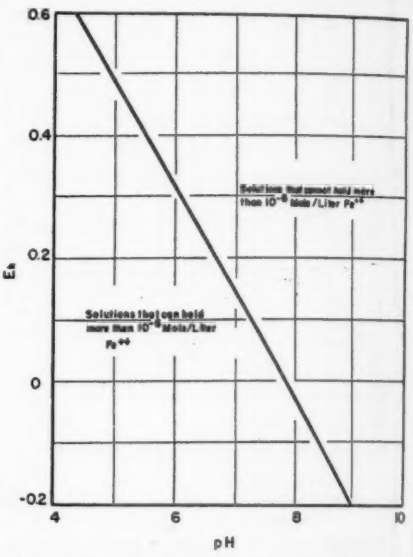

FIGURE 28.—ADAPTATION OF FIGURE 52 SHOWING THE Eh-pH STABILITY FIELD BOUNDARY SEPARATING SOLUTIONS THAT CAN CARRY APPRECIABLE AMOUNTS OF FERROUS ION FROM THOSE THAT CANNOT.

siderite deposits that have been found, even though very large volumes of solution and very long times were available. This curve is suggested as a rough upper limit, so to speak, of the most oxidizing conditions that can prevail in vein-forming solutions that precipitate abundant quantities of ferrous compounds.

Replacement of Limestone By Mixed Iron and Copper Solutions

After it was found that both copper chloride and iron chloride solutions reacted with calcite, simultaneously dissolving the calcite and precipitating an insoluble compound at the calcite surface, it was decided to determine the effect of a mixed solution. A solution was prepared of tenth molal ferrous chloride and tenth molal cupric chloride. The solution was then allowed to flow through a 6″ length of tubing filled with powdered calcite (less than 200

mesh). Movement of the solution through the powdered calcite was aided by placing the tube in a suction flask. In a very short time after the beginning of movement of the solution through the calcite, a brown precipitate formed near the upper surface of the powdered calcite and a small amount of green precipitate was found dispersed through the lower portion. The filtrate from the column had the typical equilibrium pH of approximately 7.5. It was nearly iron-free, but contained a considerable quantity of basic copper chloride (atacamite) in colloidal suspension. Tests showed that the original suspension was a true colloid in that it did not settle overnight, and it showed a very pronounced Tyndall effect. However, after a few days, recrystallization ensued and delicate crystal flakes of atacamite settled to the bottom of the container or floated on the surface of the solution. Several runs were made in which the filtrate was passed over the column several times. A little more of the colloidal atacamite "sat down" during passage through the calcite, but the suspension was truly remarkable in its ability to pass down through the calcite column.

These results are interpreted as follows: The original solution of mixed chlorides was typically acid because of hydrolysis. As it moved through the powdered calcite, reaction occurred and the solution was neutralized at the surface of the calcite fragments with a resultant local increase in the hydroxyl concentration. Then there was a competition for the hydroxyl, and the less soluble ferric oxide was formed in preference to the basic copper chloride. Consequently the grain surfaces were coated with ferric oxide. But after a very short distance of travel, hydroxyl concentration between the grains became sufficiently high to precipitate the basic chloride. Particle size of the precipitate was small indeed; consequently the particles continued downward between the fragments of calcite into the filtrate.

The results are significant in that they show, at least for this particular case, that when two solutions, each of which will replace calcite separately, are mixed, the result is not necessarily replacement by one followed by replacement farther away from the source by the second. Instead only the ferric oxide showed a replacement reaction with the calcite. The basic copper chloride simply filled spaces between the grains. Also, the role of iron in permitting copper to migrate away from outcrops in the oxidized zone is illustrated. In the absence of iron, reaction of the copper solution is almost instantaneous, and a calcite column becomes brightly green-stained at the top, removing essentially all copper present. Little or no colloidal atacamite moves downward through the pores.

It could have been predicted from the previous studies of the precipitation curve of atacamite and the oxidation precipitation curves for ferric oxide that the iron compound would react first with the calcite.

As the pH is increased at the calcite sufaces, atacamite can be expected to precipitate when its Ksp value is exceeded. In this case, the original copper ion concentration is 0.1 m, and chloride ion is 0.4 m (the solution is a mixture of 0.1 m $FeCl_2$ and 0.1 m $CuCl_2$). Substituting in the equation for Ksp, and solving for the hydroxyl concentration of the first precipitation:

$$(Cu^{++})^4(OH^-)^6(Cl^-)^2 = 10^{-66}$$
$$(10^{-1})^4(OH^-)^6(4 \times 10^{-1})^2 = 10^{-66}$$
$$(OH^-) = 10^{-10.2}$$
$$pH = 3.8$$

The original ferrous chloride solution, on the other hand, already was in equilibrium with ferric oxide, and ferric oxide was precipitated by any increase whatever in pH. Therefore, the iron oxide coating observed on the topmost grains in the reaction tube is the expected product, for atacamite will not precipitate until partial neutralization has occurred, whereas iron oxide precipitates at once.

A calculation of the completeness of precipitation is illuminating. The equilibrium pH is 7.5, corresponding to an hydroxyl concentration of $10^{-6.5}$ molal. Then:

$$(Cu^{++})^4(OH^-)^6(Cl^-)^2 = 10^{-66}$$
$$(Cu^{++})^4(10^{-6.5})^6(4 \times 10^{-1})^2 = 10^{-66}$$
$$(Cu^{++}) = 10^{-6.5}$$

Also:

$$(Fe^{+++})(OH^-)^3 = 10^{-37.5}$$
$$(Fe^{+++})(10^{-6.5})^3 = 10^{-37.5}$$
$$(Fe^{+++}) = 10^{-18}$$

At this pH, the Fe^{++}/Fe^{+++} ratio is approximately 10^4 (Fig. 26), so Fe^{++} concentration is about 10^{-14} molal, and total ionic iron left in solution, both ferrous and ferric, is about 10^{-14} mols per liter.

A rough check of this effectiveness of precipitation was obtained by an attempt to synthesize malachite by using very large volumes of very dilute copper sulfate solution. Ordinary Lake Michigan tap water was used as the solvent, and the solution was passed over a powdered calcite column. No copper was precipitated, but the upper part of the column became visibly iron-stained after about 80 liters of water had passed over it. The Evanston Municipal Water Supply Office (oral communication) informed us that the iron content of the tap water was less than 1 part per million, so the calcite column provides a rather delicate test for iron, even if a few parts per million were picked up in the pipes in transit.

The small amount of copper expected to remain at this pH suggests an explanation of the difficulties encountered by geochemical prospectors in trying to determine traces of copper in streams. Lovering, Huff, and Almond (1950, p. 508) analyzed ground water of pH averaging about 7.5, and found that copper in solution was even less than the amount calculated here. It is to be expected that, wherever ground and stream waters come into equilibrium with calcium carbonate, the iron and copper content will be reduced to low and nearly constant values. Thus geochemical tests might well give small and uniform values, regardless of the richness or proximity of the copper source.

Transportation of Iron and Copper From Oxidizing Chalcopyrite

An attempt was made to perform essentially the same experiment described before, but to simulate natural conditions more closely. Under natural conditions in the zone of oxidation, it is very common to find chalcopyrite oxidized to iron oxide at the surface and to find malachite or other oxidized minerals developed in the limestone beneath the outcrop.

In an attempt to approximate natural conditions, a tube 10 mm. in diameter was plugged at the bottom with cotton, then filled to a depth of 6 inches with powdered calcite (minus 200 mesh). On the top of the calcite was another cotton plug, approximately 1 inch long, and on top of the second cotton plug, a column of powdered chalcopyrite approximately 2 inches long. In a preliminary experiment, distilled water was dripped over the chalcopyrite, but the rate of oxidation was so small as to preclude any visible results within a reasonable length of time. It was found that a dilute solution of sulfuric acid (.01 M) caused relatively rapid oxidation of the chalcopyrite. A number of liters of the acid were used over a period of about 6 months. The permeability of the material of the column was quite low; a few milliliters were passed in 24 hours. The tube was filled to the top each morning with dilute acid, and the supply was renewed the following day. In most cases, a small amount of acid remained above the upper surface of the chalcopyrite at the time of refilling, but occasionally the chalcopyrite dried out before the tube was refilled.

The results were quite similar to those obtained using mixed ferrous chloride-cupric chloride solution. The upper part of the calcite became cavernous and heavily iron-stained. In some instances, the irregular openings filled with secondary well-developed crystals of gypsum. The experiment was run almost a month before any visible greenish copper mineral was formed, and even then it was observed only at the lower outlet of the tube and as a crust in the bottom of the catchment flask. The pH of the solution emerging from the bottom of the tube was approximately 7.5.

These relations indicate that the chalcopyrite slowly oxidized to yield ferric sulfate, cupric sulfate, and free acid. As this mixed solution passed over the calcite, the acid was neutralized, calcite was dissolved, and ferric oxide precipitated at the calcite grain surfaces. The copper, on the other hand, passed down through the tube—perhaps in colloidal form. In the upper part of the tube, where the miniature geodes formed, solution of the calcite yielded free calcium ion that reacted with the sulfate ion to form gypsum crystals in the cavities.

Unfortunately no attempt was made to protect the solution that passed through the

tube from evaporation. As a result, it is not known whether the copper mineral precipitated as a result of evaporation, or whether it was present from the beginning in colloidal form. Although roughly equivalent quantities of ferric oxide and of the basic copper mineral were expected from the oxidation of the chalcopyrite, iron staining was very heavy, whereas only traces of the green copper mineral were observed, either in the reaction tube or in the filtrate.

Relation of Grain Size to Rate of Crystallization and to the Effects of Aging

Statement

In the replacement of calcite by atacamite and ferric oxide, the replacing compound was extremely fine-grained. Electron photomicrographs of atacamite (Garrels and Stine, 1947) showed that the particles were, at most, a few microns in diameter, and electron photomicrographs of typical ferric oxide precipitates indicate that their grain size is even smaller—of the order of 0.1 micron.

It is likely that a major control of grain size is the degree of supersaturation at the reaction

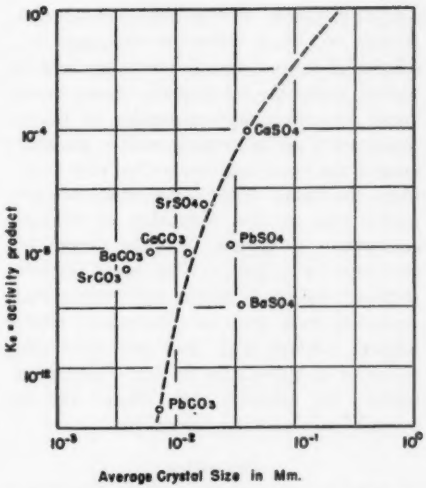

Figure 29.—Relation of Grain Size of Precipitates to Degree of Supersaturation of Solution in Which They Form.

All salts shown were precipitated by the reaction of a tenth molar solution of a soluble salt with a crystal containing sulfate or carbonate ion. The difference in position of the carbonates as opposed to the sulfates may indicate a fundamental difference in crystallizing power although data are not sufficient to more than suggest such a relation.

Table 8.—Relation of Grain Diameter to Degree of Supersaturation

Solid	Reacting Solution (0.1 M)	Time Of Run (Seconds)	Average Grain Size (mm.)	Ksp of Insoluble Compound Formed*
Na_2CO_3	$Ba(NO_3)_2$	30	0.0075	$7.0 \times 10^{-9}(BaCO_3)$
	$CaCl_2$	30	0.0125	$5 \times 10^{-9}(CaCO_3)$
	$Pb(NO_3)_2$	30	0.005	$3.3 \times 10^{-14}(PbCO_3)$
	$SrCl_2$	30	0.0037	$1.6 \times 10^{-9}(SrCO^1)$
$CuSO_4 \cdot 5H_2O$	$Ba(NO_3)_2$	30	0.035	$1.00 \times 10^{-10}(BaSO_4)$
	$CaCl_2$	480†	0.040	$6.1 \times 10^{-5}(CaSO_4 \cdot 2H_2O)$
	$Pb(NO_3)_2$	30	0.030	$1.0 \times 10^{-8}(PbSO_4)$
	$SrCl_2$	3	0.012	$2.8 \times 10^{-7}(SrSO_4)$

* Ksp values from: Snead and Maynard (1942); Kolthoff and Sandell (1938).
† No precipitate for first 300 seconds. Reaction very slow.

surface—in this case, the surface of the calcite. It is known that the rate of nucleation in crystallizing solutions increases with increase of supersaturation. The solubility of iron at a calcite surface is approximately 10^{-14} mols per liter, whereas the concentration of iron of the reacting solution used was .01 mols per liter. Consequently, the solution was tremendously supersaturated in the reaction zone, and a very high nucleation rate resulted, causing the formation of a large number of very fine particles.

To provide additional data, a series of experiments was made in which a crystal of soluble compound was allowed to react with a soluble salt, forming a precipitate of very low

solubility (Table 8; Fig. 29). For example, crystals of sodium carbonate were spun in a solution of barium chloride producing insoluble barium carbonate by reaction. These experiments are not quite comparable to the replacement of calcite by ferric oxide or atacamite because the ion in solution reacted with an ion from the solid. Eight determinations were made: four on the formation of insoluble carbonates of barium, calcium, lead, and strontium, and four on the same insoluble sulfates. Crystals of copper sulfate or sodium carbonate were spun in solutions of soluble barium, calcium, lead, and strontium salts, and after an appreciable amount of precipitate formed, the solutions were filtered and the average grain diameter determined.

Discussion

There is a fair correspondence between the size of the grains formed and the degree of supersaturation reached at the face of the crystal dissolving into the solution. Because the concentration of the original salt was the same in each case (0.1 molar), the smallness of the activity product is a rough measure of the degree of supersaturation; or, stated otherwise, the degree of supersaturation is inversely proportional to the activity product.

These experiments again indicate that the grain size of the guest mineral in a replacement deposit may be a helpful indicator of the speed of reaction at the time it was formed. By implication, replacement with textural duplication down to the limit of microscopic examination indicates that the original grain size of the guest was very small indeed, and that it was formed by a relatively rapid reaction—a rate comparable to those observed in the laboratory in these experiments.

Effect of Aging on Grain Size

It is highly unlikely that the grain size observed in a natural deposit is finer than when originally formed; the changes resulting from aging would be in the direction of coarsening of grain.

In order to get at least a qualitative measure of the amount of coarsening of grain size that might be expected as a result of aging, a number of compounds were precipitated. Half of the precipitate was removed from solution and dried; the other half sealed in the mother liquor and placed in an oven at 90°C. for 6 months. At the end of this period, the grain size of the original precipitate was compared with those that had been aged.

Two of the compounds precipitated were calcite and gypsum. The original precipitate was extremely fine with an average grain size of approximately 0.01 mm. After 6 months of aging, the average grain size was about twice as great. The original particles of calcite were irregular feathery crystals; the aged precipitate small well-formed rhombs. A precipitate of gypsum showed about the same amount of increase in average size. Sulfide precipitates did not increase sufficiently in size for the change to be measurable under the microscope, but the original and aged material showed some differences. The unaged material was powdery and earthy, whereas the aged sulfides definitely were more granular. The difference was especially noticeable in the case of lead sulfide. The aged material gave occasional sparkles when observed under a strong light, indicating the development of crystal faces; the original material had a sooty luster.

Discussion

The experiments show that the effect of aging of relatively soluble compounds (calcite and gypsum) at 90°C. was appreciable even over a 6 months period. The effect of aging on the difficulty soluble compounds (sulfides) was slight or undetectable. That aging can be observed over such a relatively short period of time, compared to the length of time available under geologic conditions, shows that observed grain size in rocks may be much greater than the original, even though aging under natural conditions may not take place at elevated temperatures.

The effect of aging in coarsening textures is, of course, the result expected, for small grains have a high surface energy relative to coarser grains. If two crystals, a large and a small, are placed side by side in a solution, the tendency is for the smaller grain to dissolve and to reprecipitate on the larger one where the surface energy is smaller (Kolthoff and Sandell, 1938, p. 96).

None of our experiments suggested any criteria by which original grain size could be determined. Several unsuccessful attempts were made to determine the presence of an original finer texture. Formvar replicas were made of the cleavage surface of galena and of crystal surfaces of pyrite from the Wisconsin lead-zinc ores, with the hope that traces of an original finer structure might be apparent under the electron microscope. The technical difficulties of making satisfactory replicas have not yet been solved.

The implication is clear, although open to much question and qualification, that the fineness of grain of many known replacement deposits indicates a reaction that proceeded at a finite rate, and further that the reacting solutions were relatively concentrated. Unless this were so—if, for example, the solutions were extremely dilute—there would be a very low degree of supersaturation at the time of precipitation, nucleation would be correspondingly slow. It is to be further noted that aging and resultant mineral growth may have a marked effect on apparent mineral paragenesis, because mineral relations change continuously with changing environments. Paragenesis may, therefore, measure diagenesis rather than syngenesis.

Replacement of Calcite by Sulfides

General

It has now been shown that the conditions for metasomatic replacement are fulfilled both by replacement of calcite by basic copper salts and by ferric oxide. The mechanism is identical —neutralization of a hydrolyzed acid heavy metal solution by calcium carbonate resulting in the simultaneous solution of the carbonate and precipitation of the mineral containing the heavy metal. In these two cases, the heavy metal precipitated as a difficultly soluble hydroxide or hydroxy-salt. It therefore seemed reasonable to investigate the possibility that a parallel mechanism might account for the replacement of limestone by metal sulfides.

The immediate difficulty, of course, was exactly one that has plagued theorists on ore transport since ores have been exploited: to find a medium in which the metal sulfides are sufficiently soluble even to permit experimentation.

The activity products of the sulfides are so low that strong reagents are necessary to bring them into solution. Two major suggestions have been made concerning the nature of the

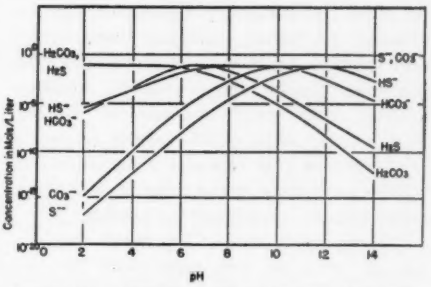

FIGURE 30.—DISTRIBUTION OF MAJOR IONIC SPECIES RESULTING FROM THE IONIZATION OF H_2CO_3 AND H_2S AS A FUNCTION OF pH

Total concentration, 10^{-1} mols per liter.

transporting medium: the first that it is acid, and that the sulfides can be carried because the bivalent sulfur in the solution is repressed into H_2S; the second that the solution is strongly alkaline, and that the metals are carried in soluble sulfide complexes. The basis for these opposing views is presented in Figure 30, which shows the distribution of bivalent sulfur among S'', H_2S, and HS' as a function of pH.

Either explanation has apparently insuperable difficulties. Solutions of high pH and consequent high S'' concentration are unsatisfactory for two major reasons. First, such solutions do not dissolve appreciable amounts of either iron or lead. The transporting medium in nature obviously is just as effective a solvent for these metals as for others. Second, in many cases, the ore-forming solutions show a marked preference for limestone. Solutions of high pH do not react with limestone; instead limestone reaches minimum solubility at high pH.

Solutions of low pH satisfy the necessary conditions better qualitatively, for they are nearly universal solvents of the metals by virtue of their repression of the sulfide ion, but they fail quantitatively. A solution sufficiently acid, for example, to dissolve appreciable

quantities of lead sulfide is capable of dissolving relatively enormous amounts of limestone. It can be predicted that, if vein solutions are sufficiently acid to carry sulfides, their effect on encountering limestone would be to leave gaping holes. Here and there in the cavities might be found a visible trace of sulfide, but no more. In laboratory experiment, all our attempts to replace calcite or limestone by acid solutions resulted in dismal failure. The limestone simply disappeared in solutions carrying even small amounts of sulfides. Furthermore, metal sulfide zoning in ores is the reverse of that expected if the control of sulfides precipitate in the order of decreasing, rather than increasing, activity product.

Consequently, neither hypothesis fits the geologic relations, and there have been no satisfactory explanations of the observed field relations. The field relations give many clues to the nature of the medium, but they lead to conditions unexplained by the chemist.

The following statements summarize some of the pertinent evidence of the nature and effects of the ore-forming fluid:

1. Limestones are generally more susceptible to massive sulfide replacement than other rocks.
2. Fluid inclusions in lead and zinc ores contain solutions of high salt content of pH approximately 7 (Newhouse, 1932).
3. Pyrite and marcasite can occur in the same deposit, indicating nearly neutral solutions, or solutions ranging in pH around neutrality (Allen, Johnson, and Larsen, 1912).
4. The distance of travel of the sulfides from their source is roughly in the order of decreasing activity products. Presumably, then, they are in the reverse order of the solubility expected if the solubility is the result of repression of the sulfide ion (Bandy, 1940).
5. Wall-rock alteration in a number of typical ore deposits indicates solutions ranging from slightly acid to alkaline. The clues to the pH of the solution are the clay minerals (Lovering, 1949).

From these relations emerges an ore solution of pH slightly on the acid side—perhaps of the order of pH = 6. It would seem to be well buffered, in that it has considerable capacity for dissolving limestone. Very likely it is high in salts of the alkali metals as well as the heavy metals. It has sufficient heavy metal sulfides in solution to take the place of any limestone dissolved, and precipitates them without regard for the activity product of the sulfides, or even in order of decreasing product.

As pointed out before, the mechanism by which such a solution can keep the heavy metals dissolved has not been elucidated. Yet the fault is more likely in our imperfect knowledge of chemistry than in the geologic reasoning. It is becoming apparent that such solutions *must* carry sulfides, despite our inability to explain how they do it.

The Silver Bisulfide Complex

A paper by Treadwell and Hepenstrick (1949, p. 1872–79) offers great promise of providing an answer to the enigma. They discovered anomalies in the solubility of silver sulfide and, upon investigation, found that a silver bisulfide complex is formed, increasing in effectiveness in solutions of increasing pH. Table 9 shows some of their data (20°C.).

They explained these solubility relations by the assumption that there are two important reactions in the solution:

$$Ag^+ + H_2S = AgHS + H^+;$$

$$\frac{(AgHS)(H^+)}{(Ag^+)(H_2S)} = 10^{9.85}\,(20°C.)$$

and:

$$AgHS = AgS^- + H^+;$$

$$\frac{(H^+)(AgS^-)}{(AgHS)} = 10^{-5.3}\,(20°C.)$$

These are, of course, in addition to the usual important equilibria:

$$\frac{(H^+)(HS^-)}{(H_2S)} = K_{H_2S}$$

$$\frac{(H^+)(S^=)}{(HS^-)} = K_{HS^-}$$

$$(Ag^+)^2(S^=) = K_{Ag_2S}$$

Using these equations, and proceeding as in the problems on solubility of calcium carbonate, we solved for silver solubility ($Ag^+ + AgHS +$

AgS^-) at pH values higher than those determined experimentally. Figure 31 shows the results of these calculations, and also the relative importance of the contributions of AgHS and AgS^- to the total solubility. Ag^+ is negligible, never rising above about 10^{-14} mols/liter.

TABLE 9.—SOLUBILITY OF SILVER IN H_2S BEARING SOLUTIONS

pH	H_2S (mols/liter)	Silver (mols/liter)
1	0.1	1.96×10^{-6}
2	0.1	1.00×10^{-6}
3	0.1	1.17×10^{-6}
4.5	0.1	1.45×10^{-6}
5.65	0.1	8.14×10^{-6}
6	0.1	11.90×10^{-6}
7	0.1	26.52×10^{-6}

Thus silver forms both soluble bisulfide and sulfide complexes, and its solubility at 20°C. is nearly constant at about 10^{-6} mols/liter in acid solutions saturated with hydrogen sulfide at 1 atmosphere pressure. The solubility increases markedly at higher pH values.

Such silver-bearing solutions would not be expected to react with calcite with resultant replacement by silver sulfide. If, for example, a solution of pH = 6 reacted with calcite, the increase in pH as the calcite dissolved would cause an increase in the solubility of silver. However, a mechanism has been discovered that renders silver sufficiently soluble to have important geological consequences. Also, the mechanism invoked is one that depends upon common constituents of vein solutions. The presence of *both* bisulfide and sulfide complexes of sufficiently low degree of ionization to render soluble one of the important metals found in ore deposits points the way to a possible answer to the problem of heavy metal transport.

Possibility of Bisulfide Complexes of Other Heavy Metals

No chemical data have been found to indicate that bisulfide complexes of other heavy metals, such as copper, lead, or zinc do form. But the discovery of the silver bisulfide complex lends much importance to the search for them.

A number of indirect lines of evidence suggest that such complexes exist. The "reverse zoning" of the sulfides is a good indication that they are not present as simple metal ions, for if they were, they would precipitate in the order expected from their activity products. Also, it is unlikely that each metal forms a different type of complex, for their behavior is, in spite of numerous exceptions, too uniform from deposit to deposit. For example, it has been shown that lead ion forms a soluble chloride complex, whereas zinc does not (Garrels, 1941, p. 738). We cannot appeal to chloride to render the lead soluble, to some other ion to render the zinc soluble, and so on. Both the present hypotheses—the "acid" and "alkaline" schools—totally agree to this, for one relies on a repression of sulfide ion into a H_2S "complex"; the other on the formation of a metal-sulfide complex. It seems inescapable that some common constituent of the vein

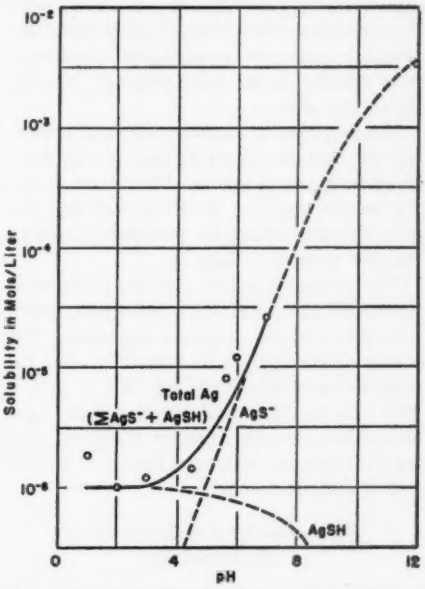

FIGURE 31.—SOLUBILITY OF SILVER AS A FUNCTION OF pH

In a solution saturated with H_2S at the temperature of 25°C. and an atmosphere pressure. The dash lines are calculated. Circles are points from data of Treadwell and Hepenstrick (1949).

solutions renders the sulfides soluble. Nor can appeal be made to gas transport, at least in many deposits formed at shallow depths. Not only do hydrostatic pressures far exceed the vapor pressure of water in these deposits, but the carbonate minerals are zoned in the order expected from their solubility products, with the iron-rich and less soluble species depositing first and deeper. So the carbonates precipitate from solution in the order expected, whereas the sulfides do not.

The fact that a bisulfide complex of silver was the first discovered is suggestive in itself, for silver is one of the best "travelers" among the metals, and one would predict that the most effective among the complexes would be the first to come to light.

The reason for lack of previous information is not difficult to ascertain, in retrospect; sulfide determinations in solutions containing H_2S are very difficult to make, especially when the order of magnitude of the solubility is 10^{-5} or 10^{-6} mols per liter. Such determinations have always been open to criticism if extreme care were not taken to assure the absence of colloids and of oxidation products.

Differential Effect of Complexes on Metal Solubility

If bisulfide complexes of the other metals do exist, it is illuminating to see what their effects would be. Several cases should be treated.

1. No sulfide or bisulfide complex is formed.
2. Only a bisulfide complex is formed.
3. Only a sulfide complex is formed.
4. Both sulfide and bisulfide complexes are formed.

CASE 1: *No sulfide or bisulfide complex is formed.* Lead sulfide has an activity product of approximately 10^{-30} at 25°C. (Verhoogen, 1938, p. 777). Assuming a solution in which H_2S solubility = $HS^- + H_2S + S^= = 0.1$, the solubility of lead is shown in Figure 32. The curve illustrates very well the reason the protagonists of acid solution, who rely entirely upon repression of sulfide ion, have quantitative difficulties in carrying metals in solution. Solubility decreases continuously with increasing pH, and is very low even at low pH values.

CASE 2: *Only a bisulfide complex is formed.* No actual examples are known of this situation. However, assume a bivalent metal sulfide with an activity product of 10^{-30} that forms a bisulfide complex so that:

$$\frac{(Me^{++})(HS^-)^2}{Me(HS)_2} = Ke = 10^{-16}$$

Such a complex would be comparable to the silver bisulfide complex, but, as no sulfide complex is assumed, the solubility occasioned by the presence of the complex would be much more sensitive to pH changes, and a solubility drop would occur at a pH of 7 (Fig. 32).

CASE 3: *Only a sulfide complex is formed.* Calculations are available for the solubility of a metal sulfide assuming only a sulfide complex is formed. It has been shown (Garrels, 1944, p. 477) that the solubility of copper sulfide is explainable on the basis of formation of a CuS_3^{-4} ion, and the solubility values shown on Figure 32 for copper sulfide are based upon the data given in that paper (p. 479).

CASE 4: *Both sulfide and bisulfide complexes are formed.* Case 4 is admirably illustrated by the solubility of silver sulfide and the curve shown on Figure 32 is taken from Figure 31.

Such solubility curves for various metals would be modified by the specific values of the constants involved, but the following generalizations may be made.

1. If no complexes are formed, simple repression of the sulfide ion by acidity is not sufficient to render the metal soluble even presuming the availability of tremendous volumes of solution and times of geologic magnitude.

2. If only a sulfide complex is formed, solubility increases progressively in alkaline solutions and such solutions would not be expected to react with carbonate rocks with concomitant precipitation of the sulfide.

3. If only a bisulfide complex is formed, the tendency is for the metal to have constant high solubility up to a pH of 7, with decreasing solubility at higher values. A solution containing a metal carried as a bisulfide complex *would* react slowly with a limestone, dissolving the limestone and precipitating the metal sulfide.

4. In the case of metals forming both metal sulfide and bisulfide complexes, the shape of

the solubility curve would depend upon the relative values of the two dissociation constants; if the bisulfide complex were the more important, a solubility maximum would be reached by reaction. On the other hand, mercury, arsenic, and antimony would not be expected to be precipitated by limestone; instead the factors controlling their precipitation would be

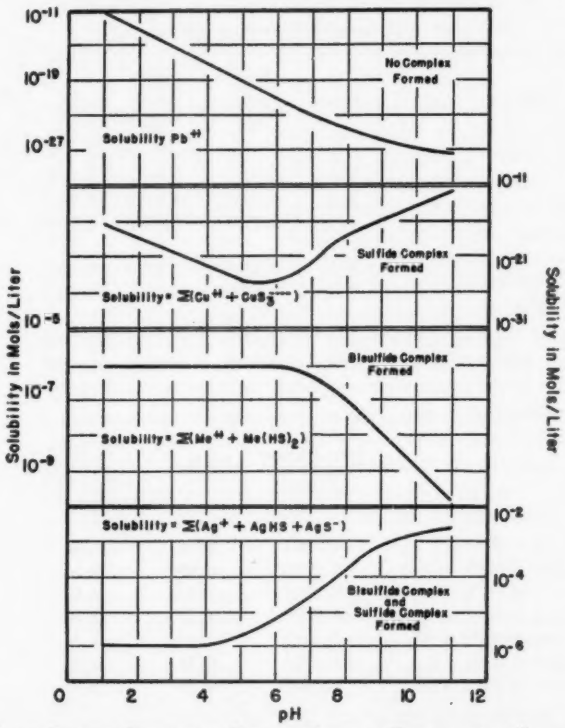

FIGURE 32.—GRAPH SHOWING EFFECTS OF VARIOUS TYPES OF COMPLEXES ON SULFIDE SOLUBILITY
Solubilities are calculated at 25° C. in a solution saturated with H_2S at atmosphere pressure.

at a pH of around 7 for a bivalent metal; if the sulfide complex constant were by far the smaller, solubility would increase with increasing pH.

It is possible to apply these conclusions toward an explanation of the differences in geologic behavior of zinc and lead, as opposed to mercury, arsenic, and antimony. It is known that lead and zinc do not form highly soluble sulfide complexes, whereas arsenic, antimony, and mercury do. If it is assumed for the moment that lead and zinc form bisulfide complexes, then slightly acid or neutral solutions containing them would tend to react with and replace limestone as pH is increased decrease of pH, temperature change, or perhaps dilution, which might destroy the complex. These chemical relations seem to fit the geologic relations reasonably well; galena and sphalerite are common limestone-replacers, whereas mercury, arsenic, and antimony (especially mercury) are much more commonly associated with siliceous rocks.

The possibility of the existence of lead and zinc sulfide complexes with nearly constant solubility up to a pH of 7 provides a possible chemical method for the formation of extensive lead and zinc sulfide replacement deposits from oxygen deficient supergene solutions. If sulfide complexes are the major factor control-

ling solubility, the simple activity products of the sulfides are no longer the sole determining factors in relative solubility. It is therefore possible that, as bisulfide complexes, lead and zinc would have essentially the same solubility. Although much work remains to be done in the investigation of sulfide and bisulfide complexes of common metals, it should be noted that the chemical composition of solutions capable of carrying lead and zinc may not be a deterrent to formation of Mississippi Valley-type lead zinc deposits from supergene solutions.

TABLE 10.—REACTION OF SOLUTIONS WITH SULFIDES

(Volume of Solution = 300 cc.)

Solution	Sulfide	Original Weight Sulfide (Grams) (W_o)	Final Weight Sulfide (Grams) (W_f)	ΔW (Grams)	$\frac{\Delta W \times 10^3}{W_o}$	Time of Reaction (Hours)
0.05 m $Cu(NO_3)_2$	PbS	0.9027	0.8984	0.0043	4.76	200
0.05 m $Cu(NO_3)_2$	ZnS	0.6803	0.6794	0.0009	1.32	200
0.05 m $Cu(NO_3)_2$	FeS_2	2.7957	2.7927	0.0030	1.08	200
0.05 m $Zn(NO_3)_2$	PbS	0.3598	0.3584	0.0014	3.89	185
0.05 m $Zn(NO_3)_2$	FeS_2	0.6095	0.6081	0.0014	2.30	185
0.05 m $Pb(NO_3)_2$	ZnS	0.6779	0.6774	0.0005	0.74	330
0.05 m $Pb(NO_3)_2$	FeS_2	0.6361	0.6360	0.0001	0.16	330

Reaction	Loss of Weight of Solid (W) (Grams)	$\frac{\Delta W \times 10^3}{W_o}$	Ratio Ionic Radius of Replacing Ion to Ionic Radius of Replaced Ion	Concentration of Replaced Ion in Solution (mols/liter)
$Cu^{++} + PbS \rightarrow CuS + Pb^{++}$	0.0043	4.76	0.84	5.4×10^{-5}
$Zn^{++} + PbS \rightarrow ZnS + Pb^{++}$	0.0014	3.89	0.61	1.7×10^{-5}
$Zn^{++} + FeS_2 \rightarrow + ZnS + S?$	0.0014	2.30	1.0	3.5×10^{-5}
$Cu^{++} + ZnS \rightarrow CuS + Zn^{++}$	0.0009	1.32	1.3	3×10^{-5}
$Cu^{++} + FeS_2 \rightarrow CuS + Fe^{++} + S?$	0.0030	1.08	1.3	7.5×10^{-5}
$Pb^{++} + ZnS \rightarrow Zn^{++} + PbS$	0.0005	0.74	1.6	1.5×10^{-5}
$Pb^{++} + FeS_2 \rightarrow PbS + Fe^{++} + S?$	0.0001	0.16	1.6	0.25×10^{-5}

REPLACEMENT OF SULFIDES BY OTHER SULFIDES

Statement

A considerable amount of work was done in attempting to investigate a different type of replacement, in which the guest has an ion in common with the host. An example is the replacement of sphalerite by galena. Experimentation was done entirely at room temperature. Crystals or cleavage fragments of galena, sphalerite, and pyrite were suspended in solutions of zinc, copper, or iron salts. A number of possible combinations were run. The solid sulfides were spun on the end of a string in the solution of the metal salt. The specimens were weighed before and after the experiment (Table 10).

Discussion of Results

No discernible replacement occurred in any of the runs. On the contrary, every experiment, regardless of the solution used or the solid suspended, resulted in a loss of weight of the solid. If any precipitation of the guest occurred, it was as a colloid in the solution. This conclusion is corroborated by a single

high temperature run in which galena fragments were suspended in a concentrated cupric chloride solution. The galena disappeared almost instantaneously with the attendant formation of a dense brown copper sulfide sol. So much galena was dissolved that the concentration of lead resulting from the reaction was sufficient to precipitate small crystals of lead chloride.

The lower part of Table 10 includes the loss of weight of the solid as well as the ratio of weight lost to the original weight, for it was not certain, even though the runs were continued over several hundred hours, whether equilibrium was established. If it were, then loss of weight should be independent of the size of the original specimen chosen. There is some suggestion that equilibrium was not attained, because one very large specimen used was "out of place" relative to the others.

There seems to be a rough relation between the amount of reaction and the ratio of the ionic radius of the replacing ion to that of the replaced ion. When such ratios are calculated and placed in the Table, it is seen that the most rapid reaction takes place when the difference between the ionic radius of the replacing ion and that of the replaced ion is a minimum. Furthermore, there is no constant relationship between the activity products of the replaced and replacing compounds. For example, it would be predicted on the basis of activity products that copper would react more rapidly with zinc sulfide than with lead sulfide, for the activity product of zinc sulfide is approximately one million times as great as that for lead sulfide (Verhoogen, 1938, p. 47). The reverse relation is found.

A reaction occurred in every case, and the rates, as measured by the concentration of the replaced ion in the solution, were all of the same order of magnitude. In this sense the results seem to correlate very well with observed geologic behavior, in that if enough ore deposits are examined, nearly every sulfide seems to show replacement relations with nearly every other sulfide.

A large number of reactions between dilute solutions and sulfides were attempted using various reagents, running the reactions at various temperatures and for different lengths of time. None produced any significant replacement. The most successful experiment produced a microscopically thin film of copper sulfide on a cleavage fragment of galena.

Experiments on replacements of the type in which an ion from the solution displaces an ion in the solid were not pursued at greater length, because of the extensive experimental work done by Schouten (1934, p. 611–659) and theoretical work by Ridge (1949, p. 522–549). Schouten's results were very different from ours, apparently because he used more concentrated solutions and higher temperatures. He produced a great many different kinds of replacements, and in his experiments the replacing material remained *in situ*, whereas in ours it apparently was lost as colloidal material in the replacing solution. Very little is known about the problem of adherence or loss of replaced film at a surface, but in most field occurrences where open space is at a premium and rate of flow of solutions probably very slow, it is unlikely that much transportation of the replacing material would take place. However, the fact that we did produce stable colloids in some of our experiments suggests that, at places of open circulation, colloids may be produced in significant quantities and transported from the site of reaction.

There is much controversy as to the mechanism of replacements of this "ion exchange type". First, is the host dissolved and the guest simultaneously precipitated at the reaction front, or is the guest formed by diffusion of the metal ion through the crystal lattice? Ridge (personal communication) conceives the process as one of solid diffusion. Presumably the original crystal lattice is not seriously changed, and replacement of galena by sphalerite, for example, would take place by migration of lead ions into and zinc ions out of the original grains. The sulfide ion might reorient when it gains its new partner, but would always be considered in the "solid" state. Second, how do the guest ions migrate through the film of new material—by "solid" diffusion or by intergranular diffusion? Ridge believes that, where one sulfide becomes surrounded by a rim of another, the "feeding" of the replacing ion to the reaction front also takes place by solid diffusion. Such a process

may occur in some of the metallic sulfides, but a demonstration of its feasibility rests upon the quantitative determination of the coefficients of solid diffusion in the sulfides.

Some of the replacements attempted in the course of our work have tended to make us lean toward a mechanism with all transport by intergranular diffusion—the host is dissolved and the guest simultaneously precipitated at the reaction face, and "feeding" to the reaction face takes place between the grains. Among these was the complete sealing off to calcite surfaces by atacamite films, which can be explained as the formation of a non-porous film at the calcite surface. Such a film would prevent intergranular diffusion, but not solid diffusion. Also several attempts to replace calcite with lead carbonate by suspending calcite in lead chloride or lead nitrate solutions resulted in no detectable reaction. The weight of the calcite rhomb used was the same at the beginning of a run as at the end. This result is explainable if it is assumed that a mono-molecular layer of lead carbonate is formed at the calcite surface which prevents further access of lead ions to the carbonate ions within the monolayer. Apparently the reaction was stopped because of lack of migration through the lattice. Also, Schouten was impressed by the high porosity of many of his replacement products. Such porosity would permit intergranular diffusion to the reaction face, but would make it extremely difficult for movement of ions through the replacing solid particles.

The two cases cited here are, of course, examples of replacement of non-metallic compounds in which solid diffusion would not be expected except at extremely high temperatures, and probably should not be used as a parallel to replacement of sulfide by sulfide, yet the nature of replacement relations in many mineral deposits does not differ strikingly between metallic sulfide and non-metallic minerals. A very high percentage of Schouten's experiments of the "ion exchange type" were of the metal sulfide—non-metallic type.

There is little doubt that both intergranular and solid diffusion are operative to some degree; migration of ions through some metallic substances goes on with considerable facility even at low temperatures. But the relative role of each is still undetermined.

Some Mechanisms of Precipitation, Exclusive of Reaction with Solids

Introduction

The only mechanism of precipitation that has been considered so far in this paper is deposition of the guest as a result of reaction with the host. Our work indicates that reaction is the major factor in metasomatism, and most of our attention has been directed toward this phase of mineral deposition. But, during the experiments, some other mechanisms were observed that may be of interest in the more general problem of mineral deposition, and some data were collected. The following discussion makes no attempt to cover the manifold mechanisms that must operate to cause mineral formation, but represents comments on but two of them.

Precipitation by Dilution

We were impressed by the number of cases we discovered in which precipitation could be caused either by dilution or concentration of the solution. If an acid (by hydrolysis' copper chloride or copper sulfate solution is partially neutralized with sodium hydroxide, so that it is just on the verge of precipitating the basic sulfate or chloride, it can be concentrated by evaporation, with the eventual precipitation of the simple sulfate or chloride. But if diluted, the basic chloride or sulfate is precipitated immediately.

The same general relation can be observed when mercury sulfide is dissolved as an $HgS_2^=$ complex in a sodium hydroxide-sodium sulfide solution. If the solution is evaporated slowly, brilliant red crystals of cinnabar as much as 0.1 or 0.2 mm. long can be obtained; if it is diluted, black metacinnabar is formed. As a sidelight, it was noted that both phases precipitated from strongly alkaline solutions—one by concentration, the other by dilution, so that the black metacinnabar can hardly be cited as evidence of acidity. A detailed discussion of mercury sulfide relationships can be found in Dreyer's work (1940).

Lead sulfide can be precipitated by dilution

of saturated acid solution rich in sodium chloride.

These three cases fall in a broad category—destruction of ionic complexes by dilution. Complexes depend for their presence on the mass action effect of individual ions; dilution usually decreases the quantity of ions held in combined form. The dilution effect can be expected where solutions mingle—the most common of these may be where juvenile and meteoric waters meet.

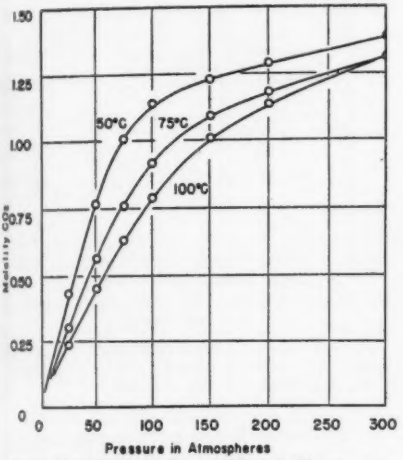

FIGURE 33.—SOLUBILITY OF CO_2 IN WATER AS A FUNCTION OF HYDROSTATIC PRESSURE AND TEMPERATURE

From Seidell (1940), after Haehnel (1920).

Precipitation by Gas Loss

Two systems of considerable geologic interest are the system CO_2-solution and H_2S-solution. In the course of this work, some data were collected on the solubilities of these gases as functions of temperature and pressure. Figure 33 shows the solubility of CO_2 in water as a function of temperature and pressure, and Figure 34 shows available data for H_2S. The H_2S curve follows the law of gas solubility (solubility α pressure) admirably, and so does CO_2 over the same range of pressure. At higher pressures, CO_2 deviates markedly from ideal behavior, and the solubility is much less than that expected for an ideal gas.

The opposite effects of temperature and pressure point up the fact that the effect of increased pressure at depth in the earth is largely offset by the corresponding temperature increase. In Figure 35, the solubility of CO_2 is shown as a function of depth, on the assumption of a hydrostatic pressure (30 feet = 1 atmosphere) and a normal geothermal gradient (1°C. = 100 feet). Solubility is almost constant at depths greater than 4000 feet, but a solution saturated at that depth would lose its CO_2 fairly uniformly between that depth and the surface.

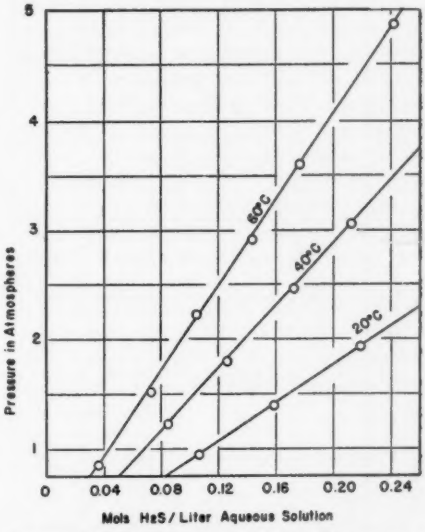

FIGURE 34.—SOLUBILITY OF H_2S IN WATER AS A FUNCTION OF HYDROSTATIC PRESSURE AND TEMPERATURE

From Seidell (1940).

The picture for H_2S probably is much the same, although data are not available at high pressures.

It is possible that in some cases the pH of a solution is controlled by its CO_2 and H_2S content, although many other factors are at work. Figure 36 shows the change in pH in such a system, where the hydrogen ion concentration is controlled entirely by dissolved CO_2, with its consequent distribution into HCO_3^-, H_2CO_3, and $CO_3^=$. The CO_2 "a" curve and the pH "a" curve are calculated for a normal geothermal gradient and a hydrostatic pressure increase

with depth; the "b" curves show the effect of a "driving pressure" and an abnormal surface temperature as well as an abnormal gradient. In both cases, the CO_2-induced pH curve

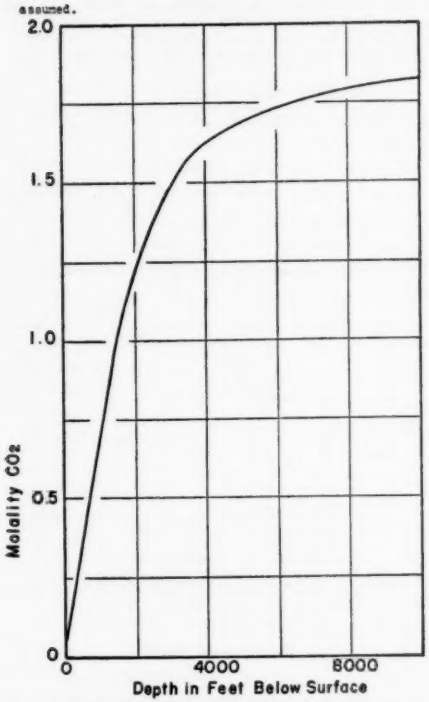

FIGURE 35.—SOLUBILITY OF CO_2 AS A FUNCTION OF DEPTH

Hydrostatic pressure and normal geothermal gradient assumed.

parallels the solubility curve, and neutralization would take place progressively by boiling off of the gas. The effect of H_2S-CO_2 mixtures should be very similar, for their first and second dissociation constants are both of the same order of magnitude.

This "boiling off" effect may conceivably be an important process in some epithermal deposits, as loss of gas and corresponding large pH change takes place in the upper 4000 feet of travel. It also, of course, may be effective whenever there is marked pressure drop, as in the passage of solution through a relatively tight rock, from a vein under high pressure to one under lower pressure.

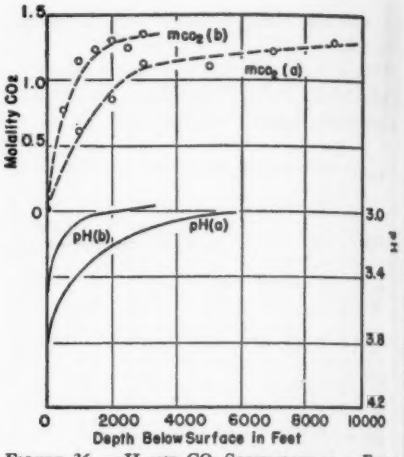

FIGURE 36.—pH AND CO_2 SOLUBILITY AS A FUNCTION OF DEPTH

Curves *a* are for normal geothermal gradient and hydrostatic pressure; curves *b* are for 1°C./10 feet and 1 atmosphere/10 feet gradient.

RELATIVE ROLES OF POROSITY AND PERMEABILITY IN CONTROL OF MINERAL DEPOSITION

Introduction

Sufficient information is now available to make semi-quantitative estimates of the relative roles of porosity and permeability in the formation of replacement deposits, and to make suggestions concerning the nature of the rocks most amenable to replacement by virtue of a proper combination of these properties.

Rove (1947, p. 57–58) has studied the permeability of a large number of mineralized limestones, and Brown (1947, p. 536–537) determined that of the rocks involved in ore deposition at the Edwards and Balmat mines. Both investigators were impressed by the very low values they obtained, and both agree that the primary permeability of the rocks they studied is too low to have permitted access of sufficient quantities of mineralizing solutions. The actual values of permeability as determined by Rove range chiefly between 10^{-4} and 10^{-6} millidarcys. Very few of his determinations gave values of 10^{-3} or less, and a great many were of the magnitude of 10^{-6}.

Such determinations always must be open to the question as to whether they represent

the permeability of the rock where it has been mineralized. The stand may be taken that the zones actually replaced were more highly permeable, and that any unmineralized specimens obtained must necessarily represent unfavorable material. This objection can be refuted, at least in part, because high permeability must extend beyond the actual zone mineralized, in order to permit passage of the necessary solutions.

TABLE 11.—PERMEABILITY OF MAJOR ORE BEDS IN THE TRI-STATE LEAD-ZINC DISTRICT
(From Rove, 1947)

Specimen No.	Horizon	No. of Tests	Ore Horizon Importance	Permeability Millidarcys
3	H	2	1	0.000,036
7	J	1	3	0.000,006,3
4	K (upper half)	6	1	0.000,002,3
5	M (middle)	2	1	0.000,035
6	M (middle to lower)	2	1	0.000,002,7
1	M (lower to middle)	2	2	0.000,036
2	M (lower)	7	2	0.000,11

Average (excluding specimen #2) approximately 10^{-4} millidarcys.

In spite of our lack of quantitative knowledge concerning the actual concentrations of the materials in the solutions that cause replacement, it still is possible to analyze the problem, for the susceptibility of a bed to mineralization can be shown to depend upon the permeability-porosity ratio, and is to a considerable extent independent of absolute concentration.

It is necessary to limit this discussion to low temperature deposits. The permeability of the mineralized rocks of the Tri-State district will be used as a representative example. For convenience in the discussion, one of Rove's tables (p. 75) is reproduced here (Table 11).

Diffusion coefficients at 100°C., the probable temperature of formation of some low-temperature replacement deposits (Newhouse, 1932, p. 749–750), are known within a relatively small percentage of error (Garrels, Dreyer, and Howland, 1949, p. 1819). If concentrations and pressure gradients are assumed, it is possible to calculate the relative quantities of material carried by diffusion and by forced flow of solution.

We can take as our problem the length of time for the formation, by replacement of limestone, of a 32 cm thick layer of galena at each wall of a planar vein. Assumptions concerning temperature, pressure, and concentration are necessary, but since the same assumptions have to be made for each calculation, the problem of relative effectiveness can be solved. If a solution is moving along a planar vertical fissure, replacement of adjacent limestone can be conceived as occurring: (1) by movement of the replacing ions into the limestone by diffusion down a concentration gradient, with concomitant solution of the limestone and back-diffusion of the dissolved ions into the vein, or (2) by horizontal forced flow of the solution from the vein through the pores of the limestone into the adjacent fissures down a pressure gradient.

Time Necessary for Replacement by Diffusion

As the solution moves along the vertical fissure, it will react with the limestone immediately adjacent to the fissure, dissolving the limestone and precipitating a sulfide or a combination of sulfides. For convenience, lead sulfide is chosen as the replacing material. After the first thin film of galena has been formed, the solution will continue to diffuse through any residual porosity that remains in the galena to the unreplaced limestone, and this process will be continued until a layer of stipulated thickness is formed (32 cm.). As shown by the calculations, the rate of replacement is so slow that a linear concentration gradient will be maintained at all times. Consequently, the length of time for the formation of a 32-cm. layer of galena under a constantly decreasing linear concentration gradient is the same as the time necessary to deliver the same total amount of galena a distance of 16 cm. under a constant linear concentration gradient.

If various concentrations of soluble lead in the solution and various residual porosities of the precipitated galena are assumed, it is possible to calculate the time in years necessary for the formation of such a galena layer. The

TABLE 12.—TIME FOR FORMATION OF A REPLACEMENT DEPOSIT OF GALENA 32 CENTIMETERS THICK AT THE WALL OF A PLANAR VEIN

Time in years

	Concentration Soluble Lead in Equivalents per Liter					
	10^{-1}	10^{-2}	10^{-3}	10^{-4}	10^{-5}	10^{-6}
A. Diffusion						
Effective Porosity of Precipitated Galena 5%.....	5.7×10^3	5.7×10^4	5.7×10^5	5.7×10^6	5.7×10^7	5.7×10^8
Effective Porosity of Precipitated Galena 10%.....	2.9×10^3	2.9×10^4	2.9×10^5	2.9×10^6	2.9×10^7	2.9×10^8
B. Forced Flow (Permeability 10^{-4} millidarcys)						
Pressure Gradient (Atmospheres per foot)						
10	1.6×10^6	1.6×10^7	1.6×10^8	1.6×10^9	1.6×10^{10}	1.6×10^{11}
1.0	1.6×10^7	1.6×10^8	1.6×10^9	1.6×10^{10}	1.6×10^{11}	1.6×10^{12}
0.1	1.6×10^8	1.6×10^9	1.6×10^{10}	1.6×10^{11}	1.6×10^{12}	1.6×10^{13}
0.01	1.6×10^9	1.6×10^{10}	1.6×10^{11}	1.6×10^{12}	1.6×10^{13}	1.6×10^{14}

Primary Permeability Necessary for Forced Flow to be as Effective as Diffusion, Expressed as a Function of Pressure Gradient

Pressure Gradient (Atmospheres per Foot)	Primary Permeability (millidarcys)
10	3×10^{-2}
1.0	3×10^{-1}
0.1	3
0.01	30

pertinent equation in this case is (Garrels, Dreyer, and Howland, 1949, p. 1826):

$$q = \frac{D(C' - C'')At}{l} \qquad (1)$$

where q is the quantity of galena deposited in equivalents, D is the diffusion coefficient expressed in cm.²/day, C' is the concentration of the diffusing substance in the vein in equivalents per cubic centimeter, C'' is the concentration at the reaction front, A is the cross sectional area in cm.² through which diffusion occurs, t is the time in days, and l is the distance of diffusion in centimeters.

In the example chosen, it is convenient to calculate the time for the formation of a prism of galena 32 cm. long and 1 cm.² in cross section. Such a prism would contain:

$32 \times 7.5 = 240$ grams of galena $= 2$ equivalents.

So q in equation #1 is 2 equivalents. The diffusion coefficient of the diffusing lead and sulfide ions is very close to 3 cm.²/day (Garrels, Dreyer, and Howland, 1949, p. 1819) at 100° C. Values of C', the concentration in the vein, can be assumed; and the value of C'', the concentration at the reaction front, can be assumed to be very small relative to C', so that $C' - C'' = C'$. The cross-sectional area of the galena prism is one square centimeter, so that the value of A, the *effective directional porosity*, must be assumed to be some fraction of 1 cm.². In the calculations values of 0.05 and 0.10 cm.² were chosen. The length l through which the lead

and sulfide ions must diffuse is 16 cm. (the average distance).

For a sample calculation, assuming a concentration in the vein of 10^{-1} equivalents per liter, or 1×10^{-4} equivalents per cc., and an effective cross-sectional area of 0.05 cm.^{2}:

$$2 = \frac{3 \times 1 \times 10^{-4} \times 5 \times 10^{-2} \times t}{16};$$

$$t = 2.1 \times 10^8 \text{ days} = 5.7 \times 10^5 \text{ years.}$$

Results of calculations based on this equation are given in Table 12.

Time Necessary for Replacement by Forced Flow

In the case of forced flow, it is assumed that the solutions move horizontally away from the fissure through the limestone down a pressure gradient, caused by a difference in pressure between the fissure carrying the solution and some adjacent fissure of easier relief of pressure. Solutions would move through the pores of the limestone, dissolving the limestone and precipitating the galena. By assuming concentrations and also pressure gradients, it is possible to calculate the length of time necessary to pass enough solution through the limestone to deposit the requisite amount of galena. A primary permeability of 10^{-4} millidarcys (ten times the average of the Tri-State rocks) is assumed.

The quantity of solution that will pass through the limestone can be calculated from the equation:

$$q = KPAt$$

where q is equal to the volume of solution that will pass through a given section, K is the permeability in Darcys, P is the pressure gradient in atmospheres per centimeter, A is the cross-sectional area in centimeters^2, and t is the time in seconds. Viscosity of the fluid is assumed to be unity. The results of these calculations also are shown in Table 12.

Discussion

The results of these calculations show that a 32 cm. thick layer of galena immediately adjacent to a vein can be formed in a much shorter time by diffusion than by forced flow under almost any conceivable pressure gradient. It is noted that the time required for replacement by forced flow is almost 300 times as great as that for diffusion, even under a pressure gradient of 10 atmospheres per foot. Such a gradient probably is much greater than any actually encountered in nature, for it would represent conditions in which a pressure of 1000 atmospheres existed in a vein within 100 feet of another opening with a pressure of but 1 atmosphere. Also it is noted that the relative effectiveness is independent of any particular assumed concentration, and that the orders of magnitude of the times involved for complete replacement by forced flow are all too great to have been effective in forming sulfide replacement deposits, even on the geologic time scale. The results of these calculations are in accord with Rove and Brown's conclusions that primary permeability is not sufficient to allow the transmittal of significant quantities of solutions through many ore-bearing rocks.

As a kind of postscript to the table, a calculation has been made of the primary permeability that would be necessary to be as effective as diffusion in forming a replacement deposit. Again it was necessary to express this permeability in terms of the pressure gradient. This calculation shows that the necessary permeabilities, even under extreme pressure gradients, are larger than any of those measured by Rove in his examination of mineralized rocks.

It must be remembered that this calculation of relative effectiveness is for the complete replacement of a rock immediately adjacent to a fissure, and the time required to form a 32 cm. thick layer of galena several hundred centimeters away from the feeding vein would be very much greater, whereas there would be no change in the time necessary to form such a deposit by forced flow.

These calculations are in accord then with the conclusion by several authors that the access of replacing solutions to rocks is through fractures, or so-called "secondary permeability". If this be true, then it is a necessary consequence that the actual replacement must be entirely by diffusion, for if it is considered that solutions are moving horizontally outward through a limestone along two parallel cracks, it is highly unlikely that there will be any significant pressure difference between the two

cracks. If the cracks are part of a zone of brecciation, we can be sure that no pressure difference will exist. Therefore, there will be no tendency whatsoever for solutions to move through the rock separating the fractures.

A picture evolves of a period of fracturing, which allows easy access of the solutions, followed by movement of the solutions through the fractures and the gradual replacement of the intervening rock masses by diffusion. It is possible to make a rough calculation of the maximum fracture spacing that will allow complete replacement of a limestone by this process. Concentrations and times must be assumed. A value of the diffusion coefficient of 3 cm.^{2} per day (corresponding to 100° C.) is used in these calculations.

TABLE 13.—REPLACEMENT OF ROCK

Concentration of Solution	Fracture Spacing	Time in Years
10^{-4} equivalents/liter	0.01 cm.	10^3
10^{-6} equivalents/liter	0.01 cm.	10^5
10^{-4} equivalents/liter	1.1 cm.	10^5
10^{-6} equivalents/liter	0.0001 cm.	10^3

If the most likely concentration of individual metals in vein solutions is taken as the range from 10^{-4} to 10^{-6} mols per liter, and the range of time available is from a thousand to a hundred thousand years, it becomes possible to calculate the spacing of the fractures that will allow complete replacement of a given rock layer (Table 13). The crack spacing would be twice the thickness of the sulfide layer that would be deposited.

In a sense, these calculations show that the assumed minimum concentration is a reasonable one, for with still smaller concentration even a time of 100,000 years would be so short that the required fracture spacing would be impossibly close. On the other hand, it suggests that the maximum concentration chosen may be too low.

The Wisconsin lead-zinc ores commonly have an alteration zone in the country rock adjacent to the fractures that extends several centimeters, and is composed, in many specimens, of approximately 50 per cent pyrite. Many such zones are isolated between mineralized fractures, so that there is little question that they represent diffusion from the fracture. The results of a calculation of the time necessary for the formation of such a zone, assuming various concentrations of iron in the fissure, are as follows:

Width of Zone, 2 Cm.; Assumed Porosity, 10%; Pyrite Content, 50%; Assumed Temperature, 100° C.

Concentration Iron	*Time*
10^{-4} mols/liter	7,000 Years
10^{-5} mols/liter	70,000 Years
10^{-6} mols/liter	700,000 Years

In this case, it can be pointed out that massive replacement would have taken place if the fracture spacing had been of the order of 1 or 2 cm.

In these ores, galena and sphalerite are confined to the fractures, and a thin layer (approximately 1 mm.) of pyrite lines the walls. It is suggested that the early stage of mineralization was very poor in lead and zinc, and that galena and sphalerite deposits did not occur until after the walls became "armored" by a non-porous film of pyrite. An alternative to this, suggested by the ore texture, is that galena and sphalerite were carried as colloids, whereas iron was in solution in significant amounts. This could account for simultaneous diffusion into the walls of the iron and sulphur, and the retention of the nondiffusing colloids in the open fractures.

SUMMARY

Metasomatic volume-for-volume replacements of limestone (in those cases in which the host rock and replacing mineral contain no common ions) again have been synthesized in the laboratory. However, we qualify the term volume-for-volume to mean a replacement providing a textural duplication of the replaced rock. The volume of replacing mineral may thus be slightly greater than the volume of the host replaced but, under the condition studied, not less. The replacement mechanism apparently involves a continual solution of the host and deposition of the guest at the replacement front. The processes involved can be considered separately. The solution of the limestone is accompanied by precipitation of the new min-

erals. In the cases studied, the changes in the character of the solution resulting from the solution of calcium carbonate are responsible for the precipitation of the new material. Consequently, the keys to the replacement process are the factors controlling calcium carbonate solubility.

Correlation of data regarding the solubility of calcium carbonate indicates that, while solubility is a function of at least five variables, pH is by far the most important; a pH decrease of one unit causes approximately a hundredfold increase in solubility. The second most important control is the ionic strength of the solution. The effect of an increase in ionic strength of 0.7 is to increase solubility by a factor of approximately 10. The effect of temperature changes of a few tens of degrees or of pressure changes of a few hundreds of bars are shown to be small. Rate of solution of calcite was studied as a function of pH and temperature. Rate of solution increases with increase in temperature by a factor of approximately two-fold for each 20° rise in temperature up to 56° C. and increases with decreasing pH by a factor of approximately twofold for each pH unit.

The replacing materials in our laboratory experiments were atacamite and brochantite whereas the product in nature usually is malachite. Concentration-pH relationships for copper chloride and copper sulfate solutions show that these products will form at calcite surfaces when concentrations are in excess of $10^{-8.5}$. The theoretical precipitation curve for malachite suggests that it is the stable form at lower concentrations. These data do much to reinforce prevalent concepts of the extreme dilution of many supergene solutions.

The replacement of calcite or of limestones by atacamite in copper chloride solutions (under the particular laboratory conditions described) results in the formation of a nonporous atacamite barrier a fraction of a millimeter in thickness. The nonporous barrier indicates an excess of precipitation over solution showing that the process is not exactly volume-for-volume in character although the textural details of the limestone are preserved. The thickness of the replacement layer is almost independent of the effective porosity of the host rock. The resulting replacement layer breaks cleanly from the replaced rock much as though the layer were formed by crustification rather than by replacement. If excess acid is added to the copper chloride solution so that the amount of dissolved calcite is increased, the replacement process is found to continue indefinitely. When solutions were forced through limestone under pressure adding actual bodily movement of the solution to the diffusion effect, much deeper replacement resulted although, as before, the process eventually stopped. The effect of pressure apparently was to break through the original layer mechanically. Solution, and thus replacement, moved outward along channels of higher permeability. In both the diffusion and forced flow experiments, the replacement process comes to a stop if the ratio of guest precipitated to host dissolved is greater than one. The depth of replacement becomes smaller as the ratio increases and also is controlled somewhat by the original porosity of the rock.

In natural replacement, open spaces characteristically fill before any significant replacement occurs. The composition of the replacement products, in many places, indicates an oscillation in composition of the replacing solutions.

Although the mineralogy of natural replacements is not the same as that of the synthetic ones, the difference is caused by the presence of more ions than could be used in a controlled system in the laboratory. On the other hand, textures are strikingly similar with the exception that grain size in the natural replacements is usually larger.

In a system containing both iron and copper chlorides, calcite was replaced both by iron oxide and by atacamite. There was a clearly marked order of reaction; iron oxide formed first. The mechanism of replacement of calcite by iron oxide or by basic copper solutions is the same.

The original grain size of the replacement products is explained as a function of their rate of formation. As indicated in numerous earlier studies, the more rapid the precipitation, the finer grain size. The grain size of the products studied was increased markedly, in some cases, by aging for 6 months at temperatures of 90° C. Fineness of grain, therefore, carries an implication of a relatively high rate of reaction.

The replacements by copper and iron indicate, by analogy, that sulfide replacements occur under conditions in which the sulfides are held as complexes, that the replacement is pH controlled, and that the mechanism is essentially identical.

Replacements of sulfides by other sulfides, using dilute solutions, were generally unsuccessful but a colloidal precipitate was produced.

Calculations of the relative importance of diffusion versus forced flow indicate that primary permeability ordinarily is too low to permit extensive replacement, and that ideal conditions for replacement occur where there are numerous small, closely spaced, secondary openings creating a somewhat higher secondary permeability.

The mechanism of natural limestone replacement is unquestionably more complex than the synthetic process we have studied. Although this study reports only one aspect of the chemical and physical environment involved in replacement, it is hoped that the data here established can be used in the examination of more complex replacement systems.

References Cited

Allen, E. T., Johnson, John, and Larsen, E. T., (1912) *The mineral sulfides of iron*, Am. Jour. Sci., 4th ser., vol. 33, p. 169–236.

Bandy, Mark (1940) *A theory of mineral sequence in hypogene ore deposits*, Pt. I, Econ. Geol., vol. 35, p. 359–382; Pt. II, pp. 546–571.

Bateman, Alan (1950) *Economic mineral deposits*, John Wiley and Sons, New York.

Becker, G. F. (1897) *Note on computing diffusion*, Am. Jour. Sci. 4th ser., vol. 3, p. 280–286.

Brown, John S. (1947) *Porosity and ore deposition at Edwards and Balmat, New York*, Geol. Soc. Am., Bull., vol. 58, p. 505–545.

Castano, J. R. and Garrels, R. M. (1950) *Experiments on the deposition of iron with special reference to the Clinton Iron Ore Deposits*, Econ. Geol., vol. 45, no. 8, p. 755–770.

Cooper, L. H. N. (1937) *Some conditions governing the solubility of iron*, Royal Soc. London, Pr., ser. B., vol. 124, p. 305.

Dreyer, R. M. (1940) *The geochemistry of quicksilver mineralization*, Econ. Geol., vol. 35, p. 17–48; 140–157.

Duffell, Stanley (1937) *Diffusion and its relation to ore deposition*, Econ. Geol., vol. 32, p. 494–510.

Ferrari, Adolfo, and Sessi, Luigi (1937) *Velocita di Soluzione Negli Acidi dei Carbonato Rombvedrici Bivalenti*, Gazetta Chimica Ital., vol. 67, pp. 501–510.

Foote, H. W., and Bradley, W. M. (1913) *Solid solution in minerals: IV. The composition of amorphous minerals as illustrated by chrysocolla*, Am. Jour. Sci., vol. 36, p. 180–184.

Garrels, R. M. (1941) *The Mississippi Valley type lead-zinc deposits and the problem of mineral zoning*, Econ. Geol., vol. 36, p. 729–744.

—— (1944) *Solubility of metal sulfides in dilute vein-forming solutions*, Econ. Geol., vol. 39, p. 477.

—— and Stine, L. P. (1947) *Replacement of calcite by atacamite in copper chloride solutions*, Econ. Geol., vol. 43, p. 21–30.

——; Dreyer, R. M.; and Howland, A. L. (1949) *Diffusion of ions through intergranular spaces in water-saturated rocks*, Geol. Soc. Am., Bull., vol. 60, p. 1809–1828.

Holser, W. T. (1947) *Metasomatic processes*, Econ. Geol., vol. 42, p. 384–395.

International Critical Tables (1929) vol. 5.

Kelley, K. K., and Anderson, C. T. (1935) *Contributions to the data on theoretical metallurgy. IV. Metal carbonates—correlations and applications of thermodynamic properties*, U. S. Bur. mines, Bull. 384, 73 pp.

Kolthoff, I. M., and Sandell, E. B. (1938) *Textbook of quantitative inorganic analysis*, Macmillan, New York, 749 pp.

Kulp, J. Laurence, and Trites, A. F. (1951) *Differential thermal analysis of natural hydrous ferric oxides*, Am. Mineral., vol. 36, p. 23-44.

Lewis, G. N., and Randall, Merle (1923) *Thermodynamics*, McGraw-Hill, New York.

Lindgren, Waldemar (1933) *Mineral deposits*, 4th ed., McGraw-Hill, New York.

Lovering, T. S. (1949) *Rock alteration as a guide to ore—East Tintic District, Utah*, Econ. Geol., Mon. 1, 64 pp.

——; Huff, L. C.; and Almond, H. (1950) *Dispersion of copper from the San Manuel Copper Deposit, Penal County, Arizona*, Econ. Geol., vol. 45, p. 493–515.

Manov, G. G.; Bates, R. C.; Hamer, W. G.; and Acree, S. F. (1943) *Values of the constants in the Debye-Huckel Equation for activity coefficients*, Am. Chem. Soc., Jour., vol. 65, p. 1765–1787.

Newhouse, W. H. (1932) *The Composition of vein solutions as shown by liquid inclusions in minerals*, Econ. Geol., vol. 27, p. 428.

—— (1933) *The Temperature of formation of the Mississippi Valley lead-zinc deposits*, Econ. Geol., vol. 28, p. 740–750.

Owen, B. B., and Brinkley, S. R. (1941) *Calculation of the effect of pressure upon ionic equilibria in pure water and in salt solutions*, Chem. Rev. vol. 29, p. 461–474.

Ridge, John D. (1949) *Replacement and the equaling of volume and weight*, Jour. Geol., vol. 57, no. 5, p. 522–549.

Robinson, R. A., and Stokes, R. H. (1949a) *The Role of hydration in the Debye-Huckel Theory*, New York Acad. Sci., Ann., vol. 51, p. 593–604 (Symposium on Molecular Interaction).

—— —— —— (1949b) *Tables of osmotic and activity coefficients of electrolytes in aqueous solutions at 25° C.*, Faraday Soc., Tr., vol. 45, p. 620.

Rove, Olaf N. (1947) *Some physical characteristics of certain favorable and unfavorable ore horizons*, Econ. Geol., vol. 42, p. 57–78, 161–193.

Schouten, C. (1934) *Structures and textures of synthetic replacements*, Econ. Geol., vol. 29, no. 7, p. 611–659.

Seidell, A., (1940) *Solubilities of inorganic and metal*

organic compounds, D. Van Nostrand, New York, p. 223, 595.

Snead, M. C., and Maynard, J. L. (1942) *General inorganic chemistry*, D. Van Nostrand, New York, 1166 p.

Sverdrup, H. U., Johnson, M. V., and Fleming, R. H., (1942) *The Oceans*, Prentice-Hall, New York.

Taylor, H. S. (1925) *A Treatise on physical chemistry*, Vol. II, D. Van Nostrand, New York, p. 942–947.

Treadwell, W. D., and Hepenstrick, H. (1949) *Solubility of silver sulfide*, Helv. Chem. Acta, vol. 32, p. 1872–1879.

Verhoogen, Jean (1938) *Thermodynamical calculation of the solubility of some important sulfides, up to 400°C.*, Econ. Geol., vol. 33, p. 34–51, 777.

Weiser, H. B. (1939) *Colloid Chemistry*, 4th ed., John Wiley, New York, p. 125.

Whitman, A. R. (1928) *Diffusion in ore genesis*, Econ. Geol., vol. 23, p. 473–488.

NORTHWESTERN UNIVERSITY, EVANSTON, ILLINOIS; UNIVERSITY OF KANSAS, LAWRENCE, KANSAS.

MANUSCRIPT RECEIVED BY THE SECRETARY OF THE SOCIETY, MARCH 19, 1951

PROJECT GRANT 486/46/S47.

(Hanover)
(Mascoma)
(Cardigan)
72°15'
72°00'
43°30'
25'
20'
A
A'
B
B'
GRANTHAM
CROYDON
NEWPORT
SPRINGFIELD
LONDON
NEW
Grantham
Croydon
Newport
Springfield
New London
Sunapee
Lake Sunapee
Mt Kearsarge
Lake Sunapee
Croydon Flat
Croydon Mills
Sunapee Harbor
Newport
North Newport P.O.
Northville
Kelleyville
Sunapee Sta
Lake Sunapee
Little Sunapee Lake
Otter Pond
Ledge Pond
Rocky Bound Pond
Stocker Pond
Spectacle Pond
Cranberry Pond
Sanborn Pond
Ruby Lake
Mud Pond
Highwood Meadows
Blueberry Mtn
Mountainview
Sunapee Mtn
Mt Sunapee Ski Run
Howe Hill
Sanborn Hill
Leavitt Hill
Prospect Hill
Pitcher Hill
Royal Arch
Pinnacle
Spectacle Pond
Rocky Bound Pond
Baptist Pond
Baldface
Lovell Mtn
Lane Hill
Barnard Hill
Bald Mtn
Coit Mtn
Tucker Hill
Ryder Corner
Camels Hump
Baldface Mtn
Baldface Pond
Perkins Pond
Baldface Brook
Baldface Circle
Baldface Circle Pond
Baldface Circle Brook
Baldface Circle Trail
Baldface Circle Trail Brook
Baldface Circle Trail Pond
Baldface Circle Trail Brook
Baldface Circle Trail Pond
Baldface Circle Trail Brook
Baldface Circle Trail Pond

SECTION A-A'

SECTION B-B'

GEOLOGIC MAP AND STRUCTURE SECTIONS OF THE SUNAPEE QUADRANGLE, NEW HAMPSHIRE

Topographic base by U. S. Geological Survey. Surveyed in 1905

APPROXIMATE MEAN DECLINATION, 1905.

Scale 1/62500

1 0 1 2 3 4 Miles

5000 0 5000 10000 15000 20000 Feet

1 0 1 2 3 4 5 Kilometers

Contour interval 20 feet

Datum is mean sea level

Geology by Carleton A. Chapman, assisted by R. W. Chapman, F. C. Kruger, J. H. Fisher, R. H. Shaver, D. H. Amos, H. H. Murray, R. S. Roth, W. H. Smith, and B. M. Gray.

Geology surveyed in 1938, 1939, 1947, 1948, and 1949, with the aid of grants from the Research Board, University of Illinois, and the Shaler Memorial fund of Harvard University.
Published 1952

DEVONIAN

Lower?

Littleton formation
Hubbard Hill member
(Zone h: chiefly quartzite, mica-quartz schist and sillimanite schist with minor amounts of interbedded lime-silicate granulite and gneiss.)

Dl

Littleton formation
Undifferentiated
(Zone m: quartzite, mica-quartz schist, mica schist and staurolite schist. Zone h: sillimanite schist and mica-quartz schist.)

SILURIAN

Middle

Sfa Sf

Fitch formation
(Zones m and h: chiefly fine- to medium-grained, actinolite-feldspar and diopside-feldspar granulites and mica schist (Sf); quartzite (Sfq); amphibolite (Sfa).

Lower or Middle

Sc

Clough formation
(Zone m: chiefly quartz conglomerate, quartzite, and quartz-mica schist. Zone h: sillimanite schist, quartz-mica schist and quartzite.)

PROBABLY ORDOVICIAN

Upper?

Oam

Ammonoosuc volcanics
(Zones m and h: amphibolite, hornblende schist, and fine-grained biotite gneiss.)

METAMORPHIC ZONES

Shown below formation symbol thus: Dlh/h

m = middle-grade
h = high-grade

CONTACTS

Accurate

Approximate and Inferred

Gradational

SPECIAL SYMBOLS

Strike and dip of bedding

Strike of vertical beds

Horizontal beds

Strike and dip of foliation

Strike of vertical foliation

Horizontal foliation

D

Normal fault; D on downthrown side

S

Silicified fault zone

BULLETIN OF THE GEOLOGICAL SOCIETY OF AMERICA
VOL. 63, PP. 381-420, 3 FIGS., 2 PLS. APRIL 1952

STRUCTURE AND PETROLOGY OF THE SUNAPEE QUADRANGLE, NEW HAMPSHIRE

By Carleton A. Chapman

Abstract

The rocks of the Sunapee quadrangle, in southwestern New Hampshire, are chiefly metamorphic in origin nd range in age from upper Ordovician (?) to lower Devonian.

The pre-Devonian rocks, constituted by the Ammonoosuc volcanics, the Clough formation, and the itch formation, are confined to the northwest part of the quadrangle. They are nearly completely separated om the rest of the area by the Grantham fault, which is probably Triassic in age. The structure northwest f this normal fault consists of an elongate dome of granodiorite gneiss flanked and overlain by concordant yers of amphibolite, biotite gneiss, quartzite, and schist.

Immediately southeast of the fault is the Bethlehem gneiss. This mass occupies the central half of the uadrangle and is composed of well-foliated, "porphyritic" granitic gneiss. East of the gneiss is the Littleton rmation. The western (older) portion of this belt of rocks consists of well-bedded mica-sillimanite schist nd quartzite. To the east the rocks of this belt become somewhat coarser-grained and more gneissic. he most easterly portions contain little schist but consist predominately of mica and microcline gneiss. ast of the Littleton formation is the Kinsman quartz monzonite. This rock resembles the Bethlehem gneiss ut is generally coarser-textured and more poorly foliated.

Metamorphism, during the late Devonian time, was not uniform throughout the quadrangle. In general oning is well developed and ranges from the staurolite-kyanite subfacies, in the western part, to the lower ortion of the granulite facies in the eastern part of the area.

The structural relations and origin of foliation, lineation, major folds, tabular inclusions, large feldspar ystals, and pegmatites are considered in detail.

It is concluded that the area southeast of the Grantham fault originally consisted of a fairly uniform quence of pelitic rocks of the Littleton formation. As a result of regional metamorphism, these rocks were large part converted to coarse-grained, "porphyritic" feldspathic gneiss (Bethlehem gneiss and Kinsman uartz monzonite). Recrystallization and reconstitution of the original sediments were the predominant rocesses involved. Certain constituents are considered to have migrated from distances up to many miles, ut the source of this nomadic material may have been largely from the more deeply buried sedimentary cks.

In the Bethlehem gneiss, bedding planes controlled the development of foliation, and recrystallization nverted much muscovite into large porphyroblasts of potash feldspar. Considerable sodium and some lcium were introduced to form oligoclase-andesine. In the Kinsman quartz monzonite, recrystallization as so severe that foliation was more poorly developed, grain size was greatly increased, and nearly all uscovite was converted to huge microcline porphyroblasts. Also contributing to the formation of micro- ne was the potassium released in the conversion of biotite in the granulite (eastern) facies. Sodium and lcium were introduced quite thoroughly to form oligoclase-andesine. In the eastern part of the area, con- derable potassium was introduced to develop the phases very rich in microcline.

The history of these metamorphic-metasomatic rocks is extremely complicated but certain processes and quences are clear. There has been, apparently, a wholesale introduction of sodium, but potassium has been troduced only locally. Recrystallization and reconstitution were long-continued processes which began ior to the introduction of material. Minor bodies of magma were intruded, largely in the form of dikes d sills, in the later stages. These intrusives replaced much of the adjacent country rock and were them- ves altered by the introduction of material which was highly mobile up to a very late stage.

CONTENTS

TEXT

	Page
Introduction	382
General lithologic features	384
Ammonoosuc volcanics	384
Clough formation	385
Fitch formation	385
Littleton formation	386
General statement	386
Undifferentiated Littleton formation	387
Hubbard Hill member	387
General statement	387
Schist	388
Gneiss	388
Quartzite	389
Lime-silicate granulite	389
Dakin Hill member	390
General statement	390
Mica gneiss	390
Microcline gneiss	391
Schist, quartzite, and quartz conglomerate	391
Thickness	391
Corydon group	391
Bethlehem gneiss	392
Kinsman quartz monzonite	394
Spaulding quartz diorite	397
Quartz monzonite	399
Concord granite	400
Structural features	400
General statement	400
Structure west of the Bethlehem gneiss	400
Grantham fault	401
Hubbard Hill member	402
Dakin Hill member	403
Bethlehem gneiss	403
Foliation	403
Lineation	404
Contact zone	406
Pegmatite and aplite	407
Kinsman quartz monzonite	408
Late quartz-feldspar rocks	408
General statement	408
Spaulding quartz diorite	408
Quartz monzonite	409
Concord granite	409
Age relations	409
Origin of the Bethlehem gneiss and Kinsman quartz monzonite	410
General statement	410
Origin of foliation	411
Origin of large feldspar crystals	411
Origin of inclusions	414
Rock similarities	414
Gradational character	414
Evidence of replacement	416
Evidence of magmatic origin	417
Preferred theory	418
Origin of the late quartz-feldspar rocks	419
Metamorphic zoning	420
Conclusions and summary	422
References cited	425

ILLUSTRATIONS

Figure	Page
1. Index map	383
2. Relation between porphyroblast and foliation	413
3. Metamorphic zones in the Sunapee quadrangle	421

Plate	Facing page
1. Geologic map and structure sections of the Sunapee quadrangle, New Hampshire	381
2. Tectonic map of the Sunapee quadrangle, New Hampshire	424

TABLES

Table	Page
1. Estimated modes of the Littleton formation	389
2. Estimated modes of the Bethlehem gneiss and inclusions	393
3. Estimated modes of the Kinsman quartz monzonite and associated rocks	397
4. Estimated modes of the late quartz-feldspar rocks	399
5. Lineation of the Hubbard Hill member	403
6. Lineation of the Bethlehem gneiss	405
7. Chemical analyses of potash feldspar, Lovewell Mountain quadrangle, New Hampshire	412
8. Chemical analyses of metamorphic and plutonic rocks from New Hampshire	415

INTRODUCTION

The present investigation represents the first detailed study of the geology of the Sunapee quadrangle in west-central New Hampshire. The mapping of this quadrangle completes a continuous belt of recent field studies which extends from the northern part of New Hampshire to the Massachusetts line (Fig. 1). The present work was undertaken in hopes of securing new information which would lead to a clearer understanding of the nature and origin of the two large bodies of granitic gneiss known as the Bethlehem gneiss and Kinsman quartz monzonite. In the northwest corner of the area is a third large foliated body which is correlated with the Oliverian magma series. The results of a study of this body were published 10 years ago (Chapman, 1942), and no further field work in that part of the quadrangle was undertaken for the present publication. To make the present report complete, however, a very brief treatment of this gneissic mass, based on the earlier work, will be included here.

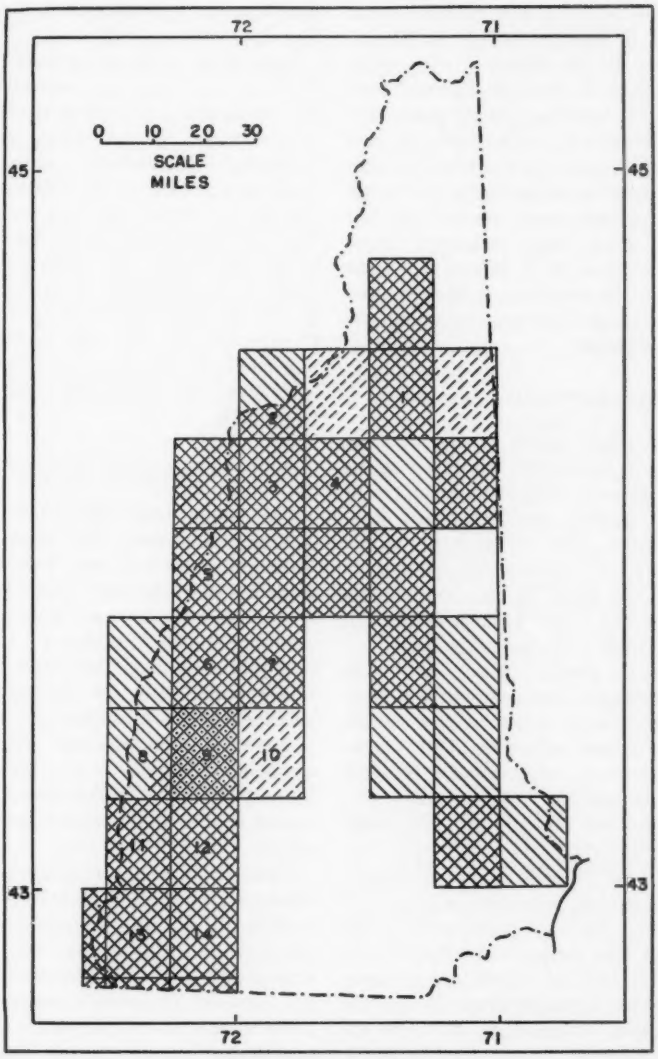

FIGURE 1.—INDEX MAP

Showing areas in New Hampshire for which geologic reports are published (cross-ruled), in which field mapping is completed (single-ruled), and in which field work is in progress (dash-ruled). Quadrangles to which reference is made are numbered: 1—Mt. Washington, 2—Littleton, 3—Moosilauke, 4—Franconia, 5—Mt. Cube, 6—Mascoma, 7—Cardigan, 8—Claremont, 9—Sunapee, 10—Mt. Kearsarge, 11—Bellows Falls, 12—Lovewell Mtn., 13—Keene, and 14—Monadnock.

The field work was carried on principally during the summers of 1947, 1948, and 1949. Shorter periods were spent in the field in 1938 and 1939. The total time spent in field work was 25 weeks.

Financial support for the field and laboratory work was made available by generous grants from the Research Board, University of Illinois and the Shaler Memorial Fund of Harvard University. The writer expresses

thanks to the following who assisted in the field studies: R. W. Chapman, F. C. Kruger, J. H. Fisher, R. H. Shaver, D. H. Amos, H. H. Murray, R. S. Roth, W. H. Smith, and B. M. Gray. The writer is especially indebted to Professor Marland P. Billings of Harvard University for suggestions in connection with the field work and for his assistance in securing the colored geologic map accompanying this report. The writer wishes to express sincere thanks to Professors A. F. Hagner and Hans Ramberg for the numerous suggestions and stimulating discussions in connection with the present investigation.

General Lithologic Features

The metamorphic rocks of the Sunapee quadrangle are represented chiefly by schist, gneiss, and quartzite with minor quantities of quartz conglomerate, amphibolite, and lime-silicate granulite. They belong chiefly to the high-grade zone of metamorphism, but middle-grade rocks are found in the northwestern corner of the area. The rocks range in age from upper Ordovician (?) to lower Devonian.

No evidence of geologic age was found in the Sunapee quadrangle. The rocks in the western part of the quadrangle, referred to as the undifferentiated Littleton formation (Pl. 1), can be traced continuously northeastward through the Mascoma and Mt. Cube quadrangles to the Littleton and Moosilauke quadrangles where Billings (1937) has determined their age to be lower Devonian. Stratigraphically below the Littleton formation is the Fitch formation which extends discontinuously northeastward to the Littleton-Moosilauke area where Billings (1937) has determined its age as middle Silurian. Stratigraphically below the Fitch formation, in descending order, are the Clough formation and Ammonoosuc volcanics. These formations can be traced almost without interruption to the Littleton-Moosilauke area. Billings (1937) showed the Clough formation to be of lower or middle Silurian age and the Ammonoosuc volcanics to be of probable upper Ordovician age. The metamorphic rocks in the eastern part of the area can be traced continuously to the Littleton-Moosilauke area where they are shown to be the high-grade metamorphic equivalents of the Littleton formation (Billings, 1937).

Three large bodies of "granite" gneiss are shown in Plate 1. In the northwest corner of the quadrangle is the gneiss of the Oliverian magma series. In the central part of the quadrangle is the Bethlehem gneiss, and in the southeastern part is the Kinsman quartz monzonite; both have been correlated with the New Hampshire magma series. Numerous small masses of younger rock ranging from quartz diorite to granite occur as sili- and dike-like bodies. Most abundant among these is the Concord granite. The large bodies of gneiss and most of the smaller masses of younger rock can be correlated with similar bodies of adjacent areas.

Ammonoosuc Volcanics

The Ammonoosuc volcanics outcrop along a nearly continuous belt from Grantham Mountain, at the north end of the quadrangle, to a point just west of the village of Northville. A somewhat smaller mass is poorly exposed west of Croydon Flat. The volcanics consist largely of amphibolite, hornblende schist, and biotite gneiss which, in adjacent areas, are believed to have been derived from volcanic tuff, breccia, and conglomerate. In the Sunapee quadrangle, however, metamorphism has apparently destroyed all evidence of their fragmental structure. A few flows may be represented.

Dark-green to black amphibolite and hornblende schist predominate. These rocks are medium-grained with more or less schistose structure. A strong lineation due to parallel arrangement of amphibole needles is occasionally observed. The essential minerals are blue-green hornblende and plagioclase (andesine or labrodorite) in approximately equal amounts and suggests that these rocks were originally basaltic. Minor constituents include epidote. Medium- to fine-grained biotite gneiss, composed of quartz, oligoclase or andesine, and biotite, occurs somewhat sporadically and is considered to represent metamorphosed dacitic rock. Apatite, sphene, and epidote occur in very minor quantities.

In the Sunapee quadrangle, only a few

hundred feet of the formation outcrop above the gneiss of the Oliverian magma series upon which the volcanics rest. On the east slope of Croydon Mountain, where the rocks have been only mildly folded, 300 feet of the formation is exposed.

Clough Formation

The Clough formation extends southward from Croydon Mountain, at the north end of the quadrangle, to just beyond Sugar River. A few small isolated patches occur immediately west and northwest of the village of Croydon Flat. The formation consists of quartz conglomerate, mica schist, and locally sillimanite schist. The quartzite is composed essentially of granoblastic quartz with a little biotite, muscovite, and plagioclase. The fresh material is white or gray but limonite staining is common. There are all gradations between quartzite and quartz conglomerate. Pebbles of the conglomerate are composed of vein quartz and quartzite and are commonly flattened parallel to the rock foliation.

All gradations appear between quartzite and mica schist. These schists are relatively coarse-grained and rich in quartz and muscovite. Biotite, garnet, and oligoclase are abundant only very locally. In the Clough formation west of Northville, considerable sillimanite occurs in the schist. Here the rock shows a pronounced lineation, a coarse texture, and a schistose to gneissose structure. Biotite, in addition to quartz, muscovite, and sillimanite, is an essential mineral in these rocks.

The maximum thickness of the Clough formation in the Sunapee quadrangle is calculated to be approximately 800 feet.

Fitch Formation

The Fitch formation outcrops in two areas in the western part of the quadrangle; along the western slope of Croydon Mountain and west of the village of Newport.

On Croydon Mountain, the formation is composed mostly of lime-silicate granulite with minor amounts of red-brown biotite schist. The lime-silicate rocks are fine- to medium-grained and exhibit a banded or blotchy appearance. Green blotches and layers consist chiefly of actinolite, oligoclase, and microcline; the white bands or blotches are comprised of diopside, oligoclase, and microcline. From this mineral composition it is concluded that the granulite was derived from arenaceous dolomite. The red-brown biotite schist is medium- to fine-grained and composed characteristically of red-brown biotite, actinolite, and calcite with varying proportions of microcline, oligoclase, and quartz. Hornblende, muscovite, garnet, epidote, and sphene are less commonly encountered. The mineral composition suggests that these schists were derived from various kinds of calcareous, dolomitic, and arenaceous shale.

From a point about 3 miles west of Newport village and extending south-southwesterly through Mt. Tug to the boundary of the area, there is a belt of rocks which was formerly correlated (Chapman, 1942) with the Ammonoosuc volcanics. More recent studies show quite conclusively, however, that these rocks are to be correlated with the rocks of the Fitch formation still further to the south-southwest. In fact the former belt can be traced continuously into the latter.

This earlier correlation was based on the following field observations. On Mt. Tug, the Bethlehem gneiss is in contact with and overlies approximately 75 feet of quartzite. The quartzite is grayish, well bedded, foliated parallel to bedding, and locally conglomeratic with quartz pebbles up to 2 inches across. Locally it contains garnet in aggregates up to an inch across and considerable sillimanite and coarse muscovite. It resembles the quartzite of the Clough formation. Immediately beneath the quartzite there is a dark amphibolite, at least 300 feet thick, which in many respects resembles the amphibolite of the Ammonoosuc volcanics. The rock ranges from medium- to coarse-grained and is composed mostly of hornblende and andesine with minor amounts of clinozoisite, quartz, sphene, and iron ores. The hornblende commonly exhibits prophyroblastic development. For these reasons the amphibolite and quartzite were mapped as belonging to the Ammonoosuc volcanics and the Clough formation respectively. To the west of the amphibolite, particularly south-southwest of Mt. Tug, exposures are poor, but the rocks observed are largely medium-grained mica schist of sedimentary origin. The more common types represented include silvery quartz-mica schist, mica schist and micaceous quartzite. Red-

brown biotite schist was less commonly encountered. These rocks consist largely of quartz, biotite, and muscovite in various proportions; biotite commonly forms as small porphyroblasts. These were earlier considered to represent special types in the Littleton formation and they were separated from the belt of amphibolite to the east by a normal fault.

Traced northward to the Sugar River, the quartzite maintains its same thickness, but here it disappears beneath the drift and valley fill. Traced southward the quartzite apparently pinches out. In the small stream immediately south of Mt. Tug, where a nearly continuous section is exposed, the amphibolite alternates with the quartzite up stream and with mica schist down stream. Bedding is well preserved in these rocks and its attitude is remarkably uniform. These facts, together with the absence of minor folds, strongly suggest that the alternation of rock types is due to interfingering relations between schist, amphibolite, and quartzite. The quartzite at the top of the section occupies a narrow belt here because of its interbedded relation with the amphibolite. This would explain why the quartzite pinches out to the south. The wide belt of amphibolite on Mt. Tug breaks down here, in the stream bed, into thin layers (1–20 feet thick) which alternate largely with mica schist. On the 1560-foot knoll to the southwest and for several miles farther southwest along the strike, the amphibolite contains few interbedded schist layers but appears to constitute a single rock unit. These facts suggest that the three rock types are interbedded and should not be mapped as separate formations.

The most characteristic rocks of the Fitch formation in western New Hampshire include lime-silicate rocks with occasional limestone or marble beds. These are found in abundance a short distance to the south-southwest of Mt. Tug, in the Claremont quadrangle. Here the light-green lime-silicate rocks are intermixed and interlayered with red-brown biotite schist. Overlying this typical assemblage is amphibolite which can be traced to the amphibolite mass on Mt. Tug. Locally this amphibolite contains considerable red-brown biotite, and the rock resembles that of the red-brown biotite schist interbedded with the underlying lime-silicate rocks. Locally one encounters hornblende, like that of the amphibolite, as a major constituent of the lime-silicate and associated rocks. Amphibolite layers, a few feet thick, were observed interbedded with the lime-silicate rocks and red-brown biotite schist.

Most of the schist beneath the amphibolite of Mt. Tug carries red-brown biotite in greater or less amounts; interbedded lime-silicate rocks, however, were not observed. When traced south-southwestward into the Claremont quadrangle, this schist appears to grade into the typical red-brown biotite schist of the Fitch formation; and the lime-silicate rocks become more abundant.

These relations strongly indicate that the large amphibolite mass should be considered as a member of the Fitch formation rather than part of the Ammonoosuc volcanics. The stratigraphic relations between the amphibolite and the overlying quartzite, as clearly seen in the little stream just south of Mt. Tug, would also favor placing the quartzite in the Fitch formation rather than correlating it with the Clough formation. The stratigraphic position of the mica schists beneath the amphibolite of Mt. Tug and the transitional nature of this rock into rocks typical of the Fitch formation, in the Claremont quadrangle, indicate the schists do not belong to the Littleton formation but are correlatives of the Fitch formation. It seems certain, therefore, that the quartzite, amphibolite and mica schist near Mt. Tug are now correctly correlated; they represent the Fitch formation which is overlain structurally by the Bethlehem gneiss.

The thickness of the Fitch formation probably does not exceed 800 feet anywhere in the area. The thickest section is believed to be in the vicinity of Mt. Tug. On Croydon Mountain, the formation is folded and the true thickness is estimated not to exceed 200 feet. To the north, the formation pinches out where it enters the Mascoma quadrangle.

Littleton Formation

General Statement

The Littleton formation is present in several widely separated areas in the Sunapee quadrangle. In the northwest corner, rocks of the Littleton formation overlie the Fitch formation and belong to the middle-grade zone of metamorphism. About 8 miles south of here and west of Kelleyville is a small area in which the rocks belong to the high-grade metamorphic zone. These rocks all lie west of the large body of Bethlehem gneiss and, for convenience, will be referred to as the undifferentiated Littleton formation. East of the Bethlehem gneiss, in the eastern third of the quadrangle, the Littleton formation occurs in a wide belt which appears to be cut into more or less disconnected masses by the Kinsman quartz mon-

zonite. These rocks belong to the high-grade zone of metamorphism.

Following Heald's work (1950) in the Lovewell Mountain quadrangle to the south, the Littleton formation in the eastern part of the Sunapee quadrangle has been subdivided into the Hubbard Hill and Dakin Hill members. The intervening May Pond member of the Lovewell Mountain quadrangle is not present in the Sunapee area. The Hubbard Hill member extends from the central part of the southern boundary of the area to the northeast corner of the quadrangle. The stratigraphic position of this member within the Littleton formation is not known because of the intervening mass of Bethlehem gneiss, but Heald (1950, p. 45) places the base of this member about 5000 feet above the base of the Littleton formation. Stratigraphically above the Hubbard Hill member is the Dakin Hill member. This unit extends from the south end of Sunapee Mountain to the village of Newbury. It is separated from the older member of the Littleton formation by a mass of Kinsman quartz monzonite.

Undifferentiated Littleton Formation

The lithologic and petrographic character of the Littleton formation west of the Bethlehem gneiss has already been described in detail (Chapman, 1939; 1942) and only the salient features will be summarized here. The relatively small area in the extreme northwest corner of the quadrangle is underlain by fine- to medium-grained mica schist and interbedded quartzite. These rocks belong to the middle-grade zone of metamorphism. The essential minerals of the schist are quartz, muscovite, and biotite; staurolite, garnet, plagioclase, and opaque minerals occur in minor amounts. Porphyroblasts are common and locally developed in great abundance. Biotite porphyroblasts a millimeter or so across usually cut the schistosity; and garnet occurs in slightly larger grains, partly cutting and partly displacing the surfaces of foliation. Staurolite is perhaps the most conspicuous porphyroblast and in places occurs abundantly (up to 10 per cent or so) in crystals up to 4 or 5 inches long. In these schists one frequently encounters quartz veins bordered by thin zones of staurolite. This phenomenon is believed (Chapman, 1950) to be due to metamorphic differentiation of the aluminous schists.

The quartzite is a common rock type. The beds are white to gray, one-half to 2 inches thick, and characteristically interbedded with various types of mica schist. Some quartzite beds are very pure but most commonly they contain much muscovite and some biotite, so that all gradations between quartzite and mica schist may be found.

The mineral composition, structure, and association of these rock types in the Littleton formation shows that originally the rocks were sedimentary in origin varying from sandstone to shale. The staurolite-rich rocks were probably derived from alumina-rich varieties.

The Littleton formation west of Kelleyville is poorly exposed due to the cover of glacial material and valley fill. Several outcrops occur at the old feldspar mine near Chandler Station and on the hill to the south. These rocks are medium- to coarse-grained schist composed essentially of quartz, muscovite, and biotite. The minor constituents are sillimanite, staurolite, garnet, and oligoclase. For simplicity, these rocks may all be grouped in the high-grade zone of metamorphism.

Hubbard Hill Member

General statement.—The Hubbard Hill member is composed predominantly of schist and gneiss with minor amounts of quartzite and lime-silicate granulite. In general the rocks in the western part of the belt, shown as the Hubbard Hill member, are slightly finer-grained and less gneissic than those to the east. In the field, the member is characterized by good bedding and marked schistosity or foliation. Beds of schist less than a foot thick are commonly observed to alternate with thinner beds of quartzite. Gneissic layers also appear to be interbedded with quartzite and schist in the eastern part of the member. Sillimanite schist, interbedded with mica-quartz schist, constitutes, perhaps, most of the member. Banding, so conspicuously expressed in many good outcrops, is due primarily to differences in composition of the original sedimentary layers. It is believed, however, that these primary compositional

differences have been exaggerated during the metamorphism by the segregation of certain minerals like sillimanite, mica, quartz, and garnet into bands and layers. Schistosity and foliation almost universally appear parallel to bedding. In many eastern exposures of the Hubbard Hill member, particularly on the west flank of Sunapee Mountain, the rocks become somewhat more gneissic and relations between bedding and foliation are not clear. But even here, where relations are descernible, a parallelism of the two structures is the rule. Lineation within the member is principally of three types. It consists of small folds and crinkles and it occasionally forms a well-developed pencil structure parallel to fold axes. Most commonly it is shown by mineral shape or orientation. Large muscovite crystals and also finer biotite flakes commonly show a linear arrangement, but less frequently sillimanite knots and long crystals show linear orientation. The schist, gneiss, and quartzite are considered to have been derived from pelitic and sandy rocks, and the lime-silicate granulites were probably originally impure dolomitic limestones.

Schist.—A great number of petrographic varieties of schist may be recognized but they are considered as a group here because of their gradational character. In hand specimen, quartz, biotite, muscovite, sillimanite, and garnet appear in various combinations. Schist with biotite and sillimanite or biotite, sillimanite, and muscovite is the most common and wide spread. Garnet, in combination with mica or mica and sillimanite, is somewhat more sporadic. The rocks are generally medium- to coarse-grained but locally very coarse- or fine-grained phases occur. A number of modes, as determined from thin section, are given in Table 1.

Quartz is the most abundant mineral and occurs as equidimensional to elongate grains (0.1–1.0 mm.). Grain boundaries are generally curved but in many specimens are sutured. Strain shadows are rarely pronounced. Tiny gas cavities (0.002–0.005 mm.) are universally present and in sufficient abundance to enable one to use their presence as a means of distinguishing quartz from feldspar in thin section. Plagioclase, usually without albite twinning, is calcic oligoclase and occurs as grains of about the same shape and size as the quartz. Red-brown biotite, as well-oriented flakes up to 2 or 3 mm., is an important constituent. Muscovite is usually much less abundant and in many cases absent. It is found as small flakes replacing biotite and quartz and as large porphyroblasts up to a centimeter long. These large crystals are feathery to poikiloblastic and lie at all angles to the schistosity. In some specimens large muscovite flakes are concentrated along definite schistosity planes, and they commonly conform to the lineation of the rock. Sillimanite occurs as tiny needle-like inclusions in quartz or as larger needles and acicular crystals (up to 5 mm.) arranged in bands, brushes, or knots replacing mica and quartz. Sillimanite knots may form eyed-structures with surfaces of schistosity wrapping around the sillimanite cores and quartz grains filling in the corners of the eyes. Most of the sillimanite appears to lie in the planes of schistosity, and in some specimens it exhibits a marked linear parallelism. These larger masses and crystals were commonly observed to be 2 to 3 cm. long and rarely 10 cm. long. The extremely rich concentration of sillimanite found in very thin layers in some rocks is believed to be due to segregation across bedding or foliation planes. Garnet is not an important constituent of the schist but is found locally as irregular grains to xenoblastic crystals up to a few millimeters across. Tiny crystals of zircon (less than 0.05 mm.) are abundant in most thin sections, and other accessory minerals consist of apatite, olive-green tourmaline, magnetite, pyrite, and graphite.

Gneiss.—Medium-grained to coarse-grained gneiss is the second important rock type in the Hubbard Hill member, and the petrographic varieties are numerous. There are all gradations between schist and gneiss, and the relative abundance of these two rocks is difficult to estimate. Both types are interbedded and mutually associated in the field, but in general the gneisses are a little more prevalent toward the south and in the eastern part of the Hubbard Hill member. The difference between the gneiss and schist is believed to be due to metamorphic processes and in part to chemical composition. Grain size is the only characteristic difference in the quartz of the gneiss and that of the schist. Its range is from 0.1 to 3.0 mm. Micas show the same features as in the schist except that they are generally poorly oriented and biotite shows a distinct tendency to form aggregates a few millimeters across. Sillimanite is present in most specimens and shows a less preferred orientation than in the schist. Garnet is more abundant and more widely distributed than in the schist. It occurs as irregular grains or poorly-formed cyrstals, generally less than 5 mm. across, and encloses numerous rounded grains of quartz or biotite and rarely sillimanite. It is clearly seen to replace quartz feldspar, biotite, and muscovite. Garnet is commonly associated with biotite and, in one locality,

garnet crystals appear wreathed with biotite. In another locality garnet crystals up to 4 cm. were abundant. Some of these form garnet-rich layers in gneiss. These large crystals are very impure and poikiloblastically enclose about 50 per cent of inclusions of biotite, quartz, muscovite, and sillimanite. For the most part they appear to replace the rock because the foliation planes can be traced through the garnet masses. Numerous modes are given in Table 1.

Quartzite.—Light-colored quartzite with varying amounts of mica is not uncommonly found in thin layers interbedded with schist, gneiss, and lime-silicate granulite. All gradations occur between quartzite and quartz-mica schist, but the latter is probably the more abundant. No microscopic study was made of the quartzite, but hand specimen study indicates that, in addition to the high percentage of quartz, it is composed of micas, sillimanite, and feldspar.

Lime-silicate granulite.—Granulose metamorphic rocks rich in lime-silicate are uncommon in the Hubbard Hill member. These rocks are referred to here as granulites. On Chandler Hill, in Goshen Township, light-gray to green granulite occurs interbedded with fine-grained red-brown biotite schist. The beds of granulite are about an inch thick, and, in contrast to the schist, stand out on the weathered surface. In hand specimen, both rock types may be seen to carry large crystals of actinolite up to 5 mm. long. The granulitic material in thin section is known to be composed largely of quartz as polygonal to rounded grains 0.1–0.3 mm. across and diopside as xenoblastic grains 0.05–0.1 mm. across. Considerable labradorite, which resembles the quartz in shape and grain size, is also

TABLE 1.—ESTIMATED MODES OF THE LITTLETON FORMATION

	Hubbard Hill Member																	Dakin Hill Member			
	1	2	3	4	5	6	7	8	9	10	11	12	13	14	15	16	17	18	19	20	21	22
Quartz	74	70	60	58	47	55	52	57	55	63	68	75	58	53	56	38	33	20	57	60	22	30
Microcline						2		12										52			27	
Oligoclase	6	5	7	10	10	1		10	10	8	4	tr	tr	3	1	5					15	7
Andesine							17												12			
Labradorite																	15					
Biotite	12	17	16	23	13	22	13	15	20	13	14	10	27	17	18	18		23	19	10	9	4
Muscovite	6	5	12	1	20	18	8	5	8	10	13	1	1	10	21	35				23		34
Chlorite																						8
Sillimanite	2	3	4	7	5	2	7	tr	4	3		10	12	13	1	1			3		10	7
Garnet	tr				5		3	tr	2	2		3	1	6	2	2	1		8		12	10
Magnetite } Ilmenite }	tr	tr	1	tr	tr	tr	tr	tr	tr	1	tr	tr	tr	tr	1	1			1	tr	tr	tr
Tourmaline		tr	tr		tr		tr		tr				tr					tr				
Pyrite			tr	tr			tr			tr		tr	1	1	tr	tr	tr	tr	tr	1		
Apatite	tr	tr	tr	tr	tr	tr					tr		tr		tr	tr		tr	tr			
Zircon	tr	tr	tr	tr	tr	tr	tr	tr	tr	tr	tr	tr	tr	tr	tr	tr	tr	tr	tr	tr	tr	tr
Sphene	tr									tr							1	2	tr			tr
Graphite	tr		tr	1	tr				tr	tr		tr		tr	tr	tr			tr	tr	tr	1
Epidote																	3	2				
Allanite																		tr				
Cordierite																				6	5	
Actinolite																		1				
Diopside																	48					

Hubbard Hill member
1. Quartz-mica schist
2. Quartz-mica schist
3. Mica-quartz schist
4. Mica-quartz schist
5. Mica schist
6. Mica schist
7. Mica-quartz gneiss
8. Mica-quartz gneiss
9. Mica-quartz gneiss
10. Mica-quartz gneiss
11. Mica-quartz gneiss
12. Mica-quartz gneiss
13. Mica gneiss
14. Mica gneiss
15. Mica gneiss
16. Mica gneiss
17. Lime-silicate granulite
18. Lime-silicate granulite

Dakin Hill member
19. Mica gneiss
20. Mica gneiss
21. Microcline gneiss
22. Muscovitized microcline gneiss

present. Highly poikiloblastic grains of garnet and crystals of actinolite are scattered through the rock in small quantities. Tiny grains of clinozoisite, sphene, and zircon are extremely numerous, but very small quantities of pyrite were observed.

The associated red-brown schist is strikingly different mineralogically in that it is composed almost entirely of equidimensional grains (0.1-0.3 mm.) of microcline, quartz, and well-oriented flakes (0.2–0.4 mm.) of red-brown biotite. A conspicuous feature is the zonal arrangement of allanite and clinozoisite. Rectangular crystals of clinozoisite with cores of allanite are abundant, and many occur in biotite flakes where strong pleochroic haloes have formed. Sphene is more abundant here than in the granulites. Well-formed crystals of actinolite, poikiloblastically enclosing most of the other mineral types, are also more numerous in the schist. These show a striking orientation in that crystallographic *b* and *c* lie in the plane of schistosity and crystallographic *c* is parallel to rock lineation. Modes of these two rock types are given in Table 1.

Along the contact with the Bethlehem gneiss, due west of Blueberry Mountain, in Sunapee Township, are garnet-pargasite rich masses of gneiss and granulite. Many of these are enclosed by Bethlehem gneiss, and will be considered in more detail in the discussion of that rock body. It should be noted that these calcium-rich rocks occur at the same stratigraphic position as the lime-silicate rocks on Chandler Hill.

Dakin Hill Member

General statement.—The Dakin Hill member is composed almost entirely of gneiss, but very minor amounts of schist, quartzite, and quartz conglomerate do occur. Like the rocks of the Hubbard Hill member, these gneisses and schists are considered to have been derived from argillaceous and somewhat arenaceous sedimentary rocks by intense metamorphism. The essential difference between these rocks and those of the Hubbard Hill member is in part textural and structural and in part mineralogical. These rocks are generally coarser-grained and show a poorer orientation of platy minerals due, undoubtedly, to more intensive recrystallization. The most striking mineralogical difference is the presence of large quantities of potash feldspar in the rocks of the Dakin Hill member. At several localities on the east slope of Sunapee Mountain, oval masses up to several feet long and composed of light-buff to greenish-gray granulite were observed. In the hand specimen they appear to be diopside and actinolite granulite and are believed to represent metamorphosed impure dolomitic concretions or lenses.

Bedding in the Hubbard Hill member is seldom seen in outcrop, but a poor foliation and commonly strong banding are characteristic. The banding is due principally to local concentration of dark and light minerals such as garnet, mica, sillimanite, and feldspar. Schistosity is relatively uncommon. The fact that bedding is difficult to detect in these rocks makes it almost impossible to state the relationship between this structure and foliation. However, in no case was bedding seen to make an angle with the foliation or banding. This would only suggest, therefore, that foliation and bedding are generally parallel. Lineation is very poor or absent throughout much of the member. Where well developed, it comprises coarse crinkles and oriented muscovite and biotite flakes. Highly elongate quartz pebbles show linear orientation in the quartz conglomerate.

Mica gneiss.—The gneiss may be conveniently subdivided into two types, the feldspathic and nonfeldspathic. The nonfeldspathic type is the more abundant, and is mineralogically similar to the gneiss of the Hubbard Hill member, being composed essentially of quartz, mica, sillimanite, and garnet. Only small quantities of plagioclase may be present. The texture is generally coarse to very coarse granoblastic, and the structure in hand specimen often appears massive. Quartz is as equidimensional grains (0.5–5 mm.) with rounded to sutured boundaries and shows moderate to strong stain effects. Tiny gas cavities are as numerous and characteristic as in the rocks of the Hubbard Hill member. In addition, tiny needles of sillimanite are abundant as inclusions. Small amounts of sodic andesine with albite and pericline twinning and slight zoning occur in some specimens. Coarse flakes of red-brown biotite, up to 5 mm. and arranged in bands or aggregates, are abundant in nearly all specimens. Muscovite is an important constituent in some thin sections but is very unevenly distributed throughout the member. Much of the muscovite, particularly in rocks where it is very abundant, is in fine-grained aggregates and appears of a different generation from the clear-cut flakes which occur with biotite and sillimanite in other parts of the rock. The shape and distribution of these aggregates

strongly suggest that this muscovite is replacing sillimanite in some cases and potash feldspar in others. In the latter case, the rock would have previously been a feldspathic gneiss. The amount of sillimanite ranges widely in these gneisses. It is most frequently seen in bundles and layers of acicular crystals usually replacing biotite and quartz but not garnet. Garnet is not abundant and forms rounded crystals up to 2 mm. across. Cordierite was found in small amounts highly replaced by biotite, muscovite, and chlorite. Accessory minerals are zircon, apatite, magnetite, pyrite, and graphite. Modes are given in Table 1.

Microcline gneiss.—The feldspathic gneiss is characterized by an abundance of microcline. Feldspar occurs as porphyroblasts up to 8 cm. long. In hand specimen many of these large crystals appear well formed, with a square to rectangular outline, and resemble the large microcline crystals of the adjacent Kinsman quartz monzonite. It is common to find the feldspar as lens-shaped and gob-like masses many of which are highly irregular. In some of the more strongly foliated rocks, the large porphyroblasts grade into highly elongate lenses and large stringers. Many of these stringers range up to 30 cm. long, and they generally conform to the foliation of the rock. Where the foliation is folded, the larger stringers follow completely around the folds. In a few places the porphyroblasts are xenoblastic, poorly oriented, and not highly elongated. In hand specimen, the microcline is seen to enclose considerable quartz and a little garnet. In thin section, the potash feldspar shows rounded to subsutured borders against the matrix of other minerals. Much is as small irregular grains more or less interstitial to the quartz. It is very fine microperthite, and high magnification reveals very fine microcline cross-hatching in the host mineral. Quartz, oligoclase-andesine, and sillimanite occur much the same as in the mica gneiss, but biotite may be a little less abundant and garnet more abundant. Cordierite, which alters to a pale pleochroic mica with pleochroic haloes, is a minor constituent of some specimens. Myrmekite is found in varying amounts and commonly replaces the large microcline porphyroblasts along their borders. In the freshest specimens, muscovite was not found; in some sections, much fine-grained muscovite occurs in aggregates constituting a third of the rock and apparently replacing microcline. Many of these masses show the rectangular outline common to this feldspar, and the pattern of the mica flakes reveals what appears to be cleavage directions in the altered host. Two modes are given in Table 1.

Schist, quartzite, and quartz conglomerate.—The schist and quartzite, which occur locally in the Dakin Hill member, so closely resemble the corresponding rock types of the Hubbard Hill member that further treatment is not justified. Quartz conglomerate was found only in two localities on Sunapee Mountain, about half a mile north of Andrews Brook at elevation 1600 feet, and 2 miles due south of Lake Solitude at elevation 1980 feet. The bed near Andrews Brook is 5 feet thick and contains stretched quartz pebbles, about an inch long, which are well lined in the direction of dip. At the other locality, the conglomerate constitutes a large block not far out of place, containing stretched pebbles up to 3 inches long.

Thickness

The thickness of the Littleton formation could not be determined with a high degree of accuracy. The undifferentiated portion of the Littleton formation exposed in the northwest part of the quadrangle probably does not exceed 2500–3000 feet. Heald (1950, p. 55) has estimated the thickness of the Hubbard Hill member as about 6000 feet in the Lovewell Mountain quadrangle to the south. This value probably holds good for the Sunapee quadrangle except in the northern half where much of the member has apparently been cut out by granitic rocks. The Dakin Hill member is considerably thinner, ranging from about 2500 feet at the south border of the area to zero just north of the village of Newbury. If Heald (1950, p. 45) is correct in placing the base of the Hubbard Hill member about 5000 feet above the base of the Littleton formation, then the undifferentiated mass of the Littleton formation in the northwestern corner of the quadrangle must all be stratigraphically below the Hubbard Hill member. In this event, the total thickness of the Littleton formation in the Sunapee quadrangle is estimated to be at least 11,000 feet.

Croydon Group

The Croydon group refers to a group of granitic-looking gneisses correlated with the Oliverian magma series. The gneiss is confined to the Croydon dome, immediately east of Croydon Mountain. The rocks are fine- to medium-grained and poorly to well foliated. Essential minerals are quartz, oligoclase,

microcline, and biotite. Epidote, magnetite, and muscovite occur in minor amounts. Hornblende is present near the contacts, and epidote is generally more abundant there also. The rock has an allotriomorphic texture and locally contains large crystals of microcline up to a centimeter long. Petrographically the gneiss is granodiorite with quartz diorite and quartz monzonite more locally developed.

Bethlehem Gneiss

The Bethlehem gneiss, the most extensive rock unit in the Sunapee quadrangle, occupies a little over half the area and is confined to a large belt extending NNE-SSW through the central part of the quadrangle. The gneiss is usually medium-gray and medium- to coarse-grained with a mineral composition ranging from quartz diorite to quartz monzonite. Granodiorite is the predominating type. The structure is usually gneissic and the foliation generally pronounced. In much of the material, thin layers of biotite and muscovite alternate with thicker layers of quartz and feldspar. The lighter layers range from 1 to 4 mm. thick, and the micaceous layers are remarkably uniformly spaced and continuous for many inches, forming a megaschistose structure. In much of the rock, the foliation is more open, in that mica layers are irregularly distributed, very discontinuous, and locally poorly oriented. In addition lens-like masses of granoblastic quartz are abundant and help to accentuate the layered structure. Lineation was detected in all but a relatively few outcrops, and in places this structure obliterates the foliation of the rock. It may be due to crinkling of mica layers, to girdle arrangement of micas, to elongate mica flakes, or to elongate masses of quartz and feldspar.

A conspicuous feature of the gneiss is the presence of large crystals of microcline with carlsbad twinning. These are generally tabular and range from anhedral to subhedral in shape; some are lenticular or augen-shaped. When viewed normal to (010), they appear rounded or irregular, but at right angles to this they are more rectangular with length-width ratios of 3:2 to 4:1. In most places {010} is well developed, but only rarely are {110} or other forms as clearly seen. The length of the crystals is commonly up to 5 cm., and in a few places it is 8 cm. Crystals up to 10 cm. are very rare. The crystals are unevenly distributed throughout the body and constitute up to about 10 per cent of the rock. The large crystals are usually oriented parallel to the rock foliation though all degrees between this and random orientation occur. In most outcrops, the foliation of the rock in part wraps around the large crystals and in part is cut off by the crystals. Inclusions of biotite, quartz, and muscovite are numerous in the feldspar. Quartz is commonly as fine granular masses up to 1 cm. across or as streaked-out lenses or phacoidal masses (2 x 25 mm) which stand out prominantly on the weathered surface and help to give the rock a much coarser appearance in the field.

In thin section, the rock shows a granoblastic texture with mica flakes more or less in parallel arrangement in a mosaic of quartz and feldspar. Quartz shows curved to sutured boundaries and moderate to strong strain shadows. Some quartz appears late and replaces mica. Gas cavities or fluid inclusions may be scarce or very abundant; many of these are in lines or layers at various angles to the foliation of the rock. In addition to its occurrence as large crystals, microcline is found abundantly in the groundmass. Plagioclase is oligoclase-andesine as equidimensional grains (0.1–4.0 mm.) with curved to subsutured boundaries. Zoning is weak but albite, pericline, and carlsbad twinning are very common. Some of the larger crystals have' been slightly bent and deformed; others appear to have been broken and partly granulated. Myrmekite is abundant in some specimens and is concentrated at the borders of microcline crystals. Biotite is as red-brown flakes (0.1–4.0 mm.) which range widely in their perfection of orientation. The content of muscovite differs greatly for different specimens, but it is almost always subordinate to that of biotite. Some fine flakes are in plagioclase, and many of these are oriented parallel to cleavage planes. Garnet and a little sillimanite were found in a few thin sections. In the field, garnet appears in the Bethlehem gneiss only near the eastern contact with the Littleton formation and near large inclusions. In thin section it was found as subhedral grains, up to 5 mm across, replacing biotite and muscovite. A very small amount of sillimanite, as needles and bundles in quartz, feldspar, and mica, occurs in the Bethlehem gneiss principally near the contact and near inclusions. Sphene appears to be a very diagnostic

minor constituent of the gneiss and is abundant as large grains associated with biotite. Very fine-grained sphene is concentrated along the cleavage planes of altered biotite suggesting that the mica was originally rich in titanium. Large crystals of allanite and numerous zircon grains have formed pleochroic haloes in biotite. Other accessories are apatite, magnetite, graphite, and green-brown tourmaline. Numerous modes of the Bethlehem gneiss are given in Table 2.

Light-colored phases of the gneiss occur locally. These appear as layers up to many feet thick and generally concordant with the foliation of the main rock. Contacts are rather sharp and the bodies have a distinct sill-like appearance. This light material has a foliated granular texture. A mode of one of these light-colored rocks is given in Table 2.

A schistose variety of the Bethlehem gneiss has developed locally, but particularly near the eastern contact of the pluton and near large inclusions. It is characterized by an excellent orientation of mica, elongate quartz and feldspar grains, and numerous thin layers of granular felsic minerals (grain size 0.05–0.5 mm.). A marked lineation of biotite is very conspicuous in many places. This phase differs from the normal gneiss in its higher quartz content and lower feldspar content (Table 2).

TABLE 2.—ESTIMATED MODES OF THE BETHLEHEM GNEISS AND INCLUSIONS

	Gneissic Phase										Schistose Phase			Inclusions			
	1	2	3	4	5	6	7	8	9	10	11	12	13	14	15	16	17
Quartz	33	20	33	25	30	28	23	18	28	38	44	64	35	38	32	15	28
Microcline	22	25	15	11	12	8	8	9	4	12	1	tr	tr				
Oligoclase - andesine	35	44	32	47	45	43	53	62	45	42	32	23	40	30	25	67	
Andesine																	17
Biotite	8	10	15	14	12	20	15	9	17	4	12	13	18	25	27	18	16
Muscovite	2	1	3	3	1	1	1	1	3	4	10	tr	2	7	11	tr	3
Chlorite			2		tr			tr	3	tr	tr						
Sillimanite											tr		1		4		
Garnet						tr				tr	tr		4				20
Magnetite, Ilmenite	tr	tr	tr	tr		tr	tr	tr					tr	tr			3
Tourmaline	tr							tr							tr		
Pyrite	tr			tr	tr			tr	tr			tr					
Apatite	tr	tr	tr	tr	tr	tr	tr	tr	tr	tr	tr	tr	tr	tr	1	tr	1
Zircon	tr	tr	tr	tr	tr	tr	tr	tr	tr	tr	tr	tr	tr	tr	tr	tr	tr
Sphene	tr		tr	tr	tr		tr	tr	1			tr		tr	tr	tr	
Graphite	tr		tr	tr	tr	tr	tr		tr	tr	tr	tr		tr			
Epidote	tr	tr	tr						tr		tr			tr	tr	tr	
Zoisite								1				tr					
Allanite			tr	tr	tr	tr	tr	tr	tr					tr			tr
Pargasite																	12
Rutile											tr						

Gneissic phase
1. Quartz monzonite
2. Quartz monzonite
3. Quartz monzonite
4. Granodiorite
5. Granodiorite
6. Granodiorite
7. Granodiorite
8. Granodiorite
9. Granodiorite
10. Light-colored granodiorite

Schistose phase
11. Quartz diorite
12. Quartz diorite
13. Quartz diorite

Inclusions
14. Medium- to fine-grained biotite gneiss
15. Medium- to fine-grained porphyroblastic biotite gneiss
16. Medium- to fine-grained porphyroblastic biotite gneiss
17. Medium-grained pargasite-garnet gneiss

It usually carries small quantities of garnet and sillimanite.

Inclusions are widely distributed throughout the body. They are perhaps only slightly more abundant near the contacts of the pluton, but at least one or two small ones were seen in the great majority of outcrops. They are lens-shaped or slablike, showing tapering ends, and are foliated parallel to their length. They range in length from a few inches to many feet but are usually only a few inches wide. The foliation and lineation of the inclusions were found in all cases to parallel the foliation and lineation respectively of the enclosing gneiss. The perfection of foliation in the inclusion is not always consistent with that of the enclosing rock, because strongly foliated inclusions have been found in poorly foliated Bethlehem gneiss. All these structural relations seem to be characteristic throughout the body. In the field, the inclusions are seen to be composed of medium- to fine-grained biotite schist and gneiss which are somewhat darker than the enclosing material because of their finer texture and higher mafic content. In many inclusions, small crystals of feldspar appear as augen-like masses more or less wedging apart the fine layers of mica. These crystals range up to about 5 mm. Microscopically the inclusions resemble some of the rocks of the Littleton formation but appear to be more or less felspathized by moderately zoned plagioclase.

The plagioclase ranges from oligoclase to adesine, and it is most abundant as polygonal or rounded grains in granoblastic texture with quartz. The large crystals of plagioclase are elongate parallel to the foliation; some show weak zoning; others appear slightly strained. They are subhedral and mica flakes usually wrap around, but in many cases the foliae have been cut off as if replaced by the large crystals. A few biotite flakes and some quartz appear as unreplaced inclusions in the large crystals, but many of the included quartz grains are rounded and show a common optical orientation suggesting a late and myrmekitic origin. Small muscovite flakes, some oriented in cleavage planes in porphyroblasts, are also probably late. Some quartz may also have been introduced or may merely have recrystallized in the rock. Potash feldspar is absent. In most other respects the inclusions closely resemble the rocks of the Littleton formation. The inclusions range widely in composition (Table 2).

In the open field 1¼ miles due west of the highest knoll on Blueberry Mountain, in Sunapee Township, lenticular masses of garnet-pargasite gneiss and garnet-pargasite granulite occur in the Littleton formation and Bethlehem gneiss. These dark-gray bodies range up to 8 feet in length and characteristically show parallel arrangement with the foliation of the enclosing rock. Many are fine-grained with garnet porphyroblasts up to 15 mm. Microscopically the garnet is subhedral and poikiloblastically encloses about 4 per cent magnetite and 25 per cent quartz. Quartz and calcic andesine are as equidimensional grains between 0.1 and 0.5 mm. Red-brown biotite flakes up to 2 mm. may or may not show parallel orientation. Pargasite as anhedral grains up to 1 mm., is uniformly distributed along with biotite. Magnetite is very abundant and apatite, as tiny slender crystals, is the principal accessory. One mode of this rock is given in Table 2. The significance of these masses will be considered later, but this material originally was probably a calcareous rich sediment.

There are sill-like bodies of gneiss in the Littleton formation near the eastern contact of the Bethlehem gneiss. These range from a fraction of an inch to many feet thick and may be up to hundreds of feet long. They are believed to be genetically related to the Bethlehem gneiss but are usually finer-grained and commonly darker. Foliation and lineation are generally good and always parallel to those structural elements of the enclosing Littleton formation. A number of thin sill-like masses of gneiss alternate with thin layers of gneiss and schist of the Littleton formation in the roadcut at the south end of Otter Pond, near the Sunapee-New London town line. The parallelism between foliation and lineation in the two formations is clearly shown. Another and even better exposure, which shows the same relations, is along the contact just northwest of Dutchman Pond in Springfield Township.

Kinsman Quartz Monzonite

The Kinsman quartz monzonite occupies about a fifth of the area and is confined to the southeastern section of the quadrangle. This mass of granitic material is part of a huge elongate body which extends for at least 25 miles to the south, through the Lovewell Mountain quadrangle (Heald, 1950) and into the Keene quadrangle (Fowler-Billing, 1949),

and for over 20 miles northward through the Mt. Kearsarge quadrangle and into the Cardigan quadrangle (Fowler-Lunn and Kingsley, 1937).

The rock composition ranges from quartz diorite to granite, but granodiorite appears to be the predominating type in the Sunapee area. The rock is typically light to medium gray, coarse-grained, and moderately gneissic. It commonly weathers to rusty brown. Locally dark-gray, medium-grained or massive phases are encountered, and these phases may be quite gradational. The foliation is roughly uniform over wide areas, but locally the strike may change as much as 90° suggesting folding on a broad scale. The foliation is made conspicuous by the parallelism of large tabular feldspar crystals which show carlsbad twinning and locally attain the length of 12 cm. but which average closer to 5 cm. These crystals not uncommonly make up 15 to 20 per cent of the rock. In hand specimen, the feldspar appears well formed with rectangular cross-sections except where prism forms give a tapering effect. Close inspection with hand lens shows somewhat irregular boundaries. Biotite wraps more or less around the ends of crystals but much abuts against and is cut off particularly by those crystals with square ends. Many of the large crystals may be seen to contain small quantities of quartz, plagioclase, and mica inclusions. The composition of the large crystals is usually microcline perthite with a relatively small amount of albitic material. Large crystals of plagioclase, however, are very abundant and widely distributed; they may be of the same size as microcline crystals. In thin section, the large crystals of microcline and plagioclase do not appear to have been deformed except very locally. Many of the large microcline crystals are replaced in their outer part by a narrow rim of myrmekite.

In the road-cut half a mile south of the village of Newbury is an excellent exposure of the Kinsman quartz monzonite with inclusions of the Littleton formation. Here the large feldspar crystals, up to 12 cm. are well developed and well oriented in both the quartz monzonite and the inclusions. The length-width ratio is 4:1 and in places the crystals are distinctly seriate. Some of the large crystals are lens-shaped (5.0 x 25.0 mm.) and smaller ones are like augen with foliation of mica wrapping around. Some large crystals appear drawn out and the foliation, revealed by oriented biotite, passes straight through them. The feldspar crystals carry much muscovite and quartz and a little biotite, and a thin layer of white mica usually surrounds each large crystal. Elsewhere in the rock muscovite is not abundant.

Microscopically these large crystals are seen to be composed of oligoclase-andesine with equally well developed pericline and albite twinning. Quartz replaces up to 50 per cent of the crystals as irregular-shaped masses with curved boundaries and moderately strong strain shadows. Some of the quartz grains are 5 mm. long. Groups of neighboring grains show optical continuity. This intergrowth resembles somewhat a very coarse myrmekite except that the quartz is not typically vermicular. In many cases the plagioclase does not form a single unit but is composed of a mosaic of smaller grains. Groups of adjacent grains are nearly in optical continuity and the orientation may change slightly from one end of the crystal mosaic to the other. In those sections where the mosaic units are smallest, the departure from parallelism is greatest. Flakes of muscovite up to 2 mm. long are abundant in the aggregate, and many have been replaced so extensively by small rounded quartz grains that they possess a striking "moth-eaten" appearance. Large muscovite flakes form a thin layer more or less completely around many of the large aggregates. Heald (1950, p. 61) believed these aggregates were pseudomorphic after large crystals of microcline because he found all stages of transition. Two additional facts suggest such an origin for these aggregates. (1) The plagioclase has a distinctly different appearance from the somewhat smaller plagioclase crystals in the rock. This difference is due principally to the prominent and equally well developed albite and pericline twinning of the feldspar in these aggregates. (2) Along the margins of many aggregates is typical myrmekite which at one time may have been replacing the borders of large microcline crystals.

The groundmass of the Kinsman quartz monzonite contains very little microcline but is most typically composed of granular quartz, plagioclase, and biotite with minor amounts of muscovite, garnet, cordierite, and sillimanite. All gradations in size are seen between large plagioclase crystals and plagioclase of the groundmass, though generally the groundmass grains are less than 6–8 mm. long.

The small to medium-sized grains show albite, periciline, and carlsbad twinning and a weak to moderate zoning. Curved twin lamellae and slight strain shadows indicate some local deformation. Sericitization of plagioclase cores seems characteristic. Many thin sections show plagioclase enclosing numerous very tiny needles of sillimanite and in addition a few equally small, irregular gas cavities. Grain boundaries are usually curved or irregular. Quartz ranges up to 8 mm. as small single grains or aggregates and lenses of grains with irregular to sutured borders. These grains are moderately to highly strained and include multitudes of tiny gas cavities, sillimanite needles, and fine particles of opaque material, possibly graphite. The gas cavities are larger and much more numerous than those in the plagioclase. Much quartz occurs as small rounded grains replacing nearly all of the other types of minerals. Muscovite is not abundant and where present is as large flakes replacing biotite or as tiny flakes in plagioclase. Red-brown biotite flakes up to 2 mm. is generally associated with the finer grains of quartz and feldspar. In most specimens, it is poorly oriented but in some the orientation is very good. In those rocks with few or no large feldspar crystals, biotite helps to give the rock a pronounced foliation. Specimens of this type can scarcely be told from the Bethlehem gneiss.

In the phases with abundant large crystals, relatively fine-grained mineral aggregates make up the rock matrix. These aggregates are highly irregular or lenticular in shape. Many possess a distinct schistose appearance and are composed of well-oriented mica flakes and elongate quartz grains. Others are coarser and more gneissic. Many of the aggregates abut against large crystals of microcline and plagioclase without a disturbance of the foliated structure. Furthermore, these masses appear to have been eaten into by the adjacent large crystals so that irregular and stringy edges remain. These aggregates most strinkingly resemble the mica schist and gneiss of the Littleton formation. Garnet is usually in small quantities and is very sporadically distributed in crystals up to 15 mm. In a few cases, crystals 2 cm. across were observed. Sillimanite is locally a minor constituent of the matrix and occurs as aggregates of needles in mica all of which appear to be eaten out by quartz and feldspar leaving scalloped contacts. Minor amounts occur as myriads of tiny needles in quartz and to a less extent in plagioclase. Small quantities of cordierite, usually altered to chlorite, occur in several thin sections. Accessories include apatite, zircon, allanite, ilmenite, and pyrite. Graphite in accessory amounts is developed in platy masses and may be seen in most hand specimens with the aid of low magnification (24×). A number of modes are given in Table 3.

Inclusions in the Kinsman quartz monzonite (Table 3) are numerous and in general resemble those found in the Bethlehem gneiss. They are widely distributed but perhaps somewhat more abundant near the contacts with the Littleton formation. They are most numerous on the north end of Sunapee Mountain. Some of these masses may be thousands of feet long. They are tabular and oriented parallel to the rock foliation. In hand specimen and under the microscope they appear to represent fragments of gneiss or schist of the Littleton formation. Like the inclusions in the Bethlehem gneiss, they have been feldspathized and altered so that all gradations between typical paragneiss (or paraschist) and Kinsman quartz monzonite occur. Layers exceedingly rich in garnet are locally encountered. These are probably partly altered masses of the Littleton formation. They have been feldspathized and contain as much as 30 per cent garnet in crystals averaging about 5 mm.

Sill-like masses of the Kinsman quartz monzonite are common in the adjacent Littleton formation. They range in thickness up to many hundreds of feet, and three large bodies are shown on the geologic map on Sunapee Mountain. On Thompson Hill and in the area to the east and northeast in Goshen Township, many small sill-like bodies of gneiss are enclosed in the Littleton formation. The rock is well foliated and commonly well lineated parallel to the foliation and lineation of the surrounding Littleton formation. The gneiss is finer-grained and darker than either the neighboring Bethlehem gneiss or Kinsman quartz monzonite which it closely resembles mineralogically, texturally, and structurally.

The modes of two of these bodies are given in Table 3. Quartz occurs as rounded to polygonal-shaped grains ranging from 0.05–1.0 mm. Oligoclase-andesine occurs as grains of the same shape as quartz but about twice as large. It shows albite, pericline, and carlsbad twinning and moderate zoning. The larger crystals of plagioclase partly displace and partly replace the parallel layers and bands of red-brown biotite. Microcline as rounded grains is about the same size as quartz. Minor constituents include muscovite, sphene, zircon,

apatite, garnet, epidote, allanite, tourmaline, and pyrite.

quadrangle. These are correlated with the Spaulding quartz diorite in its type locality in

TABLE 3.—ESTIMATED MODES OF THE KINSMAN QUARTZ MONZONITE AND ASSOCIATED ROCKS

	Kinsman quartz monzonite									Inclusions			"Sills"		Feldspathized Littleton Formation	
	1	2	3	4	5	6	7	8	9	10	11	12	13	14	15	16
Quartz	28	20	30	32	32	46	28	27	9	32	22	17	25	30	10	12
Microcline	25	20	11	7									12	tr	7	8
Oligoclase-andesine	40	49	44	47	42	43	48	57	75	26	53	58	46	48	57	55
Biotite	5	4	12	12	15	8	17	13	15	11	25	23	17	21	17	18
Muscovite	2	3	1	2	11	1	6	2	1	tr	tr	2	tr	tr		
Chlorite		3								tr				tr		
Sillimanite	tr	tr	2	tr	tr	tr	tr	tr	tr	tr		tr		tr	tr	
Garnet	tr	tr	tr			1				30			tr		8	2
Magnetite, Ilmenite	tr	1	tr	tr	tr	tr		tr	tr	tr	tr	tr			tr	tr
Tourmaline											tr		tr	tr	1	tr
Pyrite		tr				tr				tr		tr	tr			
Apatite	tr	tr	tr	tr	tr	tr	tr	1	tr	tr	tr	tr	tr	tr	tr	tr
Zircon	tr	tr	tr	tr	tr	tr	tr	tr	tr	tr	tr	tr	tr	tr	tr	tr
Sphene														1		
Graphite	tr	tr	tr	tr	tr	1	1	1	tr	1		tr			tr	
Epidote						tr	tr	tr			tr		tr	tr		
Allanite		tr		tr	tr								tr	tr	tr	tr

Kinsman quartz monzonite
1. Quartz monzonite
2. Granodiorite
3. Granodiorite
4. Granodiorite
5. Granodiorite
6. Quartz diorite
7. Quartz diorite
8. Quartz diorite
9. Quartz diorite

Inclusions
10. Coarse-grained garnet-mica gneiss
11. Medium-grained biotite gneiss
12. Medium-grained porphyroblastic biotite gneiss

"Sills"
13. Medium-grained granodiorite
14. Medium-grained quartz diorite

Feldspathized Littleton formation
15. Medium-grained biotite-garnet gneiss
16. Medium-grained biotite gneiss

Much of the rock in the neighborhood of Thompson Hill appears to be highly feldspathized. Both in hand specimen and in thin section, this rock appears intermediate between typical material of the Littleton formation and the sill-like masses of the Kinsman quartz monzonite.

Quartz, moderately zoned oligoclase-andesine, microcline, and red-brown biotite are the principal constituents and are similar to those minerals in the sill-like bodies (Table 3). Garnet is locally abundant as grains up to 2 mm. Accessories are apatite, zircon, allanite, tourmaline, ilmenite, and graphite.

SPAULDING QUARTZ DIORITE

Numerous small bodies of quartz diorite occur in the eastern part of the Sunapee the Monadnock quadrangle (Fowler-Billings, 1949) to the south. In the Sunapee area many of the bodies are too small to show on the geologic map. The bodies are most numerous in the vicinity of the Littleton formation which separates the Kinsman quartz monzonite from the Bethlehem gneiss. Some occur in the Kinsman quartz monzonite or along its contact with the Littleton formation. Contacts cannot be traced for very great distances so the true shape of some of these bodies is not well known. Many of the smaller bodies are clearly sill-like in nature, but some of the larger masses appear to cross-cut the structure of the enclosing rock. Exposures are best where the bodies of quartz diorite cross hill tops. Poor exposures on the northeast slope of Sunapee Mountain make it impossible to determine the true relations of

many isolated masses of quartz diorite found there.

The rock is dark gray with a medium- to fine-grained texture and a massive to well-foliated structure. In general, the coarser phases are the more massive and are found in the central parts of the larger bodies. Fine-grained, foliated types constitute the smaller bodies and the contact phases of the larger masses. Foliation of the fine-grained phase is due to a parallelism of biotite flakes. A lineation, which is strong in some specimens, is due to the apparent streaking out of biotite. The lineation was always observed to be parallel to that of the country rock. The coarser phases and some of the finer foliated ones show a distinct spotted appearance. Dark spots or knots, rich in mica, and light spots, rich in quartz or feldspar, are usually less than 5 mm. across.

In thin section, the quartz diorite has a very typical igneous (orthomagmatic) appearance. The texture is hypidiomorphic and usually inequigranular with porphyritic to subporphyritic phases. Plagioclase (andesine), biotite, and quartz with more or less microcline and hornblende are the chief minerals. Sphene, apatite, ilmenite, allanite, and zircon are the accessories. The composition ranges from quartz diorite to granodiorite.

Moderately zoned andesine occurs both in the groundmass and as phenocrysts. Albite and carlsbad twinning are universally well developed but pericline twinning is uncommon. The smaller grains are nearly equidimensional, but the larger crystals of the groundmass and the phenocryst are highly tabular with longer dimensions exceeding the shorter by 4 to 10 times. The feldspar of the groundmass ranges between 0.2 and 2.0 mm., but the phenocrysts commonly attain a length exceeding 5 mm. In many thin sections, tiny opaque inclusions are exceedingly abundant and seem to be confined to the inner two-thirds of the larger crystals. The line of demarkation between inclusion-rich and inclusion-free material is sharp. In a few sections the feldspars show concentric zones parallel to the pinacoidal faces in which the quantity of foreign material differs.

Quartz appears of two generations. The earlier is found in the interstices of the larger plagioclase crystals suggesting a magmatic origin. Quartz of the second generation is as rounded grains or irregular masses replacing, to a limited extent, most of the other minerals. The secondary nature of much of this quartz is also indicated by the optical continuity of neighboring but apparently isolated grains. Most of the later quartz shows moderately strong strain shadows. Quartz has replaced most frequently along grain boundaries of feldspar, and in many cases all of the feldspar crystal faces have been destroyed so the rock shows an allotromorphic granular texture. Biotite has a "moth-eaten" appearance as a result of replacement by rounded quartz grains. Locally the secondary quartz extends through feldspar crystals and across grain boundaries in a very irregular outline; nevertheless, neighboring but isolated grains show optical continuity. Where this arrangement is confined to single crystals of feldspar, a crude form of myrmekite is present. In a few sections the late quartz partially replaces the earlier interstitial quartz. Specimens from near the center of the larger quartz diorite bodies may show little secondary quartz. In these a small amount of quartz is intergrown with microcline and plagioclase to give typical micrographic textures. Small amounts of typical myrmekite are present in most sections, and this material replaces microcline which usually occurs in the groundmass as small interstitial grains. The microcline shows moderately strong crosshatch twinning and is locally perthitic.

Biotite is almost universally olive-green and commonly occurs in small aggregates associated with hornblende and accessories. Individual flakes range up to 3 or 4 mm. Blue-green hornblende is found as small crystals (1–2 mm.) poikilitically enclosing much quartz and magnetite. Much is inside biotite and appears to be altering to that mineral. Sphene is an abundant and diagnostic mineral and occurs as irregular grains of sufficient size to be detected in hand specimen without the hand lens. It encloses ilmenite and is usually confined to biotite but is seldom found in hornblende. Apatite is another diagnostic and abundant accessory and occurs as slender crystals (up to 2 mm. long) enclosed by most other minerals and as tiny needles in plagioclase. Allanite crystals rimmed with epidote are commonly 1.5 mm. long. Where enclosed in biotite, they show pleochroic haloes. Pyrite, zircon, and secondary muscovite are other minor constituents. Several modes of the Spaulding quartz diorite are given in Table 4.

The finer-grained foliated phase has a groundmass of nearly equidimensional, anhedral feldspar grains (0.1–0.5 mm.) and scattered phenocrysts up to 5 mm. long. A few glomerophenocrysts were seen. Most of these large tabular crystals have their long dimensions parallel to the rock foliation. Olive-green biotite flakes occur in parallel orientation between the feldspar crystals. Many are clustered giving the rock a spotted appearance. Quartz occurs usually as tiny rounded grains (0.05–0.5 mm.) evenly distributed throughout the

rock and much replaces all other minerals. It thus differs from the quartz of the coarser phase because only a small proportion is concentrated on the borders of large feldspar crystals. Much of the quartz may be considered late. In other respects, the finer-grained foliated phase resembles the coarser and more massive type. A mode is given in Table 4.

TABLE 4.—ESTIMATED MODES OF THE LATE QUARTZ-FELDSPAR ROCKS

	Spaulding quartz-diorite							Quartz monzonite				Concord granite						
	1	2	3	4	5	6	7	8	9	10	11	12	13	14	15	16	17	18
Quartz	15	20	17	12	13	7	23	15	18	17	27	25	20	23	22	20	27	18
Microcline	13	11	6	6	3	3	1	50	47	26	23	60	58	51	51	50	43	48
Oligoclase-andesine												16	18	17	18	23	22	30
Andesine	50	49	57	58	58	67	57	22	30	40	38							
Biotite	18	16	17	15	22	17	19	12	4	13	10	3	1	3	3	2	3	3
Muscovite	tr	1	1	tr	tr	tr	tr	1	1	2	2	6	3	6	6	5	5	1
Chlorite									tr				tr	tr			tr	
Hornblende				5		3												
Sillimanite								tr	tr	tr	tr	tr		tr			tr	tr
Garnet																tr		
Epidote	tr	tr	tr		tr	tr	tr	tr		tr			tr					
Allanite	tr	tr	tr	tr	tr	tr	tr			tr								
Zircon	tr	tr	tr	tr	tr	tr	tr	tr	tr	tr	tr	tr	tr	tr	tr	tr	tr	tr
Apatite	1	1	tr	1	1	tr	1	tr	tr	1	tr	tr	tr	tr	tr	tr	tr	tr
Sphene	3	2	2	2	3	3	tr			1	tr							
Magnetite				tr		tr		tr	tr		tr						tr	tr
Ilmenite	tr	tr	tr	tr		tr	tr			tr								
Pyrite	tr			tr	tr	tr	tr	tr		tr								
Rutile									tr					tr			tr	
Opaque												tr	tr	tr	tr			

Spaulding quartz diorite
1. Granodiorite
2. Granodiorite
3. Quartz diorite
4. Quartz diorite
5. Quartz diorite
6. Quartz diorite
7. Foliated quartz diorite

Quartz monzonite
8. Granite
9. Quartz monzonite
10. Quartz monzonite
11. Porphyritic quartz monzonite

Concord granite
12. Coarse-grained granite
13. Medium-grained granite
14. Medium-grained granite
15. Medium-grained granite
16. Fine-grained porphyritic granite
17. Fine-grained granite
18. Fine-grained quartz monzonite

QUARTZ MONZONITE

Cutting and including blocks of the quartz diorite is a light- to medium-gray, fine-grained to medium-grained rock which will be referred to as quartz monzonite. Although locally granite, the rock is predominantly quartz monzonite. In the Sunapee quadrangle it appears to be confined to the Hubbard Hill member of the Littleton formation. In a few localities it is gradational into porphyritic and weakly foliated types which were at first considered to be a variety of the Kinsman quartz monzonite. In one of these areas (west of Blueberry Mountain, in Sunapee Township) the quartz monzonite is clearly seen to include blocks of the typical Kinsman quartz monzonite. Some of the lighest-colored phases may resemble the Concord granite but it is cut by the granite and differs from it in its less granular texture, its lower content of muscovite, and abundance of certain diagnostic accessories (such as sphene). West of Blueberry Mountain some of the quartz monzonite shows a weak lineation which is due to a steep linear arrangement of biotite and small spindle-shaped masses of mafic minerals, less than an inch long.

Quartz with moderately strong strain shadows is mostly between feldspar crystals as rounded to irregular curved grains. Some appears interstitial to the subhedral crystals as in the Spaulding quartz diorite. Much is apparently late because it

replaces plagioclase and microcline with optical continuity between neighboring, isolated grains. In some specimens quartz replaces the marginal zone of larger plagioclase crystals in the form of myrmekite. In most, however, it is intergrown with small grains of plagioclase to form typical myrmekite. Plagioclase is andesine and shows weak to moderately strong zoning. Albite and carlsbad twinning are usually observed, but pericline twins are less common. Small grains are anhedral and equidimensional, but larger crystals up to 10 mm. or so have length-width ratios up to 4:1. These larger crystals resemble the large plagioclase crystals of the Spaulding quartz diorite. Microcline is abundant as anhedral grains showing strong crosshatching. Large crystals (up to 30 mm.) of microperthite with carlsbad twinning are common. Much is replaced by myrmekite. Biotite may be red-brown or olive-green. Muscovite occurs as tiny flakes in plagioclase and less abundantly as large flakes replacing biotite and other minerals. The accessory content of the quartz monzonite resembles that of the Spaulding quartz diorite. Sphene is frequently so abundant and in such large grains that it may be readily detected in hand specimen. Abundant slender crystals of apatite, large crystals of allanite (rimmed by epidote) and grains of ilmenite (rimmed by sphene) are also characteristic. Other accessories are shown in the modes in Table 4.

Concord Granite

The term Concord granite is used here to include a group of medium- to fine-grained, light-colored granites in which muscovite usually predominates over biotite. The granite occurs in dike-like masses cutting most of the other rocks in the eastern half of the area. In the vicinity of Sunapee Lake and Little Sunapee Lake, outcrops are poor but Concord granite appears as the most abundant rock type. It seems likely that the granite here constitutes a large stock-like mass.

In hand specimen the rock is light gray to buff. Some of the coarsest material is white due to the abundance of white feldspar. The fresh, fine-grained variety may have a distinct bluish-gray cast. The finer-grained varieties are usually poorly foliated parallel to contacts, but the centers of larger bodies are quite massive. Subporphyritic phases occur locally in the coarse type with large crystals of microcline up to 2 cm. long. Quartz has a slightly smoky appearance. Muscovite may occur as large flakes or books up to 5 mm. across. These large crystals are commonly euhedral with diamond-shaped or hexagonal outline. In places patches of muscovite up to a centimeter across are common.

Microscopically the rock is allotriomorphic granular and is composed mostly of microcline, plagioclase and quartz. Much of the quartz is as rounded and irregular masses replacing most other minerals and is, therefore, late in formation. Some is in myrmekite which replaces microcline and microcline perthite. Plagioclase is weakly zoned. It is oligoclase-andesine and shows albite and carlsbad twinning. Biotite is red-brown, poorly oriented but never abundant. Muscovite is as large flakes which in some specimens enclose small grains of quartz, microcline and plagioclase. Some replaces biotite and small quantities occur as tiny flakes in fledspar. In general it appears as a late mineral. The principal accessory minerals include zircon, apatite, and sillimanite. Modes are given in Table 4.

Structural Features

General Statement

The larger structural features in the Sunapee quadrangle include three masses of granitic gneiss which are more or less elongate in a NNE-SSW direction. These bodies are composed of the Croydon group, the Bethlehem gneiss, and the Kinsman quartz monzonite. The Bethlehem gneiss is separated from the Croydon group by the Grantham fault and from the Kinsman quartz monzonite by the Hubbard Hill member of the Littleton formation. The foliation and lineation of the gneisses are parallel to those structures in the adjacent metamorphic rocks. These granitic bodies appear in general to be structurally concordant to the metamorphic rocks with which they are in contact. Discordant relations are usually local.

Structure West of the Bethlehem Gneiss

The structure of the rocks west of the Bethlehem gneiss was studied by the writer 10 years ago (Chapman, 1942). No further fieldwork has been done in this part of the quadrangle except for the portion south of

Sugar River and a small area immediately north of the river. Consequently any statements concerning the interpretation of the structure or petrogenesis of the rocks in the northwest corner of the quadrangle are based entirely upon the earlier investigation.

The area northwest of the Grantham fault, which extends from Dunbar Hill at the north edge of the quadrangle nearly to Sugar River at the west border, is underlain largely by gneiss of the Croydon group. This gneiss is surrounded on the northwest, west, and southwest by successively younger belts of metamorphic rock. Bedding and foliation in these rocks dip outward away from the gneiss in most places, although the rocks show varying degrees of crumpling and folding which increase away from the gneiss. Field relations on Croydon Mountain show that the Ammonoosuc volcanics rest upon the gneiss and that this belt of rocks is overlain by the successively younger formations. Foliation within the gneiss is parallel to that of the metamorphic rocks at the contacts, but within the body it appears to have the form of large open folds. These folds trend roughly NNE-SSW parallel to the folds in the surrounding metamorphic rocks. In the earlier publication (Chapman, 1942), the gneiss is considered to have formed from a magma which intruded horizontal rocks and domed them up in laccolithic fashion. The structure is known as the Croydon dome. The small area of Ammonoosuc volcanics and Clough formation, west of the village of Croydon Flat, is considered to overlie the gneiss as a remnant of the highly eroded roof rocks.

The general structure of the metamorphic rocks south of Sugar River has already been considered in connection with the Fitch formation.

Grantham Fault

Bethlehem gneiss has been brought into contact with rocks of the Croydon group throughout most of the extent of the Grantham fault in the Sunapee quadrangle. In the Mascoma quadrangle to the north and the Claremont quadrangle to the west, it is very clear that the Bethlehem gneiss occupies a stratigraphic position somewhat above that of the Croydon group and other rocks of the Oliverian magma series. This relationship is less striking in the Sunapee quadrangle. In all three quadrangles the east side of the Grantham fault has apparently moved down relative to the west side so that stratigraphically higher units form the east block of the fault. The fault can be readily traced along most of its course by conspicuous silicified zones. In the Mascoma quadrangle and on Dunbar Hill in the Sunapee quadrangle, the general dip of the silicified zones may be determined. This dip is steep and to the east. If the silicified zones which roughly parallel the fault in strike can be assumed to parallel the fault in dip also, then the Grantham fault is of the normal type. Steep normal faults of this same general trend have been found to the southwest in the Bellows Falls quadrangle (Kruger, 1946) and Keene quadrangle (Moore, 1949) where they are correlated with the Triassic faults of the Connecticut valley in southern New England.

The most conspicuous silicified zones are found on Dunbar Hill and The Pinnacle. On the northeast slope of Dunbar Hill, the silicified zone consists of a tabular mass of nearly pure white vein quartz tending about N20°E. It appears to dip easterly at about 70° and forms the dip slope of the hill. Jointing is prominent in the quartz mass and two distinct sets may be noted. These are N15°E 70°SE and N70°E60°NW. Closer inspection reveals that the quartz body is made up of small quartz veins which have been cut by younger quartz veins and these in turn by others and so on until a very complicated network of small veins has resulted. One concludes that movement along the fault must have occurred in a large number of smaller displacements. If the fault surface were slightly curved, repeated movement could produce lens-like openings which could fill with silica, only to be shattered and opened again with the next succeeding displacement. In this manner pod or lens-like masses of silica up to thousands of feet long and several hundred feet thick accumulated. It is significant that the trend of the silicified zones and the trend of one major joint set are parallel.

In addition to silica, the silicified zones

contain irregular blocks of gneiss which are also highly veined and silicified. Quartz druses and comb-structure are common. Specular hematite and some botryoidal hematite are found on quartz crystals and in cavities.

On Dunbar Hill, to the west of the silicified zone, gneiss of the Croydon group has been greatly disturbed. Fractures trending roughly N15°E70°SE are numerous and many have been filled with quartz, forming veins up to 2 inches wide and many yards long. Here also the gneiss appears to have been shattered into large blocks. In addition, masses of biotite gneiss and schist and hornblende gneiss, resembling types in the Ammonoosuc volcanics, are abundant. The foliation of these masses is oriented at all angles. It appears that these angular blocks, intermixed with blocks of the Croydon group, constitute a very coarse fault breccia.

Instead of a single silicified zone, several narrow zones may parallel each other. Each zone may be less than 200 feet wide and form a low topographic ridge. The fault zone on The Pinnacle is about 1000 feet wide but is composed of several small parallel silicified zones. Adjacent to the silicified zones the rocks of the Croydon group and Bethlehem gneiss are sheared, shattered, and leached of biotite. Specular hematite occurs in scattered masses or in irregular, branching and parallel veins. In places the rocks are strongly silicified and brittle.

The trend of the fault zone is N25°E to N30°E whereas the silicified zones and predominant fracture sets trend N15°E to N20°E. This 10° difference indicates that the displacement has taken place along a series of fractures which are arranged en echelon to the trend of the fault zone itself. The throw along the fault is estimated to be 1000 to 2000 feet.

Hubbard Hill Member

The Hubbard Hill member forms a nearly continuous belt across the quadrangle. The interruption by the Concord granite and Bethlehem gneiss, north of Sunapee Lake, is the only break in this belt of schists for many miles. On a grand scale the structure of this belt is simple and is believed to be the east limb of a large anticline whose axis lies about 6 miles to the west.

It is not possible to detect bedding with certainty in most outcrops but, wherever conspicuous, bedding is parallel to schistosity. This relation is most frequently observed in the schist north of Little Sunapee Lake and on the west flank of Sunapee Mountain where beds range from 3–10 inches thick. In these areas minor folds are moderately open and range up to several feet in amplitude. The axial planes trend roughly parallel to the trend of the member and they dip steeply to the east. Fold axes are essentially horizontal. In the vicinity of Royal Arch Hill in Springfield Township, folding on the minor scale is fairly closed, but these smaller folds appear to have developed on a larger anticline and syncline whose amplitudes are several thousand feet. In the western part of the Hubbard Hill member, particularly south of Sunapee village, the minor folds in bedding are more nearly isoclinal, and the schistosity appears of the axial plane type. These rocks may have possessed a bedding plane schistosity which was in part destroyed as a result of the tight folding, whereas to the east and farther north the original bedding plane schistosity is still preserved.

Lineation is almost universally present, and occurs in either the direction *b* (essentially parallel to the major fold axis) or the direction *a* (essentially perpendicular to *b* and in the plane of schistosity). The lineation appears of three basic types: crinkles, elongate minerals, and streaked minerals. Elongate minerals are most commonly biotite and muscovite and much less commonly sillimanite, tourmaline, and actinolite. Muscovite crystals up to a centimeter long are arranged in girdle fashion about their long axis. Streaking of minerals is relatively uncommon and occurs most frequently in the case of biotite and muscovite. In general, down-dip lineation is more common, and strike lineation appears to have developed only where folding is pronounced (not necessarily tight) (Pl. 2). This relationship between direction of lineation and nature of folding is believed to have a genetic significance. Considerable information is contained in Table 5 which gives the frequency of the various types

of lineation in the Hubbard Hill member as determined from field notes. No attempt was made to sample the area statistically but the values give the general relationships. For example, *a*-lineation is twice as common as *b*-lineation. Mica lineation is the most common type of *a*-lineation and crinkles are the most common *b*-lineation type.

Dakin Hill Member

The massiveness of the Dakin Hill member makes structural interpretation difficult. The foliation of these relatively coarse gneisses is conspicuous in many places and folding of the gneissic banding is observed only locally. Lenses, streaks, and layers of feldspar-rich material show small folds in the feldspar gneisses. The relationship between bedding and foliation is not known, but the general impression is gained that the two structures are usually parallel. The member is believed, therefore, to be stratigraphically above the Hubbard Hill member and to possess a rather consistently steep dip to the east. If these rocks ever possessed a good lineation, it has apparently been lost through intense recrystallization. In some of the more schistose layers, crinkles may be observed and large muscovite and biotite flakes are arranged in a linear fashion. Oriented elongate quartz pebbles have already been mentioned from the quartz conglomerate of the Dakin Hill member. The pebbles range up to an inch in length and elongation is down dip. Axial ratios are 1:2:6 and 1:3:25 at the two localities where measured.

Bethlehem Gneiss

Foliation.—The Bethlehem gneiss of the Sunapee quadrangle is part of a large body (Mt. Clough pluton) which extends parallel to the regional structure in western New Hampshire for over 80 miles and ranges in width from half to about seven miles. The foliation of the gneiss is very good in most places, but locally gives way to a pronounced lineation. In the Sunapee quadrangle, it is very clear that the best foliation is not necessarily confined to the borders of the mass but in general must be considered equally good throughout. This relationship is an important one, and has already been pointed out by the writer to be true in the Mascoma quadrangle (Chapman, 1939, p. 163) immediately to the north. Another important relationship is that the foliation of the gneiss is essentially parallel to the contacts of the

TABLE 5.—LINEATION OF THE HUBBARD HILL MEMBER

	a—Lineation		% of all Lineation
	Readings	%	
Crinkles	22	21	14
Biotite	49	46	33
Muscovite	31	30	20
Sillimanite	3	3	2
	105	100	69
	b—Lineation		
Crinkles	23	50	15
Biotite	12	26	8
Muscovite	5	10	3
Sillimanite	5	10	3
Tourmaline	1	2	1
Amphibole	1	2	1
	57	100	31

body throughout its entire extent. A few exceptions to this statement will be considered later. One obvious exception is where the gneiss is bounded by a fault along its west border in the Sunapee quadrangle and part of the Mascoma quadrangle. Furthermore, the foliation at the borders (nonfaulted) of the gneiss is parallel to the foliation or schistosity of the adjacent metamorphic rocks.

Inclusions within the gneiss are tabular and are oriented with their larger dimensions parallel to each other. They are foliated parallel to their length; and this foliation, as far as the writer is aware, is universally parallel to of the enclosing gneiss. Even where inclusions occur in poorly foliated or nonfoliated rock, they are neverthless in parallel orientation. Inclusions range in size up to many hundreds of feet long, and they appear to be more or less uniformly distributed throughout the mass.

In most places foliation appears folded, flexed, or crinkled. The smaller folded and wavy structures are plainly seen in outcrop where

wavelengths range up to many feet but commonly they are less than 1 or 2 feet. Larger folds may be determined by a study of adjacent outcrops. Some of these larger structures are revealed by a study of the dip and strike symbols on Plate 1. The northern two-thirds of the gneiss show easterly dips most commonly, but horizontal foliation and westerly dips are numerous. These values indicate numerous roughly N-S open anticlines and synclines (Pl. 2). The southern third of the gneiss shows mostly easterly dips in the eastern part and many southerly dips in the western part.

Another minor structure in the foliation is the common occurrence of single flexures associated with essentially plane shears. These are referred to as shear zones. The shear plane stands at a high angle to the foliation, and the relative movement on opposite sides of the shear is such as to produce a pronounced drag in the foliation to a distance of a few inches from the shear. The shears may be traced for many feet before they are seen to decrease in amplitude and die out. These structures are essentially small faults because in some instances a definite break in the foliation has occurred along the plane of shear. In other cases merely a sharp flexure is observed, and the structures are geometrically like small monoclines. These small structures may occur singularly or in large numbers. When in groups, the planes of shear are parallel and may be spaced a foot or so apart. The direction of shear in different structures within small areas is also parallel. Locally these flexures show thin lenses or sheets of pegmatitic material confined to the central part of the structure. Normally the pegmatite masses are 1 or 2 inches wide and extend parallel to the shear plane for 5–10 feet. Beyond where the pegmatite pinches out, the zone of flexing diminishes and disappears a few feet away. Numerous localities in which these shear zones are common are shown in Plate 2.

The origin of foliation in the Bethlehem will be considered in a later section.

Lineation.—Lineation in the gneiss is due to crinkles, elongate biotite or muscovite, elongate masses of quartz, girdle biotite, and rarely elongate inclusions. It is well developed throughout the area except in the following places in Goshen and Unity Townships where none was detected: just northwest of the village of Goshen, 1¼ miles southwest of Mill Village, and 1–1½ miles northeast of Mill Village. Direction of lineation is quite uniform over wide areas and appears to be closely related to the larger folds and flexures. In other words, either *a*-lineation or *b*-lineation is present (Pl. 2). In a few places two lineations are well developed. An excellent place to observe these is 1½ miles northwest of the village of Newport. Lineation in *a* is almost universal in the eastern half of the body. The plunge is generally southeast at angles less than 45°. In the eastern extension of Bethlehem gneiss, near Little Sunapee Lake, *b*-lineation is most common and plunges at very low angles either north or south. Immediately west of the line extending southward from the silicified zone near Stocker Pond, in Grantham Township, and through the village of Newport, *b*-lineation predominates. The change from one type to the other is very abrupt when crossing this line. A little farther to the west *a*-lineation becomes common again, and throughout much of this area both types occur together. Lineation in the gneiss along the road between the villages of Newport and Kelleyville appears as a downdip type. The strike of the gneiss is roughly east-west, but this trend is somewhat wavy due to broad flexing and folding. The folds plunge southward essentially parallel to the lineation. The lineation, therefore, is *b*-lineation and not *a*-lineation as one might at first suspect. This type of lineation predominates for about 2 miles south of the road, and from there on it is seldom seen but *a*-lineation is well developed.

Before considering the significance of the distribution of the different types of lineation, a very important structural relationship should be noted. In all observations made, lineation within inclusions parallels that of the enclosing gneiss; and along nonfaulted contacts, lineation within the gneiss parallels that within the adjacent metamorphic rocks.

The statistics on lineation taken from field notes show *a*-lineation three times as common as *b*-lineation (Table 6). In each type, biotite lineation is more common than crinkling, but the relative frequency of crinkling is higher in the *b*-lineation type than in the *a*-lineation type. Too much stress should not be placed on

these figures, however, because the biotite lineation and crinkling, when parallel, are probably genetically related and commonly merely a different expression of the same structural feature. For example, crinkling is made conspicuous in the gneiss where thin, continuous layers of mica exist. Where mica layers are more discontinuous and mica flakes more isolated, crinkles are difficult to detect. The nature of intergranular movement in the gneiss with discontinuous mica layers may have been the same as in the gneiss with continuous layers, but, in the latter case, the relative displacements have been permanently recorded by the wrinkled layers of micaceous material. In the rocks with discontinuous mica layers, therefore, biotite flakes are oriented in girdle fashion (i.e. parallel to a single line) with the girdle axis constituting the direction of lineation. Had crinkles been preserved, their axes would have been parallel to the common biotite axis. Therefore, biotite lineation is so common relative to crinkles because gneiss with discontinuous mica is more extensive, and crinkling movements left little or no trace in much of the rock. In some of these rocks, so much of the biotite is turned from a common plane of foliation that the foliation itself is destroyed and the rock possesses lineation only.

TABLE 6.—LINEATION OF THE BETHLEHEM GNEISS

	a—Lineation		% of all Lineation
	Readings	%	
Crinkles	196	26	19
Biotite	472	64	47
Muscovite	28	4	3
Quartz	42	6	4
	738	100	73
	b—Lineation		
Crinkles	105	37	10
Biotite	158	56	15
Muscovite	12	4	1
Quartz	8	3	1
	283	100	27

Crinkles are abundant and strongly developed in the *b* direction, but they are usually vague and less common in the *a* direction. Crinkles of the *b* type are usually seen to be associated with larger folds of varying orders of magnitude. These crinkles parallel fold axes. The larger folds are essentially parallel to the tectonic strike, and the fold axes are roughly horizontal. These relations indicate that the crinkles formed contemporaneously with the larger folds and as a result of essentially horizontal compression normal to the *b* direction.

Crinkles in the *a* direction are in general downdip structures and usually are not seen to be associated with folded or wavy foliation. It appears, therefore, that these features formed as essentially downdip structures on the flanks of large folds and are probably due to crowding and slipping along planes of foliation in the direction of the tectonic axis. In other words, a minor amount of shortening took place in the direction of *b*.

The relation between steep shear zones, flexures, and crinkles is very clear in the outcrops, between the road and railroad, a mile east of the village of Northville. Here shear zones and shear flexures are very abundant. Foliation is essentially flat, and the shear planes strike N70°E and are vertical. One set of crinkles trends roughly N-S and another strongly developed set trends N70°E. It is apparent that the displacement along shear planes and the formation of the nearly E-W crinkles are both the result of the same deformational forces. This relationship is known to hold for a few other areas where the shear zones are numerous. Most commonly, however, the shear planes are associated with a single lineation. This lineation is either essentially parallel or normal to the strike of the steep shear zones. Where shear planes parallel lineation, both structures are probably genetically related. These general relations are apparent in Plate 2.

Muscovite lineation may be explained on the same basis as biotite lineation. It appears so infrequently because muscovite is a minor constitutent of the gneiss and, because of transparency, a difficult mineral in which to recognize lineation.

Lineation of quartz is probably equally common in the *a* and *b* directions, but intense

crinkling in *b* may make it more difficult to detect. The lineation appears as somewhat elongated masses or lenses composed of granoblastic quartz. These masses were interpreted earlier (Chapman, 1939, p. 147) as large quartz crystals which had become granulated and smeared out parallel to foliation. In the present study, these lenses are considered to have formed as a result of constructional and not destructional forces. It will become clear later why these lenses have developed in some cases in a linear fashion. For the present they may be considered to represent just another way of expressing the crinkled structure of the rock.

Contact zone.—The true nature of the contact zone may be readily studied in the Sunapee quadrangle. In Goshen Township, it may be seen in Babb Brook and the area immediately to the northeast and southwest, on Thompson Hill, on Chandler Hill, and off the road just northeast of the Rand Pond. Two good localities in Sunapee Township are 1.2 miles due west of Blueberry Mountain and half a mile southwest of Browns Hill. In Springfield Township, the zone is beautifully exposed at the base of Royal Arch Hill.

The following essential features characterize this zone. There are alternating, tabular masses of Bethlehem gneiss and schist of the Littleton formation. Sill-like bodies of the gneiss range from a fraction of an inch up to many feet thick. Inclusions and septum-like bodies of schist have similar dimensional ranges. The general appearance in many respects resembles that of a migmatite. The width of the zone ranges up to about half a mile. Foliation of the gneiss is everywhere parallel to the schistosity in the rocks of the Littleton formation, and the contacts between rock types are parallel to the planar structures within the rocks. Lineation of the gneiss is parallel to that of the schist. On the south side of Royal Arch Hill, the alternating layers of schist and gneiss form a series of north-south folds whose axes are nearly horizontal. Foliation within the gneiss shows the same pattern of folding and crinkling as the schistosity of the alternating layers of the Littleton formation. The same general relations hold for the contact zone between Little Sunapee Lake and Otter Pond. Field and laboratory studies show that certain layers of the Littleton formation have been more or less feldspathized so that in many cases it is difficult to tell what is Bethlehem gneiss and what is feldspathized schist. A detailed description and modes of these rocks types have been given in an earlier section.

The western boundary of the gneiss, along the Grantham fault, has already been described. The Bethlehem gneiss rests on quartzite and amphibolite of the Fitch formation from where the contact leaves the fault and extends south across Mt. Tug. On Mt. Tug the contact is well exposed for several hundred feet parallel to the strike. Here it can be seen to dip eastward at about 25°. The foliation of the Fitch formation, below, and Bethlehem gneiss, above, are parallel to the contact itself. It seems clear that the gneiss is resting conformably on top of the Fitch formation. There are no indications of faulting along this zone and the gneiss seems to retain its normal character. The texture is perhaps a little finer-grained than the average gneiss but this may not be very significant because fine-grained phases appear well within the mass. Lineation in the Fitch formation is parallel to that in the Bethlehem gneiss.

From these observations, the writer concludes that the Bethlehem gneiss represents a large tabular mass, essentially concordant with the adjacent metamorphic rocks, and possesses a folded structure, which in general conforms with that of the adjacent metamorphic rocks. The cross sections in Plate 1 give the general pattern of folding. The gneiss does not appear as highly crumpled as the rocks of the Hubbard Hill member. The eastward extension of gneiss, as far as Little Sunapee Lake, is due largely to folding of the eastern contact of this body with the Hubbard Hill member. The folded contact and contact zone can be observed on the south side of Royal Arch Hill, near the west end of Little Sunapee Lake, and along the main road at Otter Pond. It is very possible that this large re-entrant of gneiss into the Littleton formation can be accounted for in part by a cross-cutting relationship. The intense folding of the gneiss here and the small inlier of Bethlehem gneiss south of Otterville indicate that erosion has stripped off much of the highly folded overlying Littleton formation.

The sillicified zone east of Stocker Pond, in Grantham, resembles some of the silicified zones along the Grantham fault. The zone ex-

tends N10°E, and the principal joints in the silicified materials are N10°E 65°SE. The zone here is 10–50 feet wide and contains a little breccia of Bethlehem gneiss in fragments up to 2 inches across. It seems significant that another and more extensive silicified zone occurs 6 miles to the northeast on Banks Pinnacle, in Grafton Township, (Chapman, 1939). Perhaps these two conspicuous features outline the trace of another easterly dipping fault. The southern extension of such a fault may lie along the remarkably straight valley which extends from the silicified zone through Long Pond to the village of Newport. Brecciation without silicification may have formed a belt of weak rock, which was more readily weathered than the adjacent Bethlehem gneiss. If there is a fault here and if the displacement is relatively the same as that for the Grantham fault, then the western block of Bethlehem gneiss has been tilted to the west. If the dip and displacement are the reverse of that of the Grantham fault, then the western block of gneiss is a graben. There is little doubt that dislocation has occurred along the silicified zone, but the magnitude and direction of movement remains unknown. In any event, the Bethlehem gneiss west of this possible fault-line is structurally different from that east of the line. One principal difference is the nature of lineation already mentioned. Another difference is to be noted in the next section.

Pegmatite and aplite.—Pegmatites and aplites are abundant in the rocks of the Sunapee quadrangle. This area lies between the two well-known pegmatite districts of Keene and Grafton, New Hampshire. In general, the larger and more valuable pegmatites are found in the Littleton formation, and these bodies are more abundant in the schists immediately east of the Bethlehem gneiss. Pegmatites and aplites in the Bethlehem gneiss are very numerous although generally smaller than those in the schist. A somewhat more limited study of the Kinsman quartz monzonite shows that pegmatites in this rock are also generally smaller than those in the Littleton formation. In the present investigation, little attention was paid to pegmatites and aplites except those occurring within the Bethlehem gneiss. The attitude and structural relations for about 275 of these bodies within the Bethlehem gneiss were determined in the field. Most of these data are shown in Plate 2.

To simplify the description of the general field relations and distribution of the pegmatite-aplite bodies, they may be distinguished as concordant and discordant masses. The pegmatites and aplites are most abundant in the eastern part of the Bethlehem gneiss (Pl. 2). The distribution, as determined from the tectonic map, may be somewhat exaggerated because exposures are a little better in the eastern part of the gneiss. The pegmatites and aplites appear to be most abundant where foliation is consistently steeper and to the east. In the southern part of the area, these bodies form a band which extends nearly across the Bethlehem gneiss. In this area foliation dips fairly consistently to the east. The lack of readings in the northeast and southwest parts of the southwest ninth of the quadrangle is due to the thick cover of glacial drift.

The relation between the attitude of aplite and pegmatite and the attitude of foliation within the Bethlehem gneiss is worth noting. A preliminary study of this relationship was undertaken by Wilson (1948) and is being continued by the present writer. Only the general relations will be mentioned here. The concordant pegmatites and aplites are most abundant in the northeast part of the gneiss and are only locally developed over much of the rest of the area. In the southern third of the Bethlehem gneiss, foliation strikes about NE-SW and dips 10°–50° southeast. Most of the discordant pegmatites and aplites strike more into the east and dip 65°–90°SE. A second set of bodies (less numerous) strikes NW-SE and dips very steeply. In the east-central part of the gneiss, the foliation strikes more into the north. The pegmatites are still NE-SW in strike and the dips are generally steep to the southeast. Here, however, a few bodies dip at low angles and some even dip northwest. Here the second set of pegmatites has become relatively more abundant and the strike is NW to NNW. The dip ranges from about 40°–60°NE. In the northeastern section, foliation is variable ranging in strike from N-S to NE-SW and dipping between 20°–40° to the east. One set of pegmatites and aplites trends more or less NE-SW and dips range from low to steep. These bodies are not

numerous. The other set strikes N-S to NW-SE and dips northeast at angles greater than 45°.

Kinsman Quartz Monzonite

In many respects the major and minor structures of the Kinsman quartz monzonite resemble those of the Bethlehem gneiss. Exposures of the Kinsman quartz monzonite are relatively poor in the Sunapee quadrangle, and knowledge of the detailed structure is much more scanty than for the mass of Bethlehem gneiss. The Kinsman quartz monzonite constitutes a highly elongate body, which trends parallel to the Bethlehem gneiss for a distance of about 60 miles. It also is essentially concordant with the regional structure.

Foliation, most frequently due to parallelism of long tabular feldspar crystals, is not as good as in the Bethlehem gneiss. The general trend of foliation is NNE-SSW and the dip is steep to the east. Broad swings in the trend of foliation is an expression of open folds and flexures; folds were not observed in single outcrops. Where large feldspar crystals are lacking, foliation may be expressed by small tabular feldspar crystals and elongate masses of granoblastic quartz. Biotite orientation is generally poor. In all cases noted, foliation of the Kinsman quartz monzonite is parallel to foliation of the adjacent metamorphic rocks and, in general, to the contact of the body. Inclusions are generally tabular and universally elongated parallel to the foliation of the enclosing rock. Foliation of inclusion and Kinsman quartz monzonite are parallel.

Lineation is poor and was observed in relatively few places. It appears to be *a*-lineation and is due to crinkles and elongate biotite and muscovite. It is parallel to the lineation of inclusions and adjacent metamorphic rocks.

The contact zone of this body is similar to that of the Bethlehem gneiss and need not be described in detail. Sill-like masses of Kinsman quartz monzonite appear in the Littleton formation. Inclusions of schist, in parallel arrangement, are common in the Kinsman quartz monzonite. Foliation and lineation in one rock type are parallel to foliation and lineation in the other. Several large sill-like bodies in the Hubbard Hill member just west of Sunapee Mountain are shown in Plate 1. Other bodies too small to map are abundant. The tabular mass of Kinsman quartz monzonite which extends southwestward across Sunapee Mountain and for over 12 miles into the Lovewell Mountain quadrangle (Heald, 1950) to the south is probably the largest of these sill-like features. The feldspathization of inclusions and adjacent metamorphic rock has already been considered.

Field relations suggest that the Kinsman quartz monzonite constitutes a concordant tabular body which splits into numerous digitations at the north end of Sunapee Mountain. The disappearance of the Dakin Hill member and the upper part of the Hubbard Hill member, near the north end of Sunapee Mountain, suggests that the Kinsman quartz monzonite is replacing (taking the place of) much of the Littleton formation. The manner in which the body of Kinsman quartz monzonite was formed is reserved for consideration in a later section.

Late Quartz-Feldspar Rocks

General statement.—The term "late quartz-feldspar rocks" is used here to include the Spaulding quartz diorite, the quartz monzonite (like that near Blueberry Mountain), and the Concord granite. These rocks ard considered to be closely related both genetically and chronologically, and they may best be treated as a group. All these occur in small bodies in the Sunapee area, and lack of critical outcrops makes it difficult to determine many details regarding the shapes of these small masses. Some of the bodies appear as sills or dikes but others are perhaps quite irregular.

Spaulding quartz diorite.—The distribution of outcrops of Spaulding quartz diorite and the nature of the contacts, where observed, indicate that most of this rock type occurs in sill-like masses. Just west of Sunapee Harbor, the quartz diorite appears more irregular and cross-cutting. Foliation is restricted to the contacts in the larger masses but the smaller bodies may be foliated throughout. In the area a mile due north of Baisdell Hill, in Sunapee Township, the well-foliated phase of quartz diorite forms numerous belts, up to a few hundred feet wide and several thousand feet long, parallel to the bedding and foliation of the surrounding Littleton formation. These masses are shown on the geologic map, in a generalized fashion,

as two separate bodies. The large mass which is shown extending due south across the west end of Blueberry Mountain is believed to pinch out west of the high peak on Sunapee Mountain. As shown on the map, contact control is good only at the higher elevations. On the elongate hill 1½ miles northeast of Rand Pond, an elongate mass of the Littleton formation appears included in the quartz diorite. South of this inclusion excellent exposures occur, and the gradation between massive quartz diorite in the center and highly foliated quartz diorite at either contact can be clearly demonstrated. Some of the foliated quartz diorite is porphyritic in appearance, and small inclusions of schist were noted in the foliated phase. The inclusions are oriented parallel to the foliation of the quartz diorite. Foliation and lineation within the contact phase of quartz diorite are well developed here and are parallel to the foliation and lineation of the adjacent Littleton formation.

Where the quartz diorite crosses Blueberry Mountain, the body is actually composed of several smaller belts of moderately foliated to strongly foliated rock which alternate with Kinsman quartz monzonite and massive quartz monzonite, like that half a mile to the east. The foliation and lineation within the quartz diorite are parallel to those structures in the adjacent Littleton formation.

The true shape of the long body of Spaulding quartz diorite extending from Baisdell Hill to Blueberry Mountain is not known because outcrops are poor in this section. The linear distribution of quartz diorite, however, suggests the body is a slightly cross-cutting dike. Several good outcrops along the main road show this mass to be composed of the coarsest and most massive phase of the Spualding quartz in the quadrangle.

One striking feature of the more massive phase is the abundance of sheeting joints and steep joints which fall into several distinct sets. One set is about N-S another E-W. Two less commonly observed sets are about NE-SW and NW-SE. Many joints are filled with pegmatite, Concord granite, and quartz monzonite.

Quartz monzonite.—The rock referred to as quartz monzonite is universally associated with the Spaulding quartz diorite as small dikes following joints or as larger bodies of unknwon shape. The rock is usually massive and joints, filled by pegmatite and Concord granite, are common. On the geologic map, two small masses of the quartz monzonite are shown. One is about a mile west of the highest knoll on Blueberry Mountain, and the other is on the elongate hill 1½ miles south of Blueberry Mountain Though generalized on the map, these bodies are known to have a much more irregular outline. The mass west of Blueberry Mountain is believed to be bounded on the north and south by numerous fingers extending into the Littleton formation. The east and west boundaries are probably smooth and essentially concordant. In the belt of Spaulding quartz diorite on Blueberry Mountain, the quartz monzonite is apparently in long sill-like masses alternating with bands of the quartz diorite.

Concord granite.—Dikes of Concord granite occur abundantly in all rocks in the eastern third of the quadrangle. The presence of a large body of Concord granite around Little Sunapee Lake is based entirely on the relative abundance of granite outcrops to those of other rocks. Outcrops in this region are very poor, and so a dotted boundary is used to separate areas where Concord granite predominates from areas where the granite is subordinate to other types. In this body, the rock texture is coarse and the rock foliation poor or absent. The few readings obtained, however, show foliation roughly parallel to that of adjoining areas. Foliation within the smaller bodies is usually better than that within this large mass, and foliation is more pronounced toward the borders of bodies. The foliation, in nearly all cases, is parallel to that of the adjacent country rock. Grain size decreases with the size of the body. Joints in the granite are common and well developed and frequently are seen to have been filled with small pegmatites.

Age relations.—The relative ages of the late quartz-feldspar rocks may be determined from the following observations.

1. Spaulding quartz diorite contains numerous oriented inclusions of the Littleton formation. Small oriented inclusions of Kinsman quartz monzonite may be seen in the quartz diorite on Blueberry Mountain. The foliation of the quartz diorite is parallel to the contact wherever it was seen in contact with the Kinsman quartz monzonite. The foliation of the Kinsman quartz monzonite is nearly always

parallel to its contact with the quartz diorite, but in a few places on Blueberry Mountain it makes an angle with this contact of as much as 30°. The Kinsman quartz monzonite was never observed to be chilled or finer-grained against its contact with the Spaulding quartz diorite. On the northwest slope of the small hill half a mile WNW of Keyser Hill, in Sunapee Township, Spaulding quartz diorite has a chilled contact against a 25-foot mass of Kinsman quartz monzonite. The contact between the two bodies runs athwart the regional structure in the fashion of a cross-cutting dike or apophysis.

2. The quartz monzonite cuts the Littleton formation on the hill a mile west of Blueberry Mountain. At one place along the contact, diversely oriented tabular inclusions of the Littleton formation, a few inches long, are numerous in the quartz monzonite. The quartz monzonite some distance away contains a number of inclusions of Kinsman quartz monzonite up to several feet long. The foliation within these separate inclusions appears to conform to that of the adjacent Kinsman quartz monzonite. Inclusions of Spaulding quartz diorite (moderately to highly foliated phases) are extremely numerous in the quartz monzonite. These may be seen near the eastern limit of the quartz monzonite on the knoll a mile west of Blueberry Mountain. Hundreds of elongate inclusions occur here in sizes ranging up to a few feet, and the long dimensions are oriented parallel to a fairly prominent foliation in the quartz monzonite. Further east, in the belt of Spaulding quartz diorite, small masses of quartz monzonite cut and include masses of quartz diorite. Near by is a very coarse breccia consisting of angular blocks of Spaulding quartz diorite up to 20 feet across, enclosed in quartz monzonite. The blocks have not been moved far out of place, and the breccia zone, which is at least 50 feet wide, grades into quartz diorite heavily diked by the quartz monzonite. At the road junction just south of the "B" in "Boulders", in Sunapee Township, there are excellent outcrops in which to see large numbers of inclusions of foliated quartz diorite in what appears to be the same quartz monzonite as is found further south. Some of these appear like the exposures of breccia just described.

3. Dikes and sills of Concord granite cut the Littleton formation throughout the Hubbard Hill member, and dikes and sills of the granite are abundant in much of the Kinsman quartz monzonite. They are somewhat less numerous in the Bethlehem gneiss, and appear to be confined largely to the extreme eastern part of the body. Small dikes cutting the Spaulding quartz diorite may be seen in many localities, and dikes of Concord granite are numerous in the quartz monzonite on the hill west of Blueberry Mountain. Inclusions of the Littleton formation, the Kinsman quartz monzonite, and the Spaulding quartz diorite may be seen locally in the Concord granite. Some of these inclusions are well oriented. Behind the house immediately south of the "e" in "Boulders", in Sunapee Township, is an excellent outcrop in which to see a mass of Concord granite enclosing abundant angular and unoriented inclusions of the Littleton formation, the Spaulding quartz diorite, and small blocks of Kinsman quartz monzonite.

These observations indicate the following age relations. (1) The Spaulding quartz diorite is younger than the Littleton formation and the Kinsman quartz monzonite. (2) The quartz monzonite is younger than the Littleton formation, the Kinsman quartz monzonite, and the Spaulding quartz diorite. (3) The Concord granite is younger than the Littleton formation, the Bethlehem gneiss, the Kinsman quartz monzonite, the Spaulding quartz diorite, and the quartz monzonite.

Origin of the Bethlehem Gneiss and Kinsman Quartz Monzonite

General Statement

Three general theories for the origin of the Bethlehem gneiss and Kinsman quartz monzonite may be considered.

1. Magmatic—the rocks differentiated from basaltic or some other magma or they are of palingenetic origin.
2. Metamorphic—the rocks formed by recrystallization of a feldspathic sediment, a volcanic, or a pretectonic igneous body.
3. Replacement—the rocks formed by recrystallization of the Littleton formation and the addition of limited amounts of material from a distant source.

The main problem of origin resolves itself

into determining whether the granitic-looking rocks formed from an essentially solid or liquid state and whether any recognizable quantities of material have been introduced from without. A number of points must be given detailed consideration.

Origin of Foliation

It seems to the writer that the foliation of the Bethlehem gneiss can be explained better on the basis of the metamorphic or replacement theory than the magmatic theory. That the mass has been thoroughly recrystallized or reconstituted, in part subsequent to taking on its principal structural features, is strongly indicated by: (1) the parallelism between lineation and foliation of the gneiss and corresponding structures of the inclusions; (2) the parallelism between lineation of the gneiss and lineation of the adjacent metamorphic rocks; (3) the manner in which foliation of the gneiss universally cuts through inclusions; (4) the intense crinkling and folding of the foliation without shattered and granulated large feldspar crystals; and (5) the granoblastic texture of the rocks.

That foliation of the gneiss is the result of recrystallization, controlled by bedding, is indicated by: (1) the perfection and uniformity of foliation throughout the mass; (2) the abundance of gneiss with extensively continuous layers of mica; (3) the local development of a schistose phase; and (4) the extensive areas of flat foliation with local reversals in dip. (See cross section in Plate 1.) The foliation, therefore, has resulted from changes within a solid body and not a magma or slightly mobile fluid as the writer formerly believed (Chapman, 1939). The nature of the foliation lends credence to either the metamorphic or replacement theory.

The Sunapee quadrangle is an excellent locality in which to observe the gradual changes in structure and texture of rocks with increased intensity of metamorphism. The Littleton formation in the middle-grade zone of metamorphism on Croydon Mountain is more schistose and finer-grained than the Hubbard Hill member to the east. In crossing the Hubbard Hill member from west to east, one notes a distinct increase in abundance of coarser-grained and more gneissic material. Still further east, the Dakin Hill member is composed predominantly of coarse gneiss with highly discontinuous mica layers. In a way the same general relations hold for the large bodies of feldspathic gneiss. The mica layers of the Bethlehem gneiss in general become more discontinuous from west to east. Along the eastern contact and particularly in the eastern extension north of Little Sunapee Lake, mica layers are so discontinuous and the texture so coarse that in many outdrops one might wonder whether the rock is Bethlehem gneiss or Kinsman quartz monzonite. This similarity of rock types close to and on both sides of the Hubbard Hill member was particularly confusing to the writer in the early stages of the field work. In the northwest corner of the Mount Kearsarge quadrangle (east of Sunapee quadrangle), much of the Kinsman quartz monzonite appears identical with phases of the Bethlehem gneiss. South of Sunapee Lake, however, the abundance of large feldspar crystals makes the Kinsman quartz monzonite quite easily distinguished from the Bethlehem gneiss. This transition from well-foliated Bethlehem gneiss to poorly-foliated and coarser-textured Kinsman quartz monzonite not only suggests a close genetic relationship between the two bodies, but it is quite in agreement with the idea that processes of recrystallization and reconstitution have contributed largely to the formation of these rocks. The analogy between structural and textural evolution of the Littleton formation and the feldspathic gneisses is remarkable.

It is now clear why the micas in the matrix of the Kinsman quartz monzonite and in the coarse-textured Bethlehem gneiss exhibit a poor foliation. It is equally clear why the well-defined and continuous mica layers are so commonly exhibited in the western part of the Bethlehem gneiss. Recrystallization of the rocks along the Newport-Kelleyville road, for example, did not proceed to such a stage that it destroyed the bedded structure as it apparently did throughout much of the Kinsman quartz monzonite.

Origin of Large Feldspar Crystals

A detailed consideration of the nature and origin of the large crystals of potash feldspar

can shed much light on the problem of petrogenesis. For the following reasons the large crystals of potash feldspar cannot be considered as phenocrysts.

(1) Lack of orientation of the large feldspar crystals is common in the Bethlehem gneiss even where the rock is strongly foliated and where inclusions are well oriented.

(2) The large crystals do not appear to be deformed and granulated in spite of the severity of deformation this rock has undergone.

(3) It seems unreasonable that these large crystals are intratelluric in view of the low average microcline content for the rocks. Heald (1950, p. 84) points out that, if the large crystals were intratelluric, a second generation of microcline should be expected in the groundmass. Whereas microcline does occur in the groundmass of the Bethlehem gneiss, it is conspicuously absent in the matrix of the Kinsman quartz monzonite. Heald advances a second argument that the large crystals of feldspar are generally somewhat smaller in the small bodies of Kinsman quartz monzonite and that the development of the large crystals, therefore, was not controlled by intratelluric conditions.

If the large feldspar crystals are not intratelluric but formed during the final emplacement of a magmatic body, it is still difficult to explain why they have not suffered severe fracturing and granulation. It seems strange, furthermore, that in the Kinsman quartz monzonite practically all the microcline should succeed in accumulating around a few crystal centers to build such huge crystals during the latter part of the crystallization period. None apparently was available for the matrix. The microcline crystals are not only large in comparison with most phenocrysts, but they are unusually large to have been formed late in a magma. It is difficult to explain on this same basis the smaller microcline crystals in the small bodies of Kinsman quartz monzonite and the virtual absence of potash feldspar in the small bodies of Bethlehem gneiss. The smaller size cannot be due to chilling effects because the thermal gradient into the schist should not have been steep at the depth under which these rocks must have formed. The absence of microcline in the smaller bodies of Bethlehem gneiss and along the contact zone cannot reasonably be ascribed to effects of assimilation or chilling.

(4) In the chemical analyses of potash feldspar from the Kinsman quartz monzonite and Dakin Hill member (Table 7) the large feldspar crystal of the Kinsman quartz monzonite has a lower soda content than the potash feldspar porphyroblast from the Dakin Hill member. This low soda content seems indicative of a metamorphic or metasomatic rather than an igneous feldspar.

TABLE 7.—CHEMICAL ANALYSES OF POTASH FELDSPAR, LOVEWELL MOUNTAIN QUADRANGLE, NEW HAMPSHIRE

	1	2
SiO_2	63.90	63.94
TiO_2	0.00	0.04
Al_2O_3	20.46	19.48
Fe_2O_3 / FeO	0.09	0.06
MnO	0.00	0.00
MgO	0.08	0.18
CaO	0.16	0.36
Na_2O	2.38	1.64
K_2O	12.61	13.48
H_2O^+	0.12	0.30
BaO	0.36	0.39
	100.16	99.87

1. From porphyroblastic microcline gneiss, Dakin Hill member, Littleton formation (Heald, 1950, p. 64).
2. From Kinsman quartz monzonite (Heald, 1950, p. 64).

Many lines of evidence indicate that the large feldspar crystals formed late in essentially solid rock and are either prophyroblasts or metacrysts.[1]

(1) The shape and size of the microcline crystals are more in agreement with those expected for porphyroblasts or metacrysts than for phenocyrsts.

(2) Inclusions of biotite and rounded grains of quartz are generally observed in the large microcline crystals of the Bethlehem gneiss. The biotite shows no preferred orientation, which suggests recrystallization of biotite

[1] *Metacryst* is used in this paper to indicate a large crystal formed by replacement and as the result of the introduction of at least one major constituent from outside the rock unit.

without stress during the growth of the porphyroblast or metacryst.

(3) Large crystals of microcline and plagioclase, replacing inclusions of the Littleton formation within the Kinsman quartz monzonite and the metamorphic rocks along the contacts, have already been described in an earlier section. As far as megascopic and microscopic characters are concerned, these large crystals are identical with the other large crystals within the Kinsman quartz monzonite. In many cases it is difficult to decide where to place the boundary between the two rock types. If large crystals of this character could grow in what is unquestionably metamorphic rock, it is not unreasonable to think of all the large feldspar crystals as forming in essentially the same manner. In fact, the extensive formation of potash feldspar, much of which is in large crystals in the microcline gneiss of the Dakin Hill member, is further indication that the wide-spread development of porphyroblasts or metacrysts is not only logical but perhaps to be expected.

(4) The relationship between the large crystals and the matrix of the rocks (Fig. 2) is strong evidence in favor of the metamorphic and replacement theories. The large crystals of feldspar in part replace and in part displace foliation or schistosity regardless of whether they formed in rocks of the Littleton formation, Bethlehem gneiss, or Kinsman quartz monzonite. In thin section, these relations are even more striking. Those layers of mica coming in contact with a crystal boundary are clearly cut off where the boundary stands roughly normal to the layers but are deflected where the boundary is inclined. This relationship is believed to be the rule for many porphyroblasts and metacrysts. As the feldspar crystal begins to grow, it exerts pressure on the adjacent minerals causing those with a lower force of crystallization to be destroyed. In this case, some of the quartz grains between the flakes of mica are "dissolved" and room is made for the stronger mica flakes to be displaced outward from the growing crystal. If this process continues, in time a large number of mica layers are squeezed back as the quartz between them is removed. There results a concentration of mica at the side of the large crystal but no mica layers are cut off. If, however, the growing crystal is capable of replacing some mica as well as quartz, then less mica will appear at the margins of the large crystal. It seems logical that, in the case of mica, destruction of the flakes will proceed more rapidly

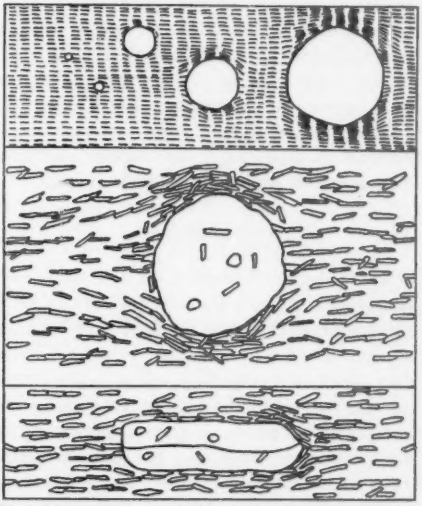

FIGURE 2.—RELATION BETWEEN PORPHYROBLAST AND FOLIATION

Upper—stages in growth showing how mica flakes are partly replaced and partly displaced. Middle—rounded microcline porphyroblast in Bethlehem gneiss. Diameter about 2 cm. Lower—tabular microcline porphyroblast in Kinsman quartz monzonite. Mica mostly displaced at wedge end and mostly replaced at square end. Length about 3 cm.

if the pressure is applied in the direction of the base rather than perpendicular thereto. In other words, since mica grows more rapidly parallel to the base, it is expected that the crystal should dissolve more rapidly in that direction under pressure. This idea has been applied to mineral orientation in metamorphic rocks for a long time, and it appears to be in good agreement with our present knowledge of crystal structure. We would expect, therefore, that the mica flakes standing nearly normal to the boundary of the growing crystal would be the ones to be replaced (destroyed) whereas the others would be pushed back as the quartz behind them was removed. If the quartz is consumed in the reconstitution of material to form the large crystal, silica merely moves

around the mica flakes to help build up the growing crystal.

(5) Many large and medium-sized crystals of microcline and plagioclase replace, in large part, what appear to be schist or fine gneiss remnants in specimens of typical Kinsman quartz monzonite and Bethlehem gneiss. Very striking examples may be seen in thin section. The old schist relics are characterized by well-oriented mica flakes and elongate or polygonal-shaped quartz grains. These relations indicate that both microcline and plagioclase crystals are replacing a metamorphic rock and that remnants of the typical schist remain.

Origin of Inclusions

The numerous inclusions of mica schist and fine-grained gneiss in the Bethlehem gneiss have already been described. If these represent inclusions oriented in a moving magma, the question arises as to why they are so well-oriented parallel to one another and to the foliation of the enclosing gneiss. If post-magmatic shear elongated these masses in the plane of foliation, we are unable to explain why orientation is equally good where foliation of the enclosing gneiss is poor. Again we are at a loss to explain why the large feldspar crystals were not sheared out along with inclusions. Another fact difficult to explain by the magmatic theory is why the inclusions are so abundant and so uniformly distributed and well oriented throughout this large body. There is no good evidence that strong penetrative movements existed which might have sheared them out into perfectly oriented tabular masses. On the contrary, the evidence seems to be strongly against the idea that these movements ever occured. On the basis of the replacement theory, the inclusions would be considered to represent unreplaced or partially replaced beds or portions of beds. On the basis of the metamorphic theory, they would be considered to represent lenses of slightly different composition or texture.

Rock Similarities

The reader has probably noted certain similarities between the mineral composition, textures, and structures of the Kinsman quartz monzonite, the Bethlehem gneiss and the Littleton formation. Many of these similarities have been pointed out, and it seems advisable to mention here that the writer considers them much more significant than coincidental. The principal differences are the lower proportions of mafics and accessories, the higher proportion of plagioclase, and the presence of microcline in the Bethlehem gneiss and Kinsman quartz monzonite. Large portions of the Dakin Hill member, however, contain potash feldspar. More intensive recrystallization of the Littleton formation, perhaps with the addition of components to form additional feldspar, would undoubtedly produce rocks like the Kinsman quartz monzonite or Bethlehem gneiss.

It is instructive to compare (Table 8) some analyses of the Kinsman quartz monzonite and Bethlehem gneiss with analyses of rocks from the Littleton formation. The compositions of the analyses of Kinsman quartz monzonite and Bethlehem gneiss are very close. These two types differ from the rocks of the Littleton formation in their higher SiO_2, Na_2O, and CaO content and lower Al_2O_3, FeO + Fe_2O_3, and MgO content. Such differences are in agreement with the magmatic theory. They also agree with the changes expected if components needed to form plagioclase and perhaps some potash feldspar were added to rocks of the Littleton formation. The differences could be explained on the basis of the metamorphic theory by assuming that the parent rocks of the feldspathic gneisses were feldspathic sediments or volcanics. Since feldspathic rocks occur in almost insignificant amounts in the Littleton formation elsewhere, including the lower zones of metamorphism, we have little evidence to support the idea that they were abundant in the regions of the feldspathic gneisses.

Gradational Character

The gradational changes in texture and structure of the rock types from west to east across the quadrangle have already been mentioned. The degree of recrystallization has been much more intense toward the east. In thin sections of the Bethlehem gneiss, one observes schistose layers composed of well-oriented mica flakes imbedded in a granoblastic matrix of quartz and a little plagioclase as elongate to polygonal-

shaped grains. In addition are layers of more gneissic material composed of equidimensional quartz and feldspar grains showing irregular to subsutured borders. Augen and highly elongate lenses of coarse quartz grains, with sutured borders, are characteristic of much of the Bethlehem gneiss. These lenses were formerly thought to be granulated phenocrysts, but this is extremely doubtful because: (1) large crystals of feldspar in these rocks are not deformed or granulated; (2) similar lenses are observed in some of the coarse schists; (3) lenses grade into the matrix of the normal Bethlehem gneiss; and (4) the structure is granoblastic not cataclastic. In fact, there is no suggestion that a cataclastic structure ever existed. These features are constructional and not destructional in origin. These gneiss layers and quartz lenses are to be compared with the larger lenses and layers which are characteristic of coarse crystalline gneisses. They represent the effects of small-scale or embryonic metamorphic differentiation in rocks transitional from schist to coarse gneiss. A schistose structure is giving place here to a gneissic structure, largely in response

TABLE 8.—CHEMICAL ANALYSES OF METAMORPHIC AND PLUTONIC ROCKS FROM NEW HAMPSHIRE

	Littleton Formation								Bethlehem Gneiss				Kinsman Quartz Monzonite		
	1	2	3	4	5	6	7	8	9	10	11	12	13	14	15
SiO_2	58.14	58.92	66.36	61.40	66.68	62.04	58.94	59.56	67.83	67.04	67.44	69.12	65.52	67.74	66.60
TiO_2	9.65	0.93	1.03	0.92	0.87	1.11	1.44	1.10	0.71	0.57	0.67	0.28	0.70	0.70	0.95
Al_2O_3	21.00	18.55	15.75	19.04	18.17	18.29	18.10	17.45	15.24	16.30	15.28	14.30	16.72	15.70	15.86
Fe_2O_3	0.33	0.94	1.16	0.63	0.90	0.33	0.49	3.10	0.55	0.74	1.02	1.32	0.60	0.85	0.35
FeO	6.32	6.63	5.37	6.90	4.98	8.45	10.04	3.84	4.04	3.94	3.76	1.92	4.75	4.30	4.48
MnO	0.06	0.08	0.08	0.07	tr	0.22	0.25	0.07	0.08	0.04	0.06	0.15	0.06	0.06	0.06
MgO	3.41	3.24	2.50	2.10	1.42	3.23	3.45	2.67	1.37	1.31	1.42	1.04	1.55	1.50	1.50
CaO	0.32	0.48	0.52	0.90	0.76	0.45	0.89	0.21	2.26	2.68	2.10	2.68	1.94	1.96	2.64
Na_2O	1.10	1.49	1.68	1.30	0.74	0.77	1.20	0.79	2.67	2.83	2.76	2.49	2.76	2.60	2.61
K_2O	3.85	3.74	3.23	3.74	2.89	3.54	3.34	3.79	3.96	4.03	4.37	5.44	3.68	4.48	3.58
H_2O^+	4.47	3.90	1.95	2.89	1.75	0.99	1.73	2.98	0.81	0.65	0.85	0.53	1.21	0.79	0.59
H_2O^-	n.d.	0.11	0.06	0.06	0.40	0.09	0.06	0.38	0.02	n.d.	n.d.	n.d.	n.d.	n.d.	0.00
CO_2	0.00	0.25	0.01	0.01	0.00	0.01	0.00	0.00	0.06	0.00	0.00	0.31	0.00	0.00	0.08
P_2O_5	0.00	0.14	0.17	0.08	tr	0.08	0.05	0.13	0.25	0.04	0.06	0.12	0.23	0.11	0.23
S	0.09	0.17	0.03	0.08	0.05	0.03	0.15	2.19	n.d.	0.11	0.06	0.06	0.19	0.10	0.14
C	n.d.	n.d.	n.d.	n.d.	n.d.	n.d.	n.d.	1.20	n.d.	n.d.	n.d.	n.d.	n.d.	n.d.	0.14
F	n.d.	n.d.	n.d.	n.d.	n.d.	0.10	0.10	0.06	n.d.	n.d.	n.d.	n.d.	n.d.	n.d.	0.08
	99.78	99.51	99.89	100.09	99.90	99.67	100.12	99.31	99.85	100.31	99.85	99.93	99.91	99.89	99.72

1. Slate, Littleton formation, Littleton quadrangle (Billings, 1937, p. 556).
2. Slate, Littleton formation, Littleton quadrangle (Billings, 1941, p. 902).
3. Staurolite schist, Littleton formation, Moosilauke quadrangle (Billings, 1941, p. 902).
4. Pseudo-andalusite schist, Littleton formation, Mt. Washington quadrangle (Billings, 1941, p. 902).
5. Sillimanite schist, Littleton formation, Franconia quadrangle (Billings, 1938, p. 292).
6. Porphyroblastic microcline gneiss, Dakin Hill member, Littleton formation, Lovewell Mtn. quadrangle (Heald, 1950, p. 77).
7. Biotite gneiss, Dakin Hill member, Littleton formation, Lovewell Mtn. quadrangle (Heald, 1950, p. 77).
8. Pyritiferous muscovite gneiss, Dakin Hill member, Littleton formation, Lovewell Mtn. quadrangle (Heald, 1950, p. 77).
9. Bethlehem gneiss, Mt. Cube quadrangle (Hadley, 1942, p. 146).
10. Bethlehem gneiss, Moosilauke quadrangle (Billings, 1937, p. 556).
11. Bethlehem gneiss, Moosilauke quadrangle (Billings, 1937, p. 556).
12. Bethlehem gneiss, Littleton quadrangle (Billings, 1937, p. 556).
13. Kinsman quartz monzonite, Moosilauke quadrangle (Billings, 1937, p. 556).
14. Kinsman quartz monzonite, Moosilauke quadrangle (Billings, 1937, p. 556).
15. Kinsman quartz monzonite, Lovewell Mtn. quadrangle (Heald, 1950, p. 84).

to increase in temperature and without the influence of significant shear.

Somewhat analogous structural changes may be seen in the Kinsman quartz monzonite, but the advanced stage which this mass is believed to have reached makes such relations less obvious. If we assume that the Sunapee area was at one time underlain entirely by the Littleton formation and if the rocks varied somewhat in composition, some being more feldspathic than others, then recrystallization alone could produce the mineralogically, texturally, and structurally different rock types in the same distribution as we now find them. But we must rule out the purely recrystallization theory as a likely one on the grounds that we have little evidence of large quantities of feldspathic material in the original rocks of the Littleton formation.

Evidence of Replacement

We do have good evidence, however, that recrystallization, combined with the introduction of greater or less amounts of material, has changed shales and sandstones into granitic material. These lines of evidence will now be considered.

(1) The extensive feldspathization of the Littleton formation about Thompson Hill, in Goshen, is quite clear. Already described is the feldspathization of the Littleton formation adjacent to the Bethlehem gneiss and Kinsman quartz monzonite and feldspathization of inclusions within these two bodies. If this same process, combined with recrystallization, could have been carried on more extensively, masses like the Kinsman quartz monzonite and Bethlehem gneiss could have been formed.

(2) Unreplaced remnants of the Littleton formation constitute one of the more convincing lines of evidence. All stages may be seen in the change over from one rock type to the other. Microscopically it is common to find remnants in the form of schist layers or gneissic layers containing mostly nonfelsic components. Streaks of biotite and muscovite are common in the Kinsman quartz monzonite. Bundles and stringers of sillimanite wend their way through these masses of mica precisely as in the sillimanite schist and gneiss of the Littleton formation. Large garnets when present appear usually in these layers. They are nearly identical to the garnet of the Littleton formation. The nature of accessories is also remarkably similar in the two rock types. Zircon, apatite, cordierite, graphite, and other opaques show the same characteristics in the two rock types. Small graphite flakes are abundant in the more coarsely crystalline parts of much of the Kinsman quartz monzonite. These may be seen with a hand lens. Sillimanite as tiny needles is well distributed through the quartz and in some sections is abundant in feldspar. Heald (1950, p. 83–84) presents several arguments to show that garnet and sillimanite of the Kinsman quartz monzonite are of metamorphic and not igneous origin. This conclusion not only agrees with the writer's contention but it further substantiates the belief that the Kinsman quartz monzonite is not of magmatic origin.

(3) Specimens of the Kinsman quartz monzonite and Bethlehem gneiss show layers of schistose material cut off cleanly by plagioclase crystals, and much quartz partially replaces flakes of mica. A close inspection of the modes in Table 2 reveals four general relationships between the amounts of quartz, plagioclase, and micas in the normal Bethlehem gneiss, the schistose phase of Bethlehem gneiss, and the inclusions within the gneiss. (1) Quartz increases in these rocks as plagioclase decreases. (2) Microcline increases as micas decrease. (3) Micas are substantially more abundant in the inclusions. (4) The schistose phase in general is very rich in quartz. The first two relations hold true for the Kinsman quartz monzonite and its inclusions. The third relation is generally true also if garnet is counted with the biotite.

The first relation indicates that plagioclase is replacing quartz for the most part. It is unlikely that plagioclase has replaced much biotite in the inclusions because the content of this mineral is as high as or higher than that of the average rock of the Littleton formation. Further indication that plagioclase largely replaces quartz is found in the Kinsman quartz monzonite where crystals of plagioclase, half a centimeter long, are seen to bulge the mica layers. The abundance of biotite along the flanks of these augen may be explained by the "porphyroblast principal" whereby quartz is

removed from betwen the mica flakes to provide room and perhaps material for the growing crystal. The less destructible mica is forced back effecting a bulge in the foliation. Destruction of a few mica flakes in a direction parallel to their cleavage would account for the slightly cross-cutting effects of these large crystals. Similar observations have been made on the large plagioclase crystals replacing fine-grained inclusions in the Bethlehem gneiss.

The second relation suggests that mica is made over into potash feldspar in these rocks. This mineralogical change is to be expected in the high-grade zone of metamorphism. Heald (1950) demonstrated the fact that potash feldspar was formed at the expense of mica in the gneisses of the Littleton formation in the Lovewell Mountain quadrangle. The same changes appear to have taken place in the Dakin Hill member on Sunapee Mountain. In these coarsely-crystallized gneisses, the potash feldspar appears as porphyroblasts and less commonly as pods and stringers. It seems reasonable to assume that much of the microcline in the Kinsman quartz monzonite has also formed from mica. Petrographic evidence indicates that the same may be true for the Bethlehem gneiss. The abundance of the mica in the oriented inclusions indicates that locally the rocks failed to develop microcline. Perhaps recrystallization did not proceed uniformly so that finer-grained patches of mica-rich rock were left as islands in a more coarsely recrystallized mass.

The third relation has been partly explained. Not only are micas generally more abundant in inclusions within the Bethlehem gneiss, but biotite is usually more abundant in these rocks than in the average schist of the Littleton formation. The question may be raised as to whether biotite components might not have been driven from the surrounding gneiss into the region occupied by the inclusion. The writer has no good evidence that such a migration has taken place, but the idea is certainly not in disagreement with field and laboratory studies.

The fourth relation, pertaining to the schistose phase of the Bethlehem gneiss, may be accounted for by considering the inclusions to be a less completely recrystallized and replaced schist than the average Bethlehem gneiss.

(4) Another line of evidence that replacement by plagioclase has occurred in the area is shown by the large pseudomorphs of plagioclase after microcline which have been described earlier. The writer agrees with Heald (1950, p. 61) that the alteration indicates an introduction of sodium and calcium and a loss of potassium. This is apparently a fairly widespread phenomenon in the rocks of the Littleton formation and Kinsman quartz monzonite.

(5) The shape and distribution of the small elongate masses of garnet-pargasite gneiss in the contact zone of the Bethlehem gneiss west of Blueberry Mountain suggests that the masses represent lenses or concretions which were so different chemically and physically from the neighboring rock that they were left unreplaced. Their original composition must have been calcareous and possibly dolomitic. These inclusions are at essentially the same stratigraphic horizon as the lime-silicate granulites further south on Chandler Hill, in Goshen Township.

(6) Evidence of preserved bedding structures may be found in contact zones where replacement has occurred along very thin layers. All gradations between unreplaced and highly replaced layers occur, ruling out the possibility that these thin layers represent sills of magmatic origin. A strong suggestion of bedding may be found in the occurrence of thin concordant masses of light-colored gneiss, a mode of which is shown in Table 2. These rocks are low in biotite and may represent replaced, light-colored beds.

Evidence of Magmatic Origin

A number of points which have been used as evidence that the Bethlehem gneiss and Kinsman quartz monzonite are of magmatic origin need consideration.

(1) Heald (1950, p. 81) expresses the view that the schists of the Littleton formation diverge at the southern termination of the Bethlehem gneiss in the Lovewell Mountain and Bellows Falls quadrangle (Fig. 1) indicating that they were probably wedged apart by intrusion of the gneiss. Whereas a bulge in the schist at this point certainly indicates intrusion, it is not in the least detrimental to the replacement hypothesis. A constriction in the schists

at this point, prior to the formation of the Bethlehem gneiss, could have made the replacement mechanism ineffective, thereby terminating the body of gneiss in the form of a wedge. Some structural control, such as is shown by Newhouse, Hagner, and DeVore (1949), may have been operative.

(2) The cross-cutting effect of the Bethlehem gneiss in the western part of the Sunapee quadrangle, the southeastern part of the Claremont quadrangle, and the northeastern part of the Bellows Falls quadrangle is another point in agreement with the magmatic theory. The evidence for a cross-cutting relation is found in the fact that the lower (western) contact of the Bethlehem gneiss rises stratigraphically from below the top of the Clough formation north of Mt. Tug, in the Sunapee quadrangle, to about 5000 feet above the base of the Littleton formation in the Bellows Falls quadrangle (Kruger, 1946) and Lovewell Mountain quadrangles (Heald, 1950, p. 71). Such a relation, however, does not oppose the theory of replacement. Replacement is expected to advance through the rock in directions of favorable composition, structure, and physical conditions. A similar explanation may account for major or minor cross-cutting relations of the Kinsman quartz monzonite.

(3) The occurrence of sillimanite in the schists adjacent to Kinsman quartz monzonite and the absence of this mineral further away has been cited by Moore (1949), in the Brattleboro quadrangle, as an effect of contact metamorphism by the quartz monzonite. Kruger (1946, p. 196) describes an isolated mass of Bethlehem gneiss in the Bellows Falls quadrangle which is resting upon schists of the staurolite zone and which encloses a large mass (septum) of coarse sillimanite-garnet-muscovite schist. This local development of high-grade metamorphic rocks he ascribes to thermal metamorphism by the gneiss. Sillimanitic zones are known to surround other granitic bodies in other parts of New Hampshire, but one should not be too hasty to conclude that contact metamorphism by the adjacent granitic rocks is the sole explanation. That the high-grade rocks should be associated with granitic rocks of replacement or metamorphic origin is also to be expected. The distribution of sillimanite zones is more in harmony with the theories of metamorphic and replacement origin than with the magmatic theory when we take into account the occurrence of sillimanite zones away from granitic looking rocks. Sillimanite schists in the Clough formation west and northwest of Kelleyville have already been described. These rocks are known to extend into the Claremont quadrangle, to the west, for about a mile. Yet they are not in contact with granitic bodies. It is possible that the Bethlehem gneiss, at one time, extended across the Grantham fault and overlaid these sillimanitic rocks. However, why should there not be a sillimanite zone all along the lower non-faulted contact of the Bethlehem gneiss? It is the writer's contention that too much stress may be placed on the distribution of the mineral sillimanite. There is danger in using this mineral solely as an indicator of metamorphic intensities, principally, perhaps, because its first appearance in progressive metamorphism is so strongly controlled by rock composition. Within a somewhat variable group of rocks, therefore, the sillimanite isograd may not serve satisfactorily to delineate regions of higher-grade metamorphism within close limits. It is particularly interesting that, whereas Moore (1949) considered that sillimanite in schist formed as a result of the intrusion of Kinsman quartz monzonite, Heald (1950, p. 83) concludes that at least part of the sillimanite in the quartz monzonite itself is metamorphic and did not form in the magma. This paradoxical relation indicates that the true significance of the sillimanite zone has not been realized.

Preferred Theory

The writer believes that the magmatic theory must be abandoned as an explanation for the Bethlehem gneiss and Kinsman quartz monzonite. The major objections to it are briefly summarized:

1. It will not explain the foliation of the rocks.
2. It will not explain the origin of the large feldspar crystals.
3. It is not in agreement with the low soda-content of the large potash feldspar crystals.
4. It will not explain the uniform distribution

and perfect orientation of slab-like inclusions.

5. It is difficult to reconcile this theory with certain mineralogical, textural, and structural similarities in the rocks of the Littleton formation, Bethlehem gneiss, and Kinsman quartz monzonite.

The metamorphic theory cannot be considered completely satisfactory for the following reasons:

1. If the granitic-looking rocks were derived from the Littleton formation, the original material must have been volcanics or feldspathic sediments. Feldspathic rocks in the Littleton formation are relatively rare elsewhere, even in the lower grades of metamorphism where they could not have lost their identity due to metamorphism.

2. If the original rocks were volcanic, why is the composition so uniform in the many thousands of feet of stratified material? Why are there no layers of more basaltic material?

3. Objections to the bodies representing pretectonic intrusions are largely structural. The extensive areas of gently dipping foliation, the abundant and perfectly oriented inclusions, and the absence of numerous discordant, satellitic bodies are all against this mode or origin.

In view of these objections, the replacement theory in combination with the metamorphic theory is now believed to offer the most satisfactory explanation for the origin of the Bethlehem gneiss and the Kinsman quartz monzonite.

Origin of the Late Quartz-Feldspar Rocks

Field and microscopic study has lead the writer to the following conclusion as to the origin of the Spaulding quartz diorite. A quartz diorite magma was intruded in more or less concordant sheets in the late stages of metamorphism and essentially after the Kinsman quartz monzonite had been formed. In the larger bodies and the central parts of the smaller bodies, crystallization proceeded more or less undisturbed by external stress and a typical magmatic rock formed. This magmatic character is indicated by the relations of hornblende and biotite, the nature of the feldspar crystals, and the interstitial occurrence of quartz. These features seem diagnostic of magmatic phenomena. Conditions were favorable at this time for extensive replacement of the wall rocks along these small intrusives so that the Littleton formation was changed over into quartz dioritic material. This replaced rock constitutes the so-called highly foliated phase of the Spaulding quartz diorite in which foliation and lineation parallel the respective structures in the adjacent Littleton formation.

Field relations indicate that the quartz monzonite has been emplaced principally within the Littleton formation and to a less extent within the Kinsman quartz monzonite and Spaulding quartz diorite. The exact nature of emplacement is not clear. That the material has entered zones of intense shattering is evinced by the outcrops of brecciated quartz diorite with a matrix of the quartz monzonite. Individual blocks in this breccia do not appear to have been rotated far from their original orientation. It is difficult to determine whether the quartz monzonite filling these breccias is magmatic or largely replacing the margins of blocks formed by intersecting fractures as suggested by A. F. Hagner (personal communication). A complicating feature is the occurrence of somewhat irregular blocks of Kinsman quartz monzonite within the quartz monzonite on the hill west of Blueberry Mountain. The foliation of the Kinsman in each block has essentially the same trend. The writer's tentative opinion is that the quartz monzonite was introduced mainly as a magma and that locally replacement phases developed.

The writer concludes that some of the bodies of Concord granite are of replacement origin whereas others probably formed from magma. The large mass around Little Sunapee Lake may be a stocklike body similar to those described from other parts of New Hampshire. Field mapping in the northwest part of the Mount Kearsarge quadrangle (to the east) shows no large body of Concord granite extending through, and the mass probably ends near the quadrangle line. This body occupies a structural position similar to the masses of Concord granite in the western part of the Cardigan quadrangle (Fowler-Lunn and Kingsley, 1937).

Many of the small bodies of Concord granite are probably magmatic. Reference is made par-

ticularly to the dike-like masses which appear to be controlled by joint sets in rocks of all ages. Coarseness of grain is a function of size in these dikes suggesting varying rates of crystallization. In other bodies, particularly the sill-like masses, foliation is strong and composition ranges greatly over very short distances. All gradations appear between Concord granite and enclosing rock. These masses are not believed to be of magmatic origin. They probably formed as a result of metamorphism and replacement.

Metamorphic Zoning

The general increase in degree of metamorphism from west to east across the Sunapee quadrangle has already been briefly considered, and this change is a continuation of the increase in metamorphic grade from the western border of the state. The rocks immediately to the west, in the Claremont quadrangle (Chapman, 1942), belong to the middle-grade zone of metamorphism. They fall within the staurolite and kyanite zones of Barrow. As the Sunapee quadrangle is approached, staurolite gives way to sillimanite in the pelitic rocks and the sillimanite zone is reached. This change, when accomplished within the pelitic sediments, is used as a basis for separating the middle-grade zone from the high-grade zone of metamorphism.

The sillimanite isograd is shown in Figure 3 extending from the Claremont quadrangle on the west to the Mascoma quadrangle on the north. The isograd enters the quadrangle, on the west, south of Mt. Tug, where it nearly coincides with the western contact of the Behtlehem gneiss. It swings west again for about a mile into the Claremont quadrangle, and returns further north across the south end of Croydon Mountain. From this point on, we have little control for determining its location; and so it is shown as a questionable line which leaves the quadrangle along the Grantham fault.

The potash feldspar isograd is shown on the map as three different lines trending NNE–SSW. Two lines separate the body of Bethlehem gneiss from lower-grade rocks. The easternmost line separates the Hubbard Hill member from the Kinsman quartz monzonite.

To the east of the potash feldspar isograd is another isograd which marks roughly the outer boundary of a zone in which both biotite and muscovite have, in large part, been converted to potash feldspar and garnet.

The existence and location of the sillimanite and potash feldspar isograds can be easily demonstrated and determined from field and laboratory study. In general, the sillimanite isograd cannot be located as precisely as the potash feldspar isograd because it passes through areas in which rock composition is not favorable to the formation of sillimanite. The potash feldspar isograd can be located somewhat more accurately because rock composition is much more uniform throughout the area east of the sillimanite isograd. The highest isograd, shown separating the zone in which potash feldspar has formed at the expense of both biotite and muscovite, is only approximately located, due to insufficient data.

Much evidence for the arrangement of metamorphic zones in the Sunapee quadrangle has already been given in the discussion on petrogenesis. A few additional points, however, might be added. The rocks of the staurolite zone are separated from those of the sillimanite zone on the basis of the following reaction:

$$\text{Staurolite} + \text{Quartz} \rightarrow \text{Sillimanite} + \text{Garnet}$$

A strong indication that the above reaction has taken place is the lack of association of staurolite and sillimanite in the same rock. An exception is found northeast of Kelleyville, in the Claremont quadrangle, where rocks containing both sillimanite and staurolite occur. These rocks are considered transitional between the staurolite and sillimanite zones (Chapman, 1942). They apparently did not reach equilibrium conditions.

The potash feldspar isograd is believed to bound the area within which potash feldspar has formed largely from muscovite. This reaction may be expressed by the following generalized change:

$$\text{Muscovite} \rightarrow \text{Potash feldspar} + \text{Sillimanite} + \text{Water}$$

In the Dakin Hill member, potash feldspar does not occur with muscovite except where it is be-

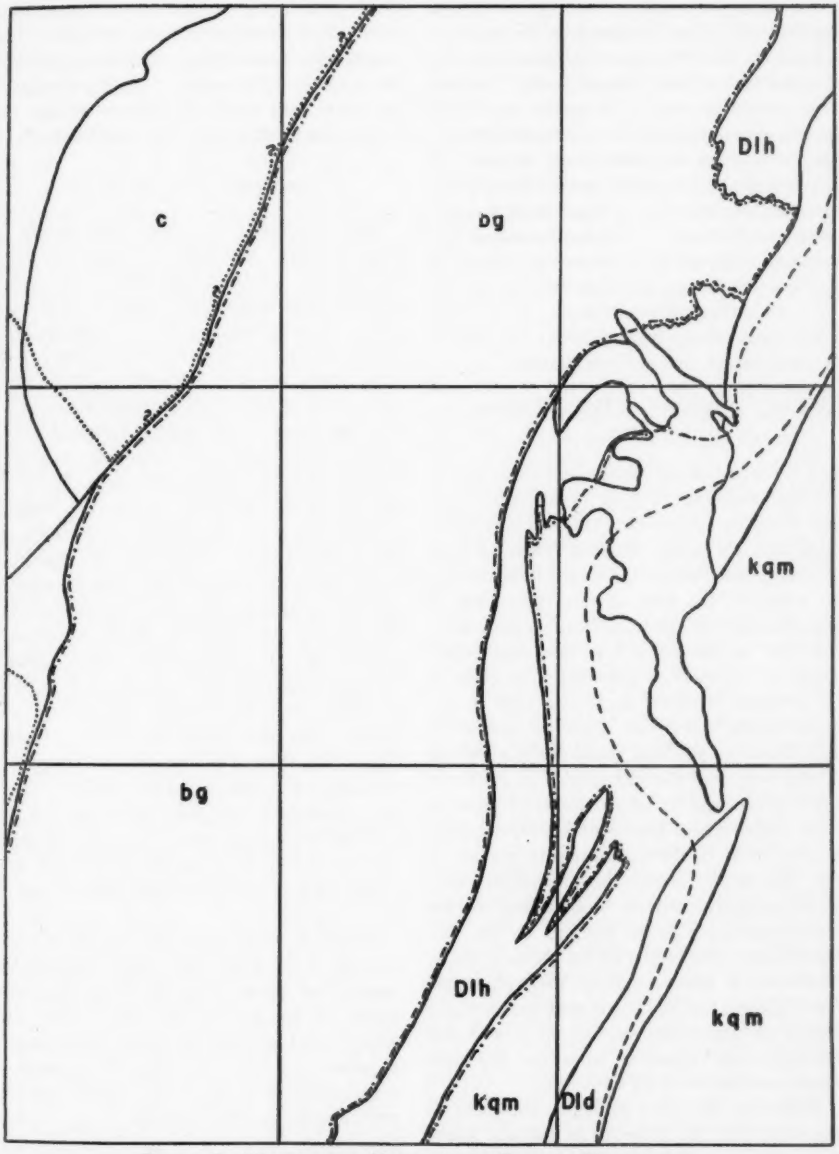

FIGURE 3.—METAMORPHIC ZONES IN THE SUNAPEE QUADRANGLE

Sillimanite isograd = dotted line, microcline isograd = dotted-dashed line, biotite → microcline isograd = dashed line.

lieved to be pseudomorphic after feldspar. In addition, many of these microcline-bearing rocks are richer in sillimanite than rocks of the Hubbard Hill member. These two relations are in agreement with the above reaction. In the Bethlehem gneiss and the extreme western part

of the Kinsman quartz monzonite, muscovite appears with potash feldspar but sillimanite is generally rare. Perhaps the potential sillimanite, liberated in the formation of potash feldspar from muscovite, was taken up by the introduced sodium and calcium to form plagioclase. Some aluminum may have been removed in this process, which would explain the slightly lower alumina content of these rocks as compared with that of the Littleton formation (see Table 8). Perhaps some aluminum found its way into the bordering schists to help develop there the narrow sillimanite zone.

The most eastern isograd has as the basis of its construction the following reaction:

Biotite + Muscovite → Potash Feldspar + Garnet

The Kinsman quartz monzonite to the east of this highest isograd is richer in microcline than that to the west of the line. This fact is in agreement with the above reaction. There is more microcline here, however, than can be accounted for solely on the basis of recrystallization of muscovite and biotite. Considerable potassium, therefore, is believed to have been introduced. There is, moreover, a noteworthy decrease in the amount of biotite and muscovite in the higher grade rocks; this is also in agreement with the above reaction. Heald (1950, p. 83) expresses very well the distribution of garnet in the Kinsman quartz monzonite when he says: "The garnetiferous phases of Kinsman quartz monzonite lie in the high-intensity portion of the high-grade zone; the nongarnetiferous types generally occur in areas of less intense metamorphism." These findings in the two quadrangles agree well with the above reaction. There is not enough garnet, however, to account for the loss in biotite; and so it is likely that some magnesium was tied up in cordierite whereas some migrated from the Kinsman quartz monzonite along with iron.

Following the facies principle, the rocks of the area may be assigned as follows. Rocks west of the sillimanite isograd are placed in the staurolite-kyanite subfacies of the amphibolite facies. Rocks between the sillimanite isograd and the potash feldspar isograd are considered to belong to the sillimanite-almandine subfacies of the amphibolite facies. The rocks in which potash feldspar has formed from muscovite alone are placed in the upper part of the amphibolite facies. Following Ramberg (1949), those which derived some of their potash feldspar from both biotite and muscovite may belong to the lower part of the granulite facies.

Conclusions and Summary

The observation that the total content of potash feldspar and mica is roughly the same within the rocks of the Bethlehem gneiss, Littleton formation, and Kinsman quartz monzonite is very significant. This antipathetic relation between micas and microcline has already been noted in an earlier section. This uniformity of potash mineral content indicates that the micas of the original Littleton formation were transformed in large part to potash feldspar to form the granitic rocks. We know this to be the case for the potash feldspar porphyroblasts in the Littleton formation. It seems logical to conclude, therefore, that little if any potassium was introduced in the western part of this area at least. Further east and in the Kinsman quartz monzonite of the Monadnock quadrangle (Fowler-Billings, 1949), potash feldspar is much more abundant. It is very probable that considerable potassium was added to the host rock in these areas. It seems likely that there was more or less transfer of potassium from one part of the Littleton formation to another over short distances, but the facts at hand do not require a wholesale introduction of potassium from depth or from some remote region except in the higher zone of metamorphism.

Potash feldspar is almost entirely as large crystals in the Kinsman quartz monzonite but most of the microcline of the Bethlehem gneiss occurs in the groundmass. This broad zonal arrangement of large feldspar crystals suggests a better and more complete development of porphyroblasts in the more intense zone of metamorphism. The increase in size of porphyroblasts from west to east is corroborative evidence that the Kinsman quartz monzonite is a more thoroughly recrystallized body than the Bethlehem gneiss or Littleton formation in the Sunapee area. The Kinsman quartz monzonite lacks the more pronounced and universal foliation and directive fabric possessed by these

other rocks. In the eastern part of the area where temperature was probably higher, the ions were more active and able to build larger crystals in the attempt to reduce the free energy of the aggregates. Even large ions like potassium were capable of migrating greater distances in order to accumulate in the minimum number of lattice structures.

Potassium feldspar is about equally abundant in the Bethlehem gneiss and Kinsman quartz monzonite. It is less abundant and generally absent in the inclusions, in the sill-like bodies, in the feldspathized schist, and within some contact zones. This distribution indicates a zonal arrangement of microcline structurally, that is, from the center of replaced masses outward into unreplaced rock. This low content or absence of microcline in the inclusions and marginal rocks may find an explanation in the fact that the rocks are less thoroughly recrystallized and reconstituted. For some reason (physical, chemical, or both) the mobility of the mineral constituents in these rocks was somewhat lower than that in adjacent rocks. As a result, reorganization here failed to keep pace with that of neighboring regions, and it was impossible for the large potassium ions to migrate and build into large porphyroblasts.

Plagioclase is abundant in the Bethlehem gneiss, the Kinsman quartz monzonite, nearly all inclusions, the feldspathized schist, and the sill-like bodies in the Littleton formation. This indicates that sodium was introduced quite thoroughly throughout the Sunapee area. This wide distribution may be attributed to the smaller size of the sodium ion. The distribution of introduced sodium is not in all cases the same as that of the large crystals of potash feldspar. On Sunapee Mountain, for example, where abundant porphyroblasts of potash feldspar have formed from mica in the Littleton formation, large amounts of plagioclase do not usually appear in the rock. As suggested by the work of Newhouse, Hagner, and DeVore (1949), it is possible that local masses of rock were isolated by some structural barrier which prevented the introduction of much sodium.

The sillimanite zones bordering the Bethlehem gneiss and Kinsman quartz monzonite have been considered. These are believed to represent constrictions in the sillimanite zone between the lower staurolitic rocks and the higher feldspathic gneisses. Apparently the processes of recrystallization and replacement were too ineffective to produce the feldspathic gneisses under metamorphic conditions much below the lower limit of the sillimanite zone. In the Bellows Falls quadrangle (Kruger, 1946), the floor of the Bethlehem mass is on the staurolite zone. Apparently the granitizing processes over-stepped, so to speak, the lower boundary of the sillimanite zone. We must not be misled by the distribution of sillimanite alone. The whole physical and chemical situation must be considered.

There is what might be termed a slight irregularity in the distribution of plagioclase and microcline in the contact zone. Some layers of rock are rich in plagioclase and not in microcline. In other layers, the relative abundance of these two minerals is reversed. Perhaps this is an indication that physical conditions favoring the formation of these two minerals are slightly different or that their formation is favored more strongly by certain chemical differences.

The sequence of introduction, expulsion, and interchange was undoubtedly complicated and probably not identical at all points. Sodium and calcium, being smaller ions, probably moved out faster and farther than potassium, and were fixed in the Bethlehem gneiss at about the same time the large microcline crystals were constituted. As the process continued, many of the porphyroblasts of microcline in the eastern part of the Kinsman quartz monzonite were enlarged still further by the incoming of greater or less amounts of potassium, but sodium and calcium were pushed westward down steep geochemical gradients and little was retained in the quartz monzonite. Still later, as the fixation of potassium was decreasing, sodium and calcium became fixed somewhat locally in the rocks, in large part by replacing earlier microcline. This is evinced by the large pseudomorphs of plagioclase with quartz and muscovite after microcline crystals. These have been described from the Kinsman quartz monzonite and adjacent Littleton formation. A similar replacement of microcline by plagioclase, quartz, and muscovite is noted in the Littleton formation and Kinsman quartz monzonite in the Lovewell Mountain quadrangle (Heald, 1950, p. 61 and

78). It is possible that some of the sodium introduced at this time was in part responsible for the formation of late myrmekite in these rocks. Some of the myrmekite, however, must have formed earlier because: (1) it is quite uniformly wide-spread; (2) it is of a slightly different appearance petrographically; and (3) it has replaced the edges of large crystals of microcline which later were altered to the distinctive assemblages of plagioclase, quartz and muscovite. At this stage of pseudomorph-development, it seems that little potassium was being fixed as microcline in the rocks. The break-down of large potash feldspar crystals may have been aided by an increase in water content so that muscovite became the stable phase; and, with the addition of sodium and calcium, plagioclase replaced most of the microcline. These changes are summarized in the following reaction:

Microcline + Sodium + Calcium + Water → Muscovite + Plagioclase + Silica + Potassium

The released silica may have formed the quartz within the pseudomorphs; some may have been freed to replace other parts of the rock. Potassium set free from this reaction would have been available to combine with sillimanite in the adjoining rocks to form the large crystals and aggregates of muscovite. It is possible that the conditions which favored the formation of muscovite at this late stage also existed in the Lovewell Mountain quadrangle to the south where potash feldspar in the Littleton formation changed to muscovite and quartz (Heald, 1950, p. 75). Released potassium may have gone to form additional mica from part of the available sillimanite.

The processes considered operative in the formation of the rocks of the Sunapee quadrangle east of the Grantham fault are now summarized in chronological fashion.

A thick series of sedimentary rocks, constituting the Littleton formation and composed essentially of shale, sandy shale, and some sandstone, were subjected to intense metamorphism. High temperature and, to a less extent, high pressure were largely responsible for the recrystallization which ensued. In certain localities and more particularly toward the east, reconstitution of material took place on a larger scale. Porphyroblasts of potash feldspar began to grow in the Kinsman quartz monzonite and Bethlehem gneiss; other effects of metamorphic differentiation were expressed in the development of local gneissic banding and the formation of small quartz and feldspar lenses, stringers, and pods. Development of potash feldspar porphyroblasts in the Dakin Hill member of the Littleton formation was accomplished at this time.

At greater depth and to the east where temperature was undoubtedly higher, certain elements were forced to leave and pass outward and upward through the rocks of the Sunapee quadrangle. These elements probably consisted mostly of sodium and calcium ions which moved more rapidly and abundantly through certain zones of strata and caused the formation of plagioclase. Potassium may have started to leave the deeper rocks at about the same time but, because of its larger ionic size, travelled more slowly and reached the rocks of the Sunapee area after much plagioclase had formed. It helped to increase the amount of potassium feldspar in part of the Kinsman quartz monzonite but little probably reached as far west as the Bethlehem gneiss.

At about this time, a quartz diorite magma was intruded into the Littleton formation and Kinsman quartz monzonite, and much country rock along the contacts of these sill-like intrusions was replaced. The quartz diorite was followed by locallized emplacement of quartz monzonite partly as a magma and partly by replacement.

The replacement processes carried on over an extended period of time, and during the later stages large crystals of potash feldspar were replaced by mixture of plagioclase, quartz, and muscovite. The potassium released in this process moved out to change sillimanite to muscovite in the adjacent schists. It is possible that much silica replaced the rocks at this time, because quartz of late formation is abundant in all the earlier rocks. This whole process appears to have culminated with the formation of the Concord granite and its associated pegmatites. Some of this granite probably formed from a magma but much appears to be of replacement origin.

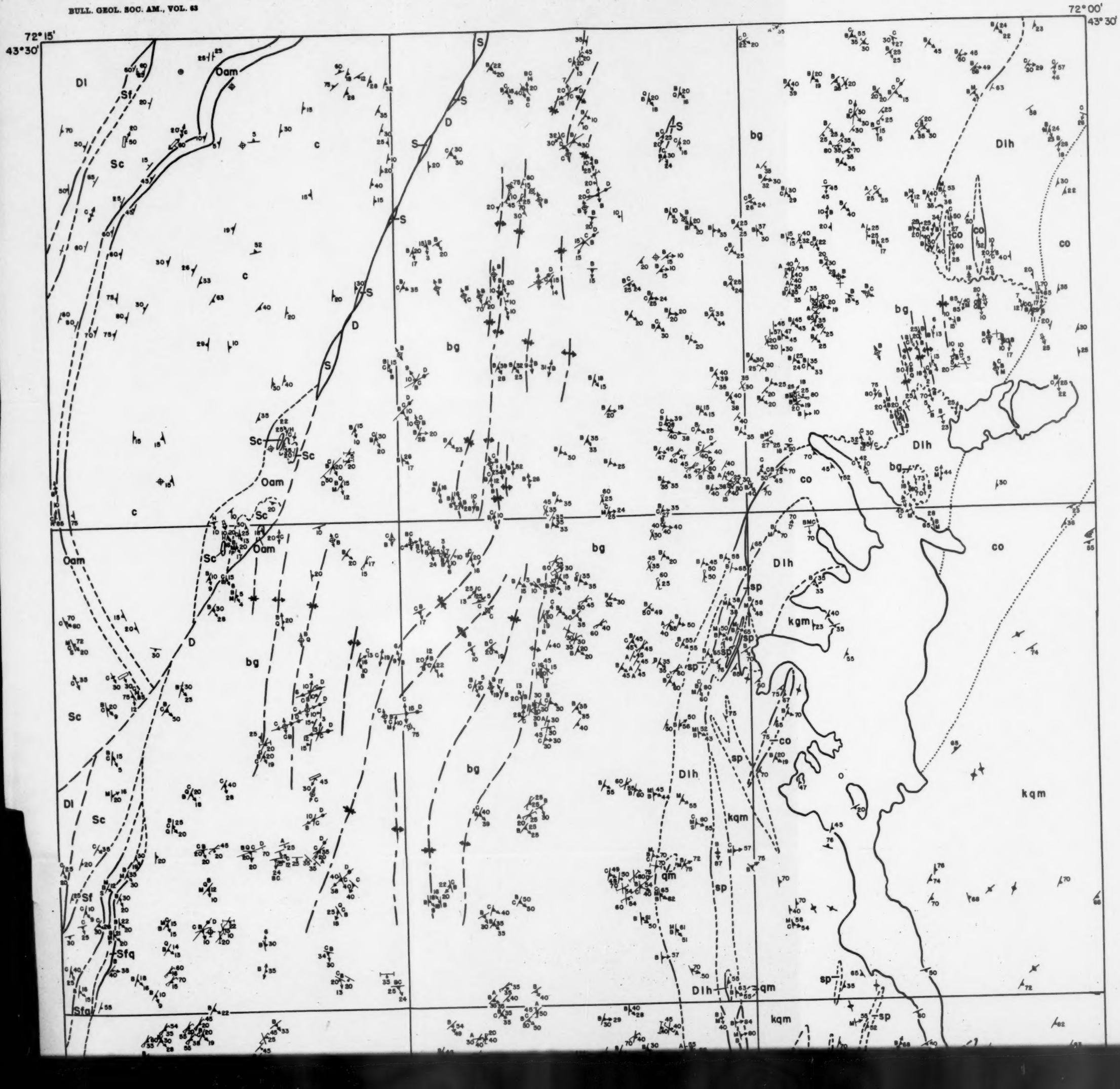
72°15'
43°30'
72°00'
43°30'
Dl
Sf
Oam
Sc
c
S
D
bg
Dlh
co
kqm
qm
sp
Sfq
Sfa

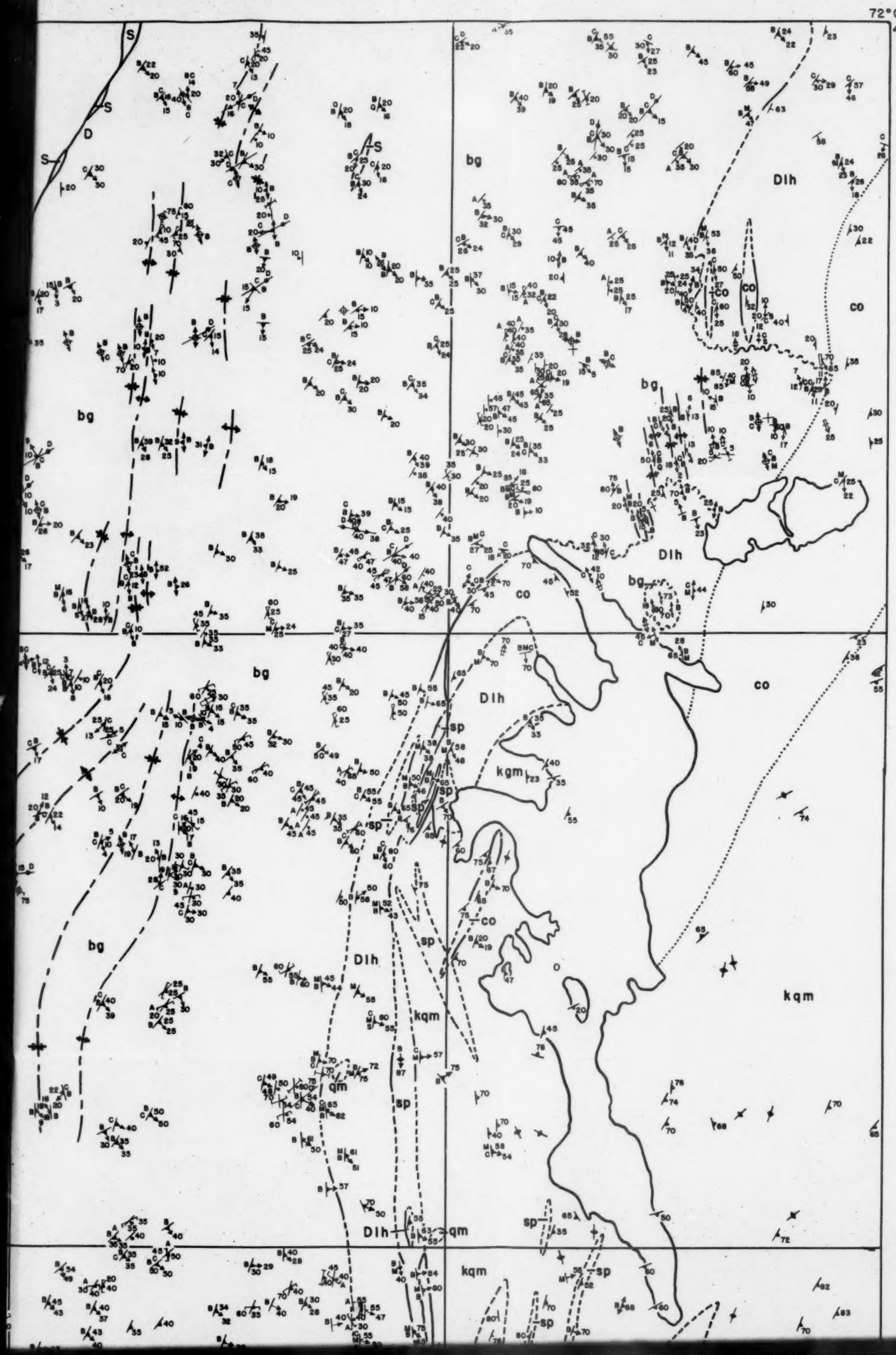

STRUCTURAL SYMBOLS

35 — BEDDING

BEDDING WHERE VERTICAL

BEDDING WHERE HORIZONTAL

35 — FOLIATION OR SCHISTOSITY

FOLIATION OR SCHISTOSITY WHERE VERTICAL

FOLIATION OR SCHISTOSITY WHERE HORIZONTAL

30 — LINEATION—STRIKE OF LINEAR ELEMENT AND VALUE OF PLUNGE

HORIZONTAL LINEATION

LINEATION SYMBOLS ARE COMBINED WITH THOSE FOR BEDDING OR FOLIATION OR SCHISTOSITY

NATURE OF LINEAR ELEMENT:

B — BIOTITE
C — CRINKLES
H — HORNBLENDE
M — MUSCOVITE
P — PEBBLES
Q — QUARTZ
S — SILLIMANITE
T — TOURMALINE

60/45 — FOLD—STRIKE AND DIP OF AXIAL PLANE AND TREND OF AXIS WITH VALUE OF PLUNGE

25 — FOLD—VERTICAL AXIAL PLANE AND VALUE OF PLUNGE OF AXIS

FOLD—VERTICAL AXIAL PLANE AND HORIZONTAL AXIS

70 — FOLD—STRIKE AND DIP OF AXIAL PLANE AND HORIZONTAL AXIS

MAJOR SYNCLINAL AXIS

MAJOR ANTICLINAL AXIS

D / 80 — SHEAR ZONE—STRIKE AND DIP OF SHEAR PLANE (D = DOWNTHROWN SIDE)

D — SHEAR ZONE—WHERE VERTICAL

PEGMATITE AND APLITE SYMBOLS
(APLITE INDICATED BY AN "A" IN THE SYMBOL)

35 — STRIKE AND DIP OF DISCORDANT PEGMATITE

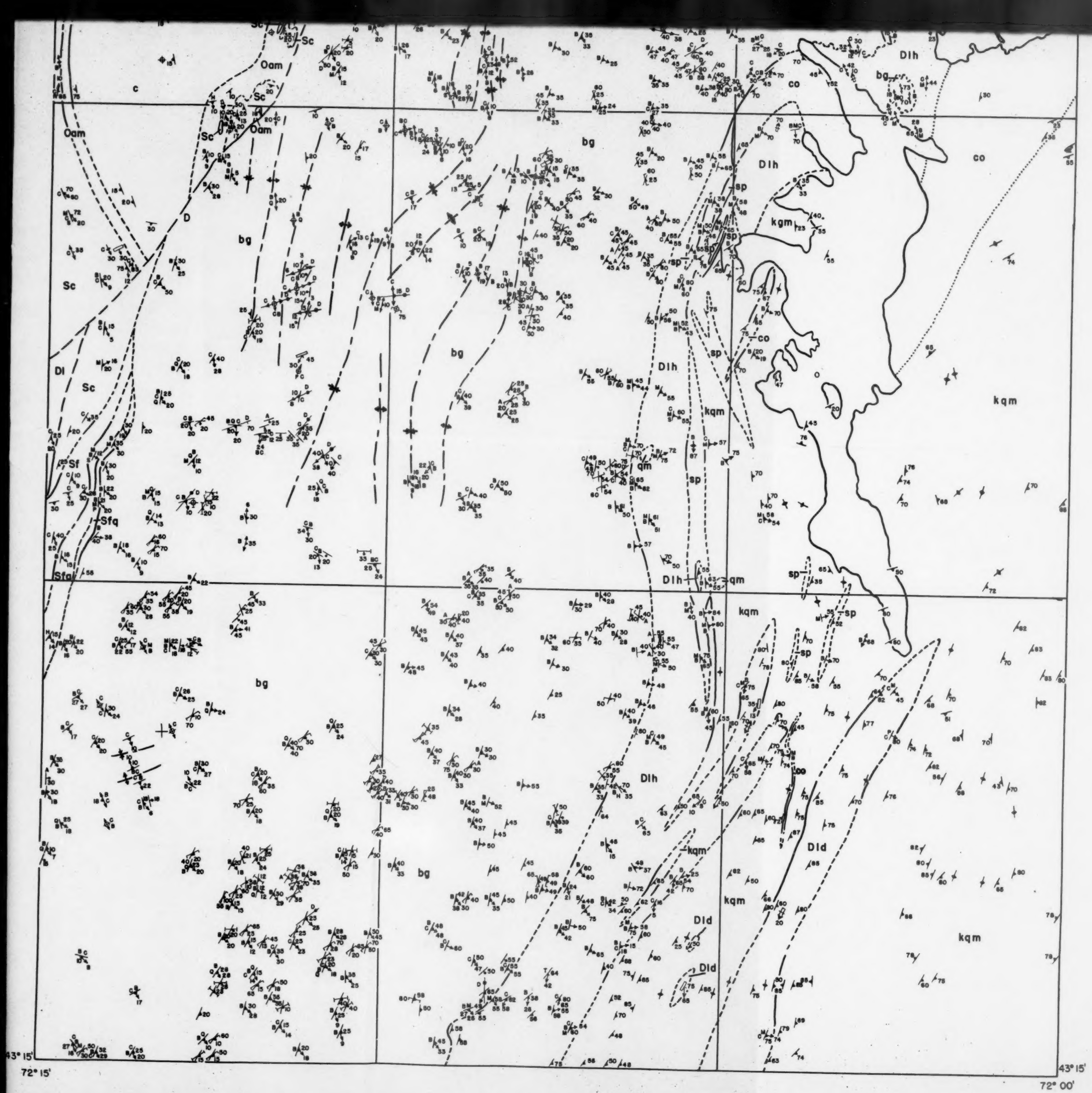
Oam
Sc
bg
D
Dl
Sf
Sfq
Dlh
Dld
qm
kqm
sp
co
43° 15'
72° 15'
72° 00'

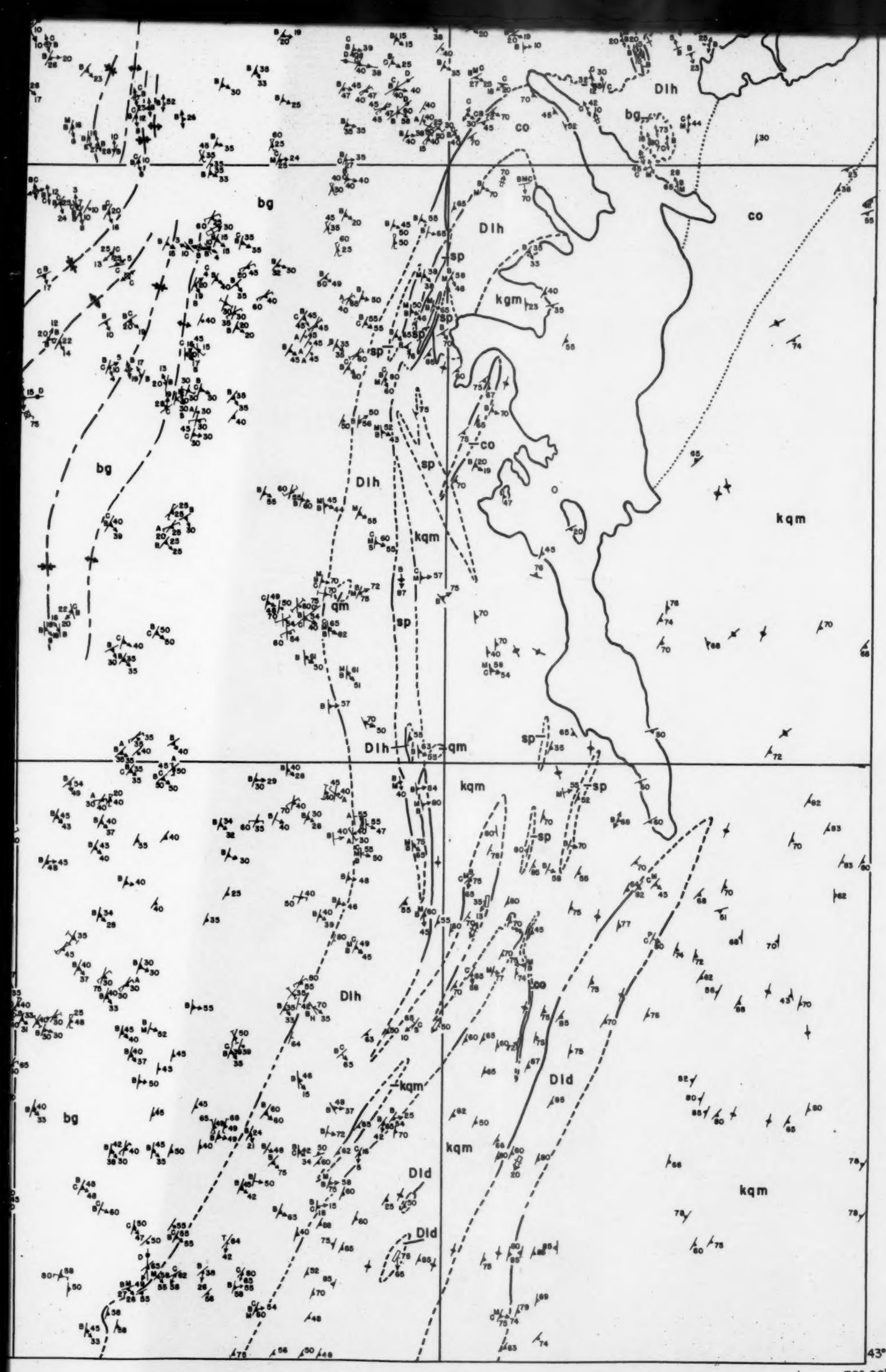

LINEATION SYMBOLS ARE COMBINED WITH THOSE FOR BEDDING OR FOLIATION OR SCHISTOSITY

NATURE OF LINEAR ELEMENT:

B — BIOTITE
C — CRINKLES
H — HORNBLENDE
M — MUSCOVITE
P — PEBBLES
Q — QUARTZ
S — SILLIMANITE
T — TOURMALINE

60→45 FOLD — STRIKE AND DIP OF AXIAL PLANE AND TREND OF AXIS WITH VALUE OF PLUNGE

25 FOLD — VERTICAL AXIAL PLANE AND VALUE OF PLUNGE OF AXIS

FOLD — VERTICAL AXIAL PLANE AND HORIZONTAL AXIS

70 FOLD — STRIKE AND DIP OF AXIAL PLANE AND HORIZONTAL AXIS

MAJOR SYNCLINAL AXIS

MAJOR ANTICLINAL AXIS

D / 80 SHEAR ZONE — STRIKE AND DIP OF SHEAR PLANE (D = DOWNTHROWN SIDE)

D SHEAR ZONE — WHERE VERTICAL

PEGMATITE AND APLITE SYMBOLS
(APLITE INDICATED BY AN "A" IN THE SYMBOL)

35 STRIKE AND DIP OF DISCORDANT PEGMATITE

STRIKE OF VERTICAL DISCORDANT PEGMATITE

35 STRIKE AND DIP OF CONCORDANT PEGMATITE

STRIKE OF VERTICAL CONCORDANT PEGMATITE

HORIZONTAL CONCORDANT PEGMATITE

FORMATION SYMBOLS
CONTACTS
FAULT
} SAME AS ON THE GEOLOGICAL MAP

0 1 2
SCALE IN MILES

TECTONIC MAP OF THE SUNAPEE QUADRANGLE, NEW HAMPSHIRE

References Cited

ings, M. P. (1937) *Regional metamorphism of the Littleton-Moosilauke area, New Hampshire*, Geol. Soc. Am., Bull., vol. 48, p. 463–566.

apman, C. A. (1939) *Geology of the Mascoma quadrangle, New Hampshire*, Geol. Soc. Am., Bull., vol. 50, p. 127–180.

– (1942) *Intrusive domes of the Claremont-Newport area, New Hampshire*, Geol. Soc. Am., Bull., vol. 53, p. 889–916.

– (1950) *Quartz veins formed by metamorphic differentiation of aluminous schists*, Am. Mineral., vol. 35, p. 693–710.

ler-Billings, Katherine (1949) *Geology of the Monadnock region of New Hampshire*, Geol. Soc. Am., Bull., vol. 60, p. 1249–1280.

ler-Lunn, Katherine, and Kingsley, Louise (1937) *Geology of the Cardigan quadrangle, New Hampshire*, Geol. Soc. Am., Bull., vol. 48, p. 1363–1386.

ld, M. T. (1950) *Structure and petrology of the Lovewell Mountain quadrangle, New Hampshire*, Geol. Soc. Am., Bull., vol. 61, p. 43–89.

Kruger, F. C. (1946) *Structure and metamorphism of the Bellow-Falls quadrangle of New Hampshire and Vermont*, Geol. Soc. Am., Bull., vol. 57, p. 161–206.

Moore, G. E. (1949) *Structure and metamorphism of the Keene-Brattleboro area, New Hampshire-Vermont*, Geol. Soc. Am., Bull., vol. 60, p. 1613–1670.

Newhouse, W. H., Hagner, A. F., and DeVore, G. W. (1949) *Structural control in the formation of gneisses and metamorphic rocks*, Science, vol. 109, p. 168.

Ramberg, Hans (1949) *The facies classification of rocks: a clue to the origin of quartzo-feldspathic massifs and veins*, Jour. Geol., vol. 57, p. 18–54.

Wilson, Virginia R. (1948) *A laboratory study in granite tectonics*, Univ. Ill., June, unpublished B.S. thesis.

University of Illinois, Urbana, Illinois.

Manuscript Received by the Secretary of the Society, August 3, 1951.

BULLETIN OF THE GEOLOGICAL SOCIETY OF AMERICA
VOL. 63, PP. 427-430 APRIL 1952

Short Notes

USE OF EQUAL-AREA OR OTHER PROJECTIONS IN THE STATISTICAL TREATMENT OF JOINTS

BY JOHN RODGERS

Howard J. Pincus' paper, *Statistical methods applied to the study of rock fractures* (1951), is a praiseworthy attempt to apply quantitative statistical methods to the study of joints, and it shows clearly the sort of advances that such treatment will make possible. It is the more unfortunate therefore that the statistical treatment in the paper is vitiated by a fundamental error.

The significance of such a statistical study of joints depends, as Pincus properly points out (p. 101), on the degree of deviation of the observed distribution of the joints from uniform (isotropic) distribution. Uniform (isotropic) distribution of joints in the field means uniform distribution of the poles of the joints in space. This uniformity ideally should be expressed graphically by uniform distribution of points representing the poles on a reference sphere, but in practice a projection of the sphere in two dimensions is required. In order however to preserve the uniform (isotropic) distribution in the projection, the projection must be an equal-area projection.

The subject of projections of spherical surfaces into two dimensions is highly developed because of its great importance in cartography, which demands the representation of the approximately spherical surface of the Earth on a two-dimensional surface (*see* any textbook of cartography or the admirable summary of projections by Deetz and Adams, 1934). A number of equal-area projections have been devised; the one commonly used for joints, as also for petrofabric or till fabric diagrams, is the Lambert zenithal (or azimuthal) equal-area projection, used by Lambert in 1772, but commonly known to geologists as the Schmidt net because introduced into petrofabrics in the 1920's by W. Schmidt.

Pincus objects to the Schmidt net (p. 96–98), principally on the ground that statistical summations cannot easily be made from it, a reasonable objection for a study such as this one. He substitutes for it however a rectangular co-ordinate diagram, plotting the strikes of joints on the abscissa and the dips on the same scale on the ordinate. By simply relabelling abscissa and ordinate (and doubling along the abscissa) this diagram becomes in fact the well-known though little-used cylindrical equal-spaced projection, which is easy to construct but has practically no other desirable properties. Above all it is not an equal-area projection, and therefore a distribution of joints that is uniform (isotropic) in space would not appear as uniform on this projection but would show a density proportional to the sine of the angle of dip (of the colatitude of the poles of the joints, in terrestrial co-ordinates). The use of this projection therefore introduces an artificial anisotropy and contravenes the basic principle that uniform distribution of observed data should be projected as uniform distribution of points; thus the statistical superstructure of the paper, especially the attempts to contour the anisotropy in the observed data, is undermined.

Pincus has attempted to refute this obvious conclusion by two arguments (p. 102, and footnote on p. 98): first, that isotropy (isotropism) can be defined arbitrarily in an infinity of ways and that there is no valid reason for preferring one definition over another, and second, that whatever the theoretical distinction between the two projections in question there is no

practical difference in the results. These objections may be dealt with separately.

An isotropic distribution (of matter, of poles, of vectors, etc.) is one in which all directions in space are quantitatively the same; isotropy has no other meaning. The idea that uniform distribution of points on the rectangular co-ordinate diagram represents some kind of isotropy of joints in space can readily be disproved. By visual inspection of the diagram, it can be seen that as much area is represented by an increment of dip angle at 0° as at 90°; therefore in a distribution graphed as uniform on this diagram dips of 0° should be as common as dips of 90°, though the dip of 0° is a single position in space and that of 90° embraces an infinity of positions that box the compass, including positions at right angles to each other that are as different from each other as either is from a horizontal position. In more general terms, strike and dip as used by geologists to describe the attitude of joints in space relate to two essentially arbitrary, though very convenient, data—the present horizontal and the present position of geographic north—but they are not truly independent variables as is assumed in plotting them as abscissa and ordinate. If the area Pincus studied were tilted appreciably in one direction, then the "isotropy" he assumes relative to the present horizontal would become an anisotropy relative to the new horizontal. To state the matter in full generality, because his projection is tied to an arbitrary datum (the present horizontal), it cannot be transformed to any other datum (a newer or older horizontal) without introducing a systematic and artificial anisotropy. The only uniform distribution of plotted points on a projection that *can* be so transformed and yet remain isotropic is that on an equal-area projection of some kind, and therefore such a projection is the only "inherently valid" kind for a statistical analysis of anisotropy concerning directions in space. To object that one "isotropy" is as good as another because "we still do not know how rocks break" is a non sequitur; studies like Pincus' are badly needed precisely because we still do not know, and from such studies we can hope to gain clues to that knowledge by studying significant *departures* from isotropy. But to use a system of plotting that introduces an artificial anisotropy related to the present-day horizontal is not the way to begin.

Pincus' second argument is that plots of the same data on the two projections are "virtually identical". His projection approaches an equal-area projection for dips of high angle (poles at low latitude), and it happens that most of Pincus' joints as observed in the field dip at a high angle (in itself a significant anisotropy, as he points out). Qualitatively, therefore, and within the specific data he is using, the two projections approach each other. But Pincus has stated that he is striving for quantitative as well as qualitative results, and quantitative results cannot be based on the argument that the two projections are qualitatively alike when demonstrably they are quantitatively different for all but vertical joints. Thus his contour diagrams can have the quantitative significance he attaches to them only after they have been replotted on an equal-area projection.

Pincus objects to the Schmidt net because it makes statistical summations more difficult, though what he is really stating is the truism that a sphere does not lend itself to simple rectangular co-ordinate; in two dimensions that would facilitate such summations. But there are many equal-area projections beside the Schmidt net, and one is not forced into a simple choice between it and the rectangular co-ordinate diagram. Specifically, the cylindrical equal-area projection (likewise known to Lambert in the eighteenth century) is theoretically impeccable and is also easy to construct, being orthographic as well as equal area (Deetz and Adams, 1934, Fig. 16). Relative to the zenithal equal-area projection (Schmidt net), its perpendicular parallels and meridians lend themselves readily to tabular summations, though the projection is less easily transformed from one datum horizontal to another, and for data taken in certain ways the excessive distortion at high latitudes (*i.e.*, for low dips) may introduce serious local anisotropies there that would not be met on the Schmidt net. Relative to the cylindrical equal-spaced projection (the rectangular co-ordinate diagram), it is a little less handy because of the unequal spacing of the parallels, but contours of anisotropy based on it really have a quantitative meaning relative to the distribution of the plotted data in space. By

plotting his data on this or some other equal-area projection, Pincus could transform his results from interesting but qualitative suggestions into rigorously quantitative conclusions.

I wish to thank my colleagues, Mr. Chester R. Longwell, Mr. and Mrs. Adolph Knopf, Mr. Horace Winchell, and Mr. Matt S. Walton, for critical reading of the manuscript of this note. I would also like to thank Mr. Pincus for his comments on the note, especially for pointing out several cases of improper use of words or phrases.

References Cited

Deetz, C. H., and Adams, O. S. (1934) *Elements of map projection with applications to map and chart construction*, U. S. Coast and Geodetic Survey, Spec. Pub. 68, 4th ed., revised.

Pincus, H. J. (1951) *Statistical methods applied to the study of rock fractures*, Geol. Soc. Am., Bull., vol. 62, p. 81–130.

Dept. Geology, Yale University, New Haven, Conn.

BULLETIN OF THE GEOLOGICAL SOCIETY OF AMERICA
VOL. 63, PP. 431-434 APRIL 1952

SOME METHODS FOR OPERATING ON ORIENTATION DATA

BY HOWARD J. PINCUS

Many geological studies include data describing orientations of groups of axes or planes. Investigations in petrofabrics, sedimentation, and structural geology are often well documented with frequency diagrams depicting orientation patterns of features of geological significance, such as crystallographic axes, long diameters of pebbles, and normals to fracture planes.

Frequency diagrams assist in, or make possible, further analysis: they are not an end in themselves. The diagrams are constructed in answer to some geological question, such as, "Do quartz c-axes in this specimen show a relation to other directions of geological significance?" Or, "Are the fractures in bed A, exposed in this quarry, part of a regional pattern?"

In using such diagrams to help answer geological questions, two requirements are imposed: (1) The type diagram to be used must necessarily be determined by the question to be put to the data. (2) The diagram selected, in turn, affects the meaning of all conclusions drawn from the data as plotted. The type of operations used in plotting and graphical summing of data determines the meaning of terms like "cluster", "band", and "girdle": thus the results obtained from operating on the same raw data in more than one way are not equivalent, even if the numerical results be identical.

In dealing with masses of three-dimensional orientation data, many authors have used the Schmidt equal-area net, a projection with many desirable properties. Typically, as in petrofabrics, orientations are plotted on the projection as (pole) points; graphic summing (Fairbairn, 1949) is performed with a unit counting circle of fixed area, usually 1 per cent of the area of the projection. The clustering of the points, as plotted, is then given in terms of the number of points in the circle at each position of the circle on the projection, divided by the number of points which would occur in the circle if all points *on the projection* were evenly distributed (1 per cent of all points plotted, if 1 per cent counting circle is used). The quotients are then contoured to give a summary graphic picture.

What do these operations imply regarding the standard thus established for measuring the concentration of orientations?

First, the selection of the Schmidt net implies that a uniform distribution of points on a sphere is the desired basic standard to which observed distributions are to be compared; also, the Schmidt net is accepted as an adequate representation of the sphere for the purposes involved.

Second, the method of summing, or "counting out", with the unit counting circle is accepted as a workable substitute for counting on the sphere itself, since equal areas on the projection are taken to represent equal (but not equally shaped) areas on the sphere.

Considering the first factor, a uniform point distribution on any surface (or even along a line, as on a scale) makes for easy visualization and comparison, within the system used. But suppose that orientations of normals to spherically concentric fractures be plotted on a sphere, then this very definite fracture pattern would show up as a uniform point distribution (Felix Chayes, personal communication). Here, other standards might provide more fruitful analyses.

Actually, uniformity on any one surface is only one type of standard for the given surface; any distribution, varying in a known way, can be used as the standard. (Along line segments, many investigators have replaced arithmetic scales with geometric scales.) Or, the investigator may use a correlation coefficient (Chayes, 1946) as a measure of "preferred orientation," neatly avoiding any *a priori* assumptions about fabric distributions in "unoriented" rocks, as plotted on the given surface.

Also, the standard of uniform point distribu-

tion on a sphere is dependent, in part, on the assumption that errors of measurement are of the same order of magnitude, or are believed to be too small to be troublesome, over the entire range of possible measurements. However, the field measurement of the strike of flatly dipping (especially irregular) surfaces is clearly subject to errors larger than those involved in measuring steeply dipping surfaces (Müller, 1933). Errors of this kind become very important where few points fall in areas of large measuring error, as in the case of fractures in gently folded rocks.

The uniform picture may be distorted by the sampling process and by the nature of the units being studied. Fabric diagrams of elongated grains are distorted by those grains whose centers lie outside the thin section; "... as the distance of the centers from the thin section increases, the grains that extend into the thin section become restricted to those whose long dimension is nearly normal to the section" (Wood and Jizba, 1950).

Thus the uniform point distribution is not flawless, and should not be blindly accepted as the last word in establishing standards.

In each investigation which does utilize uniformity as one element of the standard, there must also be established a quantitative definition of uniformity. For example, the investigator may select some value, such that a "uniform" distribution has no concentrations of value greater than the selected (density) value. Selection of the critical value should depend upon one's concept of uniformity in the light of the investigation being pursued.

But, suppose that it is decided to accept uniformity as one element of the standard; then can surfaces other than spheres be used in the analysis?

Consider the fabrics of a sedimentary rock composed of nearly parallel platy fragments, or an igneous rock with linear flow structure, or vertical fractures in horizontal beds. In the genetic sense, it means very little to compare such fabrics with a uniform distribution of points on the sphere.

Why not attempt to find, say, a quadric surface, such as a triaxial ellipsoid, on which the points plotted conform with the investigator's definition of uniformity? (The points as plotted would be the intersections of the orientation vectors with the surface used.) Then the surface used, described in terms of its equation and the orientation of its co-ordinate axes, constitutes a description (not necessarily unique) of the distribution. If the surface of some triaxial ellipsoid should satisfy the requirements of the investigation, the axial ratios and axial orientations would describe the distribution of the measured orientations, without resorting to the standard of the uniform point distribution on the sphere.

Further, suppose that, through deformation, the fabric of the rock is transformed. Then, if both the deformed and undeformed equivalents are available, the fabric transformation could be described in terms of the (secondary) concentration of points on the primary surface (ellipsoid), or in terms of the change of surfaces (ellipsoids). Using a triaxial ellipsoid, a mere tilting of the rock would involve a change in the orientation of the ellipsoidal axes, with no change in the axial ratios.

The problems of finding and projecting a surface of "best fit" (within a category of surfaces) are not insoluble. A surface, say an ellipsoid, of "best fit" might be found empirically by using projections or a series of sections through a standardized suite of ellipsoids. The projection of ellipsoids involves nothing fundamentally different from the projection of spheres.

Distributions with more than one concentration on ellipsoids would require other types of surfaces. Possibly the fascinating literature of topology (rubber-sheet geometry) holds the solution, or the means to the solution of this problem.

This author holds that *surfaces other than spheres may be used as one of the elements in analyzing orientations, just as long as the directions as plotted do not lose their identity in terms of the original measurements; the type of surface selected depends upon the question to be put to the data.* In effect, then, as stated in the author's earlier paper (Pincus, 1951), isotropy as a standard can be defined in an infinity of ways. Or, if one chooses to restrict the term "isotropy" to equivalence with a uniform point distribution on a sphere, then it can be stated that a uniform point distribution on any defined surface is a potential standard.

In each analysis, of course, the final results should consist of directions expressed in the same terms as the original measurements, but

this does not require that spheres be used throughout the analysis in order to ask productive questions of the data.

The dictum that equal-area projections of a sphere are the only valid plots for analyzing group orientation data, because measurements of orientations are made in a spherical system, is comparable to the (imaginary) argument that the 2-digit number system (binary or dyadic scale) is wrong and the 10-digit system (decimal scale) is right because we still have 10 fingers. (This would have made Leibniz quite unhappy.)

Considering the second factor mentioned above—*i.e.*, that the method of graphic summing on the Schmidt net is a workable substitute for counting on the sphere—let us assume that the uniform point distribution is the desired standard for measuring concentrations. Then it is essential that the investigator be aware of the errors involved in the counting operation. Using the same counting circle over the entire extent of the Schmidt net involves a distortion inherent in projections of this type (Deetz and Adams, 1934). Fairbairn (1949) and others have considered this problem, concluding that circular counters are "sufficiently accurate". The meaning of answers obtained in such analyses are ambiguous to at least the same degree as the expression "sufficiently accurate".

This student is not finding fault with, nor attempting to discourage the use of, the Schmidt net or any other internally consistent system: he is merely pointing out that, even in the most widely accepted method for handling three-dimensional orientation data, rigorous results are not possible until such sources of error are estimated, along with sampling and other errors.

To imply that the Schmidt net is impeccable, as has Rodgers in the preceding note, is to make a claim which is not justified for any system developed so far. Further, rotation of the horizontal in such a system can produce changes in concentrations (Osborne and Lowther, 1936), contrary to Rodgers' contentions.

The author has used a rectangular co-ordinate plot for indicating rock fracture orientations, in terms of equal linear increments along the co-ordinate axes representing equal increments of angles of dip and strike; graphic summation is effected with a unit counting square (Pincus, 1951). This type of plot is not and was not intended to be equivalent to plots on Schmidt nets, for it is used in answer to a different question. It utilizes as a standard the uniform point distribution (subject, of course, to all the limitations of "uniformity", as outlined above) over a grid based on *linear variations* in values of dip and strike.

Although the rectangular co-ordinate diagrams have been used for operating on the raw data, their inadequacy in depicting space (principally dihedral) relations led the author to use the Wulff (stereographic) net for presenting the space picture of mean fracture planes (Pincus, 1951, Figs. 14–16).

To say (as has Rodgers) that this plot is a type of projection of a sphere constitutes a restricted view of a relation stated earlier as a requirement—*i.e.*, that orientations measured in a spherical system must not lose their identity when plotted in some other system. To brand as incorrect the rectangular plot, or any other plot not an equal-area projection of a sphere requires special restrictions for which this author knows no valid basis. Such restrictions would block entry into a potentially fruitful field by designating as incorrect those standards based on different operations, simply because they are different. A given standard may be less preferable for a specific purpose, but this is quite different from being incorrect.

With regard to specific points made by Rodgers, the following require examination:

"... the statistical treatment of the paper (Pincus, 1951) is vitiated by a fundamental error." It is presumed that Rodgers' intended target is the standard consisting of the uniform point distribution on rectangular co-ordinates, but this statement levels a blast at a host of targets.

Under the heading of "statistical treatment", workers in the field of statistics regard the gathering of the raw data as the most important single operation in the entire sequence of statistical operations. (*See* almost any introductory text.) Yet Rodgers' statement covers the gathering of the data and, in addition, determination of sample size, the A-test and related treatments (applicable to any type of plot, including equal-area projections), etc. Part IV deals with dips of individual fracture planes, treated independently of three-dimensional plots, yet this too is "statistical treatment".

Rodgers also states that, by plotting the data on an equal-area projection of a sphere, the results could be transformed "from interesting but qualitative suggestions into rigorously quantitative conclusions". One should be puzzled reading about a paper which is based on a "fundamental error", yet has "interesting but qualitative suggestions".

More important, there is almost no recognition of the fact that the raw data have been studied on both the rectangular net and the Schmidt net (Pincus, 1951, p. 102; footnote 4), and that the A-test yielded similar results in both systems. (Except for Figure 8, only the rectangular plots have been published.) Further, these analyses are accompanied by statements indicating that this similarity in results does not mean that the results are equivalent. However, if the rectangular system were wiped off the record (which the author is not as yet prepared to do, at least not on the basis of Rodgers' arguments), the numerical results of the paper would remain approximately the same.

Also, the author does not understand what Rodgers means by terms such as "qualitative suggestions" and "rigorously quantitative conclusions". As a matter of record, both plots yield quantitative conclusions which serve as bases for different qualitative suggestions. The terms "quantitative" and "qualitative" are not mutual exclusives, nor can they be ranked. (*See* Webster's Unabridged.) No type of analysis can yield "rigorous" results until estimates are made of the order and distribution of the errors involved; the type of plot used cannot, in itself, make the results "rigorously quantitative".

The author wishes to express his sincere thanks to John Rodgers for having given considerable time and thought to this aspect of analyzing orientation data, and for presenting a clear exposition of a point of view which is probably shared by many investigators (Fairbairn, 1949, footnote p. 289). But this view is incomplete and unjustifiably restricted, unless the concepts presented earlier in this note can be proved incorrect; if incorrect, the author will readily concede error, and expand his thanks to congratulations for keeping our literature "correct".

The comments of interested colleagues on this and related subjects will be most welcome; it is believed that discussions should center on

(1) Suitability of various standards for studying orientation data (Chayes, *in* Fairbairn, 1949).

(2) Orders of error involved in measuring, plotting, and averaging. Spherical projection errors are available but are little used.

(3) Areas of geological research most susceptible to productive quantitative analyses, and those most susceptible to "counting beans", and little more.

(4) The meaning of the terms "qualitative" and "quantitative", as applied to geological evidence, and techniques for using both productively.

References Cited

Chayes, F. (1946) *Application of the coefficient of correlation to fabric diagrams*, Am. Geophys. Union, Tr. vol. 27, p. 400.

Deetz, C. H., and Adams, O. S. (1934) *Elements of map projection with applications to map and chart construction*, U. S. Coast and Geodetic Survey, Sp. Pub. 68, 4th ed. revised.

Fairbairn, H. W. (1949) *Structural petrology of deformed rocks*, Addison-Wesley Press, Cambridge.

Müller, L. (1933) *Untersuchungen über statistische Kluftmessung*, Geol. u. Bau., Jahrb. 5, p. 231.

Osborne, F. F., and Lowther, G. K. (1936) *Petrotectonics at Shawinigan Falls, Quebec*, Geol. Soc. Am., Bull., vol. 47, p. 1343–1370.

Pincus, H. J. (1951) *Statistical methods applied to the study of rock fractures*, Geol. Soc. Am., Bull. vol. 62, p. 81–130.

Wood, W. H., and Jizba, Z. V. (1950) *Effects of grain elongation on fabric diagrams* (Abstract), Geol. Soc. Am., Bull., vol. 61, p. 1534–1535.

The Ohio State University, Columbus, Ohio